AB INITIO STUDIES OF ELECTRONIC STRUCTURE AND PROPERTIES OF DIATOMIC MOLECULES CONTAINING ALKALINE-EARTH ATOMS

Ph.D. THESIS

by

Renu Bala

DEPARTMENT OF PHYSICS
INDIAN INSTITUTE OF TECHNOLOGY ROORKEE
ROORKEE - 247 667 (INDIA)
MAY, 2019

AB INITIO STUDIES OF ELECTRONIC STRUCTURE AND PROPERTIES OF DIATOMIC MOLECULES CONTAINING ALKALINE-EARTH ATOMS

A THESIS

Submitted in partial fulfilment of the requirements for the award of the degree

of

DOCTOR OF PHILOSOPHY

in

PHYSICS

by

RENU BALA

DEPARTMENT OF PHYSICS
INDIAN INSTITUTE OF TECHNOLOGY ROORKEE
ROORKEE - 247 667 (INDIA)
MAY, 2019

INDIAN INSTITUTE OF TECHNOLOGY ROORKEE
ROORKEE

CANDIDATE'S DECLARATION

I hereby certify that the work which is being presented in the thesis entitled **"*AB INITIO* STUDIES OF ELECTRONIC STRUCTURE AND PROPERTIES OF DIATOMIC MOLECULES CONTAINING ALKALINE-EARTH ATOMS"** in partial fulfillment of the requirements for the award of the Degree of Doctor of Philosophy and submitted in the Department of Physics of the Indian Institute of Technology Roorkee is an authentic record of my own work carried out during a period from January, 2014 to May, 2019 under the supervision of **Dr. H. S. Nataraj**, Assistant Professor, Department of Physics, Indian Institute of Technology Roorkee, Roorkee, INDIA.

The matter presented in the thesis has not been submitted by me for the award of any other degree of this or any other institute.

(RENU BALA)
Signature of the Candidate

This is to certify that the above statement made by the candidate is correct to the best of my knowledge.

(H. S. Nataraj)
Signature of Supervisor

The Ph.D. Viva-Voce Examination of **Ms. Renu Bala**, Research Scholar, has been held on 5^{th} August, 2019 at the Department of Physics, IIT Roorkee, Roorkee, INDIA.

Chair, SRC **Signature of External Examiner**

This is to certify that the student has made all the corrections in the thesis.

Signature of Supervisor **Head of the Department**

Dated: .....

ABSTRACT

With recent advancements in experimental techniques, the study of diatomic molecules at cold and ultracold temperatures has attracted considerable recognition in various areas of research such as controlled chemical reactions, quantum computing, quantum phase transitions, fundamental interactions, fundamental physical constants, etc. In this context, the theoretical knowledge of numerous electronic and vibrational properties of diatomic molecules plays an important role in the design and development of various such experiments.

In this thesis, we have investigated singly charged alkaline - earth lithides ($AELi^+$): $BeLi^+$, $MgLi^+$ and $CaLi^+$, which have recently been considered for the examination of elastic - and inelastic processes occurring during the ion - atom collisions and for predicting the feasibility of formation of these ions via photoassociation processes [1–4]. We have performed all electron calculations for the potential energy curves (PECs), spectroscopic constants: equilibrium bond lengths (R_e), dissociation energies (D_e), harmonic frequencies (ω_e), anharmonic frequencies ($\omega_e x_e$) and rotational constants (B_e and α_e), and the molecular properties: dipole moments (μ_0), quadrupole moments (Θ_{zz}), components of dipole polarizabilities ($\alpha_\parallel$, $\alpha_\perp$, $\bar{\alpha}$, γ) and dipole polarizabilities at the asymptotic limit (α_{100}) for the ground state of these molecular ions

using higher - order correlation methods and large optimized basis sets. The results of quadrupole moments and dipole polarizabilities are reported for the first time in our work, to the best of our knowledge. The errors due to the size of basis sets and correlation methods are also estimated for all diatomic constants and molecular properties of ground electronic states. Further, the effect of diffuse functions on molecular properties has also been investigated. It has been found that the inclusion of relativistic effects alters the electronic energies for the ground states of the molecular ions considered in this work noticeably. However, the difference between the results of diatomic constants calculated with the relativistic and the non - relativistic methods is small and lies within the estimated error bars at the non - relativistic level of theory.

In addition, by using the PECs and permanent dipole moment (PDM) curves of ground electronic states, we have calculated the vibrational parameters: energies, wavefunctions, rotational constants and transition dipole moments (TDMs) between the vibrational levels. The lifetimes of vibrational states are then computed using relative vibrational energy spacings and vibrational TDMs. The lifetimes of ro - vibrational ground states are found to be 4.67 s for $BeLi^+$, 2.81 s for $MgLi^+$, and 3.19 s for $CaLi^+$. The lifetime of highest vibrational level of the ground electronic state of $MgLi^+$ ($CaLi^+$) is calculated to be 19.3 s (2.38 s) which is much larger than (comparable to) the lowest vibrational level.

We have also investigated the low - lying excited states of these ions for their PECs, diatomic constants and PDM curves. Further, the transition energies (T_e) and the TDMs for the transitions from the ground to the excited electronic states are reported. We have made detailed comparison of our calculations for electronic and vibrational properties of $AELi^+$ with the results available in the literature and emphasized on the high accuracy attained in our work. Since very few calculations, particularly, for the excited states are reported in the literature, our all - electron calculations computed with large active space could stand as benchmarks for the theoretical studies on these

molecular ions in future.

Another sub - species of diatomic molecules, *viz.*, the heavier members of alkaline - earth monofluorides (AEMFs), BaF and RaF, are the potential candidates for probing the nuclear anapole moment that is of immense interest in contemporary physics [5–7]. In this connection, we have studied the molecular properties such as PDMs, components of dipole polarizability (DP), parity ($\mathcal{P}$) and time - reversal ($\mathcal{T}$) - odd interaction constants: W_d and W_s, and hyperfine structure (HFS) constants for the ground state of AEMFs, and also the static DPs of alkaline - earth and fluorine atoms. The PDM of RaF, molecular polarizabilities for CaF and RaF, HFS constants of BeF and W_s for BeF, MgF, CaF and SrF molecules are computed and reported for the first time. Further, the effect of augmentation of the basis sets on the valence properties; and the contribution of triple excitations and also the contributions of inner - core electrons on the HFS constants of lower members of this series are investigated. The calculated results using frozen core approximation show good agreement with the existing data, wherever available. We have observed, however, that the accurate calculations of the HFS constants require the inclusion of core electrons as well as triple excitations at the correlation level.

We believe that the results presented as part of this thesis using sophisticated many - body theories and sufficiently large optimized basis sets would serve as benchmarks for similar calculations in the future. They would also be beneficial for the experimental spectroscopists who might consider working on these molecular systems in future.

ABBREVIATIONS AND NOTATIONS

$AELi^+$	Singly Charged Alkaline - Earth Lithides
AEMFs	Alkaline - Earth Monofluorides
BOA	Born - Oppenheimer Approximation
IPM	Independent Particle Model
HF	Hartree - Fock
SCF	Self Consistent Field
RHF	Restricted HF
UHF	Unrestricted HF
DF	Dirac - Fock
CI	Configuration Interaction
MBPT	Many - Body Perturbation Theory
MP2	Second - Order MBPT/Møller - Plesset Perturbation Theory of Second - Order
CC	Coupled - Cluster
CCSD	CC with Singles and Doubles
CCSD(T)	CCSD with Partial Triples

CCSDT	CCSD with Full Triples
MRCI	Multi - Reference CI
MRCI + Q	MRCI Including Davidson Correction
KRCI	Kramers - Restricted CI
KRCISD	KRCI with Singles and Doubles
GAS	Generalized Active Space
EOM - CC	Equation - of - Motion CC
PRCC	Perturbed Relativistic CC
GHF - ZORA	Generalized HF - Zeroth - Order Regular Approximation
ECC	Extended CC
CPF	Coupled Pair Functional
ECP	Effective Core Potential
RAS	Restricted Active Space
CPP	Core Polarization Potential
FC	Frozen Core
FS	Fock - Space
EO	Effective Operator
CIPSI	Configuration Interaction by Perturbation of a Multiconfiguration Wavefunction Selected Iteratively
DIRAC	Direct Iterative Relativistic Atomic and Molecular Code
CFOUR	Coupled - Cluster Techniques for Computational Chemistry
MOLCAS	Molecular Complete Active Space
DBOC	Diagonal Born - Oppenheimer Correction
STO	Slater Type Orbital
GTO	Gaussian Type Orbital
cc - pVXZ	Correlation - Consistent Polarized Valence [X] Zeta
aug - XZ	Augmented cc - pVXZ [basis]
a.u.	Atomic Unit
amu	Atomic Mass Unit

NIST	National Institute of Standard and Technology
BBR	Black - Body Radiation
PEC	Potential Energy Curve
PDM	Permanent Dipole Moment
eEDM	Electric Dipole Moment of an Electron
S - PS	Scalar - Pseudoscalar
TDM	Transition Dipole Moment
HFS	Hyperfine Structure
DP	Dipole Polarizability
QM	Quadrupole Moment
NMM	Nuclear Magnetic Moment
IR	Irreducible Representation
α_A	Atomic Polarizability
$\mathcal{P}$	Parity
$\mathcal{T}$	Time - Reversal
R_e	Equilibrium Bond Length
D_e	Dissociation Energy
ω_e	Harmonic Frequency
$\omega_e x_e$	Anharmonic Frequency
α_e, B_e	Rotational Constants
μ_0	Dipole Moment
Θ_{zz}	Quadrupole Moment
$\alpha_\parallel$	Parallel Component of DP
$\alpha_\perp$	Perpendicular Component of DP
$\bar{\alpha}$	Average Polarizability
γ	Polarizability Anisotropy
α_{100}	Polarizability at 100 a.u. Distance
v	Vibrational Quantum Number
J	Rotational Quantum Number

E_v	Vibrational Energy
B_v	Vibrational Rotational Constant
T_e	Transition Energy
Γ_{spon}	Spontaneous Transition Rate
Γ_{BBR}	BBR Induced Transition Rate
τ	Lifetime
$\mathcal{I}$	Nuclear Spin
ε_{eff}	Effective Electric Field
W_d, W_s	$\mathcal{P}$, $\mathcal{T}$ - Odd Interaction Constants

CONVERSION FACTORS FROM ATOMIC UNITS TO S.I. UNITS

Physical quantity	Symbol	a.u.	S.I. unit
Electron mass	m_e	1	$9.110 \times 10^{-31}\,\mathrm{Kg}$
Electron charge	e	1	$1.602 \times 10^{-19}\,\mathrm{C}$
Distance	a_0	1	$5.292 \times 10^{-11}\,\mathrm{m}$
Energy	E_h	1	$4.360 \times 10^{-18}\,\mathrm{J}$
Angular momentum unit $(h/2\pi)$	$\hbar$	1	$1.055 \times 10^{-34}\,\mathrm{J\,s}$
Speed of light $(1/a_0)$	c	137.036	$2.998 \times 10^{8}\,\mathrm{m/s}$
Electric field $(E_h/e\,a_0)$	ε	1	$5.1422 \times 10^{11}\,\mathrm{V/m}$
Dipole moment $(e\,a_0)$	μ_0	1	$8.4784 \times 10^{-30}\,\mathrm{C\,m}$
Quadrupole moment $(e\,a_0^2)$	Θ	1	$4.4866 \times 10^{-40}\,\mathrm{C\,m^2}$
Dipole polarizability $(e^2\,a_0^2\,E_h^{-1})$	α	1	$0.16488 \times 10^{-40}\,\mathrm{C^2\,m^2\,J^{-1}}$
Fermi constant $(E_h\,a_0^3)$	G_F	2.22249×10^{-14}	$1.1663787 \times 10^{-5}\,\mathrm{Gev^{-2}}$

ACKNOWLEDGEMENTS

During the difficult but exciting and rewarding journey of more than five years, I have met several people who directly or indirectly became a part of this expedition. I am pleased to have this opportunity to show my sincere gratitude to all of them.

Firstly, I wish to express my heartfelt gratitude and deep respect to my supervisor ***Dr. H. S. Nataraj***, Assistant Professor at the Department of Physics, Indian Institute of Technology Roorkee, as without his guidance the dream of writing "Dr." before my name would have not been realized. His advice and valuable discussions have made this thesis possible. His cooperation, consistent encouragement, positive criticism and suggestions have helped me in improving my overall performance and self - confidence. I am also thankful to him for giving me enough space for independent thinking.

I am grateful to the members of my Student Research Committee: ***Dr. L. Sharma*** (Internal member), ***Dr. P. Debnath*** (external member) and ***Prof. R. Srivastava*** (***Prof. B. D. Indu***) present (former) Chairman, for their valuable time and comments for each and every presentation of this work. I am also thankful to ***Prof. A. K. Jain*** and ***Prof. K. L. Yadav***, former and present Head of Department of

Physics, Indian Institute of Technology Roorkee, for providing the basic infrastructure to pursue my research work in a better manner.

My sincere gratitude to our collaborators ***Dr. M. K. Nayak***, ***Dr. M. Abe***, and ***Prof. M. Kajita*** for their valuable discussions that encouraged and aided me to evolve as a better scientist. I am grateful to ***Dr. G. Gopakumar*** and ***Dr. C. N. Ramachandran*** for the several fruitful discourses that helped me to understand the various concepts of molecules. I also thank my teachers from school to college for believing in me and motivating me.

During this wonderful journey, I have got friends: Pragati, Gagan, Priti, Swati and Vidhi, for the rest of my life. Thank you all for supporting me and cheering me, whenever I was in low spirits. I also want to thank Rohit, Sanjeev, Ankita Joshi, Tiku sir, Mona di, Karunava, Kavita, Avijeet, Ankita di, Avijit, Atin and Shailesh, for their support. I would like to present my gratitude towards my former and present labmates Bhoomika di, Swati Modi di, Dipti di, Lata di, Rakhi ma'am, Anita ma'am, Archana, Neeraj, Shivam, Swati Bharti, Neelam, Shubham, Mujeeb, Shubhalaxmi, Salman and Radhika for providing a healthy environment to work. I have relished the several academic and non - academic debates that we have had over time. A big thanks to Meena ma'am for her motherly love and care at IITR.

My sincere thanks to Archana Jayaprakash for helping me during my visit to Japan. I must not forget my school friends: Deepak, Mukesh, Mangat, Preety, Sameena, Neha, Manisha, Rohini, Rubina, Arsh, Sonia, Beenu, Chandni, Hema, Heena, Aman and Rupinder, and college friends: Veenu di, Gurpreet di, Shareena, Geetu, Pooja, Manpreet, Nisha, Sukhjeet, Amanpreet, Kuljeet, Shilpy, Sukhdeep and Madhvi for contributing to my journey in one way or the other.

Although they are beyond any expressible appreciation, I still would like to pay

homage to my family, to whom I owe everything. My great reverence and enormous thanks are due to my grand parents: Sri Rajinder Kumar and Smt. Kamla, for the values they inculcated in me that contributed to my life in various ways and provided me the ability to grow without any inhibitions. Although, they are not in this world physically, but wherever they are, I hope they feel proud of their grand daughter. I deeply thank my parents for their unconditional love, continuous support and encouragement. I would never have been able to be at this level without their immense blessings and impeccable patience. I am indebted to Ashwani chachu (late), Shiv chachu, Sanjeev chachu, Rekha chachi, Anita chachi and Ranju chachi, for always being there for me. I can not think life without my siblings: Yodh and Deepika, and my cousins: Harish, Meenakshi, Koshal, Neelam, Suhani and Sanjana, I love you all.

All calculations reported in this thesis were performed on the computing facility available in the Department of Physics, Indian Institute of Technology Roorkee, India and in the Department of Chemistry, Tokyo Metropolitan University, Japan. The financial assistance from Ministry of Human Resource Development, India and Students' Aid Committee (StAC), Indian Institute of Technology Roorkee, during the period of this research is highly acknowledged. The financial aid received from the JST CREST fund for visiting TMU is also appreciated.

Above all, I would like to thank God for EVERYTHING!

Date:. . . . . (Renu Bala)

Dedicated to my beloved parents

Sri Shanti Saroop and Smt. Suman Rani

List of Publications

Refereed articles:

1. *Ab initio calculations of permanent dipole moments and static dipole polarizabilities of alkaline - earth monofluorides*,
   R. Bala, H. S. Nataraj, and M. K. Nayak, Journal of Physics B: Atomic, Molecular and Optical Physics **52**, 085101 (2019).

2. *Calculations of electronic properties and vibrational parameters of alkaline - earth lithides: $MgLi^+$ and $CaLi^+$*,
   R. Bala, H. S. Nataraj, M. Abe, and M. Kajita, Molecular Physics **117**, 712 (2019).

3. *Accurate ab initio calculations of spectroscopic constants and properties of $BeLi^+$*,
   R. Bala, H. S. Nataraj, M. Abe, and M. Kajita, Journal of Molecular Spectroscopy **349**, 1 (2018).

4. *Spectroscopic Studies of $^1\Sigma^+$ States of HfH^+ and PtH^+ Molecular Ions*,
   R. Bala, H. S. Nataraj, and M. Abe (Accepted for publication in Springer Proceedings of 7^{th} Topical Conference of the Indian Society of Atomic and Molecular Physics).

5. *Calculations of $\mathcal{P}$ & $\mathcal{T}$ -odd interaction constants of alkaline - earth monofluorides using KRCI method*,
   R. Bala, and H. S. Nataraj (Under preparation).

Papers in Conferences/Symposium:

1. *Many - body calculations of ground - and low - lying excited states of PtH^+*,
   R. Bala, H. S. Nataraj, and M. Abe, 13^{th} Asian International Seminar on Atomic and Molecular Physics, December 3 - 8, 2018, Tata Institute of Fundamental Research/Indian Institute of Technology Bombay, Mumbai, India.

2. *Ab initio calculations of spectroscopic parameters of HfH^+ and PtH^+*,
   R. Bala, H. S. Nataraj, and M. Abe, 7^{th} Topical Conference of the Indian Society of Atomic and Molecular Physics, January 6 - 8, 2018, Indian Institute of Science Education and Research/Indian Institute of Technology Tirupati, Tirupati, India.

3. *Calculations of magnetic hyperfine structure constants for alkaline - earth monofluorides*,
   R. Bala, H. S. Nataraj, and M. K. Nayak, Theoretical Design of Materials with Innovative Functions Based on Element Strategy and Electronic Relativistic Theory, December 8 - 9, 2017, Tokyo Metropolitan University, Tokyo, Japan.

4. *Correlation effects for diatomic constants of group - IVa monoxides*,
   R. Bala, and H. S. Nataraj, 21^{st} National Conference on Atomic and Molecular Physics, January 3 - 6, 2017, Physical Research Laboratory, Ahmedabad, India.

Workshops/Conferences/Symposia Attended:

1. 3^{rd} North - West Meeting on Spectroscopy, Structure and Dynamics, April 5 - 7, 2019, Indian Institute of Technology Roorkee, Roorkee, India.

2. 13^{th} Asian International Seminar on Atomic and Molecular Physics, December 3 - 8, 2018, Tata Institute of Fundamental Research/Indian Institute of Technology Bombay, Mumbai, India.

3. Workshop on Improving Awareness and Plagiarism, October 31, 2018, Indian Institute of Technology Roorkee, Roorkee, India.

4. 7^{th} Topical Conference of the Indian Society of Atomic and Molecular Physics, January 6 - 8, 2018, Indian Institute of Science Education and Research/Indian Institute of Technology Tirupati, Tirupati, India.

5. Theoretical Design of Materials with Innovative Functions Based on Element Strategy and Electronic Relativistic Theory, December 8 - 9, 2017, Tokyo Metropolitan University, Tokyo, Japan.

6. TIFR School on Advances in atomic Collisions, March 5 - 18, 2017, Homi Bhabha Centre for Science Education, Mumbai, India.

7. 21^{st} National Conference on Atomic and Molecular Physics, January 3 - 6, 2017, Physical Research Laboratory, Ahmedabad, India.

8. Author Workshop on Book Publishing, September 26, 2016, Indian Institute of Technology Roorkee, Roorkee, India.

9. Intel HPC Code Modernization (Parallelization) Workshop, October 16 - 17, 2015, Indian Institute of Technology Roorkee, Roorkee, India

10. Exploring Fundamental Physics using Atomic Systems, May 6 - 8, 2015 at Physical Research Laboratory, Ahmedabad, India.

11. 20^{th} National Conference on Atomic and Molecular Physics, December 9 - 12, 2014, Indian Institute of Space Science and Technology, Thiruvananthapuram, India.

CONTENTS

LIST OF FIGURES

LIST OF TABLES

CHAPTER 1

INTRODUCTION

"Everything that is living can be understood in terms of the jiggling and wiggling of atoms" − Richard Phillips Feynman

Atoms are the basic building blocks of matter. It is, therefore, natural that their meticulous study is required to comprehend various phenomena occurring in nature. Indeed, the advancement in laser cooling and trapping techniques has opened up newer perspectives in research with cold and ultracold atoms[1]. The developments in experiments have also led to headways in theory and vice - versa. In fact, the theoretical knowledge of various structural parameters of atoms form the backbone of several such experiments.

Over the course of time, various combinations of atoms forming a variety of molecules have also undergone such theoretical and experimental scrutiny which provides a

[1]The Nobel Prize in 2005, awarded to J. L. Hall and T. W. Hänsch for their contribution to the development of laser - based precision spectroscopy including the optical frequency comb technique [8], and in 2012 to S. Haroche and D. J. Wineland for providing the experimental methods that facilitate measuring and manipulation of individual quantum systems [9] also bear a testimony to the rigorous progress in this field.

brand new and an exciting array of scientific opportunities for fundamental research and technological development. In particular, diatomic molecules have garnered special attention as they have the simplest electronic structure beyond an atom. A special class of these diatomic molecules containing alkaline - earth atoms form the crux of this thesis, in which we have performed several *ab initio* structure and property calculations for their ground - and excited states. Nevertheless, before we delve deeper into the realm of these diatomic molecules, we consider recollecting some of the basic concepts that are pre - requisites for a better understanding of the physical and chemical properties of diatomics. Although, there exists numerous authoritative textbooks [10–18] on this subject, the spectroscopic terms that are calculated and discussed in the later chapters are introduced in the following sections.

1.1 Basics of Diatomic Molecules

1.1.1 The Rotations of a Diatomic Molecule

Consider a diatomic system containing two atoms of masses m_1 and m_2, separated by a fixed internuclear distance, R_e, and center - of - mass, C, as shown in Figure (1.1), so that,

$$R_e \;=\; R_1 \;+\; R_2. \tag{1.1}$$

In a center - of - mass frame, the radii of rotation and masses of atoms are related as,

$$m_1\, R_1 \;=\; m_2\, R_2. \tag{1.2}$$

The moment of inertia (I) of the system about C is given by [10],

$$\begin{aligned} I \;&=\; m_1 R_1^2 \;+\; m_2 R_2^2, \\ &=\; R_1 R_2\, (m_1 \;+\; m_2), \qquad \text{using Eq. (1.2).} \end{aligned} \tag{1.3}$$

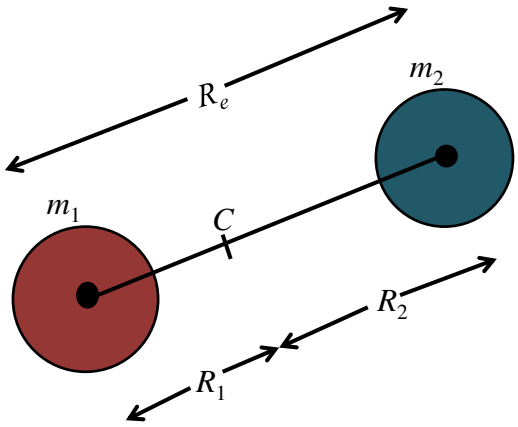

Figure 1.1: A diatomic molecule with a fixed internuclear distance between its constituent atoms, R_e, and center - of - mass, C.

Plugging the values of R_2 and R_1 from Eq. (1.1) into Eq. (1.2), we obtain,

$$R_1 = \frac{m_2\, R_e}{m_1 + m_2}, \qquad R_2 = \frac{m_1\, R_e}{m_1 + m_2}. \tag{1.4}$$

On substituting these values of R_1 and R_2 into Eq. (1.3), we get,

$$\begin{aligned} I &= \frac{m_1\, m_2}{m_1 + m_2}\, R_e^2, \\ &= \mu\, R_e^2, \end{aligned} \tag{1.5}$$

where μ is the reduced mass of the system.

In rigid rotator approximation, the energies of rotational levels, E_J, can be calculated as,

$$\begin{aligned} E_J &= \frac{\hbar^2}{2\,\mu\, R_e^2}\, J\,(J+1), \\ &= B_e\, J\,(J+1), \end{aligned} \tag{1.6}$$

where $\hbar \left(= \frac{h}{2\pi}\right)$ is the modified Planck's constant, $J\,(=\ 0,\ 1,\ 2,\ \ldots)$ is the rotational quantum number and $B_e \left(= \frac{\hbar^2}{2\,\mu\,R_e^2}\right)$ is the rotational constant of a diatomic molecule at equilibrium bond distance. The energy required to raise a molecule from a state J to a state $(J\ +\ 1)$ is given by [10],

$$\Delta E_J\ =\ E_{J+1}\ -\ E_J\ =\ 2\,B_e\,(J\ +\ 1). \tag{1.7}$$

Thus, the absorption spectrum in the rigid rotator approximation consists of equally spaced lines at $2B_e$, $4B_e$, $6B_e$, ..., in terms of energy units.

For a real molecule, on the other hand, the internuclear position changes from R_e to R, in the rotating molecular reference frame, under the action of a centrifugal force, $|\vec{F_c}|$, which is given by [13, 18],

$$\begin{aligned} |\vec{F_c}|\ &=\ \mu\,\omega^2\,R, \\ &=\ \frac{|\mathbf{J}^2|}{\mu\,R^3}, \qquad\qquad \text{as}\ \ |\mathbf{J}|\ =\ \mu\,R^2\,\omega, \end{aligned} \tag{1.8}$$

with ω being the angular velocity and $\mathbf{J}\left(\ =\ \sqrt{J\,(J\ +\ 1)}\,\hbar\right)$ being the rotational angular momentum of a molecule. The centrifugal force given by Eq. (1.8) is balanced by the restoring force, $|\vec{F_r}|$, around the equilibrium point and therefore,

$$|\vec{F_c}|\ =\ |\vec{F_r}|\ \Longrightarrow\ \frac{|\mathbf{J}^2|}{\mu\,R^3}\ =\ k\,(R\ -\ R_e), \tag{1.9}$$

where k is the force constant. Thus, the rotational energy gets modified as [18],

$$E_J\ =\ \frac{|\mathbf{J}^2|}{2\,\mu\,R^2}\ +\ \frac{1}{2}\,k\,(R\ -\ R_e)^2. \tag{1.10}$$

For $(R - R_e) << R_e$, Eq. (1.9) becomes,

$$(R - R_e) = \frac{|\mathbf{J}^2|}{\mu R^3 k} \cong \frac{|\mathbf{J}^2|}{\mu R_e^3 k}. \tag{1.11}$$

On substituting the value of $(R - R_e)$ from Eq. (1.11) into Eq. (1.10), we obtain,

$$E_J = \frac{|\mathbf{J}^2|}{2\mu R^2} + \frac{1}{2}\frac{|\mathbf{J}^4|}{\mu^2 R_e^6 k}. \tag{1.12}$$

R can be expressed in terms of R_e, from Eq. (1.11), as,

$$R = R_e\left(1 + \frac{|\mathbf{J}^2|}{\mu k R_e^4}\right) = R_e(1 + x), \quad \text{with } x << 1,$$

and therefore, one can write,

$$\frac{1}{R^2} = \frac{1}{R_e^2}\left[1 - \frac{2|\mathbf{J}^2|}{\mu k R_e^4} + 3\left(\frac{|\mathbf{J}^2|}{\mu k R_e^4}\right)^2 - \dots\right]. \tag{1.13}$$

Hence, the energy of a non-rigid rotator given by Eq. (1.12) becomes,

$$\begin{aligned} E_J &= \frac{|\mathbf{J}^2|}{2\mu R_e^2} - \frac{|\mathbf{J}^4|}{2k\mu^2 R_e^6} + \frac{3|\mathbf{J}^6|}{2k^2\mu^3 R_e^{10}} + \dots, \\ &= B_e J(J+1) - \mathcal{D}_e J^2(J+1)^2 + \mathcal{H}_e J^3(J+1)^3 + \dots, \end{aligned} \tag{1.14}$$

where $\mathcal{D}_e$ and $\mathcal{H}_e$ are called centrifugal distortion constants and these are defined via [18],

$$\mathcal{D}_e = \frac{\hbar^4}{2k\mu^2 R_e^6}, \tag{1.15a}$$

and

$$\mathcal{H}_e = \frac{3\hbar^6}{2k^2\mu^3 R_e^{10}}, \tag{1.15b}$$

respectively. The centrifugal distortion constant, $\mathcal{D}_e$, can be shown to be equal to [18],

$$\mathcal{D}_e = \frac{4B_e^3}{\omega_e^2}. \tag{1.16}$$

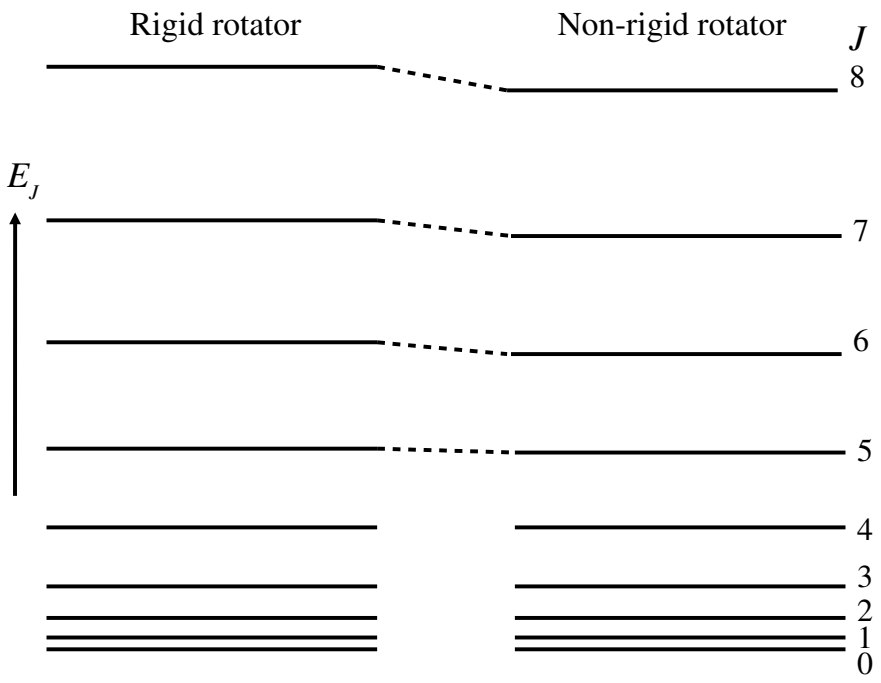

Figure 1.2: Comparison of the rotational energy levels of a rigid and a non - rigid diatomic molecule.

where ω_e is the harmonic frequency of oscillation around the equilibrium point. The change in the energies of rotational levels after evolving from a rigid to a non - rigid diatomic molecule is as shown in Figure (1.2).

1.1.2 The Vibrations of a Diatomic Molecule

In the simple harmonic approximation, it is assumed that the compression and extension of the bond which holds the nuclei together, is equivalent to a vibrating spring with a spring constant, k, as shown in Figure (1.3). It obeys Hooke's law force and the corresponding potential energy, V, of the system is given by,

$$V = \frac{1}{2} k (R - R_e)^2. \tag{1.17}$$

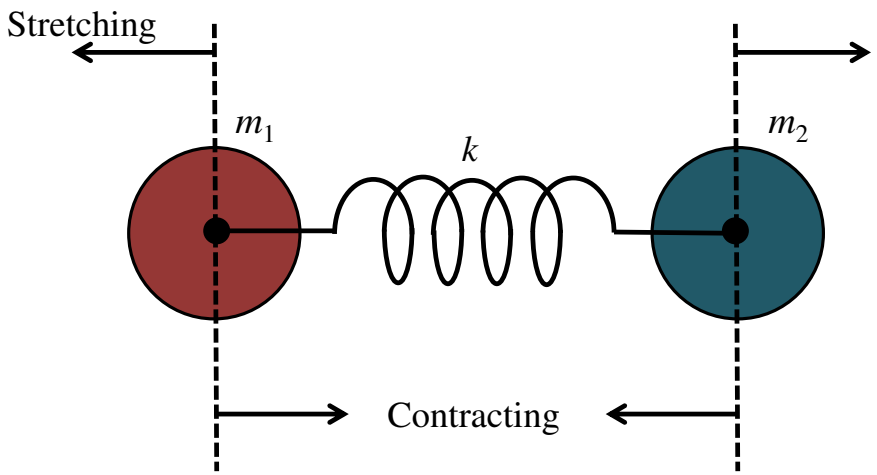

Figure 1.3: Vibrations of a diatomic molecule.

The energy of vibrational levels of a molecular system in the quantum harmonic oscillator approximation is given by,

$$E_v = \left(v + \frac{1}{2}\right) \hbar\omega_e, \tag{1.18}$$

where $v\,(= 0, 1, 2, \ldots)$ is the vibrational quantum number and $\omega_e \left(= \frac{1}{2\pi}\sqrt{\frac{k}{\mu}}\right)$ represents the harmonic frequency of oscillation. The energy corresponding to $v = 0$, *viz.*, $E_0 = \frac{1}{2}\hbar\omega_e$ is called zero point energy of a molecule in the harmonic approximation. It never being zero indicates that the atoms bound in a molecule are always in motion with respect to each other.

For a realistic molecule, on the other hand, if a bond between the two atoms is stretched too far, the molecule will dissociate into constituent atoms at a particular distance known as the dissociation limit. At this point, the force constant is zero and any further increase in R does not change the potential energy of a system. Hence,

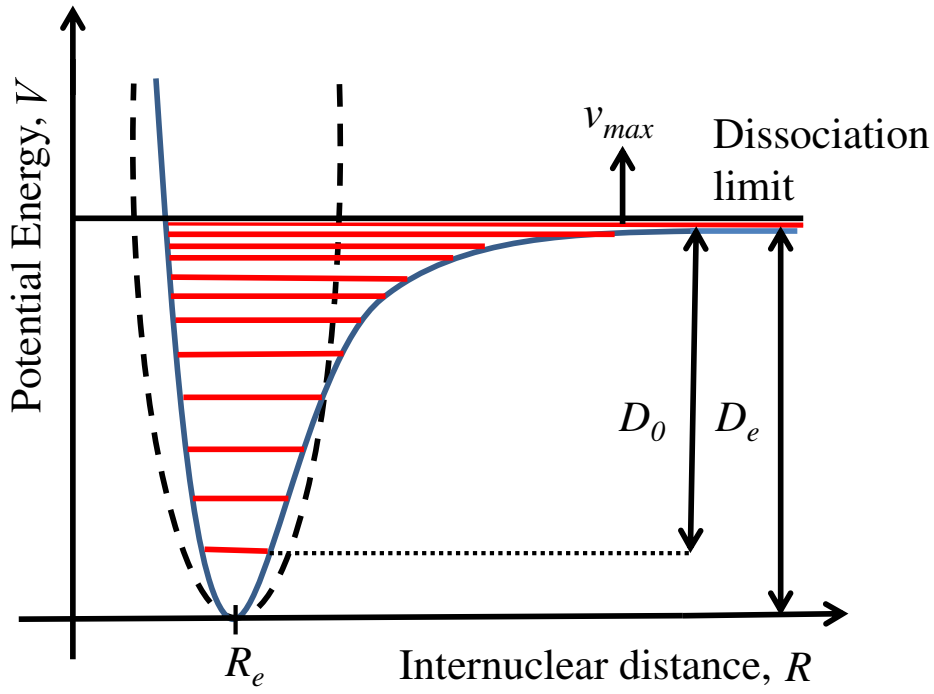

Figure 1.4: Potential energy curve and energy levels of a diatomic molecule behaving as an anharmonic oscillator, together with the ideal simple harmonic parabola (shown by dashed curve).

the potential energy curve (PEC) flattens out at $V = D_e$, where D_e is the equilibrium dissociation energy[2] measured with respect to the potential energy at $R = R_e$, as shown in Figure (1.4). The comparison of PEC for a real molecule (solid blue) with the parabolic (dashed black) curve due to harmonic oscillator approximation is also shown in Figure (1.4). The deviations in the PEC for a real molecule from the one resulting from the harmonic oscillator approximation are due to anharmonic effects. The empirical expression to define the anharmonic motion was given by P.

[2]However, the true dissociation energy of any molecule is equal to

$$D_0 = D_e - ZPE, \tag{1.19}$$

where ZPE is zero point energy, the vibrational energy, E_v, as in Eq. (1.21), in the limit $v = 0$.

M. Morse and is called the *Morse potential* [13],

$$V \,=\, D_e \left(1 \,-\, exp\left[\,-\, a\,(R \,-\, R_e)\right]\right)^2, \tag{1.20}$$

where 'a' is a positive constant for a given molecule having dimensions of inverse distance. The energies of the vibrational levels corresponding to the Morse potential are given by,

$$E_v \,=\, \left(v \,+\, \frac{1}{2}\right) \hbar\,\omega_e \,-\, \left(v \,+\, \frac{1}{2}\right)^2 \hbar\,\omega_e\,x_e, \tag{1.21}$$

where x_e is the anharmonicity constant corresponding to quadratic term of vibrational energy, which is positive and small. It is related to D_e and ω_e as [11, 17],

$$\omega_e\,x_e \,=\, \frac{\hbar\,\omega_e^2}{4\,D_e}. \tag{1.22}$$

The more general expression for the vibrational energy, however, is written as a power series in $\left(v \,+\, \frac{1}{2}\right)$ as [18],

$$E_v \,=\, \left(v \,+\, \frac{1}{2}\right) \hbar\,\omega_e - \left(v \,+\, \frac{1}{2}\right)^2 \hbar\,\omega_e\,x_e + \left(v \,+\, \frac{1}{2}\right)^3 \hbar\,\omega_e\,y_e - \left(v \,+\, \frac{1}{2}\right)^4 \hbar\,\omega_e\,z_e + \ldots, \tag{1.23}$$

where y_e and z_e represent the anharmonicity constants corresponding to cubic and quartic terms of vibrational energy with a rapidly decreasing magnitude. Hence, these higher - order terms are dropped in the current work. The analytic expression for the potential corresponding to this general expression for energy, however, is not available.

The energy difference between the two neighbouring vibrational levels when only the leading order anharmonic term is considered, is given by,

$$\Delta E_v \,=\, E_{v+1} \,-\, E_v,$$

$$= \hbar\,\omega_e\big[1 - 2\,x_e\,(v + 1)\big]. \tag{1.24}$$

As one moves towards the higher vibrational levels, the relative spacing between the adjacent levels decreases due to the anharmonic effects and $\Delta E_v \rightarrow 0$ at the dissociation limit. Therefore, the maximum number of vibrational levels, v_{max}, can be calculated using [10],

$$\begin{aligned} \hbar\,\omega_e\big[1 - 2\,x_e\,(v + 1)\big] &= 0, \\ \implies v_{max} &= \frac{1}{2x_e} - 1. \end{aligned} \tag{1.25}$$

On substituting the value of x_e from Eq. (1.22) into Eq. (1.25), we obtain,

$$v_{max} = \frac{2\,D_e}{\hbar\,\omega_e} - 1. \tag{1.26}$$

1.1.3 Diatomic Molecule as a Vibrating Rotator

The diatomic molecule must be considered as a vibrating rotator as it completes several vibrational periods (typically 10 - 100) during a full single rotation, as shown in Figure (1.5) [18]. The energy of a vibrating rotator molecule can be calculated as the sum of the energies of anharmonic oscillator and non - rigid rotator when the coupling between the vibrational and rotational motion is ignored. It is defined upto leading order terms in anharmonicity and centrifugal distortion, as below:

$$E_v + E_J = \hbar\,\omega_e\left(v + \frac{1}{2}\right) - \hbar\,\omega_e\,x_e\left(v + \frac{1}{2}\right)^2 + B_e\,J\,(J + 1) - \mathcal{D}_e\,J^2\,(J + 1)^2. \tag{1.27}$$

It has, however, been observed that as one move towards higher 'v', the rotational constant of a system decreases due to the coupling between vibrational and rotational motion. Therefore, the vibrationally coupled rotational constant associated with a particular 'v' is denoted as B_v and it is related to the equilibrium rotational constant,

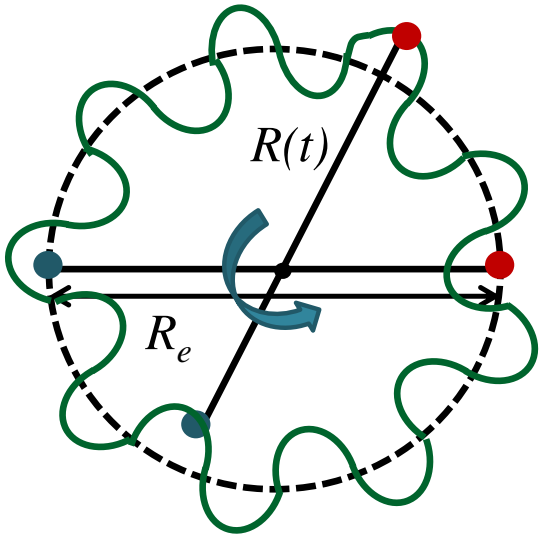

Figure 1.5: Vibrating rotator.

B_e, (for a diatomic molecule) as [13, 17],

$$B_v = B_e - \alpha_e \left(v + \frac{1}{2}\right) + \dots . \tag{1.28}$$

Similarly,

$$\mathcal{D}_v = \mathcal{D}_e - \beta_e \left(v + \frac{1}{2}\right) + \dots , \tag{1.29}$$

where α_e and β_e are small positive constants that depend on the shape of the PEC.

Within a given electronic state, as one moves from the lowest bound vibrational state that lies near the minima of a PEC to the highest vibrational state at the dissociative limit, the relative energy spacing between the vibrational states decreases from few 1000 cm^{-1} to $\sim$ 1 cm^{-1}. Further, a single vibrational state contains several rotational states with energy spacing typically increases from 1 cm^{-1} to $\sim$ 100 cm^{-1} as one moves from the lowest to the highest rotational state. A vibrational transition, therefore, is accompained by a change in rotational levels. The selection rules for the

ro - vibrational transitions, in general, are [10, 11],

$$\begin{aligned} \Delta v &= \pm 1, \pm 2, \pm 3, \ldots, \\ \Delta J &= \pm 1. \end{aligned} \tag{1.30}$$

The rotational transitions corresponding to $\Delta J = +1$ and $\Delta J = -1$ give the set of lines called R - branch and P - branch, respectively. The energies of these lines can be obtained by applying the selection rules $\Delta J = \pm 1$ to the energy expression given by Eq. (1.27) for $B_e = B_v$ and $D_e = D_v$. By considering the transition from (v'', J'') to (v', J'), we have,

$$\begin{aligned} E^R &= \hbar\,\omega_e\,(v' - v'')\,[1 - x_e\,(v' + v'' + 1)] + 2B_{v'} - 4\,\mathcal{D}_{v'} + J''^4\,(\mathcal{D}_{v''} - \mathcal{D}_{v'}) \\ &\quad + 2\,J''^3\,(\mathcal{D}_{v''} - 3\,\mathcal{D}_{v'}) + J''^2\,(B_{v'} - B_{v''} + \mathcal{D}_{v''} - 13\,\mathcal{D}_{v'}) \\ &\quad + J''\,(3B_{v'} - B_{v''} - 12\,\mathcal{D}_{v'}), \\ &\qquad\qquad \text{for } \Delta J \equiv J' - J'' = +1, \end{aligned} \tag{1.31}$$

and

$$\begin{aligned} E^P &= \hbar\,\omega_e\,(v' - v'')\,[1 - x_e\,(v' + v'' + 1)] + J''^4\,(\mathcal{D}_{v''} - \mathcal{D}_{v'}) + 2\,J''^3\,(\mathcal{D}_{v''} + \mathcal{D}_{v'}) \\ &\quad + J''^2\,(B_{v'} - B_{v''} + \mathcal{D}_{v''} - \mathcal{D}_{v'}) - J''\,(B_{v'} + B_{v''}), \\ &\qquad\qquad \text{for } \Delta J \equiv J' - J'' = -1, \end{aligned} \tag{1.32}$$

where $(v'',\ J'')$ and $(v',\ J')$ represent the quantum numbers of lower and upper state, respectively, and ω_e is the energy of the harmonic vibrational transition with $J' = J'' = 0$. The rotational transition lines corresponding to R - branch and P - branch are labelled according to the J values of lower state as $R(J'')$ and $P(J'')$, respectively. The pictorial representation of the vibrational - rotational transitions is depicted in Figure (1.6).

If the component of the orbital angular momentum quantum number along the in-

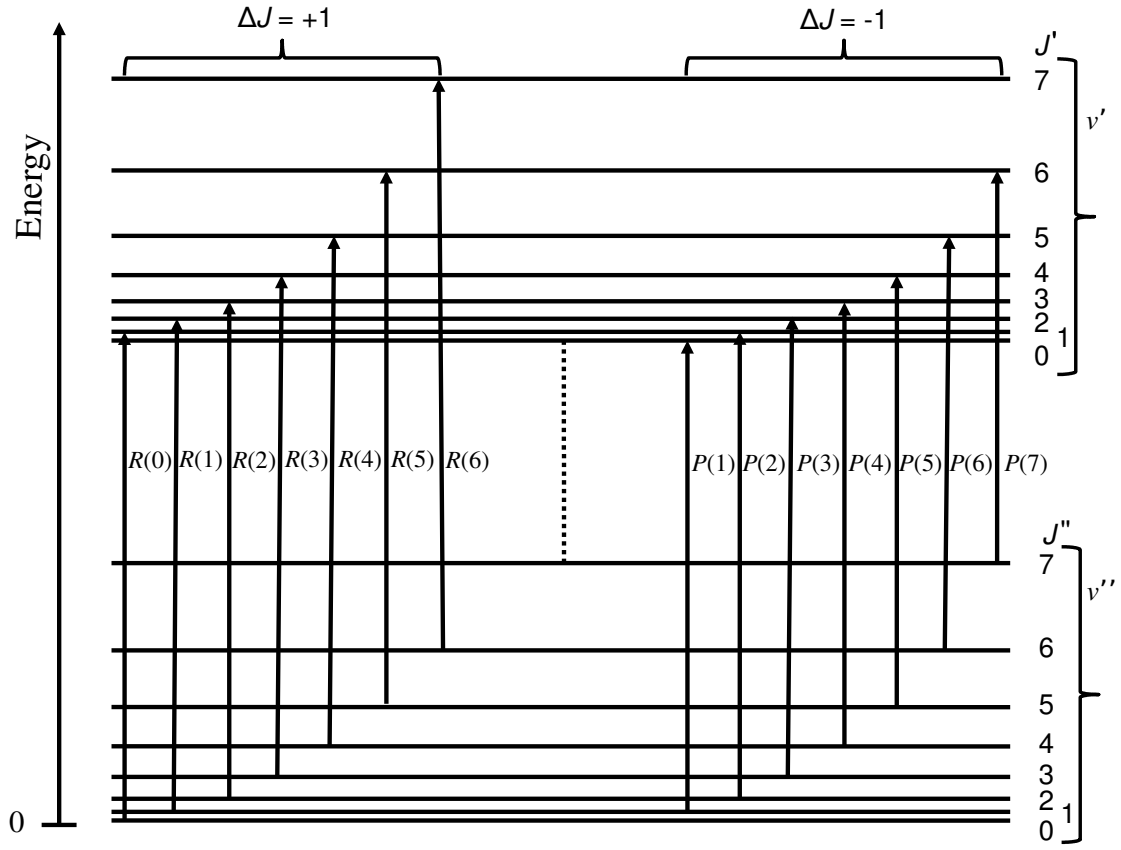

Figure 1.6: The vibrational - rotational absorption spectrum arising due to the transitions from (v'', J'') to (v', J').

ternuclear axis is non - zero, (i.e., $\Lambda \neq 0$, non - Σ states), there exists an additional branch in the vibrational - rotational spectrum. This branch, called Q - branch, arises due to the rotational transitions with the selection rule $\Delta J = 0$. The energies of transition lines corresponding to the Q - branch are given by,

$$E^Q = \hbar\omega_e (v' - v'') [1 - x_e (v' + v'' + 1)] + (J''^4 + 2J''^3)(\mathcal{D}_{v''} - \mathcal{D}_{v'}) + J''^2 (B_{v'} - B_{v''} + \mathcal{D}_{v''} - \mathcal{D}_{v'}) + J''(B_{v'} - B_{v''}), \quad \text{for } J' = J''. \tag{1.33}$$

1.1.4 Electric Properties of Molecules

The electrostatic potential, $\varphi^{\rho}(\vec{r'})$, at a point $\vec{r'}$ due to a continuous charge distribution with charge density $\rho(\vec{r})$ is given by [14],

$$\varphi^{\rho}(\vec{r'}) = \frac{1}{4\pi\epsilon_0} \int_{\vec{r}} \frac{\rho(\vec{r})}{|\,\vec{r'} - \vec{r}\,|}\, d\vec{r}, \tag{1.34}$$

where $\rho(\vec{r})$ is the charge density and $d\vec{r} = dx\, dy\, dz$ is the volume element. An alternative expression for the electrostatic potential (which is often used in the calculations) is derived using the Taylor series expansion of $\dfrac{1}{|\,\vec{r'} - \vec{r}\,|}$ about $\vec{r} = \vec{r}_o$ is given by,

$$\begin{aligned}\frac{1}{|\,\vec{r'} - \vec{r}\,|} &= \frac{1}{|\vec{r'} - \vec{r}_o|} + \sum_{\alpha} \left(\frac{\partial}{\partial r_\alpha} \frac{1}{|\,\vec{r'} - \vec{r}\,|}\right)_{\vec{r}=\vec{r}_o} (r_\alpha - r_{o,\alpha}) \\ &+ \frac{1}{2} \sum_{\alpha\beta} \left(\frac{\partial^2}{\partial r_\alpha \partial r_\beta} \frac{1}{|\,\vec{r'} - \vec{r}\,|}\right)_{\vec{r}=\vec{r}_o} (r_\alpha - r_{o,\alpha})\,(r_\beta - r_{o,\beta}) \\ &+ \ldots .\end{aligned} \tag{1.35}$$

The subscripts α and β represent Cartesian components. On substituting the above Taylor series expansion into Eq. (1.34), we get,

$$\begin{aligned}\varphi^{\rho}(\vec{r'}) = \frac{1}{4\pi\epsilon_0} \Bigg[&\frac{1}{|\,\vec{r'} - \vec{r}_o\,|} \int_{\vec{r}} \rho(\vec{r}) d\vec{r} \\ &+ \sum_{\alpha} \left(\frac{\partial}{\partial r_\alpha} \frac{1}{|\,\vec{r'} - \vec{r}\,|}\right)_{\vec{r}=\vec{r}_o} \int_{\vec{r}} \rho(\vec{r})\,(r_\alpha - r_{o,\alpha})\, d\vec{r} \\ &+ \frac{1}{2} \sum_{\alpha\,\beta} \left(\frac{\partial^2}{\partial r_\alpha \partial r_\beta} \frac{1}{|\,\vec{r'} - \vec{r}\,|}\right)_{\vec{r}=\vec{r}_o} \int_{\vec{r}} \rho(\vec{r})\,(r_\alpha - r_{o,\alpha})\,(r_\beta - r_{o,\beta})\, d\vec{r} \\ &+ \ldots \Bigg],\end{aligned} \tag{1.36}$$

$$\varphi^{\rho}(\vec{r'}) = \frac{1}{4\pi\epsilon_0} \left[\frac{1}{|\,\vec{r'} - \vec{r}_o\,|}\, q + \sum_{\alpha} \left(\frac{\partial}{\partial r_\alpha} \frac{1}{|\,\vec{r'} - \vec{r}\,|}\right)_{\vec{r}=\vec{r}_o} \mu_\alpha \right.$$

$$+\frac{1}{2}\sum_{\alpha\,\beta}\left(\frac{\partial^2}{\partial r_\alpha \partial r_\beta}\,\frac{1}{|\,\vec{r'}\,-\,\vec{r}\,|}\right)_{\vec{r}=\vec{r}_o} Q_{\alpha\,\beta}\,+\,\ldots\Bigg], \tag{1.37}$$

where,

$$q\;=\;\int_{\vec{r}}\rho(\vec{r})\,d\vec{r}\quad\text{is the total charge,} \tag{1.38a}$$

$$\mu_\alpha(\vec{r}_o)\;=\;\int_{\vec{r}}\rho(\vec{r})\,(r_\alpha\,-\,r_{o,\,\alpha})\;d\vec{r}\quad\text{is the electric dipole moment,} \tag{1.38b}$$

and

$$Q_{\alpha\beta}(\vec{r}_o)\;=\;\int_{\vec{r}}\rho(\vec{r})\;(r_\alpha\,-\,r_{o,\,\alpha})\;(r_\beta\,-\,r_{o,\,\beta})\;d\vec{r}\quad\text{is the quadrupole} \tag{1.38c}$$

moment (QM, *viz.*, second - order electric moment) tensor.

Further, the traceless[3] QM tensor, $\Theta_{\alpha\beta}$, can be defined as,

$$\Theta_{\alpha\beta}(\vec{r}_o)\;=\;\frac{1}{2}\int_{\vec{r}}\Big[3\,(r_\alpha-r_{o,\,\alpha})\,(r_\beta-r_{o,\,\beta})\;-\;\delta_{\alpha\beta}\,(\vec{r}\;-\;\vec{r}_o)^2\Big]\,\rho(\vec{r})\,d\vec{r}. \tag{1.39}$$

The electric field in molecules is generated due to the charges of the electrons as well as the nuclei. In the Born - Oppenheimer approximation (BOA)[4], the charge distribution due to the electrons, $\rho_{el}\,(\vec{r}\,)$, is continuous, whereas the nuclei form a discrete charge distribution, $\rho_N\,(\vec{R}_A)$. Therefore, the α - component of the permanent dipole moment for the molecules is gives as [14],

$$\mu_\alpha(\vec{r_o})\;=\;\int_{\vec{r}}(r_\alpha\,-\,r_{o,\,\alpha})\,\rho_{el}(\vec{r})\,d\vec{r}\,+\,\sum_A Z_A\,e\,(R_{A,\,\alpha}\,-\,r_{o,\,\alpha}), \tag{1.40}$$

where $Z_A\,e$ is the charge on the nucleus located at $\vec{R}_A$.

[3]The sum of diagonal components is zero, i.e., $\sum_\alpha \Theta_{\alpha\alpha}\;=\;0$.

[4]This approximation is discussed in Chapter 2.

In quantum mechanics, the charge density due to n-electrons is defined as,

$$\rho_{el}(\vec{r}) \;=\; -e\left\langle \Psi_0 \,\middle|\, \sum_i^n \delta(\vec{r_i} \,-\, \vec{r}) \,\middle|\, \Psi_0 \right\rangle. \tag{1.41}$$

Hence,

$$\begin{aligned}
\mu_\alpha(\vec{r_o}) \;&=\; \int_{r_\alpha} (r_\alpha \,-\, r_{o,\alpha})\,(-e)\left\langle \Psi_0 \middle| \sum_i^n \delta(r_{i,\alpha} \,-\, r_{o,\alpha}) \middle| \Psi_0 \right\rangle dr_\alpha \,+\, \sum_A Z_A\, e\,(R_{A,\alpha} \,-\, r_{o,\alpha}), \\
&=\; \left\langle \Psi_0 \middle| -\, e \sum_i^n (r_{i,\alpha} \,-\, r_{o,\alpha}) \middle| \Psi_0 \right\rangle \,+\, \sum_A Z_A\, e\,(R_{A,\alpha} \,-\, r_{o,\alpha}), \\
&=\; (\mu_{el})_\alpha \,+\, (\mu_{nucl})_\alpha,
\end{aligned} \tag{1.42}$$

where $(\mu_{el})_\alpha$ and $(\mu_{nucl})_\alpha$ represent the electronic and nuclear contributions to the total dipole moment, respectively.

Similarly, the quantum mechanical expressions for $Q_{\alpha\beta}$ and $\Theta_{\alpha\beta}$ are [14],

$$\begin{aligned}
Q_{\alpha\beta}(\vec{r_o}) \;=\; &\left\langle \Psi_0 \middle| -\, e \sum_i^n (r_{i,\alpha} \,-\, r_{o,\alpha})\,(r_{i,\beta} \,-\, r_{o,\beta}) \middle| \Psi_0 \right\rangle \\
&+\, \sum_A Z_A\, e\,(R_{A,\alpha} \,-\, r_{o,\alpha})\,(R_{A,\beta} \,-\, r_{o,\beta}),
\end{aligned} \tag{1.43}$$

and

$$\begin{aligned}
\Theta_{\alpha\beta}(\vec{r_o}) \;=\; &\frac{1}{2}\left\langle \Psi_0 \middle| -\, e \sum_i^n 3\,(r_{i,\alpha} \,-\, r_{o,\alpha})\,(r_{i,\beta} \,-\, r_{o,\beta}) \,-\, \delta_{\alpha\beta}\,(\vec{r_i} \,-\, \vec{r_o})^2 \middle| \Psi_0 \right\rangle \\
&+\, \frac{1}{2}\sum_A Z_A\, e\Big[3\,(R_{A,\alpha} \,-\, r_{o,\alpha})\,(R_{A,\beta} \,-\, r_{o,\beta}) \,-\, \delta_{\alpha\beta}\,(\vec{R}_A \,-\, \vec{r_o})^2\Big],
\end{aligned} \tag{1.44}$$

respectively.

It has been suggested by Diercksen *et al.* [19] that the finite-field approach should be taken as the "legitimate" method to perform the electric property calculations

that are directly related to experimentally measurable quantities. Therefore, we have described this method briefly below.

Finite - Field Method

In the presence of an external electric field, $\vec{\varepsilon}$, and the field gradients, $\tilde{\varepsilon}$, the energy $E(\vec{\varepsilon}, \tilde{\varepsilon})$ of a system can be written as a Taylor expansion [20],

$$E\,(\vec{\varepsilon},\,\tilde{\varepsilon}\,) \;=\; q\,\varphi^{\varepsilon}\,(\vec{r}_o) \;-\; \sum_{\alpha} \mu_{\alpha}(\vec{r}_o)\,\varepsilon_{\alpha}(\vec{r}_o) \;-\; \frac{1}{3}\sum_{\alpha\,\beta} \Theta_{\alpha\,\beta}(\vec{r}_o)\,\varepsilon_{\alpha\beta}(\vec{r}_o) \;+\; \ldots, \quad (1.45)$$

where,

$$\mu_{\alpha}(\vec{r}_o) \;=\; -\left.\frac{\partial E}{\partial \varepsilon_{\alpha}(\vec{r}_o)}\right|_{\vec{\varepsilon}=0}, \quad (1.46)$$

and

$$\Theta_{\alpha\,\beta}(\vec{r}_o) \;=\; -\,3\left.\frac{\partial E}{\partial \varepsilon_{\alpha\,\beta}(\vec{r}_o)}\right|_{\tilde{\varepsilon}=0}. \quad (1.47)$$

If z - axis is considered as the internuclear axis of a molecule, then the z - component of the QM (Θ_{zz}) can be expressed as the negative sum of other diagonal components as,

$$\Theta_{zz} \;=\; -\,(\Theta_{xx} \;+\; \Theta_{yy}). \quad (1.48)$$

Further, $\Theta_{xx} \;=\; \Theta_{yy}$ for a linear molecule which has a cylindrical symmetry about the internuclear axis, and therefore,

$$\Theta_{zz} \;=\; -2\,\Theta_{xx}. \quad (1.49)$$

Further, dipole polarizability (DP, $\alpha_{\alpha\beta}$), which is a second - rank tensor can be calculated as,

$$\alpha_{\alpha\beta} \;\equiv\; \left.\frac{\partial \mu_{\alpha}}{\partial \varepsilon_{\beta}}\right|_{\vec{\varepsilon}=0} \;\equiv\; \left.\frac{\partial^2 E}{\partial \varepsilon_{\alpha}\partial \varepsilon_{\beta}}\right|_{\vec{\varepsilon}=0}. \quad (1.50)$$

By calculating parallel ($\alpha_{\parallel} \equiv \alpha_{zz}$) and perpendicular components ($\alpha_{\perp} \equiv \alpha_{xx} \equiv \alpha_{yy}$), one can calculate the average ($\bar{\alpha}$) and the anisotropic (γ) polarizabilities, respectively, through the equations,

$$\bar{\alpha} = \frac{(\alpha_{\parallel} + 2\,\alpha_{\perp})}{3}, \tag{1.51}$$

and

$$\gamma = (\alpha_{\parallel} - \alpha_{\perp}). \tag{1.52}$$

The finite - field method discussed above comes with some disadvantages though, such as [21],

(i) As the electric properties in this method are calculated using the numerical differentiation of the energy with respect to the external perturbation, the accuracy of energy calculations should be much higher than usual. This then becomes computationally expensive.

(ii) To calculate each property, one has to perform at least two (or more) separate energy calculations with different electric field strengths at the SCF and also, at the correlation level. In contrast, computations of the property using the expectation value method requires only single calculation using the unperturbed Hamiltonian. Hence, the finite - field method increases the computational cost several fold.

1.1.5 Electronic Quantum Numbers

The most suitable coupling scheme to designate the electronic states for diatomic molecules is that which is equivalent to the Russell - Saunders scheme for atoms [12]. If there is no heavy nucleus available in the molecule or in other words, when the spin - orbit interaction is weak, the orbital angular momentum, **L**, gets strongly coupled to the internuclear axis by the electrostatic field created by the nuclei[5]. Hence,

[5]This situation is referred to Hund's coupling case (a), as shown in Figure (1.7) [11, 12, 15].

L is no longer a good quantum number, while the component of **L** along the internuclear axis, i.e., $\Lambda = \left|\sum_{i=1}^{n} m_l(i)\right| = |M_l|$, is a good quantum number [11, 12]. The symbol m_l represents the projection of orbital angular momentum of an electron and M_l represents the projection of total electronic orbital angular momentum of an n-electron diatomic molecule on the molecular/symmetry axis. In this scenario, the molecular orbitals are labeled as σ, π, δ, ..., corresponding to the values of $|m_l| = 0, 1, 2, \ldots$, while the molecular electronic states are designated by the symbols Σ, Π, Δ, Φ, ... corresponding to the positive integer values of $\Lambda = 0, 1, 2, 3, \ldots$.

The spin angular momentum, **S**, on the other hand, is not coupled with the electrostatic field but with the magnetic field component along the internuclear axis due

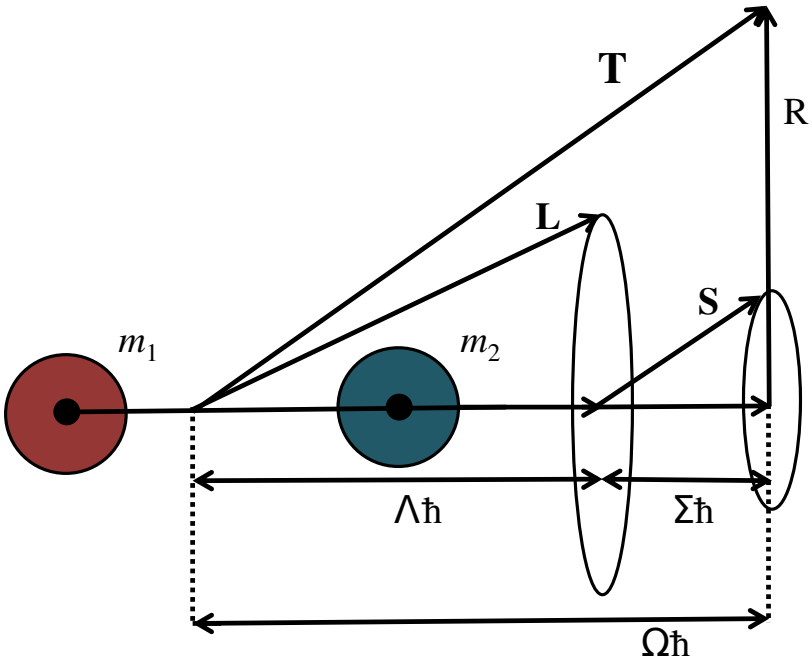

Figure 1.7: Hund's coupling case (a).

to the orbital motion of the electrons. The projection of **S** along the internuclear

axis, i.e., Σ[6], can take the values,

$$\Sigma = S, S-1, \ldots, -S.$$

The multiplicity of any molecular state is specified by $(2S+1)$ and is represented by an upper left prefix to the electronic state symbol. As an example, consider electrons in the π ($m_l = \pm 1$) and δ ($m_l = \pm 2$) orbitals, such that the total orbital angular momentum projection, $\Lambda = 1$ or 3. For such a scenario, the molecular state symbol would be either Π or Φ. Further, if the spins of the two electrons are parallel (anti-parallel), the state is designated as $^3\Pi$ or $^3\Phi$ ($^1\Pi$ or $^1\Phi$).

For the same set of quantum numbers: S and Λ, the molecular states can be distinguished by the prefixes X[7], 2, 3, ..., in the order of increasing energies.

The projection of total angular momentum along the symmetry axis is equal to the sum of the projections of **L** and **S** in Hund's coupling case (a) and it is given as,

$$\Omega = |\Lambda + \Sigma|.$$

Thus, the term symbol for molecules is $^{2S+1}\Lambda_\Omega$.

On the other hand, if there is at least one heavy nucleus present in the molecule, the spin - orbit interaction is sufficiently large. Due to this large spin - orbit coupling, **L** and **S** can not be decoupled by the electrostatic field of the nuclei and hence, the total angular momentum $\mathbf{T}\,(= \mathbf{L} + \mathbf{S})$ couples directly to the molecular axis. This coupling scheme is referred to as Hund's coupling case (c)[8] as shown in Figure (1.8), where Λ and Σ are not good quantum numbers, while Ω is.

[6]This Σ is different from the electronic state symbol corresponding to $\Lambda = 0$.

[7]By convention, the electronic ground state is labeled with the prefix X.

[8]Here, we have not discussed the Hund's coupling cases (b) and (d), as they are not common in practice. However, one can find the details of these cases in Refs. [11, 15].

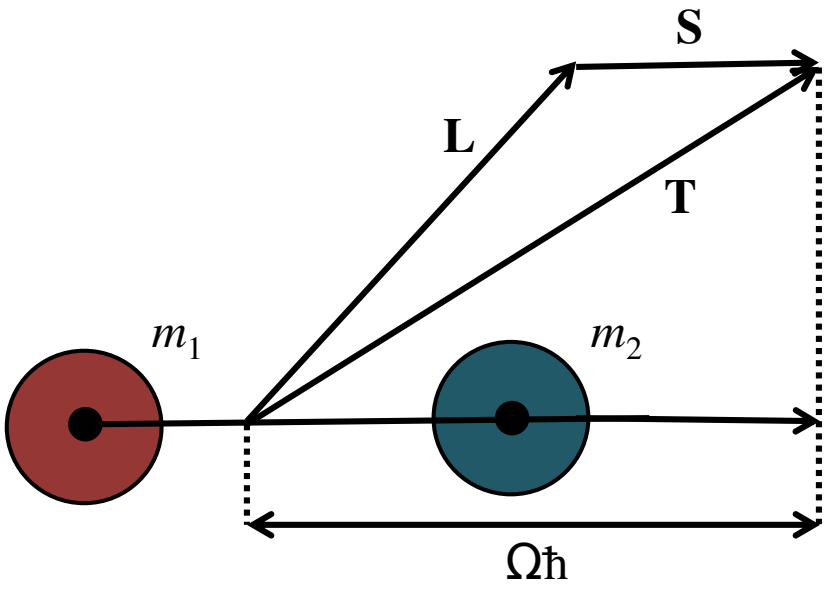

Figure 1.8: Hund's coupling case (c).

Apart from the electronic angular momentum quantum numbers, one may need one (for heteronuclear) or two (for homonuclear) additional symmetries: reflection $(+/-)$ and inversion (g/u: *gerade/ungerade*), to define the wavefunction of a diatomic molecule. All linear diatomic molecules have a plane containing the molecular axis and the nuclei, which is known as the *plane of symmetry*. The electronic wavefunction may either be symmetric $(+)$ or anti-symmetric $(-)$ with respect to such reflection. Hence, this reflection symmetry is applicable to all linear diatomic molecules. In contrast, the inversion symmetry is relevant only for homonuclear diatomic molecules such as Be_2, Li_2 etc. This symmetry is associated with the inversion of coordinates of all electrons through the origin located at the center-of-mass. Therefore, this symmetry is known as the *center of inversion symmetry*.

This thesis comprises of the structural studies of heteronuclear diatomic molecules and they possess cylindrical symmetry about the internuclear axis. There are infinite

rotations about C_∞ axis[9] and reflections in the vertical planes[10] (σ_v). Hence, these molecules belong to the $C_{\infty v}$ point group. However, we have made use of C_2 and C_{2v} symmetry to carry out the *ab initio* calculations reported in this thesis. The character tables of C_2 and C_{2v} groups are given by Table (1.1) and Table (1.2),

Table 1.1: Character table of C_2 point group symmetry.

C_2	E	C_2	linear functions, rotations	quadratic functions
A	1	1	z, R_z	x^2, y^2, z^2, xy
B	1	-1	x, y, R_x, R_y	xz, yz

Table 1.2: Character table of C_{2v} point group symmetry.

C_{2v}	E	C_2	$\sigma_v(xz)$	$\sigma_v^{'}(yz)$	linear functions, rotations	quadratic functions
A_1	1	1	1	1	z	x^2, y^2, z^2
A_2	1	1	-1	-1	R_z	xy
B_1	1	-1	1	-1	x, R_y	xz
B_2	1	-1	-1	1	y, R_x	yz

respectively [22, 23]. The symmetry element E is the identity operation that leaves the molecule unchanged; C_2 is a twofold symmetry axis; $\sigma_v(xz)$ and $\sigma_v^{'}(yz)$ represent the reflection symmetry with respect to xz and yz planes. The symmetry labels A (B) in the first column of Table (1.1) and Table (1.2) indicate symmetry (antisymmetry) with respect to the C_2 operation, and the subscripts 1 (2) to the symmetry labels A and B in Table (1.2) indicate symmetry (antisymmetry) with respect to the reflection operation about xz plane, $\sigma_v(xz)$. Some additional details on the molecular symmetries and symmetry groups are discussed in Appendix A.

[9] Rotation by any angle about this axis produces an identical configuration.
[10] A plane containing principal axis is known as vertical plane.

1.1.6 Selection Rules for Electronic Transitions

In BOA, consider two electronic states of a diatomic molecule which are given by [17],

$$\left|\Psi'(\vec{r},\vec{R}\,)\right\rangle \;=\; \left|\Psi'_{el}(\vec{r};\vec{R}\,)\right\rangle \left|\Psi_{v'}(\vec{R}\,)\,\Psi_{J'}(\vec{R}\,)\right\rangle, \tag{1.53a}$$

and

$$\left|\Psi''(\vec{r},\vec{R}\,)\right\rangle \;=\; \left|\Psi''_{el}(\vec{r};\vec{R}\,)\right\rangle \left|\Psi_{v''}(\vec{R}\,)\,\Psi_{J''}(\vec{R}\,)\right\rangle, \tag{1.53b}$$

where Ψ_{el} is the electronic wavefunction, Ψ_v is the vibrational wavefunction and Ψ_J is the rotational wavefunction. The wavefunctions with single prime ($'$) correspond to the upper state, while the wavefunctions with double prime ($''$) correspond to the lower state.

The dipole matrix element corresponding to the $E1$ transitions, if the molecular rotation is ignored, can be written as[11],

$$\begin{aligned}
\left\langle \Psi'(\vec{r},\vec{R}\,)\,\middle|\,\vec{\mu}\,\middle|\,\Psi''(\vec{r},\vec{R}\,)\right\rangle \;&=\; \left\langle \Psi'_{el}(\vec{r};\vec{R}\,)\,\Psi_{v'}(\vec{R}\,)\,\middle|\,\vec{\mu}\,\middle|\,\Psi''_{el}(\vec{r};\vec{R}\,),\Psi_{v''}(\vec{R}\,)\right\rangle, \\
&=\; \left\langle \Psi'_{el}(\vec{r};\vec{R}\,)\,\Psi_{v'}(\vec{R}\,)\,\middle|\,\vec{\mu}_{el}\;+\;\vec{\mu}_{nucl}\,\middle|\,\Psi''_{el}(\vec{r};\vec{R}\,)\,\Psi_{v''}(\vec{R}\,)\right\rangle, \text{ from Eq. (1.42)} \\
&=\; \left\langle \Psi'_{el}(\vec{r};\vec{R}\,)\,\middle|\,\Psi''_{el}(\vec{r};\vec{R}\,)\right\rangle \left\langle \Psi_{v'}(\vec{R}\,)\,\middle|\,\vec{\mu}_{nucl}\,\middle|\Psi_{v''}(\vec{R}\,)\right\rangle \\
&+\; \left\langle \Psi'_{el}(\vec{r};\vec{R}\,)\,\Psi_{v'}(\vec{R}\,)\,\middle|\,\vec{\mu}_{el}\,\middle|\Psi''_{el}(\vec{r};\vec{R}\,)\Psi_{v''}(\vec{R}\,)\right\rangle.
\end{aligned} \tag{1.54}$$

As the electronic states are orthogonal to each other, the first term in the above equation is equal to zero and the matrix element in second term becomes,

$$\int d\vec{R}\,\Psi^*_{v'}(\vec{R}\,)\,\Psi_{v''}(\vec{R}\,)\int d\vec{r}\,\Psi'^*_{el}(\vec{r};\vec{R}\,)\,\vec{\mu}_{el}\,\Psi''_{el}(\vec{r};\vec{R}\,) \;\equiv\; \int d\vec{R}\,\Psi^*_{v'}(\vec{R}\,)\,\Psi_{v''}(\vec{R}\,)\,M_e(\vec{R}\,). \tag{1.55}$$

where $M_e(\vec{R}\,)$ represents the electronic transition moment function. It is assumed that the variation of $M_e(\vec{R}\,)$ with the bond distance, $\vec{R}$, is slow and therefore, $M_e(\vec{R}\,)$

[11]The details of selection rules presented in the subsection (1.1.6) are taken mostly from Ref. [17].

can be approximated by its average value. Hence, Eq. (1.54) becomes,

$$\begin{aligned} \left\langle \Psi'(\vec{r},\vec{R}\,) \,\middle|\, \vec{\mu} \,\middle|\, \Psi''(\vec{r},\vec{R}\,) \right\rangle &= \overline{M_e(\vec{R}\,)} \int d\vec{R}\, \Psi^*_{v'}(\vec{R}\,)\, \Psi_{v''}(\vec{R}\,), \\ &= \overline{M_e(\vec{R}\,)}\, \langle\, v' \,|\, v'' \,\rangle, \end{aligned} \tag{1.56}$$

where $\overline{M_e(\vec{R}\,)}$ is the average of electronic transition moment function. The electronic transition probability is then given by,

$$\left| \left\langle \Psi'(\vec{r},\vec{R}\,) \,\middle|\, \vec{\mu} \,\middle|\, \Psi''(\vec{r},\vec{R}\,) \right\rangle \right|^2 = \left| \overline{M_e(\vec{R}\,)} \right|^2 \left| \langle\, v' \,|\, v'' \,\rangle \right|^2, \tag{1.57}$$

where $\left| \langle\, v' \,|\, v'' \,\rangle \right|^2$ is called the *Franck - Condon Factor* (FCF).

For the electronic transition matrix element, $M_e(\vec{R}\,) = \left\langle \Psi'_{el} \,\middle|\, \vec{\mu}_{el} \,\middle|\, \Psi''_{el} \right\rangle$, to be non - zero, it is necessary for the direct product of irreducible representations (IRs)

$$\Gamma(\Psi'_{el}) \otimes \Gamma(\vec{\mu}_{el}) \otimes \Gamma(\Psi''_{el}) \tag{1.58}$$

to contain totally symmetric IR, i.e., Σ^+ in $C_{\infty v}$ and Σ^+_g in $D_{\infty h}$. Because the parallel component of the dipole moment $[\,(\,\vec{\mu}_{el})_z\,]$ transforms as Σ^+_u, while the perpendicular component $[\,(\,\vec{\mu}_{el})_{x,y}\,]$ as Π_u in $D_{\infty h}$, therefore, the direct products

$$\Gamma(\Psi'_{el}) \otimes \begin{pmatrix} \Pi_u \\ \\ \Sigma^+_u \end{pmatrix} \otimes \Gamma\,(\Psi''_{el}) \tag{1.59}$$

must contain the Σ^+_g representation for $E1$ transitions in homonuclear diatomic molecules. If the ground electronic state ($|\Psi''_{el}\rangle$) of a homonuclear diatomic molecule is, say $X^1\Sigma^+_g$ which is often the case, then the transition from this state to the excited electronic state ($|\Psi'_{el}\rangle$) is $E1$ - allowed if and only if $\Gamma(\Psi'_{el})$ is Π_u for the operator $(\,\vec{\mu}_{el})_{x,y}$ and Σ^+_u for $(\,\vec{\mu}_{el})_z$. Thus, the selection rules for $E1$ - allowed electronic

transitions can be written as,

$$\Delta\Lambda = 0, \pm 1, \tag{1.60a}$$

$$+ \leftrightarrow +, \; - \leftrightarrow -, \; + \nleftrightarrow -, \text{ in } \Sigma - \Sigma \text{ transitions}, \tag{1.60b}$$

$$g \leftrightarrow u, \; g \nleftrightarrow g, \; u \nleftrightarrow u. \tag{1.60c}$$

Note that the transitions $\Sigma^+ \leftrightarrow \Pi$ and $\Sigma^- \leftrightarrow \Pi$ are also allowed transitions.

As the dipole moment operator does not depend on the spin - coordinates, the spin selection rules for small spin - orbit coupling, i.e., for Hund's coupling case (a), must be,

$$\Delta S = 0. \tag{1.61a}$$

$$\Delta\Sigma = 0. \tag{1.61b}$$

For Heteronuclear diatomic molecules, on the other hand, the selection rule given by Eq. (1.60c) is not applicable as they do not possess centre of symmetry.

For Hund's coupling case (c), when spin - orbit coupling is sufficiently large so that Λ and Σ are no longer good quantum numbers, then the selection rules given by Eq. (1.60a), Eq. (1.61a) and Eq. (1.61b) are not applicable.

1.2 Literature Survey

Atoms and molecules have been extensively surveyed to better understand the fundamental theories, fundamental constants and the properties of fundamental quantities. The recent advancements in both theoretical and experimental methods make the field of atomic and molecular spectroscopy even more fascinating and fruitful that brings together the researchers from various areas such as nuclear physics, condensed matter physics, astrophysics, atomic, molecular and optical physics, and chemistry for new scientific explorations [24–26]. Ultracold atoms in optical lattices have opened up the

door for the exploration of various interrelated areas of physics ranging from non-linear dynamics to quantum computation. Trapped atoms in their Rydberg states can be used in the field of quantum information processing [27, 28], while atoms trapped in the optical lattices at ultracold temperatures have been used to illustrate the quantum phase transitions [29–31]. Several neutral and singly charged atoms have been studied theoretically as well as experimentally to improve the accuracy of current time standard [32–38], which can be further used to improve the global positioning system (GPS) measurements [39].

On the other hand, the presence of additional vibrational and rotational degrees of freedom in the molecules makes the comprehension of their structure more complex, challenging and non-trivial. Nevertheless, careful investigations on such systems can provide a wealth of information which can be utilized for the exploration of various interrelated areas of research [26, 40]. To mention, cold and ultracold molecules can be used in the study of the controlled chemical reactions [41, 42], quantum computation [40, 43–45], anisotropic- and long-range dipole-dipole interactions [46, 47], the variation of fundamental physical constants such as the proton-to-electron mass ratio (m_p/m_e) [48–51], the fine structure constant (α) [50], etc. The heavy polar molecules such as ThO, PbO, BaF, RaF, YbF, HfH^+, PtH^+, etc., have been investigated for the search of the electric dipole moment (EDM): a symmetry violating exotic property of an electron which hitherto has evaded detection [5–7, 52–56] and that plays a key role in understanding the physics beyond the standard model of particle physics.

The small natural linewidths and systematic shifts (black-body radiation, quadrupole, Stark and Zeeman) in the ro-vibrational transitions of isotopomers: H_2^+ and HD^+ make them suitable candidates for a molecular ion clock which would be insightful for the study of variation in the mass ratios (m_p/m_e, proton-to-deutron: m_p/m_d) [57–59]. Recently, a hybrid system of ultracold atom and ion, Li-Yb^+, has

been studied by Bissbort *et al.* [60] to imitate the properties of solid - state physics. More recently, Kondov *et al.* have demonstrated the molecular lattice clock which is based on vibrations in diatomic molecules [61]. The other emerging fields including the study of two - species Bose - Einstein condensates [62–65], ultracold plasmas [66, 67], atom - molecule collisions at low temperatures [68–70], and different quantum phases such as checkerboard (CB), supersolid (SS), superfluid, etc., [47,71], use ultracold gases of atoms and diatomic molecules.

A number of experimental techniques have been developed to unravel the complex structure and properties of molecules. For such purposes, neutral molecules have been formed using magnetic trapping via buffer gas cooling [72] and electrostatic trapping of Stark decelerated molecules [73, 74]. Photoassociation [75–80] and Feshbach resonance [81, 82] methods have been employed for the formation of ultracold molecules. The formation of molecular ions by radiative association of cold atoms and ions has been discussed in Ref. [83]. The cold molecular ions can also be formed by sympathetic cooling using laser - cooled atomic ions [84–86]. An excellent review of such and several other experiments related to high - precision measurements is presented in Ref. [87].

Such advancements in the experimental techniques for precision measurements obviously need sound theoretical inputs to better understand various experimental aspects and sometimes to complement the experimental results. For example, the accurate determination of the PECs for the ground - and suitable excited electronic states is required to analyze the transition lines in the molecular spectra [88–90], and to elucidate various complicated processes occurring in the molecular systems [91–93]. In addition to the spectroscopic constants that can be extracted from the PECs [equilibrium bond lengths (R_e), harmonic frequencies (ω_e), anharmonic constants ($\omega_e x_e$), dissociation energies (D_e), electronic excitation energies (T_e) and rotational constants (B_e and α_e)] [94], the molecular formation rates [95,96], the molecular properties [per-

manent dipole moments (PDMs, μ_0), QMs (Θ), DPs (α), transition dipole moments (TDMs) between the electronic states, hyperfine structure (HFS) constants, effective electric field (ε_{eff}), and parity ($\mathcal{P}$) and time-reversal ($\mathcal{T}$) symmetry violating interaction constants] [52, 55, 97–102], and also the vibrational parameters [energies (E_v), vibrationally coupled rotational constants (B_v), FCFs, lifetimes (τ), TDMs, spontaneous- and black-body radiation (BBR-) induced transition rates between the vibrational levels], are of interest to the experimentalists [59, 103–107]. The accurate theoretical predictions of these properties could shed light on different experimental aspects. Therefore, meticulous calculations of the aforementioned properties require the use of sophisticated many-body theories, some of which particularly the ones we have used in this thesis work will be discussed briefly in the forthcoming chapter.

Having been motivated by the numerous applications of diatomic molecules in various fields of fundamental importance, we set modest goals for this thesis as: (i) to provide electronic and vibrational properties of ground- and low-lying excited states of singly charged alkaline-earth lithides ($AELi^+$: AE = Be, Mg, Ca), (ii) to calculate the atomic polarizabilities of alkaline-earth atoms, and molecular properties *viz.* PDMs, components of molecular polarizabilities ($\alpha_{\parallel}$ and $\alpha_{\perp}$), HFS constants and $\mathcal{P}$ & $\mathcal{T}$-odd interaction constants of alkaline-earth monofluorides (AEMFs: AE = Be, Mg, Ca, Sr, Ba, Ra). We aim to perform systematic calculations taking large optimized basis sets together with large active space for correlation calculations using accurate many-body theories.

1.3 Overview of the Thesis

A brief overview of the preceding chapters of the thesis is presented below:

Chapter 2: This chapter presents the basics of many-body methods that can be used for the structural studies of atoms and molecules. First, we have given a brief

description of the Born - Oppenheimer approximation. Then, the self consistent field (SCF) method that provides the zeroth - order wavefunction for the post - SCF calculations is presented. Further, a few of the most widely used post - SCF methods such as configuration interaction (CI), many - body perturbation theory (MBPT) and coupled - cluster (CC) theory including equation - of - motion CC (EOM - CC) method are discussed. These methods are used for calculating spectroscopic parameters and molecular properties reported in this thesis. Furthermore, the elementary concepts of basis sets and diagonal Born - Oppenheimer corrections (DBOC) are also discussed. In addition, a brief introduction to the quantum chemistry program packages: DIRAC, CFOUR, MOLCAS, and LEVEL that are used for the calculation of electronic and vibrational properties studied in Chapter 3 - Chapter 5 is provided.

Chapter 3: This chapter includes the calculations of spectroscopic constants (R_e, D_e, $\omega_e, \omega_e x_e, B_e$ and α_e), and the molecular properties ($\mu_0, \Theta_{zz}, \alpha_{\parallel}, \alpha_{\perp}, \bar{\alpha}, \gamma$ and α_{100}) for the ground state ($X\,^1\Sigma^+$) of $BeLi^+$ at different levels of correlation: second - order many - body perturbation theory (MP2), coupled cluster method with single and double excitations (CCSD) and CCSD with perturbative triples (CCSD(T)). The correlation - consistent polarized valence Double/Triple/Quadruple Zeta (cc - pVXZ: X = D, T, Q) basis sets and also their augmented counterparts are used together with the non - relativistic and relativistic Hamiltonians. Further, by solving the vibrational Schrödinger equation using the PEC obtained via the CCSD(T)/QZ method, we have calculated the vibrational parameters such as energies, rotational constants, PDMs, lifetimes, TDMs, spontaneous - and BBR - induced transition rates between different vibrational levels of the electronic ground state. In addition, electronic and vibrational parameters of a few low - lying electronic excited states are calculated using the EOM - CCSD/QZ method. The electric dipole moments for the transitions from the electronic ground - to the excited singlet states are also studied. In short, the work published in Ref. [108] is the major content of this chapter.

Chapter 4: In this chapter, we have reported the theoretical calculations of electronic and vibrational parameters of $MgLi^+$ and $CaLi^+$ molecular ions. These ions have an electronic structure similar to that of $BeLi^+$. The $^1\Sigma^+$ electronic ground states of $MgLi^+$ and $CaLi^+$ molecular ions have been investigated for their diatomic constants and electric properties using sophisticated correlation methods as employed in Chapter 3. The non - relativistic and relativistic Hamiltonians are used in conjunction with TZ and QZ basis sets to carry out the calculations of ground state parameters. The vibrational energies, the wavefunctions and the relevant vibrational parameters are obtained by solving the vibrational Schrödinger equation using the PEC and the PDM curve of the molecular electronic ground state. Thereafter, spontaneous - and BBR - induced transition rates are calculated to obtain the lifetimes of the vibrational states. Further, a few low - lying electronic excited states of Σ and Π symmetries have been investigated for their electronic and vibrational properties using EOM - CCSD/QZ method. This work has been published by us in Ref. [109].

Chapter 5: This chapter reports the atomic polarizabilities of fluorine - and alkaline - earth atoms, and also molecular properties such as: PDMs, components of molecular polarizabilities, HFS constants and $\mathcal{P}$ & $\mathcal{T}$ - odd interaction constants (W_d, and W_s) of AEMFs. A generalized active space (GAS) technique is applied to carry out the atomic and molecular property calculations using the Kramers - restricted CI method limited to single and double excitations (KRCISD). These calculations are performed using frozen - core approximation together with the QZ basis sets for lighter atoms (Be, Mg, F) and relativistic Dyall basis sets of similar standard for heavy atoms (Ca, Sr, Ba, Ra), in uncontracted form. The calculated atomic and molecular properties are compared with the existing experimental and theoretical results, wherever available. A part of this work has been published by us in Ref. [110]. some of the results are being reported here in this thesis for the first time.

Chapter 6: This chapter presents the concluding remarks along with the future out-

look of the work reported in this thesis.

At the end, we have given a couple of **appendices** that contain the illustrative input files which may be necessary for running the softwares used to carry out the work reported in this thesis.

CHAPTER 2

BASICS OF MANY - BODY METHODS

"The quantum is that embarrassing little piece of thread that always hangs from the sweater of space-time. Pull it and the whole thing unravels" – Fred Alan Wolfe

The theoretical study of any quantum system involves finding a solution to the Schrödinger equation,

$$H\,\Psi \;=\; E\,\Psi. \tag{2.1}$$

In most of the cases, however, it is either impossible or extremely non - trivial to solve the Schrödinger equation exactly. Hence, different approximations are employed in order to simplify the task. A crucial first step in this regard is to invoke the Born - Oppenheimer approximation in which the coupled motion between the electrons and the nuclei is ignored.

2.1 Born - Oppenheimer Approximation

The Hamiltonian for a molecular system containing n - electrons in the presence of N nuclei is given as [12, 111],

$$\begin{aligned} H &= T_e + T_N + V_{eN} + V_{ee} + V_{NN}, \\ &= -\frac{\hbar^2}{2\,m_e}\sum_{i=1}^{n}\nabla_i^2 - \frac{\hbar^2}{2}\sum_{A=1}^{N}\frac{1}{M_A}\nabla_A^2 + \frac{1}{4\,\pi\,\epsilon_0}\Bigg[-\sum_{i=1}^{n}\sum_{A=1}^{N}\frac{Z_A\,e^2}{r_{iA}} \\ &+ \sum_{i=1}^{n}\sum_{j>i}^{n}\frac{e^2}{r_{ij}} + \sum_{A=1}^{N}\sum_{B>A}^{N}\frac{Z_A\,Z_B\,e^2}{R_{AB}}\Bigg], \end{aligned} \tag{2.2}$$

where $\nabla^2 \left(\equiv \frac{\partial}{\partial x^2} + \frac{\partial}{\partial y^2} + \frac{\partial}{\partial z^2} \right)$ is the Laplacian operator in Cartesian coordi-

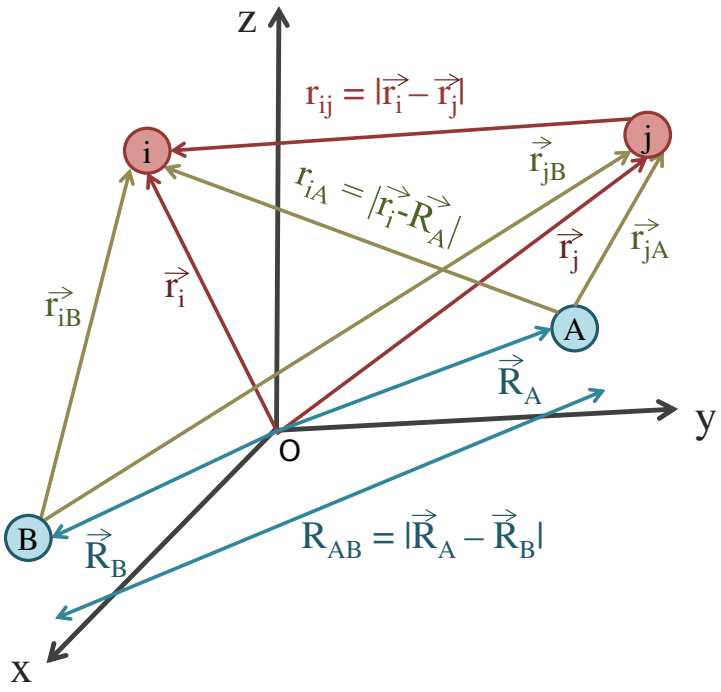

Figure 2.1: A molecular coordinate system showing all interactions between electrons (i, j) and nuclei (A, B). The origin 'O' of the coordinate system is chosen at the center - of - mass of two nuclei.

nates; M_A is the mass of nucleus; $r_{iA} = |\vec{r}_i - \vec{R}_A|$ is the distance between the i^{th} electron and A^{th} nucleus; $r_{ij} = |\vec{r}_i - \vec{r}_j|$ is the distance between the i^{th} and j^{th} electron; $R_{AB} = |\vec{R}_A - \vec{R}_B|$ is the distance between the two nuclei A and B, as shown in Figure (2.1). The first - and second terms in Eq. (2.2) represent the kinetic energy operators for electrons and nuclei, respectively. The third term corresponds to the attractive Coulomb interaction between the electrons and nuclei. The fourth - and fifth terms correspond to interelectronic and internuclear Coulomb repulsions, respectively.

Since the mass of even the lightest nucleus is much larger than the mass of an electron ($\sim$ 1800 times), one can assume that the relative motion of the nuclei within a molecule is small and negligible in comparison to the motion of the electrons. In other words, it is safe to consider that the positions of the nuclei are fixed with respect to the electronic motion. This approximation is known as the **Born - Oppenheimer approximation**.

For fixed nuclei, the second term of Eq. (2.2) can be ignored and the last term of Eq. (2.2) can be treated as a constant quantity. The remaining terms in Eq. (2.2) constitute what is known as the electronic Hamiltonian, H_{el}, *viz.*,

$$H_{el} = -\frac{\hbar^2}{2\,m_e}\sum_{i=1}^{n}\nabla_i^2 + \frac{1}{4\,\pi\,\epsilon_0}\left[-\sum_{i=1}^{n}\sum_{A=1}^{N}\frac{Z_A\,e^2}{r_{iA}} + \sum_{i=1}^{n}\sum_{j>i}^{n}\frac{e^2}{r_{ij}}\right], \tag{2.3}$$

and the corresponding electronic Schrödinger equation is,

$$H_{el}\,\Psi_{el} = E_{el}\,\Psi_{el}. \tag{2.4}$$

The H_{el} defined by Eq. (2.3) depends on the electronic coordinates explicitly, while it has a parametric dependence on the nuclear coordinates. Therefore, the eigenfunc-

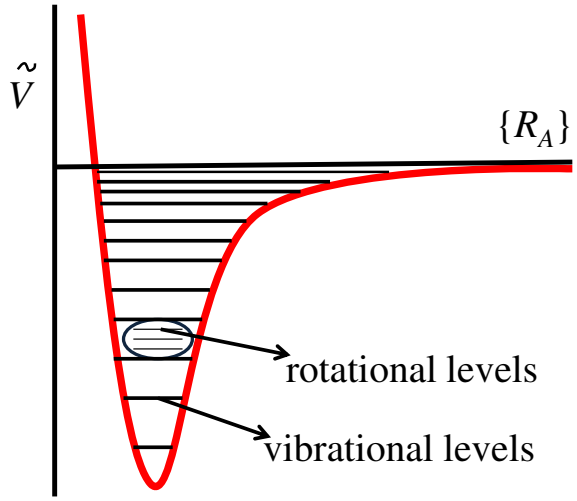

Figure 2.2: Potential energy curve of a diatomic molecule.

tions of H_{el} depend on both electronic as well as the nuclear coordinates.

$$\Psi_{el} = \Psi_{el}\big(\{\vec{r}_i\};\{\vec{R}_A\}\big). \tag{2.5}$$

The sum of the eigenvalues of H_{el} and the constant nuclear repulsion energies at different internuclear distances form a potential energy curve for the nuclear motion as shown in Figure (2.2).

$$\tilde{V} = E_{el} + \frac{1}{4\,\pi\,\epsilon_0}\sum_{A=1}^{N}\sum_{B>A}^{N}\frac{Z_A\,Z_B\,e^2}{R_{AB}}. \tag{2.6}$$

Therefore, the nuclear Hamiltonian, H_{nucl}, can be written as,

$$H_{nucl} = -\frac{\hbar^2}{2}\sum_{A=1}^{N}\frac{1}{M_A}\nabla_A^2 + \tilde{V}, \tag{2.7}$$

and the corresponding Schrödinger equation for the nuclear motion is given by,

$$H_{nucl}\,\Psi_{nucl} \;=\; E\,\Psi_{nucl}, \tag{2.8}$$

where E represents the total energy of a given system that includes the electronic (E_{el}), vibrational (E_v) and rotational (E_J) energies, and Ψ_{nucl} represents the nuclear wavefunction. It follows from the BOA that the total wavefunction, Ψ, of a molecular system can be written as,

$$\Psi \;=\; \Psi_{el}\big(\{\vec{r}_i\};\,\{\vec{R}_A\}\big)\,\Psi_{nucl}\big(\{\vec{R}_A\}\big). \tag{2.9}$$

Further, the Ψ_{nucl} can be factorized into vibrational and rotational terms so that one can write Ψ as,

$$\Psi \;=\; \Psi_{el}\,\Psi_v\,\Psi_J, \tag{2.10}$$

where v and J represent the vibrational and rotational quantum number, respectively.

2.2 Hartree - Fock Theory

The electronic Schrödinger equation for a molecular system given by Eq. (2.4) in the previous section cannot be solved exactly due to the presence of two - body interaction term, i.e., the Coulomb repulsion between the electrons. To overcome this problem, D. R. Hartree [112] proposed an approximation based on independent particle model (IPM) in which each electron moves independently in an average potential created by nuclei and by all other electrons in a given system. However, the total wavefunction for a system is not antisymmetric in this approximation. The generalization of the Hartree approach which incorporates the antisymmetry requirement was carried out by V. A. Fock and the method is now known as the Hartree - Fock (HF) approximation. The relativistic equivalent of this is called Dirac - Fock (DF) or Dirac - Hartree - Fock (DHF) approximation, which uses Dirac Hamiltonian in place of Eq. (2.3). Thus, the electronic Hamiltonian given by Eq. (2.3) can be written

as [111, 113, 114],

$$H_{el} \;=\; H_0 \;+\; V_{res}. \tag{2.11}$$

The first term, H_0, in the above equation represents the Hamiltonian in the HF/DF approximation. For the non - relativistic case,

$$H_0 \;\equiv\; H_0^{HF} \;=\; -\frac{\hbar^2}{2\,m_e}\sum_{i=1}^{n}\nabla_i^2 \;-\; \frac{1}{4\,\pi\,\epsilon_0}\sum_{i=1}^{n}\sum_{A=1}^{N}\frac{Z_A\,e^2}{r_{iA}} \;+\; \sum_{i=1}^{n}u^{HF}(r_i), \tag{2.12a}$$

where u^{HF} represents the average one - body potential in the HF approximation. On the other hand, for the relativistic case,

$$H_0 \;\equiv\; H_0^{DF} \;=\; \sum_{i=1}^{n}\left[c\,\alpha_i\,.\,p_i \;+\; (\beta_i - 1)\,m_e\,c^2\right] \;-\; \frac{1}{4\,\pi\,\epsilon_0}\sum_{i=1}^{n}\sum_{A=1}^{N}\frac{Z_A\,e^2}{r_{iA}} + \sum_{i=1}^{n}u^{DF}(r_i), \tag{2.12b}$$

where c is the speed of light, p_i is the momentum operator of the i^{th} electron, u^{DF} is the average one - body potential in the DF approximation, while α and β are the Dirac matrices. The standard representation of α and β is given by,

$$\alpha_i \;=\; \begin{pmatrix} 0 & \sigma_i \\ \sigma_i & 0 \end{pmatrix},\ \text{where } i \;=\; 1,\, 2,\, 3; \qquad\qquad \beta \;=\; \begin{pmatrix} I & 0 \\ 0 & -I \end{pmatrix}, \tag{2.13}$$

where σ_i are the Pauli spin matrices and I is a 2×2 unit matrix. These matrices are shown below [115]:

$$\sigma_1 \;=\; \begin{pmatrix} 0 & 1 \\ 1 & 0 \end{pmatrix}, \qquad\qquad \sigma_2 \;=\; \begin{pmatrix} 0 & -i \\ i & 0 \end{pmatrix},$$

$$\sigma_3 \;=\; \begin{pmatrix} 1 & 0 \\ 0 & -1 \end{pmatrix},\ \text{and} \qquad I \;=\; \begin{pmatrix} 1 & 0 \\ 0 & 1 \end{pmatrix}. \tag{2.14}$$

The second term, V_{res}, in Eq. (2.11) is the residual potential, defined as the difference between the exact two - body Coulomb potential between electrons and the average one - body potential in the HF approximation[1],

$$V_{res} = \frac{1}{4\,\pi\,\epsilon_0} \sum_{i=1}^{n} \sum_{j>i}^{n} \frac{e^2}{r_{ij}} - \sum_{i=1}^{n} u^{HF}(r_i). \tag{2.15}$$

The eigenfunctions of HF Hamiltonian given by Eq. (2.12a) can be written as a single Slater determinant of orthonormal basis as,

$$\Phi(r_1, r_2, ..., r_n) = \frac{1}{\sqrt{n!}} \begin{pmatrix} \phi_1(r_1) & \phi_2(r_1) & \phi_3(r_1) & \cdots & \phi_n(r_1) \\ \phi_1(r_2) & \phi_2(r_2) & \phi_3(r_2) & \cdots & \phi_n(r_2) \\ \vdots & \vdots & \vdots & \ddots & \vdots \\ \phi_1(r_n) & \phi_2(r_n) & \phi_3(r_n) & \cdots & \phi_n(r_n) \end{pmatrix}. \tag{2.16}$$

The columns in a Slater determinant represent single - electron orbitals, whereas the electron coordinates are shown along the rows.

For a closed shell system, there is a restriction that each spatial orbital in a Slater determinant should occupy two electrons with opposite spin. The electronic wavefunctions formed from such Slater determinants are known as the restricted HF (RHF) wavefunctions [116, 117]. On the other hand, if there are no restrictions on the total spin of the system, i.e., the alpha and beta spin orbitals have different spatial orbitals, the wavefunction is known as the unrestricted HF (UHF) [116,117]. The UHF method is also known as different orbitals for different spins (DODS) method.

The average one - body potential, known as the HF potential, is defined as,

$$u^{HF}\,|\,\phi_i\rangle = \frac{1}{4\,\pi\,\epsilon_0} \sum_{i=1}^{n} \sum_{j>i}^{n} \left[\langle \phi_j \,|\, \frac{e^2}{r_{ij}} \,|\, \phi_j \rangle \,|\, \phi_i \rangle - \langle \phi_j \,|\, \frac{e^2}{r_{ij}} \,|\, \phi_i \rangle \,|\, \phi_j \rangle \right]. \tag{2.17}$$

[1]From here onwards, all equations of this section are written in terms of the HF potential.

The first term in the above equation is called the *direct term* which represents the electrostatic Coulomb interaction of the i^{th} electron with the charge density of all other electrons. The second term is called the *exchange term* of the HF potential which has no classical analog and it appears solely due to the antisymmetric nature of the determinantal wavefunction. Thus, the HF equation can be written as,

$$\sum_{i=1}^{n} \left[-\frac{\hbar^2}{2\,m_e} \nabla_i^2 \; - \; \frac{1}{4\,\pi\,\epsilon_0} \sum_{A=1}^{N} \frac{Z_A\,e^2}{r_{iA}} \; + \; u^{HF}(r_i) \right] |\phi_i\rangle = \sum_{i=1}^{n} \epsilon_i\,|\phi_i\rangle. \tag{2.18}$$

Since the HF potential given by Eq. (2.17) has a functional dependence on the spin orbitals $|\phi_i\rangle$, the set of equations given by Eq. (2.18) need to be solved iteratively in a self consistent manner. Hence, this method is also known as the self consistent field (SCF) method.

The single particle wavefunctions and energies are obtained by minimizing the functional, $\langle \Phi_0 \,|\, H_0^{HF} \,|\, \Phi_0 \rangle \; - \; E\,[\Phi_0] \; = \; 0$, using the variational principle. The integro - differential equations given in Eq. (2.18) can be defined in terms of matrix eigenvalue equations known as the Roothaan equations [111, 118],

$$F\,C \; = \; \epsilon\,S\,C, \tag{2.19}$$

where F, C, ϵ, and S represent the Fock matrix, eigenvector matrix, eigenvalue matrix, and overlap matrix, respectively. For the orthogonal and normalized basis set, $S \; = \; I$ (the identity matrix); the eigenvalues (orbital energies) and the eigenvectors (expansion coefficients) can be found by diagonalizing the Fock matrix similar to the general eigenvalue problem. However, in case when the basis sets that are used for the molecular structure calculations are not orthogonal to each other, i.e., $S \; \neq \; I$,

one has to find a transformation matrix[2] (X) so that,

$$X^{\dagger}SX = 1, \tag{2.20}$$

and

$$\tilde{C} = X^{-1}C \quad \Longrightarrow \quad C = X\tilde{C}, \tag{2.21}$$

where $\tilde{C}$ is the transformed coefficient matrix. On substituting $C = X\tilde{C}$ in Eq. (2.19), one obtains,

$$FX\tilde{C} = \epsilon SX\tilde{C}. \tag{2.22}$$

Multiplying on the left by $X^{\dagger}$ gives,

$$(X^{\dagger}FX)\,\tilde{C} = \epsilon\,(X^{\dagger}SX)\,\tilde{C}. \tag{2.23}$$

By defining a transformed Fock matrix as $\tilde{F} = X^{\dagger}FX$ and using Eq. (2.20), we get,

$$\tilde{F}\,\tilde{C} = \epsilon\,\tilde{C}. \tag{2.24}$$

These equations are known as the transformed Roothan equations that can be solved for $\tilde{C}$ by diagonalizing $\tilde{F}$.

The difference between the exact energy (E_{exact}) and the SCF energy (E_{SCF}) is known as the correlation energy (E_{corr}). To calculate E_{corr}, one has to consider the post - SCF methods, which are discussed briefly in the next section.

2.3 Post - Mean - Field Methods

The accurate calculations involving interacting many - electron systems are non - trivial and go beyond the simple mean - field methods such as the HF method. Unlike

[2]This matrix should be non - singular, i.e, inverse of a matrix should exist.

the mean - field method, where each electron is assumed to interact with the effective potential created combinedly by the nucleus and all other electrons, the post - mean - field methods treat the instantaneous Coulomb repulsion between the electrons. Resorting to the post - mean - field methods for many - electron systems is inevitable for any accurate calculation of electron correlation effects. The most commonly and widely used many - body methods are: configuration interaction (CI) method, many - body perturbation theory (MBPT), and coupled - cluster (CC) method. All of these methods are built over the HF wavefunction, which serves as their zeroth - order approximation. These methods are briefly discussed here. Further details of these methods can be found elsewhere, for example in Refs. [111, 119–121].

2.3.1 Configuration Interaction Method

The simplest approach for treating electron correlation is the configuration interaction (CI) method. The CI method is more appropriately referred to as the method of superposition of configurations as it involves the expansion of the many - electron wavefunction as a linear combination of determinantal functions [111],

$$|\Psi\rangle = C_0\,|\,\Phi_0\rangle + \left(\frac{1}{1!}\right)^2 \sum_{a,\,p} C_a^p\,|\,\Phi_a^p\rangle + \left(\frac{1}{2!}\right)^2 \sum_{ab,\,pq} C_{ab}^{pq}\,|\,\Phi_{ab}^{pq}\rangle + \ldots, \qquad (2.25)$$

here $|\Phi_0\rangle$ is the reference HF determinant, $|\Phi_a^p\rangle$ represents the singly excited determinant in which one of the occupied spin orbital χ_a is replaced by one of the virtual spin orbital χ_p, $|\Phi_{ab}^{pq}\rangle$ represents the doubly excited determinant in which two spin orbitals χ_a and χ_b are replaced by χ_p and χ_q, and so on, and C_a^p, C_{ab}^{pq}, ... are the corresponding amplitudes of excitations. The summation index a, b, ... represent the filled orbitals, while p, q, ... represent the virtual orbitals. A factor of $\left(\frac{1}{n!}\right)^2$ is added in front of each term to avoid multiple counting. The optimized coefficients of various determinants can be calculated by the application of the variational principle. The exact solution, for the given basis set, is obtained by using all the terms

of CI expansion upto n - tuple excitations. This method is known as full CI. In the symbolic form, the CI wavefunction can be rewritten as,

$$|\Psi\rangle \;=\; C_0\,|\,\Phi_0\rangle \;+\; C_S\,|\,S\rangle \;+\; C_D\,|\,D\rangle \;+\; \ldots, \tag{2.26}$$

where $|S\rangle$ includes all those determinants that arise due to single excitation. Similarly, $|D\rangle$ includes all determinants involving double excitations, and so on. The coefficients C_S and C_D are the amplitudes for single - and double excitations, respectively. The matrix representation of the Hamiltonian operator in the basis $|\Phi_i\rangle$ is a $n \times n$ matrix with elements,

$$(H)_{ij} \;=\; \langle\Phi_i\,|\,H\,|\,\Phi_j\rangle. \tag{2.27}$$

Using the symbolic notation, the full CI matrix can be written as,

$$\begin{array}{c} \\ \\ \langle\Phi_0| \\ \langle S| \\ \langle D| \\ \langle T| \\ \langle Q| \\ \vdots \end{array}
\begin{array}{c}
\begin{array}{ccccccc} & & |\Phi_a^p\rangle & |\Phi_{ab}^{pq}\rangle & |\Phi_{abc}^{pqr}\rangle & |\Phi_{abcd}^{pqrs}\rangle & \ldots \\ & |\Phi_0\rangle & |S\rangle & |D\rangle & |T\rangle & |Q\rangle & \ldots \end{array} \\
\begin{pmatrix}
\langle\Phi_0|H|\Phi_0\rangle & 0 & \langle\Phi_0|H|D\rangle & 0 & 0 & \ldots \\
 & \langle S|H|S\rangle & \langle S|H|D\rangle & \langle S|H|T\rangle & 0 & \ldots \\
 & & \langle D|H|D\rangle & \langle D|H|T\rangle & \langle D|H|Q\rangle & \ldots \\
 & & & \langle T|H|T\rangle & \langle T|H|Q\rangle & \ldots \\
 & & & & \langle Q|H|Q\rangle & \ldots \\
 & & & & & \vdots
\end{pmatrix}
\end{array}$$

As the CI matrix is Hermitian[3], only the upper triangle elements are shown here. The eigenvalues and the corresponding eigenvectors can be obtained by diagonalizing the CI matrix. Further, it has to be noted that:

(i) $\langle\Phi_0\,|\,H\,|\,S\rangle \;=\; \langle\Phi_0\,|\,H\,|\,\Phi_a^p\rangle \;=\; 0$, i.e., the singly - excited determinants, $|\Phi_a^p\rangle$, do not mix with the HF reference state, $|\Phi_0\rangle$. However, they can mix with $|\Phi_0\rangle$ indirectly through the doubly excited determinants. This is a consequence of

[3]A matrix is said to be Hermitian if it is equal to its own conjugate transpose, i.e., $H_{ij} \;=\; H_{ji}^{*}$.

Brillouin's theorem [111].

(ii) The reference state can not be coupled with those determinants involving triple - or quadruple excitations, *viz.*, $\left[\langle \Phi_0 \,|\, H \,|\, \Phi^{pqr}_{abc} \rangle \;=\; \langle \Phi_0 \,|\, H \,|\, \Phi^{pqrs}_{abcd} \rangle \;=\; 0 \right]$. Similarly, singles do not mix with quadruples $\left[\langle \Phi^{p}_{a} \,|\, H \,|\, \Phi^{pqrs}_{abcd} \rangle \;=\; 0 \right]$. This is a consequence of the fact that all those matrix elements in which two Slater determinants differ by more than two spin orbitals are zero [111]. It indicates that the blocks which are not zero in the CI matrix are scarce. For instance, consider the matrix element,

$$\langle D \,|\, H \,|\, Q \rangle \;\leftrightarrow\; \langle \Phi^{pq}_{ab} \,|\, H \,|\, \Phi^{rstu}_{cdef} \rangle. \tag{2.28}$$

This matrix element is non - zero only if the indices a and b are the subset of $\{c, d, e, f\}$ and the indices p and q are the subset of $\{r, s, t, u\}$.

For actual calculations, it is nearly impossible to consider all n - tuple excitations for reasonably large basis sets because of practical limitations, such as the availability of computer resources. Therefore, most often one uses the truncated CI expansion. Usually, the truncation is done after the double excitation level, which is termed as CISD (configuration interaction with single - and double excitations) method.

The main disadvantage of this method is that it is not *size - consistent* in its truncated form, which is one of the desired properties for any many - body theory. A method is said to be size - consistent if the energies of two systems say, A and B, and of the combined system AB with A and B separated by sufficiently large distance, calculated in similar ways, satisfy [119],

$$E(AB) \;=\; E(A) \;+\; E(B). \tag{2.29}$$

In a more general way, the size - consistency can also be defined for the interacting particles, when the energy of a many - particle system becomes proportional to the

number of particles (n) in the limit $n \to \infty$ [111].

2.3.2 Many - Body Perturbation Theory

In the perturbation method, the Hamiltonian of the system is divided into two parts: a model Hamiltonian or a zeroth - order Hamiltonian (H_0) and a perturbation (H') so that [120, 122],

$$H = H_0 + H'. \tag{2.30}$$

The Hamiltonian H_0 has known eigenvalues and eigenfunctions given by their solvable Schrödinger equation,

$$H_0 \left|\Phi^{(j)}\right\rangle = E^{(j)} \left|\Phi^{(j)}\right\rangle. \tag{2.31}$$

If the set $\{\Phi^{(j)}\}$ is complete and $|\Phi^{(0)}\rangle$ is a good approximation to exact wavefunction, $|\Psi\rangle$, then one can write,

$$|\Psi\rangle = |\Phi^{(0)}\rangle + \sum_{j=1}^{\infty} K^{(j)} \left|\Phi^{(j)}\right\rangle. \tag{2.32}$$

where $K^{(j)}$ is the j^{th} - order perturbation coefficient. The coefficient for the zeroth - order wavefunction is often chosen to be $K^{(0)} = 1$, which can be achieved by proper renormalization of $|\Psi\rangle$. Similar to the wavefunction, the exact energy E can be expanded in a perturbation series as,

$$E = E^{(0)} + E^{(1)} + E^{(2)} + \dots . \tag{2.33}$$

The goal of perturbation theory is to obtain the perturbation coefficients $K^{(j)}$ and matrix elements of the perturbing part of the Hamiltonian between the eigenfunctions of H_0. Terms that involve products of n such matrix elements are grouped together to comprise the n^{th} - order perturbation theory.

In modern perturbation theory, the functional space for the wavefunction is divided

into *model space* (P) and *complementary space* (Q) such that [120],

$$P + Q = 1. \tag{2.34}$$

The basic idea is to find *effective operators* which act only on limited space known as *model space*, but generate the same result as the original operators acting on the whole functional space. Thus, the proper choice of model space plays an important role in the success of perturbation calculations.

Note that MBPT is a fully size - consistent theory at any given order of perturbation. This can be proved by using the *linked - cluster theorem*, which states that the perturbation expansion of the energy of a many - electron system can be represented only by linked diagrams, while the unlinked diagrams representing the disjoint excitations completely cancel out [120]. Some of the disadvantages of MBPT approach are given below [119, 120]:

(i) This method, in general, is non - variational so that there is no upper bound on the energy.

(ii) The number of terms beyond the second - order become too large to handle, and it is impractical to consider MBPT to all orders of perturbation in any computational calculation.

2.3.3 Coupled - Cluster Method

In a single reference approximation, the CC wavefunction is obtained by operating the exponential operator on the reference wavefunction, $|\Phi_0\rangle$. It can be written as [119, 123],

$$\begin{aligned} |\Psi\rangle &= e^T |\Phi_0\rangle, \\ &= \left[1 + T_1 + \frac{1}{2}T_1^2 + T_2 + \frac{1}{3!}T_1^3 + T_1 T_2 + T_3 + \ldots\right] |\Phi_0\rangle, \end{aligned} \tag{2.35}$$

where $T\,(=\,T_1\,+\,T_2\,+\,T_3\,\ldots)$ is the cluster operator; T_1, T_2, T_3, …, T_n represent the excitation operators corresponding to single excitation, double excitation, triple excitation, …, n - tuple excitation. In second quantized notation, these operators can be defined as,

$$T_1 \;=\; \sum_{a,\,p} t_a^p\, \mathbf{a}_p^\dagger\, \mathbf{a}_a, \tag{2.36a}$$

$$T_2 \;=\; \frac{1}{4} \sum_{ab,\,pq} t_{ab}^{pq}\, \mathbf{a}_p^\dagger\, \mathbf{a}_q^\dagger\, \mathbf{a}_b\, \mathbf{a}_a, \tag{2.36b}$$

and so on, where $\mathbf{a}$ and $\mathbf{a}^\dagger$ refer to the annihilation and creation operator, respectively. The subscripts a, b, c, … denote the filled orbitals, and p, q, r, … denote the virtual orbitals. Therefore, Eq. (2.36a) represents the annihilation of an electron from the filled orbital a, with the simultaneous creation of a virtual electron in orbital p, and the amplitude of this single excitation is t_a^p. Similarly, in Eq. (2.36b), a pair of electrons is annihilated simultaneously from the filled orbitals (a, b) and created in virtual orbitals (p, q) with an amplitude t_{ab}^{pq}. The diagrammatic representation of these excitation operators are shown in Figure (2.3), where the horizontal line refers

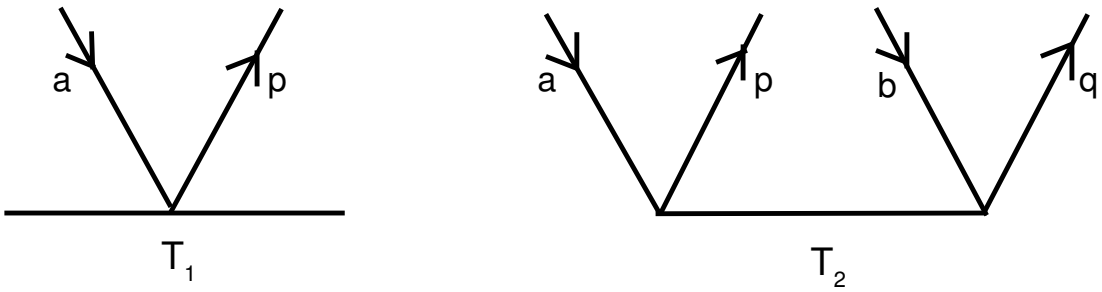

Figure 2.3: The coupled - cluster amplitude diagrams for single - and double - excitations.

to the HF reference state.

If one considers only first two terms in the definition of cluster operator, *viz.*, $T = T_1 + T_2$, one obtains CCSD (CC with singles and doubles) method; if one considers first three terms, *viz.*, $T = T_1 + T_2 + T_3$, one obtains CCSDT (CCSD with full triples) method, and so on.

As the CC wavefunction is of exponential form, it includes linear as well as nonlinear terms and hence, it takes into account a large class of correlation effects compared to other methods at similar truncation levels. It has to be noted that the CC theory is neither *perturbative* nor *variational*. The key features of this method are that it is equivalent to all - order MBPT and fully size - consistent at any given level of truncation. Due to these advantages, CC theory has proved extremely useful for the study of wide range of many - body systems such as atoms, molecules, nuclei, etc. Thus, CC theory has been referred to as the universal many - body theory [124, 125].

Equation - of - Motion CC Method

The conventional CC method, in general, is very successful for predicting an accurate description of most molecular ground states, particularly when they are dominated by a single - determinant. However, most of the excited, ionized and electron - attached states are open - shell states with contributions from more than one - determinant, which renders the CC method inadequate to provide reliable results. The EOM - CC method is one of those methods that can be used to describe such states accurately. The Schrödinger equation for the final target state is given by,

$$H\,\Psi_f \;=\; E\,\Psi_f. \tag{2.37}$$

In this method, the energies and properties of desired excited electronic states are obtained by applying the linear operator like CI on the ground - or initial state CC

wavefunction ($|\Psi_0\rangle$). The wavefunction for the final excited state is given by [119,126],

$$|\Psi_f\rangle \;=\; R\,|\Psi_0\rangle, \tag{2.38}$$

where the subscripts 0 and f correspond to the ground - and excited electronic state wavefunctions, respectively, and R is the linear excitation operator that can be written as the sum of all relevant excitations as,

$$R \;=\; R_0 \;+\; R_1 \;+\; R_2 \;+\; R_3 \;+\; \ldots\,. \tag{2.39}$$

If the initial and final states are of different symmetry then $R_0 \;=\; 0$. The n^{th} order excitation operator is given by,

$$R_n \;=\; \left(\frac{1}{n!}\right)^2 \sum_{\substack{abc\ldots,\\ pqr\ldots}} r^{pqr\ldots}_{abc\ldots}\, p^\dagger a\, q^\dagger b\, r^\dagger c\, \ldots, \tag{2.40}$$

where a, b, c, ... are the filled orbitals, and p, q, r, ... are the virtual orbitals. On substituting the Eqs. (2.35) and (2.38) into the Schrödinger equation given by Eq. (2.37), we obtain,

$$H\,R\,e^T\,|\Phi_0\rangle \;=\; E\,R\,e^T\,|\Phi_0\rangle. \tag{2.41}$$

On multiplying Eq. (2.41) by e^{-T} on the left side and using commutation between R and T operator, we obtain,

$$\left[e^{-T}\,H\,e^T \;-\; E\right]\,R\,|\Phi_0\rangle \;=\; 0. \tag{2.42}$$

The term ($e^{-T}\,H\,e^T$) in the above eigenvalue equation is called effective Hamiltonian ($\tilde{H}$). As $\tilde{H}$ is non - Hermitian due to the non - unitary nature of CC operator e^T, $\tilde{H}$ has left eigenfunction with the same energy eigenvalue, E, in addition to the right eigenfunction,

$$\langle\tilde{\Psi}| \;=\; \langle\Phi_0|\,L\,e^{-T}, \tag{2.43}$$

$$|\Psi\rangle \;=\; e^{T}\, R\,|\Phi_0\rangle. \tag{2.44}$$

Here L, being the de - excitation operator, is defined as,

$$L \;=\; L_0 \;+\; L_1 \;+\; L_2 \;+\; L_3 \;+\; \ldots, \tag{2.45}$$

with

$$L_n \;=\; \left(\frac{1}{n!}\right)^2 \sum_{\substack{pqr\ldots,\\ abc\ldots}} l^{abc\ldots}_{pqr\ldots}\, a^{\dagger}p\, b^{\dagger}q\, c^{\dagger}r\;\ldots\,. \tag{2.46}$$

It is important to mention here that the T, R, and L operators should be truncated to some level of excitation so that the computations can be made manageable. In general, the truncation is made after single - and double excitations. With this constraint, the EOM - CC method is known as the EOM - CCSD method.

Two sets of eigenfunctions satisfy the property of biorthogonality and therefore,

$$\langle\tilde{\Psi}|\Psi\rangle \;=\; 1. \tag{2.47}$$

The energies and properties (θ) can be calculated, respectively, as,

$$\begin{aligned} E \;&=\; \langle\tilde{\Psi}\,|\,H\,|\,\Psi\rangle, \\ &=\; \langle\Phi_0\,|\,L\,\tilde{H}\,R\,|\,\Phi_0\rangle, \end{aligned} \tag{2.48}$$

and

$$\theta \;=\; \langle\tilde{\Psi}\,|\,\Theta\,|\,\Psi\rangle, \tag{2.49}$$

where Θ is a linear property operator.

The dipole strength for an electronic transition between the states Ψ_0 and Ψ_f can be calculated as,

$$D_{0f} \;=\; \langle\tilde{\Psi}_0\,|\,\mu\,|\,\Psi_f\rangle\,\langle\tilde{\Psi}_f\,|\,\mu\,|\,\Psi_0\rangle, \tag{2.50}$$

here μ is the dipole moment operator defined by Eq. (1.38b). Further, D_{0f} is related to the oscillator strength, f_L, as,

$$f_L \;=\; \frac{2\,m_e}{3\,\hbar^2\,e^2}\,(\Delta E)\,D_{0f}, \tag{2.51}$$

where $\Delta E \;=\; (E_f \;-\; E_0)$ is the electronic transition energy between the states Ψ_0 and Ψ_f.

2.4 Basis Sets in Brief

The *ab initio* study of any atomic/molecular system essentially involves the introduction of a basis set. A basis set is a set of known functions, $\{\chi_i\}$, which is used to construct a wavefunction[4], Φ, as [12, 116],

$$\Phi \;=\; \sum_{i\,=\,1}^{M} C_i\,\chi_i, \tag{2.52}$$

where C_i are the expansion coefficients and M is the total number of basis functions. A wavefunction formed from the known basis functions is not an approximation if the basis set is complete. Nevertheless, an exact wavefunction is extremely difficult to realize in actual calculations as a complete basis set requires a very large number of basis functions and hence, large computational resources. Thus, one has to choose a set of functions which has optimal qualities from the computational point of view while producing the desired accuracy of the wavefunction for a particular problem.

In principle, the basis functions can be of several types: exponential, Gaussian, plane wave, polynomial, etc. However, two types of basis functions: Slater type orbitals (STOs) and Gaussian type orbitals (GTOs), are commonly used for atomic/molecular

[4]This wavefunction is the electronic wavefunction for atomic/molecular structure calculations.

structure calculations. Mathematically, STOs can be defined as [116, 121],

$$\chi_{\xi,n,l,m}(r,\,\theta,\,\phi) \;=\; N\,Y_{l,m}(\theta,\,\phi)\,r^{n-1}\,e^{-\xi r}, \tag{2.53}$$

where N is the normalization constant, n is the principle quantum number, r is the radial distance, and $Y_{l,m}(\theta,\,\phi)$ are the spherical harmonic functions. The parameter ξ is called Slater orbital exponent. The GTOs, on the other hand, can be described as [116, 121],

$$\chi_{\zeta,n,l,m}(r,\,\theta,\,\phi) \;=\; N\,Y_{l,m}(\theta,\phi)\,r^{2n-2-l}\,e^{-\zeta r^2}, \tag{2.54}$$

with ζ being the exponent of the Gaussian function.

The major difference between STO and GTO is the dependence on the radial variable in the exponent. The presence of the r^2 term in the exponent of GTOs forces them to have zero slope at the nucleus and also, GTOs fall off more rapidly away from the nucleus than STOs. These features indicate that more GTOs are required (roughly three times) than STOs to achieve the same level of accuracy [116]. Nevertheless, the electron integral calculations are easier and faster with the GTOs than STOs. Therefore, GTOs are considered to form the most successful expansion set to perform electronic structure calculations [117, 127].

The smallest basis set that includes only one basis function for each filled atomic orbital is called minimal basis set. For example, minimal basis set for H and He atom is single s - function (1s); for second - row elements, it includes two s - functions (1s, and 2s) and one p - function (p_x, p_y, p_z). On the other hand, the commonly used double - zeta (DZ) basis sets incorporate two functions for each atomic orbital, while triple - zeta (TZ) uses three, and so on. Depending upon the nature of the molecular property to be calculated, the accuracy of the results can be improved either by the inclusion of core functions or by the inclusion of diffuse functions to the basis sets. To mention, the valence properties such as electric moments and polarizabilities largely

depend on tail part of the wavefunction and therefore, additional diffuse functions are required for the accurate description of the outer part of the wavefunction [116]; the properties such as HFS, $\mathcal{P}$ & $\mathcal{T}$ - odd interaction constants depend on the wavefunction near the nuclear region and hence, extra core functions are required for accurate calculations.

If one diffuse function at each angular momentum (L) level is added to the basis set, the basis set is known as singly augmented (s - aug -) basis set, if two diffuse functions are added, the basis set is known as doubly augmented (d - aug -) basis set, and so on. On the other hand, if tight functions are added to the basis set to determine the core - core and core - valence correlations, the basis set is known as core - valence (CV -) basis set.

In this thesis, we have used cc - pVXZ[5] (X = D, T, Q) basis sets of Dunning *et al.* and Koput *et al.* [128, 129] for the lighter elements, and Dyall basis sets[6] [130] of a similar standard for the heavier elements.

2.5 Diagonal Born - Oppenheimer Correction

For the majority of the molecular calculations, the BOA discussed in Section (2.1), is a very good approximation. However, demand in the high accuracy calculations for ro - vibrational spectroscopy, quantum nuclear dynamics, molecular properties involving different isotopes, etc., require the inclusion of finite nuclear mass effects [131–134]. These effects can be included in the PEC via first - order adiabatic correction to the electronic energy calculated using BOA. This adiabatic correction is known as

[5]The exponents for s- and p basis functions are optimized using the HF method, whereas the exponents for the polarized functions: $d, f, g, \ldots$, are obtained using the CISD method.

[6]These basis sets are optimized using the DF Hamiltonian with Gaussian nuclear charge distribution.

diagonal Born - Oppenheimer correction (DBOC) that can be evaluated using [135],

$$\Delta E_{DBOC} = -\frac{\hbar^2}{2}\sum_{A=1}^{N}\frac{1}{M_A}\sum_{i=x,y,z}\langle\Psi_{el}|\,\nabla^2_{R_{Ai}}\,|\Psi_{el}\rangle, \tag{2.55}$$

where M_A is the mass of the nucleus A and $\nabla_{R_{Ai}} = \frac{\partial}{\partial R_{A_i}}$; R_{Ai} are the nuclear coordinates. The details of this correction term at different levels of correlation methods can be found in Refs. [136–138].

2.6 Softwares for Structure Calculations

Several software packages such as CFOUR [139], GAUSSIAN [140], GAMESS [141], MOLPRO [142], DIRAC [143], MOLCAS [144], LEVEL [145], etc., have been developed for performing the structure calculations of atomic and molecular systems at various levels of correlation. Most of these softwares can be run on UNIX operating systems. In the current section, we briefly discuss the capabilities of the softwares that are used to calculate the spectroscopic constants and molecular properties of diatomic molecules, reported in this thesis.

2.6.1 CFOUR

Coupled - Cluster techniques for Computational Chemistry (CFOUR) is a software suite developed by Stanton *et al.* [139] for performing atomic and molecular properties based on Møller - Plesset perturbation theory and CC theory at the non - relativistic level. Further, the DBOC, thermodynamic and several relativistic corrections can be calculated with this software.

The ground state calculations for various spectroscopic constants and molecular properties can be performed with various approximations such as HF, CCSD, CCSD with partial triples [CCSD(T)], CCSDT, linearized CCSD (LCCSD), LCCSD(T),

LCCSDT, CISD, CISD including triples (CISDT), etc. The calculations of excited electronic states of molecules for their PECs, equilibrium geometries, harmonic frequencies, rotational constants, anharmonic constants, PDMs, static DP components, QMs, oscillator strengths, TDMs between the electronic levels can be performed using different theoretical approaches such as CI, EOM - CC method, etc. The correlation calculations beyond the quadrupole excitation can be performed with the MRCC program [146] interfaced to CFOUR. CFOUR program reads the ZMAT input file that includes the information about atoms, basis sets, correlation method for the calculation of molecular properties (SCF and correlation energies, molecular geometries, first - and second - order properties, etc.). A sample input to calculate energy and first - order properties of singly charged BeLi molecule at SCF and CCSD(T) level of theory for the cc - pVQZ basis set is shown in Appendix (B.1).

2.6.2 DIRAC

Direct Iterative Relativistic Atomic and Molecular Code (DIRAC) developed by Bast *et al.* [143] is a program package for performing the relativistic calculations on atoms and molecules. A number of theoretical methods such as DF - SCF, CI, CCSD, CCSD(T), second - order MBPT (MBTP2), KRCI, and KRMCSCF (Kramers - restricted multiconfiguration SCF), etc., have been implemented in this package together with the 2 - component, and 4 - component Hamiltonians. These theoretical methods can be used for performing various calculations for the ground electronic state, *viz.*, the energies, Mulliken population analysis, DPs, dipole moments, hyperpolarizabilities, QMs, and magnetic properties, etc. In addition, the EOM - CC and KRCI methods are available for calculating excited state properties: energies, dipole moments, TDMs between the electronic states, etc.

DIRAC software requires two input files, (1) $*.mol$ file that includes the information about molecular geometry, symmetry group and the basis set used for the cal-

culation, and (2) $*.inp$ file that seeks the required theoretical method, Hamiltonian, energy threshold, nuclear charge distribution, active space, etc., for calculating any particular property specified in the same file. A few sample input files for the DIRAC program are given in Appendix (B.2).

2.6.3 MOLCAS

Molecular Complete Active Space (MOLCAS) is a quantum chemistry package developed by Karlström *et al.* [144] is useful for calculating the spectroscopic constants and properties of molecules using multi - configurational approach where the single - reference determinant is not enough to define the actual state of the system. Various methods, such as complete active space SCF (CASSCF), restricted - active space SCF (RASSCF), generalized active space SCF (GASSCF), complete - active space second - order perturbation theory (CASPT2), multi - reference configuration interaction (MRCI) and multiconfiguration Pair - Density Functional Theory (MCPDFT) etc., based on multi - configuration approach are available in MOLCAS.

The VIBROT (A Program to determine vibration - rotation spectrum of Diatomic Molecules) module of the MOLCAS package is available for performing the vibration - rotation spectroscopic calculations of diatomic molecules. This program can be used independently by feeding the numerical data of the PEC and PDM curve as input. The cubic - spline fitting is available to interpolate the given potential. The ro - vibrational parameters such as vibrational energies, rotational constants, vibrational wavefunctions and TDMs between the vibrational levels can be computed by solving the vibrational Schrödinger equation numerically using Numerov's method. The sample input file for the VIBROT program to calculate vibrational parameters is provided in Appendix (B.3).

2.6.4 LEVEL

LEVEL is a FORTRAN program written by Le Roy [145] that can be used for solving the nuclear Schrödinger equation for bound and quasi - bound levels. A number of analytical functions are available to generate potential energy functions. Further, the potential energy functions can be corrected with the atomic - mass - dependent Born - Oppenheimer breakdown correction. Depending upon the number of data points, point piecewise polynomials/ cubic spline interpolation/ low - order piecewise polynomials can be used for the interpolation. On the other hand, the inward extrapolation can be performed using an exponential function fitted to three turning points and outward extrapolation can be performed either as an exponential - type function or as a sum of inverse - power terms. This program can be used for the calculation of (i) vibrational - rotational energies, rotational constants, centrifugal distortion constants, etc., for the vibrational levels of a single PEC (ii) TDMs, FCFs and radiative lifetimes for all allowed transitions between the vibrational - rotational levels of a single molecular state or of two different electronic states of a molecule. The sample input file for the LEVEL program is given in Appendix (B.4).

CHAPTER 3

SPECTROSCOPIC CONSTANTS AND MOLECULAR PROPERTIES OF $BeLi^+$

"The shortest interval between two points is the awareness that they are not two" – Eric Micha'el Leventhal

3.1 Introduction

The diatomic molecules containing alkaline - earth elements have been studied extensively for over decades and yet, they continue to attract the attention of both experimentalists and theorists alike even today. Some of the AEMFs have been laser cooled and trapped [147–153] for the study of fundamental symmetry violating effects [5–7, 154, 155]. The alkaline - earth - monohydrides (both AEH and AEH^+) have been observed in several astrophysical atmospheres such as solar, stellar, cometary and interstellar medium [156–160]. They have been studied both the-

oretically [161–169] and experimentally [72, 170, 171]. The BeH molecules have been considered for the molecular diagnostics of the fusion plasmas such as the one used in International Thermonuclear Experimental Reactor (ITER) [162, 172, 173]. Further, MgH^+, CaH^+ and SrH^+ have been proposed for the tests of temporal variation in the fundamental physical constants such as m_p/m_e ratio [174].

The diatomic molecules containing alkali - and alkaline - earth metals have strong long - range interactions owing to their large dipole moments [99, 100, 175]. Their spectroscopic constants and molecular properties have been investigated by several research groups [1, 2, 99, 100, 176]. Both CaLi and SrLi molecules have also been proposed for the study of possible variation in m_p/m_e [49]. To observe the ultracold atom - ion interactions, the elastic collisions between laser - cooled fermionic lithium atoms and calcium ions have been studied by Haze *et al.* [3]. The long lifetimes of the highly excited vibrational states in $LiBe^+$, $LiMg^+$, $NaBe^+$ and $NaMg^+$ enable these molecules to be used in ultracold experiments [177].

The $BeLi^+$ ion is the simplest ionic system among alkali - alkaline - earth molecular ions. Although, there is no experimental data available for this system yet, to the best of our knowledge, it is being considered by Rakshit *et al.* [1] and Ghanmi *et al.* [2]. There exist, however, several calculations in the literature, such as, the calculation of spectroscopic constants of 1-2 $^1\Sigma^+$ and 1 $^3\Sigma^+$ using SCF method by Safonov *et al.* [178], theromodynamical stability and physicochemical reaction of several molecular ions including $BeLi^+$ by Nicolaides *et al.* [179], the calculation of ground state spectroscopic constants at MP2 (full) level by Boldyrev *et al.* [180] using the Gaussian 92 program, calculations of the ground state and low - lying $^1\Sigma^+$ electronic states of $BeLi^+$ by Farjallah *et al.* [181] using full valence CI, the studies of ground - and first excited state PECs for predicting the feasibility of the formation of cold molecular ion via photoassociation process by Rakshit *et al.* [1], studies of the ground - and several low - lying excited states by Sun *et al.* [182] using MRCI + Q method and

multi - reference averaged quadratic coupled - cluster (MRAQCC) methods including Davidson correction. An *ab initio* study of ground - and low - lying excited states has been done by You *et al.* [183] using MRCI method. Recently, Ghanmi *et al.* [2] have reported their theoretical investigations for a large number of excited electronic states of $BeLi^+$ molecular ion. Those authors have reported the PECs, spectroscopic constants, PDM curves, and also the TDM curves for several of these excited states for the first time, and use those results for the photoassociation prediction of $BeLi^+$ molecular ion. Their calculations are based on the full CI method, however, considering only two active valence electrons that are moving in the field of Be^{2+} and Li^+ cores using the pseudo - potential approach. More recently, spectroscopic constants and vibrational state lifetimes of diatomic alkali - alkaline - earth cations have been studied by Fedorov *et al.* [177]. An accurate knowledge of spectroscopic constants would always be advantageous both theoretically and experimentally. However, the non - inclusion of all electrons and lack of higher basis sets in the calculations may not lead to the level of accuracy desirable for experimental purposes.

In the present work, in order to achieve reliable accuracy, we have employed the higher levels of correlation methods and also used a successive hierarchy of three optimized basis sets, which enable us to extrapolate the results easily to the CBS limit. This is required to achieve saturation of the results with respect to the basis set size effects. The configuration space considered for electron correlation calculations in our work is also quite large compared to many of the previous works. Thus, the spectroscopic constants, PECs and PDM curves for the ground state ($X\,^1\Sigma^+$) of $BeLi^+$ are calculated systematically and more accurately in our work when compared to many of those available in the literature. In addition, we have calculated the components of DP and the QM for the ground state of $BeLi^+$ ion, which are being reported for the first time known to our knowledge. Using PEC calculated at the CCSD(T) level of correlation for the QZ basis set, vibrational Schrödinger equation is solved to obtain the spectroscopic parameters of vibrational energy levels. Thereafter, we have

studied low - lying excited electronic states and their vibrational spectroscopy at the EOM - CCSD level of correlation. We hope that our results would be useful for the experimentalists who are seeking accurate theoretical data for $BeLi^+$ molecular ion.

3.2 Methodology

CFOUR [139] and DIRAC15 [143] software suites are used to carry out the non - relativistic and relativistic ground state calculations, respectively, of the spectroscopic constants such as: R_e, D_e, ω_e, $\omega_e x_e$, B_e, and α_e together with the molecular properties such as: μ_0, Θ_{zz}, and components of static DP ($\alpha_{\parallel}$, $\alpha_{\perp}$) at MP2, CCSD, and CCSD(T) level of correlation. The uncontracted cc - pVXZ and aug - cc - pVXZ basis sets of Dunning *et al.* [128] with X = [D, T, Q], available in the DIRAC15 package, are used in the present calculations. The details of the basis sets used in this work are shown in Table (3.1). The nuclear mass of 9.0121822 amu for Be and of 7.0160030 amu for Li has been used. Further, only for calculational purpose, C_{2v} molecular point

Table 3.1: Details of the basis sets for Be and Li in uncontracted form.

Atom	Basis
Be	cc - pVDZ: 9s, 4p, 1d
	cc - pVTZ: 11s, 5p, 2d, 1f
	cc - pVQZ: 12s, 6p, 3d, 2f, 1g
Li	cc - pVDZ: 9s, 4p, 1d
	cc - pVTZ: 11s, 5p, 2d, 1f
	cc - pVQZ: 12s, 6p, 3d, 2f, 1g

group symmetry has been used in our calculations. Furthermore, the origin of the coordinate system is chosen at the center - of - mass of the molecule. All the electrons are kept active both for diatomic constants and also for property calculations. Furthermore, the energies and PDMs are calculated for the range 0.4 - 30 Å with a step size of 1 Å and around the known equilibrium point a finer step size of 0.001 Å is adopted. The maximum distance of 30 Å is chosen based on the saturation of

energies limited to the threshold set. The dissociation energies (D_e) are evaluated by taking the difference between the energies at equilibrium bond length and those at a distance of 30 Å.

For non - relativistic calculations, the basis sets have been taken from the EMSL library [184]. The harmonic frequencies and anharmonic constants are calculated using the second - order vibrational perturbation theory, i.e., with VPT2 keyword in the CFOUR package. By convention, the internuclear axis is taken to be along the z - direction, (i.e., along internuclear axis) and hence, $\alpha_{zz} \equiv \alpha_{\parallel}$. Similarly, on calculating the other two perpendicular components ($\alpha_{\perp}$) of DP (i.e., α_{xx} and α_{yy}), we have obtained the average ($\bar{\alpha}$) and the anisotropic (γ) polarizability components according to the Eq. (1.51) and Eq. (1.52), respectively.

Further, we have performed vibrational spectroscopic calculations for the ground electronic state using VIBROT program available in MOLCAS package [144]. PEC and dipole moment data for bond distance varying from 0.4 to 30 Å at CCSD(T) level of correlation are used to obtain vibrational wavefunctions, vibrational parameters: E_v, B_v and TDMs between the vibrational levels.

The spontaneous - ($\Gamma^{spon}_{v,J}$) and black - body radiation - (BBR -) induced transition rates ($\Gamma^{BBR}_{v,J}$) at the surrounding temperature, *viz.* $T = 300$K, are calculated using TDM and relative energy differences between the vibrational levels as [185],

$$\Gamma^{spon}_{v,J} = \sum_{v'',J''} \Gamma^{emis}(v,\, J \rightarrow v'',\, J''), \tag{3.1}$$

$$\Gamma^{BBR}_{v,J} = \sum_{v'',J''} \bar{n}(\omega)\, \Gamma^{emis}(v,\, J \rightarrow v'',\, J'') + \sum_{v',J'} \bar{n}(\omega)\, \Gamma^{abs}(v,\, J \rightarrow v',\, J'), \tag{3.2}$$

where the indices (v'', J'') and (v', J') denote the ro - vibrational levels with energies lesser and higher than that of (v, J) level, respectively. The average number of

photons $\bar{n}(\omega)$ at frequency ω is given by the relation,

$$\bar{n}(\omega) = \frac{1}{e^{(\hbar\omega/k_B T)} - 1}, \tag{3.3}$$

where $\hbar\omega = |E_{v,J} - E_{\tilde{v},\tilde{J}}|$ is the energy difference between the two ro - vibrational levels involved, with $(\tilde{v}, \tilde{J})$ is (v'', J'') for emission and (v', J') for absorption, and k_B is the Boltzmann constant. In dipole approximation, the emission and absorption rates are calculated using the equation,

$$\Gamma\,(v,\, J \rightarrow \tilde{v},\, \tilde{J}) = \frac{8\,\pi}{3\,\epsilon_0}\,\frac{1}{h\,c^3}\,\omega^3\,(TDM_{v,J\rightarrow\tilde{v},\tilde{J}})^2. \tag{3.4}$$

Finally, the lifetimes (τ) of the ro - vibrational states are obtained as,

$$\tau = \frac{1}{\Gamma^{total}}, \tag{3.5}$$

where $\Gamma^{total}(= \Gamma^{spon} + \Gamma^{BBR})$ is the of sum of spontaneous - and BBR - induced transition rates.

Further, we have also studied a few low - lying electronic excited states using EOM - CCSD/QZ method. The details of EOM - CCSD method are discussed in Section (2.3.3). Similar to the ground state, all electrons are kept active for the excited state calculations.

For the relativistic case, on the other hand, the Dirac - Fock - Coulomb Hamiltonian is used with the DIRAC15 package. The contribution from the (SS|SS) integrals is taken in an approximate manner, as suggested in Ref. [186], by including an interatomic (SS|SS) correction. The energy calculations at MP2, CCSD and CCSD(T) levels are carried out with the RELCCSD module [187]. The VIBROT program of MOLCAS is used for calculating the spectroscopic constants. The results calculated systematically using the three progressively large basis sets, both for relativistic and non - relativistic

cases, are extrapolated to CBS limit using a function of the form [188, 189],

$$f(x) = f_{CBS} + B\, e^{-(x-1)} + C\, e^{-(x-1)^2}, \tag{3.6}$$

where B and C are constant parameters, $x\,(=\ 2,\ 3,\ 4)$ is the cardinal number for basis sets DZ, TZ and QZ, respectively. Here, $f(x)$ is the property that is calculated with the basis set characterized by cardinal number x and f_{CBS} is the complete basis set limit for the property of interest.

The estimation of uncertainty on the results of the calculated quantities, in general, is little involved; there can be two possible error sources: one arising due to the choice of the basis set (*viz.* the size) and the other arising from the negligence of higher order correlation effects beyond what is considered in the present work. As we have done a series of calculations with a successive hierarchy of optimized basis sets, and extrapolated the results systematically to the CBS limit, we least expect the error to come from the former source. As the contributions from the higher order correlation effects are not expected to be larger than that of the leading order triples considered perturbatively in our work, we have quoted the entire contribution from the latter, i.e. CCSD(T) - CCSD at CBS level, as the maximum possible error bar (Δ) on our results. Thus, we recommend the final result, f_{final}, of the calculated property to be,

$$f_{final} \ = \ f_{CCSD(T)@CBS} \ \pm \ (|\Delta|), \tag{3.7}$$

where $f_{CCSD(T)@CBS}$ is the CBS value of the property of interest at CCSD(T) level.

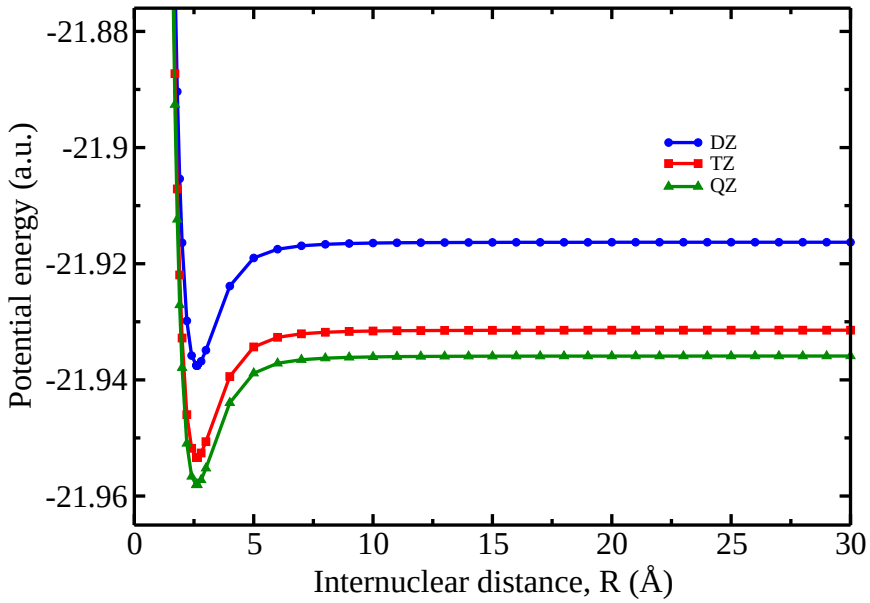

Figure 3.1: Potential energy curves for the ground state of $BeLi^+$ using CCSD(T) method, in the non - relativistic case.

3.3 Results and Discussion

3.3.1 Ground State Parameters

Figures (3.1) - (3.2) show the PECs for the ground state of $BeLi^+$, obtained at the CCSD(T) level of correlation with DZ, TZ and QZ basis sets, using the non-relativistic and relativistic Hamiltonian, respectively. The spectroscopic constants computed, using the non - relativistic Hamiltonian, at various levels of correlation, considered in this work, are shown in Table (3.2). In addition, the results extrapolated to CBS limit at each level of correlation are also shown. Our results of the spectroscopic constants show a good agreement with those available in the literature [2, 177–183, 190]. The difference between our CBS values at the SCF level and those quoted in Ref. [178] is not more than 7% in all the spectroscopic constants barring the anharmonic constant. The latter which depends on other diatomic constants shows a larger deviation. The MP2 results of Ref. [180] also compare quite well with our results at the similar level of approximation. The results reported in Ref. [181], calculated at full valence CI

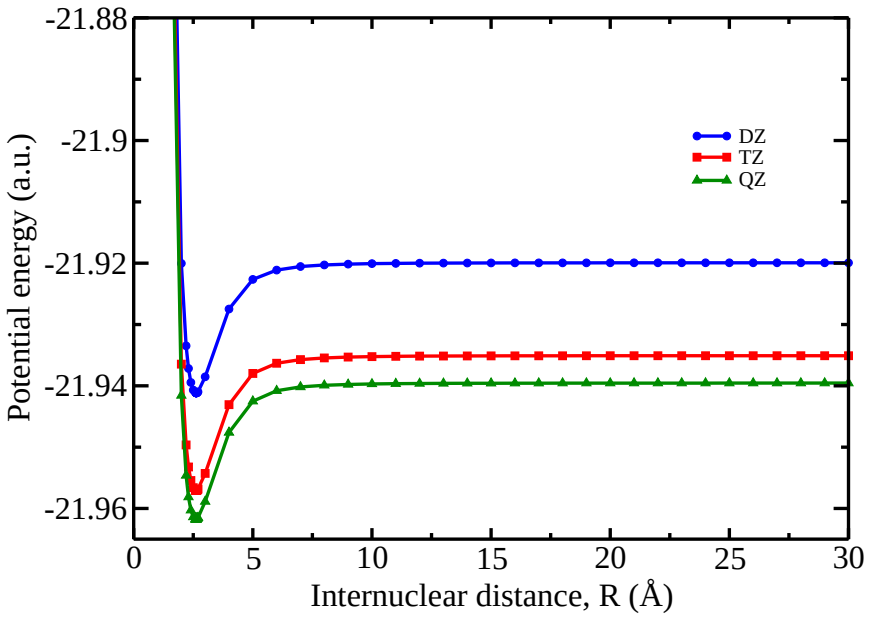

Figure 3.2: Potential energy curves for the ground state of $BeLi^+$ using CCSD(T) method, in the relativistic case.

level and our recommended CCSD(T) values, highlighted in bold fonts, agree extremely well. Leaving aside the anharmonic constant, the difference between our CBS results at CCSD(T) level and those reported in Ref. [183] and Ref. [2] at MRCI and valence FCI level of correlation, respectively, is less than 3% for all diatomic constants. The values for R_e, D_e and ω_e obtained in the current work at CCSD(T) level with cc-pVQZ basis set are very close to those reported in Ref. [177] at MRCI level of correlation with cc-pCVQZ basis set. The difference between present results for R_e, D_e and ω_e using cc-pVQZ basis set and CCSD(T) method is not more than 1.2% from those reported in Ref. [177] at CCSDT level with cc-pCVQZ basis set. The fundamental vibrational frequency (ω_0) of $BeLi^+$ ion calculated via equation, $\omega_0 = \omega_e(1 - 2x_e)$, using the CBS results of ω_e and $\omega_e x_e$ at the CCSD(T) level of theory is 314.26 cm^{-1}.

In order to understand the dissociative nature of the ground state of $BeLi^+$, we have calculated the ionization energy using the electronic state energy of neutral

Table 3.2: The computed spectroscopic constants for the ground state of $BeLi^+$, in the non-relativistic case. Comparison with the available results in the literature.

Basis	Method	$R_e\,(a_0)$	$D_e\,(\mathrm{cm}^{-1})$	$\omega_e\,(\mathrm{cm}^{-1})$	$\omega_e x_e\,(\mathrm{cm}^{-1})$	$B_e\,(\mathrm{cm}^{-1})$	$\alpha_e\,(\mathrm{cm}^{-1})$
DZ	SCF	5.006	5068	305	5.01	0.608	0.0138
	MP2	4.966	4994	320	4.80	0.618	0.0130
	CCSD	4.957	4644	318	4.84	0.621	0.0131
	CCSD(T)	4.955	4655	318	4.93	0.621	0.0131
TZ	SCF	5.008	5105	302	5.16	0.608	0.0139
	MP2	4.947	5145	324	4.82	0.623	0.0129
	CCSD	4.942	4799	319	4.84	0.624	0.0131
	CCSD(T)	4.940	4812	319	4.82	0.625	0.0131
QZ	SCF	5.004	5116	300	5.15	0.609	0.0144
	MP2	4.930	5222	326	4.95	0.627	0.0132
	CCSD	4.927	4859	321	4.86	0.628	0.0134
	CCSD(T)	4.923	4868	322	4.85	0.629	0.0133
CBS	SCF	5.001	5122	299	5.14	0.610	0.0147
	MP2	4.919	5269	327	5.04	0.630	0.0134
	CCSD	4.917	4894	322	4.87	0.631	0.0136
	CCSD(T)	**4.912**	**4900**	**324**	**4.87**	**0.631**	**0.0134**
Error bar		**±0.005**	**±6**	**±2**	**±0.00**	**±0.001**	**±0.0002**
published works							
	SCF [178]	5.027	5001	320	8.2	0.601	–
	MP2 [180]	4.968	–	320	–	–	–
	MP4 [180]	–	4757	–	–	–	–
	QCISD(T) [180]	–	4617	–	–	–	–
	FCI [181]	4.96	4849	321.2	6.48	0.6395	–
	CCSD(T) [182]	4.964	–	315.5	–	0.623	–
	MRCI [183]	4.913	4903.6	318.4	4.310	0.6173	–
	FCI [2]	4.940	4862	323.7	5.45	0.6395	–
	CCSDT [177]	4.919	4881.0	325.9	5.6	–	–
	MRCI [177]	4.921	4870.7	323.3	5.1	–	–
	MRD-CI [190]	5.083	–	–	–	–	–

Table 3.3: The computed spectroscopic constants for the ground state of $BeLi^+$, in the relativistic case.

Basis	Method	$R_e\,(a_0)$	$D_e\,(\mathrm{cm}^{-1})$	$\omega_e\,(\mathrm{cm}^{-1})$	$\omega_e x_e\,(\mathrm{cm}^{-1})$	$B_e\,(\mathrm{cm}^{-1})$	$\alpha_e\,(\mathrm{cm}^{-1})$
DZ	SCF	5.005	5067	320	5.13	0.607	0.0116
	MP2	4.966	4993	322	5.05	0.616	0.0113
	CCSD	4.955	4644	320	5.13	0.619	0.0116
	CCSD(T)	4.954	4654	320	5.11	0.620	0.0116
TZ	SCF	5.006	5104	318	4.99	0.605	0.0112
	MP2	4.947	5149	323	4.73	0.619	0.0109
	CCSD	4.942	4799	321	5.24	0.622	0.0115
	CCSD(T)	4.940	4811	322	5.22	0.623	0.0114
QZ	SCF	5.003	5114	319	5.02	0.605	0.0113
	MP2	4.929	5221	327	4.99	0.622	0.0106
	CCSD	4.926	4858	324	5.31	0.626	0.0116
	CCSD(T)	4.922	4868	324	5.30	0.627	0.0116
CBS	SCF	5.001	5119	320	5.05	0.605	0.0114
	MP2	4.917	5264	330	5.18	0.624	0.0104
	CCSD	4.916	4893	326	5.35	0.629	0.0116
	CCSD(T)	**4.910**	**4901**	**325**	**5.35**	**0.630**	**0.0117**
Error bar		**±0.006**	**±8**	**±1**	**±0.00**	**±0.001**	**0.0001**

BeLi and singly charged ion, $BeLi^+$. We have found that the first ionization energy of BeLi is 43437 cm^{-1}, which agrees with the ionization energy (= 43487.1 cm^{-1}) of Li atom but not with the ionization energy (= 75192.6 cm^{-1}) of Be atom, reported in NIST database [191]. Therefore, we can say that the ground state of $BeLi^+$ will dissociate as $Be + Li^+$. In addition, D_e calculated by taking the difference between the sum of Be and Li^+ energies, and the energy at the equilibrium point of $BeLi^+$ molecule in the PEC reassures the dissociative atomic states of $BeLi^+$ is atomic Be and ionic Li.

The results of spectroscopic constants derived from the PECs computed using the relativistic Hamiltonian are given in Table (3.3). Except for $\omega_e x_e$ and α_e, we did not observe an appreciable difference between the relativistic and non-relativistic results of other spectroscopic constants. Thus, we continue to use the non - relativistic Hamiltonian for the calculation of molecular properties such as dipole moments, QMs,

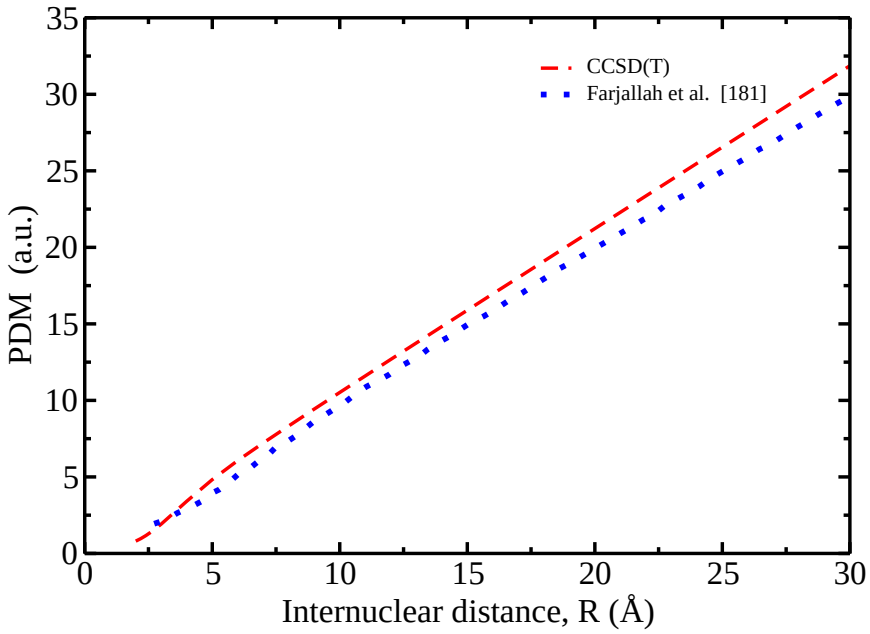

Figure 3.3: Permanent dipole moment curve for the ground state of $BeLi^+$ using CCSD(T)/QZ method.

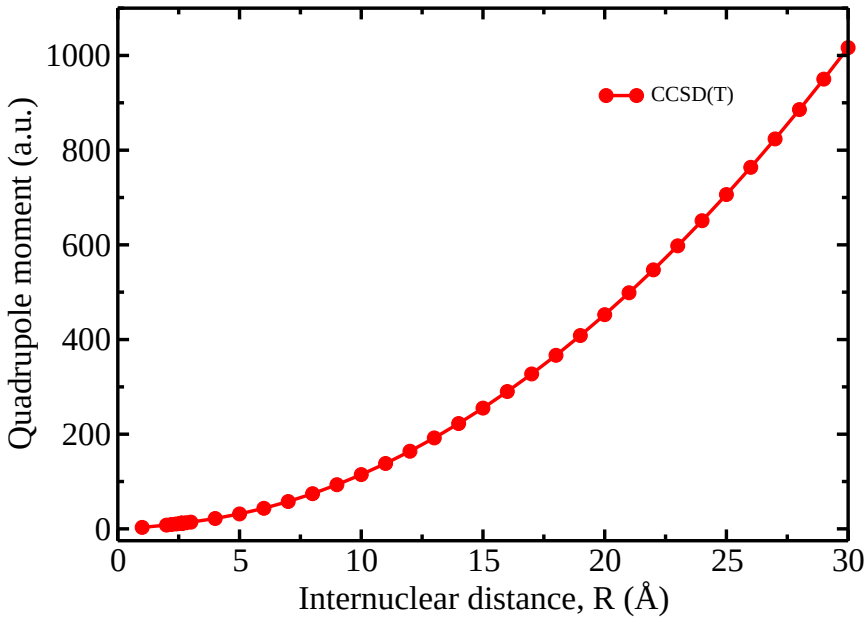

Figure 3.4: Quadrupole moment curve for the ground state of $BeLi^+$ using CCSD(T)/QZ method.

components of static DP and parallel - component of the DP at super molecular limit (100 a.u.) symbolized as α_{100}, and these results are tabulated in Table (3.4). Figure (3.3) shows the absolute value of PDM as a function of internuclear distance R at CCSD(T) level of correlation using QZ basis set. This dipole moment curve shows an almost linear behaviour from 6 Å to 30 Å exactly in agreement with that reported by Farjallah *et al.* [181]. The value of PDM at equilibrium point reported in the current work using CCSD(T) method is 0.005 a.u. larger and 0.018 a.u. smaller than those reported in Ref. [177] at CCSDT and MRCI levels of theory, respectively, at the similar standard of basis set. We have observed that, as we go towards the higher basis set, the results for spectroscopic constants and molecular properties converge. Further, the R - variation of QM and components of DP at CCSD(T) level of correlation using QZ basis set is shown in Figure (3.4) and Figure (3.5), respectively. The complete list of the computed values of potential energies, PDMs, QMs and DPs are collected together and are reported in the Supplementary Table S1 of Ref. [108].

Table 3.4: The permanent dipole moments (in units of $e\,a_0$), quadrupole moments (in units of $e\,a_0^2$), components of dipole polarizabilities (in units of $e^2\,a_0^2\,E_h^{-1}$) at the equilibrium point, and polarizabilities (in units of $e^2\,a_0^2\,E_h^{-1}$) at super-molecular limit, for the ground state of $BeLi^+$.

Basis	Method	$\lvert\mu_0\rvert$	Θ_{zz}	$\alpha_\parallel$	$\alpha_\perp$	$\bar{\alpha}$	γ	α_{100}
DZ	SCF	1.274	12.642	46.086	36.843	43.005	9.243	44.586
	MP2	1.335	12.713	43.881	34.285	37.483	9.596	40.403
	CCSD	1.449	11.732	42.010	32.071	35.384	9.939	35.921
	CCSD(T)	1.450	11.712	41.942	32.006	35.318	9.936	35.838
TZ	SCF	1.276	12.622	45.941	36.713	42.865	9.228	45.520
	MP2	1.310	12.130	43.652	34.306	37.421	9.346	41.348
	CCSD	1.421	11.711	42.223	32.347	35.639	9.876	37.012
	CCSD(T)	1.422	11.687	42.143	32.273	35.563	9.870	36.911
QZ	SCF	1.274	12.621	45.895	36.745	42.845	9.150	45.721
	MP2	1.291	12.097	43.499	34.407	37.438	9.092	41.572
	CCSD	1.405	11.680	42.197	32.466	35.710	9.731	37.191
	CCSD(T)	1.406	11.645	42.087	32.363	35.604	9.724	37.037
CBS	SCF	1.273	12.621	–	–	42.836	9.098	45.826
	MP2	1.279	12.095	–	–	37.452	8.929	41.691
	CCSD	1.395	11.660	–	–	35.749	9.635	37.274
	CCSD(T)	**1.396**	**11.617**	–	–	**35.623**	**9.628**	**37.085**
Error bar		**±0.001**	**±0.043**	–	–	**±0.126**	**±0.007**	**±0.189**
	CCSDT [177]	1.401	–	–	–	–	–	–
	MRCI [177]	1.424	–	–	–	–	–	–

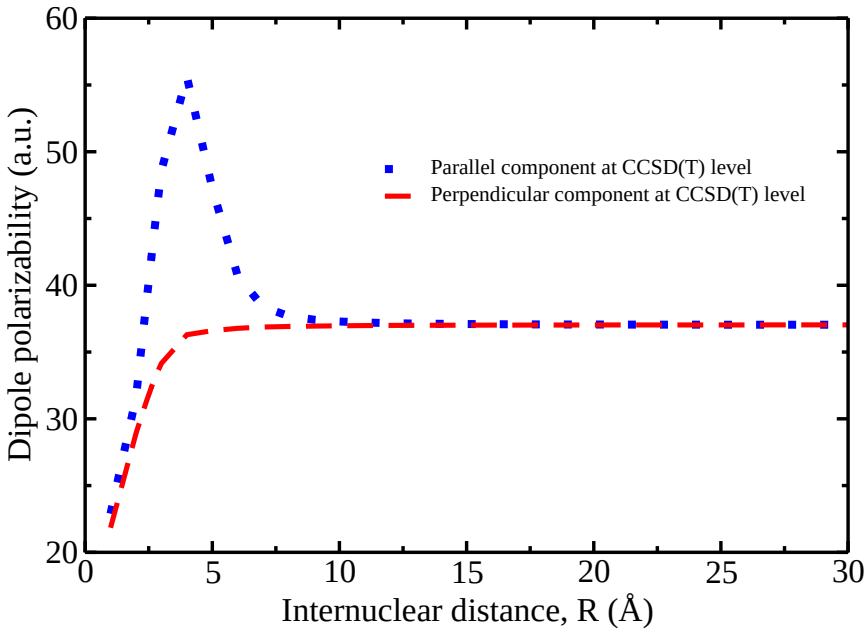

Figure 3.5: Components of dipole polarizability of $BeLi^+$, as a function of R, using CCSD(T)/QZ method.

The augmentation of the basis sets with diffuse functions does not appreciably alter the results of the spectroscopic constants and the molecular properties. The difference in our final results between the augmented and un-augmented basis sets is about 0.001 a.u. in R_e, 1 cm^{-1} in both D_e and ω_e, 0.2 cm^{-1} in $\omega_e x_e$, 0.0003 cm^{-1} in B_e, 0.0001 cm^{-1} in α_e, 0.0004 a.u. in both μ_0 and Θ_{zz}, 0.066 a.u. in $\bar{\alpha}$, and 0.051 a.u. in γ, at the CCSD(T) level. All of these, except $\omega_e x_e$ and γ, are well within the error bars that we have reported in Table (3.2) and in Table (3.4). The polarizability results, with and without augmentation, in the super-molecular limit seem to have a noticeable difference. At the CCSD(T) level, the CBS value of $\alpha_{100} = (37.944 \pm 0.167)$ a.u. with augmented basis set, while $\alpha_{100} = (37.085 \pm 0.189)$ a.u. without augmentation. The former is significantly close to the sum of atomic polarizabilities (α_A) of the Be [127] and Li^+ [192], *viz.*, $\alpha_{Be} + \alpha_{Li^+} = 37.71 + 0.191 = 37.901$ a.u. Due to the unavailability of experimental value of polarizability for Li^+ in the literature, we have taken its calculated value at the CCSD(T) level from the Ref. [192], and combined it with the experimental value for Be. The recent work in Ref. [2] also

reports $\alpha_{Be} = 37.4932$ a.u., which lies almost in the middle of our two estimates for α_{100} discussed above.

In order to understand the effects of higher - order electron correlation, beyond the CCSD(T) level considered here for most of the calculations, we have performed potential energy calculations at the CCSDT level using QZ basis set. The difference in the potential energies calculated using CCSD(T) and CCSDT method, in the vicinity of equilibrium point is about 9 cm^{-1}, while at the dissociative limit, it is about 6 cm^{-1}. We have found that the values of R_e and B_e remain unaffected by the inclusion of missing non - leading order triples to CCSD(T) at least for up to the accuracies reported in this work. On the other hand, the value of D_e increases by 3 cm^{-1}. These contributions are well within the error bars that we have quoted in Table (3.2). Further, the adiabatic effects are also estimated by including the DBOC at the CCSD level of theory using QZ basis set. The calculated DBOC energy correction is significantly large, about 332 cm^{-1}, similar to that reported for BeH molecule in Ref. [132]. However, the consideration of DBOC for the energy in our calculation does not seem to alter the R_e as well as the D_e results since it has been observed to be more or less uniform throughout the region of PEC of $BeLi^+$. The computed values of DBOC are given in the Supplementary Table S2 of Ref. [108].

Using PEC and PDM curve obtained at CCSD(T) level of correlation with QZ basis sets, we have solved the vibrational Schrödinger equation taking the rotational quantum number, $J = 0$, and obtained the vibrational parameters. The vibrational parameters: E_v, B_v, μ_v, $\Gamma^{spon}_{v,0}$, and $\Gamma^{BBR}_{v,0}$, are tabulated for some low - lying vibrational states in Table (3.5). The relative energy spacings between the adjacent vibrational states observed in this work compare well with those reported by Fedorov *et al.* [177]. However, the actual energies are different in both works because of the different reference points. In our case, we have reported the energies of vibrational states by taking minima of a potential as zero, whereas in Ref. [177], the authors have reported

Table 3.5: Energies, rotational constants, permanent dipole moments, spontaneous - and BBR - induced transition rates for vibrational levels of the ground electronic state of $BeLi^+$.

v	$E_v\,(\mathrm{cm}^{-1})$	$B_v\,(\mathrm{cm}^{-1})$	$\lvert\mu_v\rvert\,(e\,a_0)$	$\Gamma^{spon}_{v,0}\,(\mathrm{s}^{-1})$	$\Gamma^{BBR}_{v,0}\,(\mathrm{s}^{-1})$
0	159.72	0.623	1.435	–	0.214
1	471.78	0.609	1.509	0.731	0.649
2	773.92	0.596	1.588	1.426	1.102
3	1066.1	0.582	1.671	2.078	1.571
4	1348.19	0.568	1.759	2.682	2.048
5	1620.14	0.554	1.852	3.239	2.541
6	1881.78	0.539	1.951	3.726	3.018
7	2132.99	0.524	2.057	4.168	3.504
8	2373.58	0.509	2.169	4.516	3.946
9	2603.42	0.494	2.290	4.811	4.462
10	2822.31	0.478	2.418	4.978	4.932
11	3030.08	0.462	2.556	5.105	5.253
12	3226.55	0.445	2.705	5.140	5.564
13	3411.53	0.428	2.865	5.077	5.747
14	3584.84	0.410	3.039	4.913	5.945
15	3746.34	0.391	3.227	4.705	6.021
16	3895.91	0.372	3.430	4.411	5.577
17	4033.44	0.353	3.653	4.081	3.700
18	4158.92	0.332	4.151	3.013	0.930

actual energies. As expected, the value of dipole moment for $v = 0$ is close to the dipole moment calculated at the equilibrium point of the PEC. We have observed that the PDM increases as the vibrational quantum number increases because the average R ($\langle R \rangle$) increases, whereas the rotational constant decreases as it is inversely proportional to $\langle R \rangle$. It has been reported in the literature [193] that the TDMs between the vibrational states and hence, the lifetimes of vibrational states depend on the numerical grid size used for the integration for solving vibrational Schrödinger equation. In order to verify this, we have used four different grid sizes ranging from 1000 to 2200. The grid dependent TDM values used to calculate transition rates can be found in the Supplementary Table S3 of Ref. [108]. From the reciprocal of total transition rates, the lifetimes of the vibrational states are evaluated and plotted in

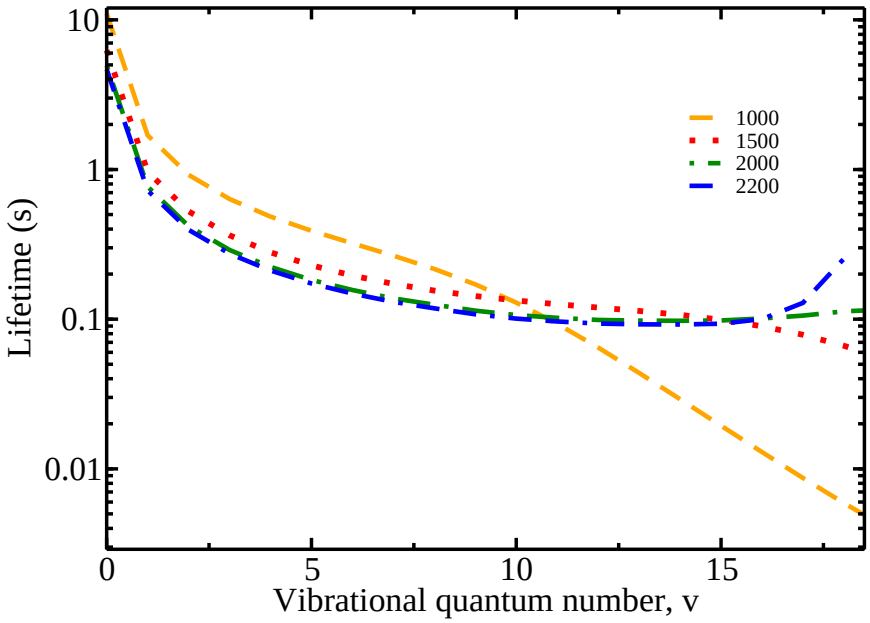

Figure 3.6: Lifetimes of the pure vibrational states of the electronic ground state of $BeLi^+$, at $T = 300$K, calculated with different grid size.

Figure (3.6) for different grid sizes. It can be seen explicitly that the lifetime curves with 2000 and 2200 grid sizes almost overlap each other upto $v = 16$ and hence, we report the lifetime for the ro-vibronic ground state to be 4.67 s calculated with 2200 grid size. This result is 1.89 s larger than the value reported in Ref. [177]. The reason for this discrepancy could be from the difference in the PDM values between the two calculations and the numerical convergence issues related to grid size considered in Ref. [177]. The lower vibrational states have longer lifetimes than that of the higher vibrational states and also, the difference between the lifetimes of consecutive states for higher 'v' is much smaller than the lower states.

3.3.2 Excited State Parameters

The PECs for the excited states: $1\,^3\Sigma^+$, $1\,^3\Pi$, $2\text{-}4\,^1\Sigma^+$ and $1\text{-}2\,^1\Pi$, as a function of internuclear distance, R, at EOM-CCSD level of theory using QZ basis set are shown in Figure (3.7). The corresponding data for the PECs is provided in the Supplemen-

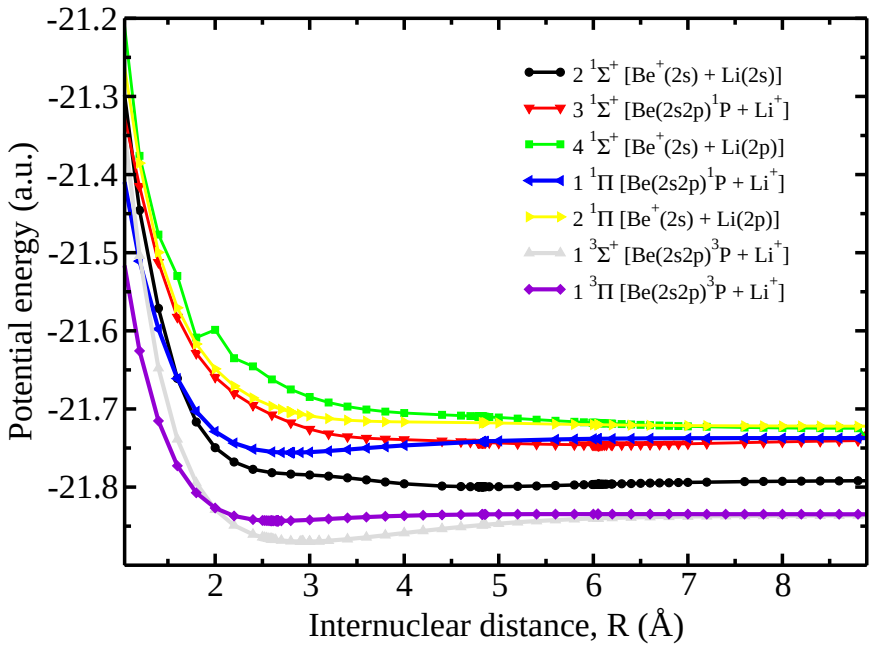

Figure 3.7: Potential energy curves for the excited states of $BeLi^+$ using EOM - CCSD/QZ method.

tary Table S4 of Ref. [108]. These calculations are performed using the EOM - CCSD method alone due to the current unavailability of higher - order EOM - CC methods. By extracting the spectroscopic constants from the PECs of the excited states, and on comparing them with the available results, we have confirmed the accuracy of our results. The calculated spectroscopic constants for the excited states are shown in Table (3.6). The dissociative product states of these electronic excited states are shown in Table (3.7). In order to identify the molecular states to which these excited states dissociate, we have compared their energies at dissociation limit (100 a.u.) with the sum of atomic/ionic energies taken from the NIST database [191]. The maximum percentage error between our values and those from Ref. [191] is 1.97% as shown in the last column of Table (3.7).

Both of the triplet excited states considered here: $1\,^3\Sigma^+$ and $1\,^3\Pi$ dissociate into the same final states: $Be\,(2s\,2p)\,^3P + Li^+$. There is a small energy separation of

Table 3.6: The spectroscopic constants for the excited states of $BeLi^+$ computed using EOM - CCSD/QZ method. Comparison with the available results in the literature.

State	$R_e\,(a_0)$	$D_e\,(\mathrm{cm}^{-1})$	$T_e\,(\mathrm{cm}^{-1})$	$\omega_e\,(\mathrm{cm}^{-1})$	$\omega_e x_e\,(\mathrm{cm}^{-1})$	$B_e\,(\mathrm{cm}^{-1})$	$\alpha_e\,(\mathrm{cm}^{-1})$	Ref.
$2^1\Sigma^+$	9.121	1937	34656.36	126	2.15	0.185	0.0025	This work
	9.150	1976	34729	123.15	2.04	0.1836	–	[2]
	Repulsive							[182]*
$1^3\Sigma^+$	5.556	7603	19262.19	270	1.62	0.484	0.0042	This work
	5.530	7615	19648	275.47	4.06	0.5016	–	[2]
	5.605	6976.85	–	271.9	2.679	0.489	0.00678	[182]*
	5.546	7527.0	–	274.2	2.290	0.4949	0.006894	[183]
$1^3\Pi$	5.040	1793	25077.82	245	6.22	0.597	0.0163	This work
	5.02	1650	25613	244.33	7.57	0.6100	–	[2]
	5.104	1661.54	–	236.4	6.848	0.589	0.02025	[182]*
	5.029	1754.2	–	244.6	5.501	0.5984	0.01402	[183]
$3^1\Sigma^+$	11.439	1803	46457.07	83	0.81	0.111	0.0015	This work
	11.74	737	35967	75.50	9.24	0.1111	–	[2]
	Repulsive							[182]*
$1^1\Pi$	5.285	4027	44238.18	267	4.61	0.545	0.0115	This work
	5.320	3183	45279	256.6	5.12	0.5428	–	[2]
	5.365	3395.67	–	256.6	4.446	0.533	0.01228	[182]*
	5.263	7224.7	–	281.1	1.572^+	0.5329	0.004875	[183]
$4^1\Sigma^+$	16.863	418	51087.32	37	1.18	0.056	0.0023	This work
	17.27	535	51075	37.17	1.90	0.0515	–	[2]
$2^1\Pi$	Repulsive							This work
	Repulsive							[2]

*At muti - reference averaged quadratic coupled - cluster (MRAQCC) level.

$^+$In Ref. [183], this number is given as 1.572×101 that might be a typographical error.

Table 3.7: Energies of a few low - lying electronic states of $BeLi^+$ at the dissociative limit.

		E (cm^{-1})		
Molecular state	Asymptotic molecular state	This work	NIST [191]	% difference
$X^1\Sigma^+$	$Be\,(2s^2) + Li^+$	0.0	0.0	–
$2^1\Sigma^+$	$Be^+(2s) + Li(2s)$	31734	31706	0.09
$1^3\Sigma^+$	$Be\,(2s\,2p)\,^3P + Li^+$	22009	21979.49	0.13
$1^3\Pi$	$Be\,(2s\,2p)\,^3P + Li^+$	22011	21979.49	0.14
$3^1\Sigma^+$	$Be(2s\,2p)\,^1P + Li^+$	43403	42565.35	1.97
$1^1\Pi$	$Be(2s\,2p)\,^1P + Li^+$	43405	42565.35	1.97
$4^1\Sigma^+$	$Be^+\,(2s) + Li(2p)$	46644	46609.83	0.07
$2^1\Pi$	$Be^+\,(2s) + Li(2p)$	46647	46609.83	0.08

$\sim 2\,cm^{-1}$ between these triplet states at the dissociation limit in our calculation, however, they are shown to be degenerate in NIST database [191]. The spectroscopic constants that we have obtained for these states are reasonably in good agreement with other published calculations [2, 182, 183]. The disagreement ranges between 0.01 - 0.06 a.u. for R_e, 12 - 626 cm^{-1} for D_e, 0.4 - 8.6 cm^{-1} for ω_e, 0.62 - 2.4 cm^{-1} for $\omega_e x_e$, 0.001 - 0.002 cm^{-1} for B_e and 0.002 - 0.003 cm^{-1} for α_e.

We have evaluated the contribution of relativistic effects for the $^3\Pi$ state using KR-CISD method available in the KRCI module of DIRAC15 [143]. The $^3\Pi_1$ and $^3\Pi_2$ states are found to lie 1.96 cm^{-1} and 3.92 cm^{-1}, respectively, above the $^3\Pi_0$ state at the equilibrium point. Hence, the transition energy, T_e, reported in Table (3.6) may have an error of about 4 cm^{-1}, while the error in the reported dissociation energy, harmonic frequency and anharmonic constant for $^3\Pi$ state is estimated to be 0.8 cm^{-1}, 0.01 cm^{-1} and 0.001 cm^{-1}, respectively, due to the negligence of relativistic effects.

There is an apparent disagreement between the results of Sun *et al.* [182] and Ghanmi *et al.* [2] for the case of 2 - 3 $^1\Sigma^+$ states. The former reports these PECs as repulsive, while the latter reports them to be attractive with a potential depth of 1976 cm^{-1} for $2\,^1\Sigma^+$ and 737 cm^{-1} for $3\,^1\Sigma^+$. In the present work, we have found both of these

states to be attractive similar to that of Ref. [2], and calculated the potential depths to be 1937 cm^{-1} and 1803 cm^{-1}, respectively. The relative difference between our results and those reported in Ref. [2] is; $\Delta(R_e) < 0.32\,\%$, $\Delta(\omega_e) < 2.32\,\%$, $\Delta(\omega_e x_e) < 5.4\,\%$, and $\Delta(B_e) < 0.8\,\%$ for $2\,^1\Sigma^+$ state. However, for $3\,^1\Sigma^+$ state, some of our results show a noticeable disagreement. Our dissociation energy ($D_e = 1803\,cm^{-1}$) is 1066 cm^{-1} larger and the anharmonic constant ($\omega_e x_e = 0.81\,cm^{-1}$) is 8.43 cm^{-1} smaller than that of [2]. The difference in the values of potential depths may arise due to the method of calculation employed and the choice of basis set. On the other hand, our findings for $4\,^1\Sigma^+$ state compare well with those given in Ref. [2]. Our results of all spectroscopic constants, except D_e, of $1\,^1\Pi$ state are in good agreement with the results available in literature [2, 182, 183]. On the other hand, the $2\,^1\Pi$ molecular state is found to be repulsive in our work and as well as in Ref. [2].

The molecular states [$2\,^1\Sigma^+$], [$3\,^1\Sigma^+$, $1\,^1\Pi$] and [$4\,^1\Sigma^+$, $2\,^1\Pi$] dissociate, respectively, into [$Be^+(2s) + Li(2s)$], [$Be(2s\,2p)\,^1P + Li^+$] and [$Be^+(2s) + Li(2p)$]. The nature of the asymptotic molecular states for $X\,^1\Sigma^+$, $2\,^1\Sigma^+$ and $1\,^3\Sigma^+$ reported in this work agree well with those reported in Ref. [2]. However, the dissociative nature of $^{1,3}\Pi$ electronic states reported in Ref. [2] seems to be ambiguous to compare with.

The variation of PDMs against the internuclear distance, R, for the excited electronic states is shown in Figure (3.8), and the corresponding data is provided in the Supplementary Table S5 of Ref. [108]. As the structure of the molecule changes from $BeLi^+$ to Be^+Li, the polarity of the dipole moment changes from negative to positive at large distance in the present work, *viz.*, the following electronic states: $2\,^1\Sigma^+$, $4\,^1\Sigma^+$ and $2\,^1\Pi$, which dissociate into Be^+Li, as can be seen from Table (3.7), show a common trend together, while the remaining electronic states, shown in Table (3.7), which dissociate into $BeLi^+$ show an opposite trend at large distances in Figure (3.8). The phase convention adopted in Ref. [2], however, seems to be the opposite. The electronic TDMs from ground state to singlet excited states as a function of R are

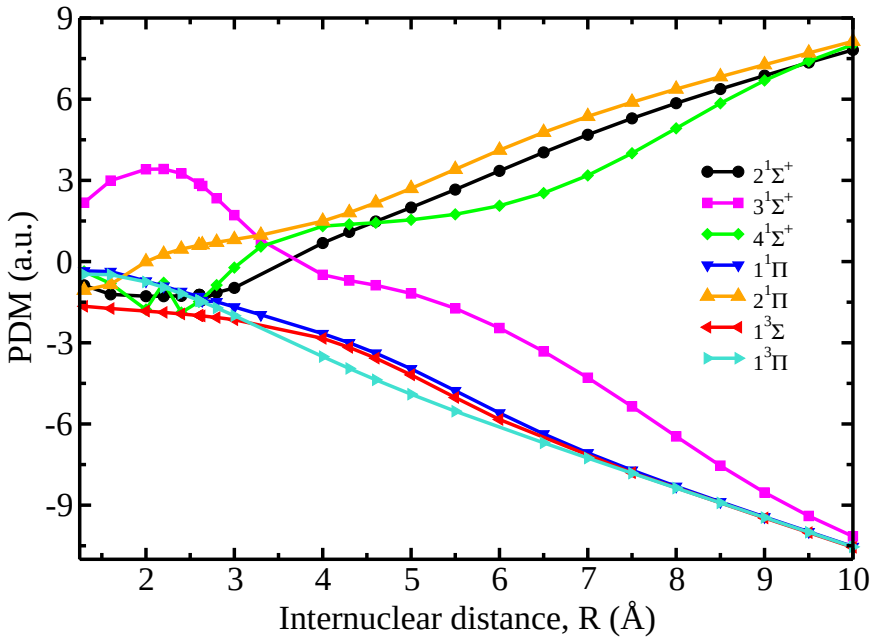

Figure 3.8: Permanent dipole moment curves for the excited states of $BeLi^+$ using EOM-CCSD/QZ method.

shown in Figure (3.9), and the corresponding TDM values are provided in the Supplementary Table S6 of Ref. [108]. The behaviour of TDM curves for $X\,^1\Sigma^+ \rightarrow 2\,^1\Sigma^+$ and $X\,^1\Sigma^+ \rightarrow 3\,^1\Sigma^+$ electronic transitions compares well with those reported in Ref. [181]. The TDM value, for the electronic transitions: $X\,^1\Sigma^+ \rightarrow 2\,^1\Sigma^+$, $X\,^1\Sigma^+ \rightarrow 4\,^1\Sigma^+$ and $X\,^1\Sigma^+ \rightarrow 2\,^1\Pi$, goes to zero at large internuclear separation. The molecular excited states involved in these transitions are dissociating into $Be^+(2s) + Li(2s \text{ or } 2p)$. On the other hand, the remaining transitions: $X\,^1\Sigma^+ \rightarrow 3\,^1\Sigma^+$ and $X\,^1\Sigma^+ \rightarrow 1\,^1\Pi$ whose TDM attains a constant non-zero value after 13 Å bond distance, are dissociating into $Be(2s\,2p) + Li^+(2s^2)$. The value of TDM ($= 1.889$ a.u.) at the dissociative limit for $X\,^1\Sigma^+ \rightarrow 3\,^1\Sigma^+$ and $X\,^1\Sigma^+ \rightarrow 1\,^1\Pi$ molecular transitions agrees extremely well with the value of 1.887 a.u., reported in Ref. [181]. This is also comparable to the theoretical ($= 1.801$ a.u.) [194] and as well as experimental ($= 1.645 \pm 0.278$ a.u.) [195] value of TDM available in the literature for the pure allowed atomic transition between $Be(2s^2)$ to $Be(2s\,2p)$. The maximum TDM value of $X\,^1\Sigma^+ \rightarrow 2\,^1\Sigma^+$ transition

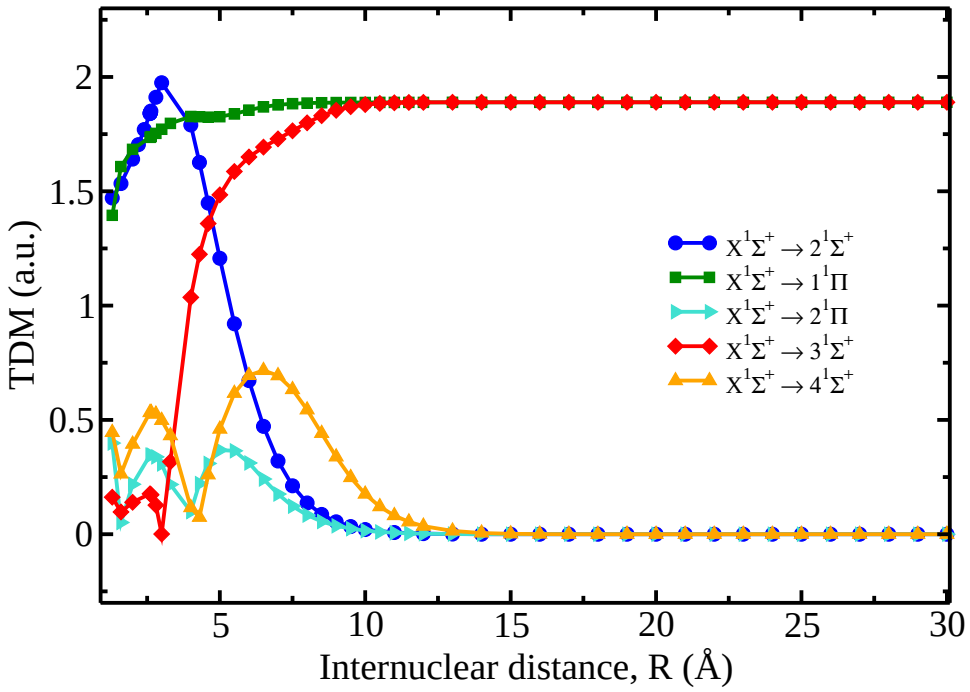

Figure 3.9: Transition dipole moment, as a function of R, from the ground state to the excited singlet electronic states of $BeLi^+$ calculated using EOM - CCSD/QZ method.

is found to be 1.975 a.u. at 3 Å bond distance.

The electronic excitation energies (T_e) as reported in Ref. [2] and our results shown in Table (3.6) are in very good agreement. The maximum difference between the two is about 2.3% for all states, except for the $3\,^1\Sigma^+$ state for which the difference is about 29%. On solving the Schrödinger equation using the electronic energies calculated at different bond lengths varying from 0.4 to 30 Å, we have obtained the maximum vibrational levels to be: 45 for $1\,^3\Sigma^+$, 11 for $1\,^3\Pi$, 31 for $2\,^1\Sigma^+$, 41 for $3\,^1\Sigma^+$, 32 for $4\,^1\Sigma^+$, and 25 for $1\,^1\Pi$. The Table (3.8) provides the relative energies of vibrational states and the vibrationally coupled rotational constants for all the excited electronic states considered. We have shown variation of the energy spacing between the adjacent vibrational states, ($\Delta E_v = E_v - E_{v-1}$), for the ground - and for the low - lying excited electronic states as a function of vibrational quantum number in Figure (3.10). This separation which is not a constant is a hallmark of anharmonic

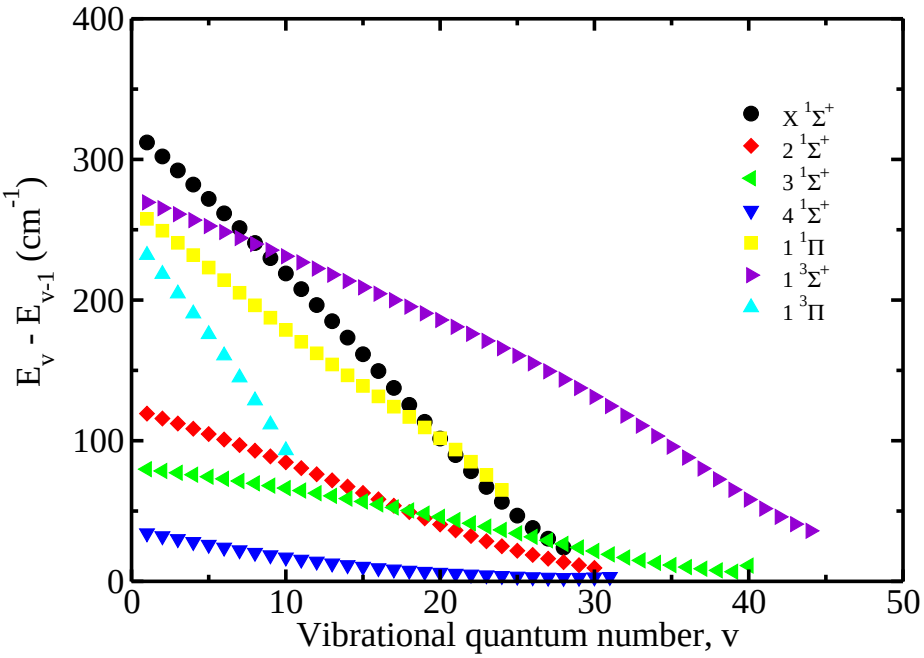

Figure 3.10: Energy spacing between the adjacent vibrational levels of the electronic ground state (using CCSD(T)/QZ method) and of the excited states (using EOM-CCSD/QZ method) of $BeLi^+$.

effects.

3.4 Summary

To summarize, we have carried out the *ab initio* calculations of the spectroscopic constants and the molecular properties of the ground state ($X\,^1\Sigma^+$) of $BeLi^+$ molecular ion that dissociates into $Be + Li^+$. We have investigated the effect of including DBOC, and the contribution of non-leading order triples which were missing in CCSD(T) on the spectroscopic parameters. Although, the DBOC in itself is significant, it does not affect the spectroscopic constants. As anticipated, the contributions of CCSDT-CCSD(T) are well within the error bars that we have quoted. Our findings of diatomic constants and equilibrium dipole moment are reasonably in good agreement with the available results. Furthermore, the results of the DP and the QM for this ion are

Table 3.8: Relative energies and rotational constants for vibrational levels of the excited electronic states of $BeLi^+$. The results are quoted in cm^{-1}.

	$2^1\Sigma^+$		$3^1\Sigma^+$		$4^1\Sigma^+$		$1^3\Sigma^+$		$1^3\Pi$		$1^1\Pi$	
v	ΔE_v	B_v	ΔE_v	B_v	ΔE_v	B_v	ΔE_v	B_v	ΔE_v	B_v	ΔE_v	B_v
0	–	0.1823	–	0.1165	–	0.0530	–	0.4909	–	0.5908	–	0.5405
1	119.24	0.1799	79.75	0.1163	34.26	0.0516	269.46	0.4843	231.98	0.5706	257.73	0.5289
2	115.78	0.1774	78.51	0.1160	32.19	0.0502	265.29	0.4777	218.47	0.5496	249.32	0.5169
3	112.22	0.1747	77.2	0.1158	30.12	0.0486	261.1	0.4711	204.59	0.5277	240.73	0.5047
4	108.54	0.1719	75.82	0.1155	28.07	0.0469	256.88	0.4645	190.36	0.5047	231.99	0.4923
5	104.75	0.1690	74.39	0.1152	26.06	0.0452	252.64	0.4580	175.68	0.4804	223.12	0.4795
6	100.87	0.1659	72.9	0.1149	24.09	0.0435	248.39	0.4514	160.53	0.4547	214.17	0.4665
7	96.93	0.1626	71.35	0.1146	22.19	0.0416	244.11	0.4449	144.86	0.4271	205.2	0.4533
8	92.93	0.1592	69.74	0.1142	20.38	0.0398	239.81	0.4384	128.55	0.3972	196.27	0.4400
9	88.86	0.1555	68.07	0.1138	18.66	0.0379	235.49	0.4318	111.44	0.3641	187.44	0.4266
10	84.71	0.1517	66.34	0.1134	17.04	0.0361	231.16	0.4253	93.12	0.3259	178.78	0.4131
11	80.49	0.1476	64.56	0.1129	15.52	0.0342	226.79	0.4187	–	–	170.35	0.3998
12	76.18	0.1433	62.71	0.1125	14.12	0.0324	222.4	0.4121	–	–	162.16	0.3865
13	71.8	0.1387	60.81	0.1119	12.81	0.0306	217.99	0.4054	–	–	154.21	0.3733
14	67.36	0.1338	58.85	0.1113	11.6	0.0289	213.54	0.3988	–	–	146.47	0.3602
15	62.86	0.1288	56.82	0.1107	10.49	0.0272	209.05	0.3920	–	–	138.92	0.3471
16	58.33	0.1234	54.74	0.1100	9.47	0.0255	204.52	0.3853	–	–	131.52	0.3340
17	53.78	0.1178	52.59	0.1092	8.53	0.0239	199.94	0.3784	–	–	124.21	0.3208
18	49.26	0.1119	50.4	0.1083	7.68	0.0224	195.3	0.3715	–	–	116.88	0.3074
19	44.8	0.1059	48.17	0.1073	6.89	0.0209	190.59	0.3645	–	–	109.43	0.2935
20	40.45	0.0997	45.9	0.1060	6.17	0.0195	185.82	0.3574	–	–	101.76	0.2789
21	36.26	0.0934	43.6	0.1045	5.52	0.0181	180.96	0.3502	–	–	93.71	0.2634
22	32.26	0.0870	41.29	0.1026	4.92	0.0168	176.01	0.3429	–	–	85.09	0.2463
23	28.5	0.0807	38.94	0.1003	4.38	0.0155	170.95	0.3354	–	–	75.64	0.2271
24	24.99	0.0745	36.56	0.0975	3.89	0.0144	165.78	0.3277	–	–	64.98	0.2044

Table 3.8: Continued...

	$2^1\Sigma^+$		$3^1\Sigma^+$		$4^1\Sigma^+$		$1^3\Sigma^+$	
v	ΔE_v	B_v	ΔE_v	B_v	ΔE_v	B_v	ΔE_v	B_v
25	21.75	0.0684	34.15	0.0942	3.44	0.0132	160.47	0.3198
26	18.79	0.0624	31.68	0.0904	3.04	0.0121	155.01	0.3117
27	16.09	0.0566	29.18	0.0861	2.69	0.0112	149.37	0.3034
28	13.66	0.0510	26.65	0.0813	2.5	0.0109	143.54	0.2947
29	11.48	0.0456	24.1	0.0761	2.61	0.0112	137.48	0.2856
30	9.54	0.0405	21.6	0.0707	2.91	0.0117	131.19	0.2762
31	–	–	19.2	0.0653	3.2	0.0120	124.63	0.2663
32	–	–	16.96	0.0600	–	–	117.8	0.2559
33	–	–	14.94	0.0551	–	–	110.7	0.2450
34	–	–	13.15	0.0504	–	–	103.34	0.2336
35	–	–	11.58	0.0462	–	–	95.75	0.2216
36	–	–	10.19	0.0422	–	–	88.02	0.2093
37	–	–	8.95	0.0385	–	–	80.24	0.1966
38	–	–	7.85	0.0350	–	–	72.56	0.1839
39	–	–	6.87	0.0318	–	–	65.15	0.1712
40	–	–	11.19	0.0260	–	–	58.17	0.1589
41	–	–	–	–	–	–	51.73	0.1472
42	–	–	–	–	–	–	45.9	0.1361
43	–	–	–	–	–	–	40.66	0.1256
44	–	–	–	–	–	–	35.97	0.1158

being reported here for the first time, to the best of our knowledge. On solving vibrational Schrödinger equation, we have obtained vibrational wavefunctions, spectroscopic constants and TDMs for all vibrational states. Further, we have also calculated the spontaneous - and the BBR - induced transition rates, and hence the lifetimes of vibrational states. The lifetime of the ro - vibronic ground state ($X\,^1\Sigma^+$ with $v = 0$ and $J = 0$) of $BeLi^+$, at room temperature, is found to be 4.67 s.

In addition, we have calculated the spectroscopic parameters, and studied the PDM curves of a few low - lying electronic excited states using the EOM - CCSD method and compared them with the available results in the literature. The nature of electronic TDM curves for the transitions from the ground to the excited singlet states is also presented and analyzed.

We have considered all electrons as well as virtual orbitals active for correlation calculations even in the largest basis sets considered, and also we have used accurate correlation methods available. We have taken extreme care in estimating the error bars, limited to the theoretical approximations considered, on the ground state spectroscopic parameters by extrapolating our results to complete basis set limit. Further, the complete convergence of the results, with respect to numerical grid size, of the vibrational lifetimes of the electronic ground state are obtained. Thus, the results reported in this work for the ground state should be considered more reliable than many of the existing calculations for this molecular ion. Our results on the excited state PECs, and the derived spectroscopic parameters settle the discrepancies in some of the existing theoretical calculations.

CHAPTER 4

ELECTRONIC STRUCTURE AND VIBRATIONAL PARAMETERS OF $MgLi^+$ AND $CaLi^+$

"Nothing in life is to be feared, it is only to be understood. Now is the time to understand more, so that we may fear less" – Marie Curie

4.1 Introduction

This work is a continuation of our previous study on $BeLi^+$ reported in Chapter 3. Here, we have performed the calculations of PECs, the spectroscopic constants: R_e, D_e, ω_e, $\omega_e x_e$, B_e and α_e, and the molecular properties: μ_0, Θ_{zz}, $\alpha_{\parallel}$, $\alpha_{\perp}$, $\bar{\alpha}$, γ at molecular equilibrium point and α_{100}, for the ground state of $MgLi^+$ and $CaLi^+$ ionic systems at different levels of correlation with fully optimized basis sets. Further, vibrational spectroscopic calculations are performed by solving the vibrational Schrödinger equation taking PECs and PDM curves as inputs. Furthermore, we have

extended this work to the low - lying excited states for both the molecular ions using EOM - CCSD method.

There is no experimental data available in the literature yet, although there exists a few theoretical studies of $MgLi^+$ and $CaLi^+$. The spectroscopic constants such as R_e, D_e and ω_e are calculated for $MgLi^+$ using the primitive 6 - 31G* basis set together with HF and MP2 by Pyykkö *et al.* [196]. For the same ion, Boldyrev *et al.* [180] have calculated R_e, ω_e at MP2 (full) level, and D_e at many - body perturbation theory of fourth-order (MP4), and quadratic configuration interaction with singles and doubles including perturbative triples (QCISD(T)) level, using 6 - 311 + G* basis set for the ground state. An *ab initio* study of ground - and low - lying excited states of MgLi and $MgLi^+$ have been reported by Gao and Gao [197] using valence FCI and MRCI method. Calculations of adiabatic PECs have been presented for these molecular species using MRCI + Q method, and also the scalar relativistic effects are included using third - order Douglas - Kroll - Hess Hamiltonian (DKH3). The study of spectroscopic constants, PECs, PDM curves, and TDM curves of ground - and several excited electronic states of $MgLi^+$ have been reported by ElOualhazi and Berriche [4] using CIPSI package (configuration interaction by perturbation of a multiconfiguration wavefunction selected iteratively). They have used nonempirical pseudo - potential approach that considers the $MgLi^+$ molecular ion as an effective two electron system moving in the effective potential created by Mg^{2+} and Li^+ core. *Ab initio* calculations for ground state spectroscopic constants, PDMs and lifetimes of alkali - alkaline - earth cations have been reported by Fedorov *et al.* [177].

The perturbed - stationary - state method has been employed by Kimura *et al.* [198] to charge transfer in $Li^+ + Ca$ collisions and have calculated the diatomic constants for the ground state using pseudo - potential technique and STO basis sets. Russon *et al.* [89] have reported *ab initio* all - electron calculations for R_e, ω_e and ionization energy of $X\,^1\Sigma^+$ state using QCISD(T), and also using complete active space

self consistent field MRCI with single - and double - excitation (CASSCF - MRCISD) method. To determine the effect of the core - valence correlation on dissociation energy of the ground state, they have presented QCISD(T, full) results including all electrons with the geometry optimized at QCISD(T) level. Habli *et al.* [175] also have performed FCI calculations for electronic and vibrational properties of ground - and excited states of $CaLi^+$ by treating two valence electrons explicitly with core polarization potentials (CPP) approach.

4.2 Methodology

The electronic structure calculations reported in this work are carried out systematically at different levels of correlation: SCF, MP2, CCSD and CCSD(T) using CFOUR [139] and DIRAC15 [143] software packages, for non - relativistic and relativistic cases, respectively. The nuclear masses used for Li, Mg and Ca are 7.01600 amu 23.98504 amu and 39.96259 amu, respectively. The uncontracted TZ and QZ basis sets are used [128, 129] together with the C_{2v} point group symmetry. The number of functions in each basis set is given in Table (4.1). Despite using such large basis

Table 4.1: Details of the basis sets for Mg, Ca and Li in uncontracted form.

Atom	Basis
Mg	cc - pVTZ: 15s, 10p, 2d, 1f
	cc - pVQZ: 16s, 12p, 3d, 2f, 1g
Ca	cc - pVTZ: 20s, 14p, 6d, 1f
	cc - pVQZ: 22s, 16p, 7d, 2f, 1g
Li	cc - pVTZ: 11s, 5p, 2d, 1f
	cc - pVQZ: 12s, 6p, 3d, 2f, 1g

sets, neither the valence orbitals are truncated nor the core electrons are frozen. All the electrons, *viz.*, core, valence and virtual orbitals are kept active for the calculations of diatomic constants, and molecular properties that are reported in this work.

The center-of-mass of the molecular system is taken as the origin of the coordinate system. Further, the electronic energies are computed at different internuclear distances (R) ranging from 0.4 Å to 30 Å with a step size of 1 Å. Also, around the vicinity of the potential minimum, a small refined step size of 0.001 Å is considered. From the PECs that are plotted, the dissociation energies are calculated as a difference between the energies at equilibrium point and those at a distance of 30 Å. Note that the energy difference between this ceiling distance and that of conventional asymptotic limit of 52 Å or 100 a.u. distance is less than 0.7 cm^{-1} for $MgLi^+$, and 1.5 cm^{-1} for $CaLi^+$.

The harmonic frequencies, and anharmonic constants are calculated using second-

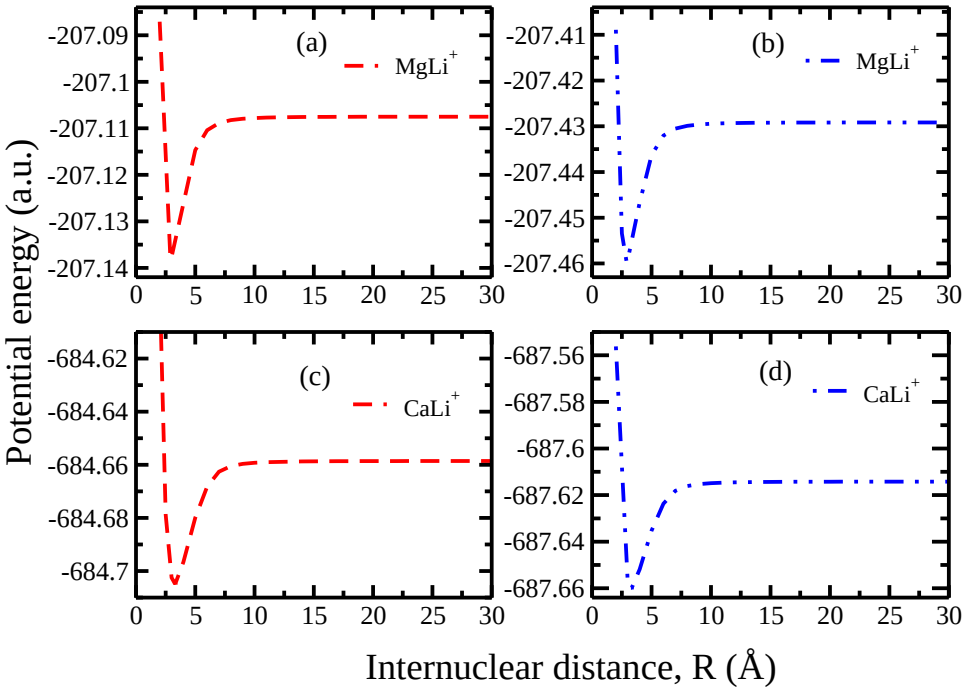

Figure 4.1: Potential energy curves obtained using CCSD(T)/QZ method for the ground state of (a) $MgLi^+$, a non-relativistic case, (b) $MgLi^+$, a relativistic case, (c) $CaLi^+$, a non-relativistic case, and (d) $CaLi^+$, a relativistic case.

order vibrational perturbation theory adopted in the CFOUR package. Similar to the case of $BeLi^+$, the $\bar{\alpha}$ and γ of these molecules are obtained using Eq. (1.51) and

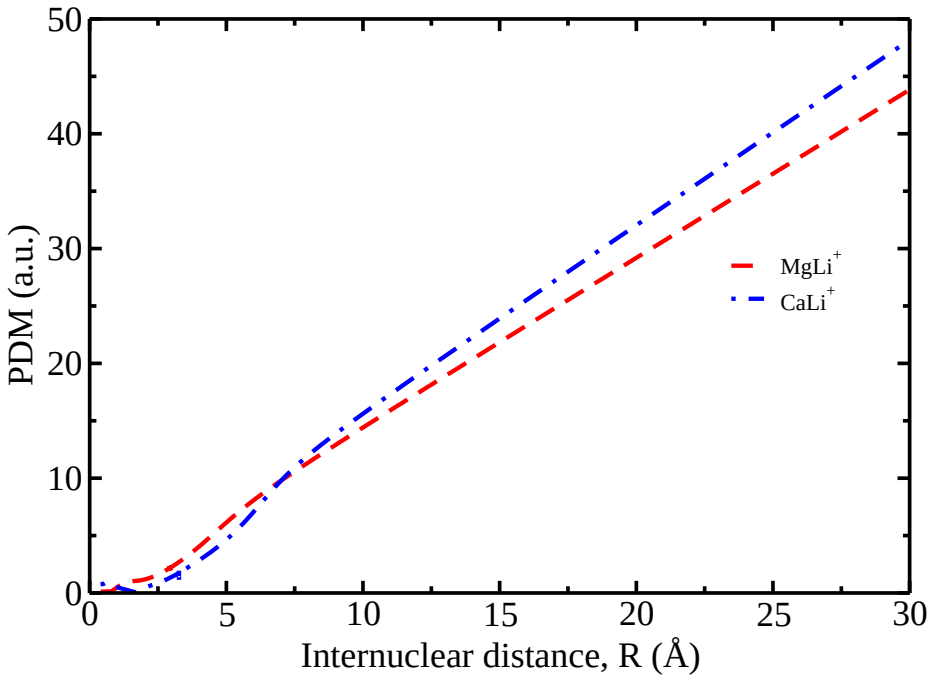

Figure 4.2: Permanent dipole moment curves for the ground state of $MgLi^+$ and of $CaLi^+$ using CCSD(T)/QZ method.

Eq. (1.52), respectively.

Using the PECs shown in Figure (4.1) and PDM curves shown in Figure (4.2), we have solved the vibrational Schrödinger equation using Le Roy's LEVEL16 program [145] and obtained the vibrational parameters, *viz.*, wavefunctions, E_v, B_v, and TDMs between different vibrational states. An appropriate step size required for numerical calculations of these parameters is estimated using equation (3) of Ref. [145], and cubic spline fitting is used for interpolation.

Further, the vibrational energy differences and TDM values between the vibrational states are used to calculate the spontaneous- and BBR-induced transition rates at the surrounding temperature, *viz.*, $T = 300\,\mathrm{K}$, according to the Eq. (3.1)-Eq. (3.4) [185]. Further, electronic energies of the low-lying excited states are calculated, by keeping all occupied- and virtual orbitals as active, using EOM-CCSD method im-

plemented in CFOUR program taking the QZ basis set. The spectroscopic constants are obtained using VIBROT program available in MOLCAS package [144]. Furthermore, the vibrational parameters for the excited states are computed using LEVEL16 program [145].

The relativistic calculations for the ground state molecular constants are carried out using DIRAC15 software package. After generating the reference state using SCF method, the energy calculations at MP2, CCSD and CCSD(T) level are carried out using RELCCSD module. The Dirac - Coulomb Hamiltonian is used with the approximation proposed by Visscher [186] in which contribution from the (SS|SS) integrals is replaced by an interatomic (SS|SS) correction. The diatomic constants are calculated using VIBROT program.

Errors in our calculation may come from two sources: one, from the choice of the basis set - particularly its size, and the other, from the higher - order terms in the CC expansion that are neglected in the present work. The error due to the former source (Δ_1) is not expected to be larger than the difference between the TZ and the QZ results, and yet, we have taken this entire difference as the maximum possible error. Since the contribution from the correlation effects converges with the higher hierarchy of correlation levels, the error (Δ_2) due to this source is not expected to be larger than the difference, *viz.*, CCSD(T) - CCSD. With this, the final value of the calculated property (P) can be quoted as,

$$P_{final} = P_{CCSD(T)@QZ} \pm (|\Delta_1| + |\Delta_2|), \tag{4.1}$$

where $P_{CCSD(T)@QZ}$ is the result of the property of interest calculated using QZ basis set at the CCSD(T) level of approximation.

4.3 Results and Discussion

4.3.1 Structure Constants & Properties of Ground states

The ground state PECs of $MgLi^+$ and $CaLi^+$ molecular ions are shown in Figure (4.1). The sub - figures (a) & (c) correspond to non - relativistic case and (b) & (d) refer to relativistic case. These PECs reflect the well known fact that the relativistic energy levels are lower than their non - relativistic counterparts. The computed results of the spectroscopic constants at the non - relativistic level are compared with the available results in the literature in Table (4.2) and their relativistic variants are shown in Table (4.3). The relativistic contributions to the spectroscopic constants: R_e, D_e and ω_e are smaller than the error bars quoted in Table (4.3).

In order to understand whether or not our results of the spectroscopic constants are saturated with respect to basis set size, we have performed CCSD(T) calculations using 5Z basis set for both the ions considered in this work. The calculated results are: R_e = 5.452 a.u., D_e = 6748.39 cm^{-1}, ω_e = 268.8 cm^{-1}, $\omega_e x_e$ = 2.25 cm^{-1}, B_e = 0.3731 cm^{-1}, and α_e = 0.0052 cm^{-1} for $MgLi^+$; while for $CaLi^+$: R_e = 6.142 a.u., D_e = 10134.28 cm^{-1}, ω_e = 246.96 cm^{-1}, $\omega_e x_e$ = 1.48 cm^{-1}, B_e = 0.2674 cm^{-1}, and α_e = 0.0025 cm^{-1}. Except R_e, B_e and α_e, other diatomic constants for both the molecular ions lie within the error bars reported in Table (4.2).

Further, to estimate the higher - order correlation effects beyond CCSD(T)/QZ, we have calculated the diatomic constants using the CCSD with full triples, *viz.*, CCSDT/ QZ method. From the comparison of these two sets of results, we infer that the contribution of the missing triples in CCSD(T) method is negligible, at least up to the accuracies that we have reported here, for the diatomic constants R_e, B_e and α_e for both the molecular ions. However, D_e increases by 4.91 cm^{-1} (27.61 cm^{-1}), while ω_e decreases by 0.02 cm^{-1} (0.24 cm^{-1}) for $MgLi^+$ ($CaLi^+$). In addition, the value of anharmonic constant changes by -0.22 cm^{-1} for $MgLi^+$ and 0.17 cm^{-1} for $CaLi^+$.

Table 4.2: The spectroscopic constants for the electronic ground state of $MgLi^+$ and $CaLi^+$ at various levels of correlation, computed for the non-relativistic case, and compared with the published results.

Molecule	Method/basis	R_e (a_0)	D_e (cm^{-1})	ω_e (cm^{-1})	$\omega_e x_e$ (cm^{-1})	B_e (cm^{-1})	α_e (cm^{-1})
$MgLi^+$	SCF/TZ	5.599	6396.1	256.8	2.47	0.3537	0.0048
	MP2/TZ	5.516	6595.9	264.5	2.46	0.3645	0.0049
	CCSD/TZ	5.510	6634.6	265.8	2.49	0.3652	0.0047
	CCSD(T)/TZ	5.509	6641.9	265.7	2.26	0.3655	0.0047
	SCF/QZ	5.599	6409.3	256.6	2.49	0.3537	0.0049
	MP2/QZ	5.501	6659.7	265.8	2.49	0.3665	0.0048
	CCSD/QZ	5.497	6702.2	267.0	2.32	0.3670	0.0047
	CCSD(T)/QZ	**5.493**	**6712.4**	**267.3**	**2.30**	**0.3675**	**0.0046**
	Error bar	**±0.02**	**±80.7**	**±1.9**	**±0.06**	**±0.0025**	**±0.0002**
	CCSDT/cc-pCVQZ [177]	5.476	6658.8	265.9	2.0	–	–
	MRCI/cc-pCVQZ [177]	5.481	6649.2	265.4	2.0	–	–
	HF/6-31 G* [196]	5.629	6264.5	255	–	–	–
	MP2/6-31 G* [196]	5.569	6456.4	262	–	–	–
	MP2(full)/6-311 +G* [180]	5.546	6470.5	261	–	–	–
	MRCI/AV5Z + Q [197]	5.546	6508.9	263.5	2.37	0.3606	–
	MRCI/AV5Z + Q + DK [197]	5.533	6557.3	266.4	2.48	0.3623	–
	MRCI/AVQZ + Q [197]	5.548	6484.7	262.9	2.35	0.3603	–
	MRCI/AVQZ + Q + DK [197]	5.544	6476.6	262.9	2.36	0.3608	–
	FCI/Gaussian [4]	5.47	6575	264.22	2.63	0.372138	–
	SCF/STO-6G [199]	5.633	–	–	–	–	–

Table 4.2: Continued...

Molecule	Method/basis	$R_e\,(a_0)$	$D_e\,(\mathrm{cm}^{-1})$	$\omega_e\,(\mathrm{cm}^{-1})$	$\omega_e x_e\,(\mathrm{cm}^{-1})$	$B_e\,(\mathrm{cm}^{-1})$	$\alpha_e\,(\mathrm{cm}^{-1})$
$CaLi^+$	SCF/TZ	6.329	9734.4	240.2	1.79	0.2518	0.0024
	MP2/TZ	6.178	9328.0	246.6	1.82	0.2643	0.0026
	CCSD/TZ	6.189	9987.6	247.6	1.43	0.2633	0.0024
	CCSD(T)/TZ	6.193	10008.5	245.8	1.60	0.2630	0.0024
	SCF/QZ	6.327	9744.7	240.3	1.67	0.2520	0.0024
	MP2/QZ	6.153	9428.0	246.2	1.68	0.2664	0.0025
	CCSD/QZ	6.172	10083.4	246.8	1.37	0.2648	0.0023
	CCSD(T)/QZ	**6.170**	**10092.9**	**245.1**	**1.31**	**0.2650**	**0.0023**
	Error bar	**±0.025**	**±94**	**±2.4**	**±0.23**	**±0.0022**	**±0.0001**
	FCI/Gaussian [175]	6.120	9973.27	242	–	–	–
	FCI/STO's [198]	6.20	8952.8	235	–	0.263	–
	QCISD(T) [89]	6.274	10012.7	239	–	–	–
	CASSCF-MRCISD [89]	6.272	–	239	–	–	–
	QCISD(T,full) [89]	–	9678.7	–	–	–	–

Table 4.3: The computed spectroscopic constants for the electronic ground state of $MgLi^+$ and $CaLi^+$ at different levels of correlation, in the relativistic case.

Molecule	Method/basis	$R_e\,(a_0)$	$D_e\,(\mathrm{cm}^{-1})$	$\omega_e\,(\mathrm{cm}^{-1})$	$\omega_e x_e\,(\mathrm{cm}^{-1})$	$B_e\,(\mathrm{cm}^{-1})$	$\alpha_e\,(\mathrm{cm}^{-1})$
$MgLi^+$	SCF/TZ	5.597	6377.6	254	2.25	0.3484	0.0036
	MP2/TZ	5.513	6579.2	261.7	2.17	0.3569	0.0031
	CCSD/TZ	5.508	6618.7	264.1	2.11	0.3580	0.0029
	CCSD(T)/TZ	5.505	6625.9	263.4	2.03	0.3593	0.0031
	SCF/QZ	5.595	6391.3	254.5	2.29	0.3495	0.0038
	MP2/QZ	5.497	6644.5	263.9	2.26	0.3597	0.0033
	CCSD/QZ	5.493	6685.7	266	2.14	0.3624	0.0034
	CCSD(T)/QZ	**5.490**	**6696.1**	**265.7**	**2.12**	**0.3628**	**0.0034**
	Error bar	**±0.02**	**±80.6**	**±2.6**	**±0.1**	**±0.004**	**±0.0003**
$CaLi^+$	SCF/TZ	6.321	9649.0	240.2	1.45	0.2475	0.0018
	MP2/TZ	6.169	9323.9	246.3	1.51	0.2586	0.0018
	CCSD/TZ	6.182	9911.2	245.5	1.17	0.2554	0.0013
	CCSD(T)/TZ	6.185	9933.8	243.3	1.08	0.2563	0.0014
	SCF/QZ	6.321	9661.1	240.7	1.50	0.2488	0.0020
	MP2/QZ	6.147	9355.4	246.4	1.52	0.2622	0.0020
	CCSD/QZ	6.166	9999.9	245.2	1.18	0.2575	0.0014
	CCSD(T)/QZ	**6.165**	**10010.4**	**243.2**	**1.11**	**0.2561**	**0.0012**
	Error bar	**±0.02**	**±87.1**	**±2.1**	**±0.1**	**±0.002**	**±0.0004**

Except $\omega_e x_e$ for $MgLi^+$, the contributions of the non - leading order triples to CCSD(T) are well within the error bars that are reported in Table (4.2). From these two additional calculations: one, using CCSD(T)/5Z and the other, using CCSDT/QZ; we infer that our results reported in Table (4.2) are more saturated with respect to correlation effects than with respect to the basis set size effects. For achieving better accuracies, as a trade - off to higher - order correlation effects, one may need to consider either the basis sets larger than 5Z or one may extrapolate the results to CBS limit.

The DBOC is calculated for both the ions at the CCSD level of theory in conjunction with the QZ basis sets. In the vicinity of the equilibrium geometry, the DBOC is found to be 1001.32 cm^{-1} and 1823.36 cm^{-1} for $MgLi^+$ and $CaLi^+$, respectively. Although the magnitude of DBOC is significant, its inclusion to PEC does not seem to affect R_e. However, it lowers the D_e of $MgLi^+$ by 0.65 cm^{-1} and D_e of $CaLi^+$ by 1.35 cm^{-1}. Thus, it is very small when compared to the error bars quoted on D_e in Table (4.2) and Table (4.3).

We have calculated several molecular properties such as the electric dipole moments, QMs and static DPs, however, all at non - relativistic level as they are not available at the relativistic level in the software package used. These results are tabulated in Table (4.4). The parallel - component of the dipole polarizability at super - molecular limit, i.e. at a bond distance of 100 a.u., denoted as α_{100}, is also reported in the last column of Table (4.4). With the convention that the direction of interatomic axis is considered from the heavier element to the lighter one, we have obtained negative values of PDM throughout the curve. However, we have reported the absolute values to compare them with the other calculations. The behaviour of PDM as a function of bond distance R, observed with CCSD(T)/QZ method, for both the molecular ions is shown in Figure (4.2). Our results calculated at the equilibrium point are compared directly with those available in the literature and with those extracted from the

Table 4.4: The permanent dipole moments (in units of $e\,a_0$) and traceless quadrupole moments (in units of $e\,a_0^2$) together with the components of static dipole polarizabilities (in units of $e^2\,a_0^2\,E_h^{-1}$) at the molecular equilibrium point, and the latter at super molecular limit for the ground state of $MgLi^+$ and $CaLi^+$.

Molecule	Method/basis	$\lvert\mu_0\rvert$	Θ_{zz}	$\alpha_\parallel$	$\alpha_\perp$	$\bar{\alpha}$	γ	α_{100}
$MgLi^+$	SCF/TZ	2.086	20.045	84.464	61.236	68.979	23.228	81.386
	MP2/TZ	2.112	19.308	79.383	57.217	64.606	22.165	73.387
	CCSD/TZ	2.139	19.165	78.408	57.216	64.280	21.192	72.273
	CCSD(T)/TZ	2.146	19.122	78.145	56.975	64.032	21.170	71.823
	SCF/QZ	2.085	20.041	84.485	61.339	69.054	23.146	81.544
	MP2/QZ	2.103	19.214	78.642	57.128	64.299	21.514	73.652
	CCSD/QZ	2.129	19.075	77.885	57.151	64.062	20.734	72.938
	CCSD(T)/QZ	**2.135**	**19.017**	**77.533**	**56.863**	**63.753**	**20.669**	**72.462**
	Error bar	**±0.017**	**±0.163**	–	–	**±0.588**	**±0.566**	**±1.115**
	CCSDT/cc-pCVQZ [177]	2.140	–	–	–	–	–	–
	MRCI/cc-pCVQZ [177]	2.140	–	–	–	–	–	–
	MRCI/AV5Z + Q + 3DK [197]	2.126	–	–	–	–	–	–
	FCI/Gaussian [4]	3.075	–	–	–	–	–	–
$CaLi^+$	SCF/TZ	1.441	24.140	181.719	117.212	138.714	64.507	185.046
	MP2/TZ	1.827	23.401	165.102	102.065	123.077	63.037	144.279
	CCSD/TZ	1.695	23.344	163.684	108.221	126.708	55.463	163.853
	CCSD(T)/TZ	1.751	23.328	161.008	107.309	125.209	53.700	161.862
	SCF/QZ	1.439	24.121	181.668	117.329	138.776	64.339	185.461
	MP2/QZ	1.814	23.182	162.911	101.711	122.111	61.199	143.741
	CCSD/QZ	1.685	23.157	162.699	107.947	126.198	54.752	163.386
	CCSD(T)/QZ	**1.748**	**23.120**	**159.409**	**106.738**	**124.295**	**52.671**	**160.812**
	Error bar	**±0.066**	**±0.245**	–	–	**±2.817**	**±3.11**	**±3.624**
	FCI/Gaussian [175]	2.713	–	–	–	–	–	–

dipole moment curves in the case of non-availability of these values. As the calculated values of PDM are fairly large, these ions might be useful for the study of long-range dipole-dipole interactions. The R-variation of QM and components of DP for both the molecular cations is shown in Figure (4.3) and Figure (4.4), respectively. The behaviour of QM and DP curve is similar to that observed for $BeLi^+$ ion in Chapter 3. Our recommended values of the results obtained at the highest level of correlation, i.e., CCSD(T) and with the largest basis sets, i.e., QZ, are highlighted, together with the error bars, in bold fonts at the bottom of Table (4.4). The results

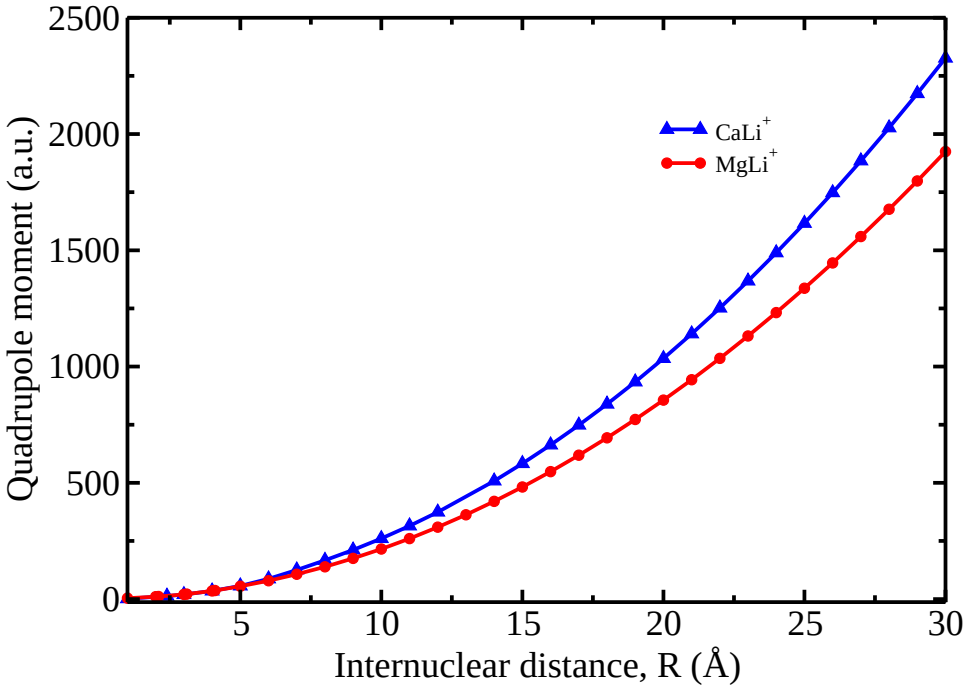

Figure 4.3: Quadrupole moment curves for the ground state of $MgLi^+$ and $CaLi^+$ using CCSD(T)/QZ method.

of QMs and electric DPs for these molecular ions are not available in the literature, to the best of our knowledge. These results could serve as benchmarks for other calculations in future and also they may be useful for experimentalists who would consider working on these molecular systems in future.

We have also investigated the effect of adding diffuse functions on the results of

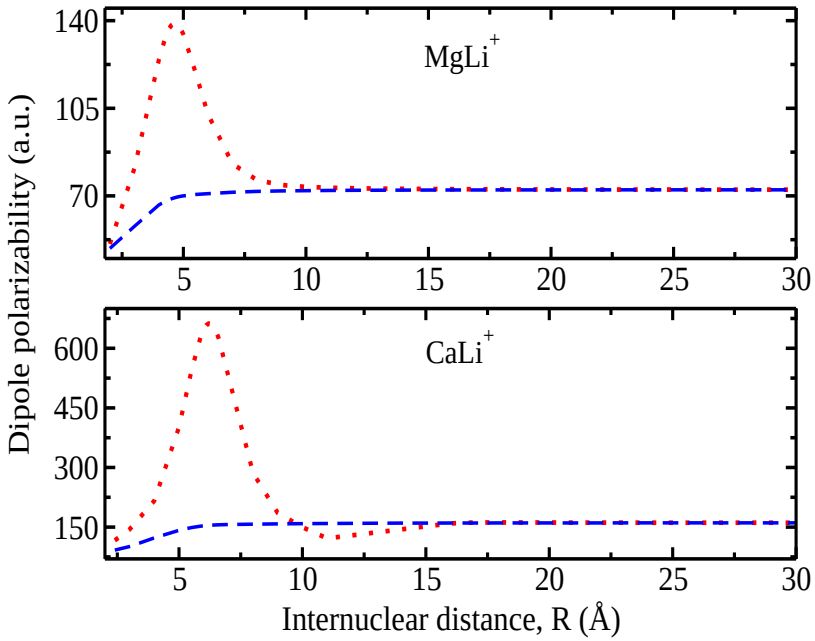

Figure 4.4: Parallel- (red dotted line) and perpendicular (blue dashed line) components of dipole polarizability, as a function of R, using CCSD(T)/QZ method.

molecular properties by considering singly augmented QZ basis sets together with the CCSD(T) method. The corresponding results for $MgLi^+$ ($CaLi^+$) are: μ_0 = 2.135 (1.749) a.u., Θ_{zz} = 19.015 (23.134) a.u., $\bar{\alpha}$ = 63.795 (124.404) a.u., γ = 20.581 (52.550) a.u., and α_{100} = 73.099 (160.882) a.u. It is thus observed that the contribution of diffuse functions to the dipole-, quadrupole- moments and polarizabilities is well within the error bars quoted on these properties in Table (4.4).

In order to determine the molecular products to which the ground state of $MgLi^+$ and $CaLi^+$ dissociate into, at asymptotic limits, we have calculated the first ionization energies by taking the difference between the energies of neutral and singly charged molecules at 100 a.u. bond distance. The first ionization energy of both MgLi and CaLi molecules is the same, *viz.*, 43437.6 cm^{-1} and it matches remarkably well with the value of ionization energy of Li atom (43487.1 cm^{-1}), reported in NIST database [191] to within 0.11%. Hence, we realize that the ground state

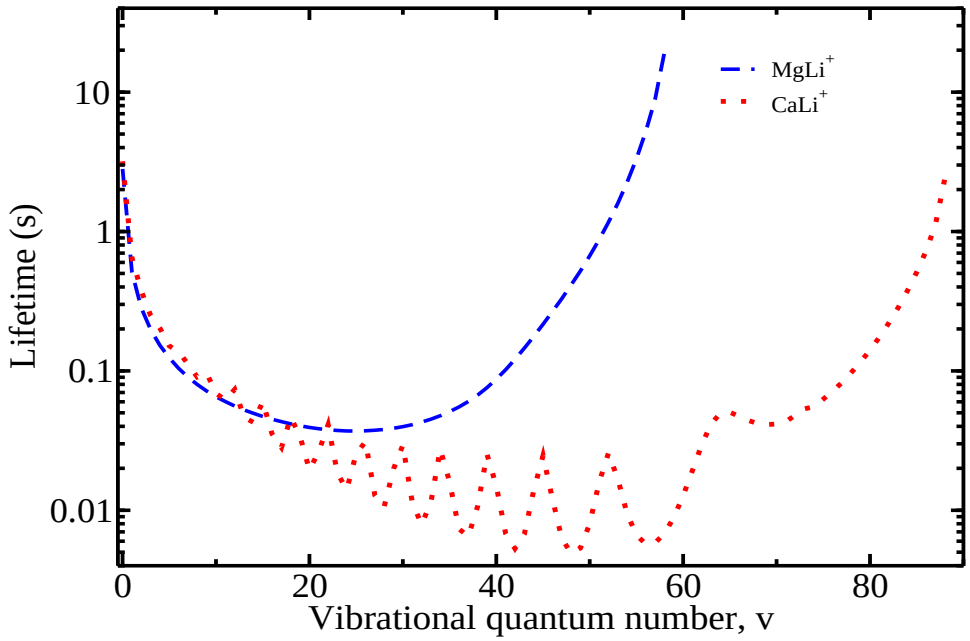

Figure 4.5: Lifetimes of the pure vibrational states for the electronic ground state of $MgLi^+$ and $CaLi^+$ at $T = 300$K.

of these ions will dissociate to $X(ns^2) + Li^+$ with $n = 3$ for Mg and 4 for Ca. On solving the vibrational Schrödinger equation using PEC and PDM curve obtained at CCSD(T)/QZ level, we have obtained 59 and 89 vibrational states for the electronic ground state of $MgLi^+$, and $CaLi^+$, respectively. The energy separation between the last two vibrational levels in both cases is less than 0.3 cm^{-1}. The ΔE_v and B_v for the electronic ground states of $MgLi^+$ and $CaLi^+$ are reported in Table (4.5) and Table (4.6), respectively. The TDMs between different vibrational states of ground electronic state for $MgLi^+$, and $CaLi^+$ can be found in the supplementary Tables S1 and S2, respectively [109]. The calculated lifetime for the electronic ground state with $v = 0$ and $J = 0$ is 2.81 s for $MgLi^+$ and 3.19 s for $CaLi^+$. The variation of the lifetimes of vibrational states against vibrational quantum number, 'v', is shown in Figure (4.5).

In the following subsections, we will discuss the spectroscopic constants, and molec-

Table 4.5: Relative energies and rotational constants for vibrational levels of the ground electronic state of $MgLi^+$. The results are quoted in cm^{-1}.

$X^1\Sigma^+$					
v	ΔE_v	B_v	v	ΔE_v	B_v
0	–	0.3651	36	63.84	0.1368
1	262.65	0.3604	37	57.27	0.1278
2	257.52	0.3554	38	50.87	0.1188
3	252.16	0.3505	39	44.76	0.1097
4	247.54	0.3458	40	38.98	0.1008
5	243.56	0.3408	41	33.67	0.0922
6	240.09	0.3354	42	28.88	0.0839
7	236.71	0.3298	43	24.61	0.0760
8	232.91	0.3241	44	20.84	0.0686
9	228.56	0.3184	45	17.52	0.0615
10	223.69	0.3127	46	14.57	0.0548
11	218.49	0.3070	47	12.02	0.0485
12	213.21	0.3014	48	9.80	0.0425
13	207.90	0.2958	49	7.89	0.0370
14	202.53	0.2902	50	6.25	0.0318
15	197.10	0.2846	51	4.86	0.0269
16	191.58	0.2788	52	3.71	0.0225
17	185.96	0.2731	53	2.76	0.0184
18	180.26	0.2672	54	1.99	0.0148
19	174.51	0.2613	55	1.38	0.0115
20	168.70	0.2554	56	0.91	0.0086
21	162.80	0.2493	57	0.56	0.0061
22	156.80	0.2431	58	0.30	0.0037
23	150.67	0.2367	–	–	–
24	144.40	0.2301	–	–	–
25	138.03	0.2234	–	–	–
26	131.59	0.2165	–	–	–
27	125.05	0.2095	–	–	–
28	118.44	0.2023	–	–	–
29	111.74	0.1948	–	–	–
30	104.96	0.1871	–	–	–
31	98.08	0.1792	–	–	–
32	91.17	0.1711	–	–	–
33	84.27	0.1628	–	–	–
34	77.42	0.1543	–	–	–
35	70.58	0.1456	–	–	–

Table 4.6: Relative energies and rotational constants for vibrational levels of the ground electronic state of $CaLi^+$. The results are quoted in cm^{-1}.

$X^1\Sigma^+$								
v	ΔE_v	B_v	v	ΔE_v	B_v	v	ΔE_v	B_v
0	–	0.2637	36	148.22	0.1792	72	13.78	0.0387
1	242.17	0.2614	37	145.30	0.1766	73	11.94	0.0354
2	239.46	0.2591	38	142.33	0.1739	74	10.28	0.0321
3	236.70	0.2567	39	139.31	0.1712	75	8.76	0.0290
4	233.92	0.2544	40	136.24	0.1685	76	7.43	0.0261
5	231.25	0.2520	41	133.11	0.1657	77	6.29	0.0234
6	228.55	0.2497	42	129.91	0.1629	78	5.25	0.0208
7	225.87	0.2473	43	126.64	0.1599	79	4.34	0.0184
8	223.19	0.2450	44	123.30	0.1569	80	3.54	0.0161
9	220.49	0.2427	45	119.87	0.1539	81	2.86	0.0140
10	217.81	0.2404	46	116.35	0.1507	82	2.26	0.0120
11	215.15	0.2380	47	112.74	0.1474	83	1.76	0.0101
12	212.50	0.2357	48	109.02	0.1441	84	1.34	0.0084
13	209.85	0.2334	49	105.19	0.1406	85	1.00	0.0069
14	207.21	0.2311	50	101.26	0.1370	86	0.72	0.0055
15	204.58	0.2288	51	97.19	0.1332	87	0.49	0.0042
16	201.95	0.2266	52	93.01	0.1293	88	0.29	0.0026
17	199.32	0.2243	53	88.70	0.1253	–	–	–
18	196.70	0.2220	54	84.27	0.1211	–	–	–
19	194.08	0.2197	55	79.72	0.1167	–	–	–
20	191.46	0.2174	56	75.06	0.1122	–	–	–
21	188.85	0.2151	57	70.32	0.1075	–	–	–
22	186.23	0.2128	58	65.50	0.1027	–	–	–
23	183.61	0.2105	59	60.65	0.0977	–	–	–
24	180.98	0.2082	60	55.81	0.0927	–	–	–
25	178.35	0.2059	61	51.03	0.0876	–	–	–
26	175.71	0.2035	62	46.37	0.0824	–	–	–
27	173.06	0.2012	63	41.88	0.0774	–	–	–
28	170.39	0.1988	64	37.62	0.0724	–	–	–
29	167.71	0.1965	65	33.63	0.0675	–	–	–
30	165.00	0.1941	66	29.93	0.0628	–	–	–
31	162.28	0.1916	67	26.53	0.0583	–	–	–
32	159.53	0.1892	68	23.44	0.0540	–	–	–
33	156.75	0.1867	69	20.65	0.0499	–	–	–
34	153.95	0.1842	70	18.12	0.0460	–	–	–
35	151.10	0.1817	71	15.83	0.0423	–	–	–

ular properties for the electronic state of individual ionic systems considered in this work in detail, and compare them with the available calculations.

4.3.1.1 $MgLi^+$

The results reported in Refs. [180, 196, 199] for R_e, D_e and ω_e at SCF and MP2 levels differ from ours, at the similar level of approximation, by a maximum of about 1.2%, 3% and 1.8%, respectively, despite the fact that they all have used minimal basis sets as against our QZ basis sets which are quite large in comparison. Our recommended value of R_e, *viz.*, (5.493 ± 0.02) a.u., as shown in Table (4.2), and the MRCI result quoted in Ref. [197] and also the FCI result of Ref. [4], agree extremely well to within 1%. Similar is the situation for all other diatomic constants which have a maximum difference of 4% to ours, except the anharmonic frequency for which the FCI result is larger than ours by about 14%. Our other results at CCSD(T)/QZ level differ from those reported in Ref. [177] at CCSDT and MRCI level with cc - pCVQZ basis set by less than 1%.

Further, in order to make quantitative comparison of our results, we choose the work of Ref. [177] since in both works, all - electron calculations are performed at CCSDT level with the similar quality of basis sets. Our value of D_e at CCSDT/cc - pVQZ for $MgLi^+$ is 6717.3 cm^{-1} which is comparable to the value of 6658.8 cm^{-1} at CCSDT/cc - pCVQZ as reported in Ref. [177]. The difference of about 58.5 cm^{-1} in the two results can be explained as below: (a) The value of $R_{max} = 20$ Å in Ref. [177], whereas we have used $R_{max} = 30$ Å in our work. It has been observed, from our results, that there is a potential energy difference of about 3.15 cm^{-1} between $R = 20$ Å and $R = 30$ Å at CCSDT/QZ level. Although, this difference of 3.15 cm^{-1} does not account for explaining the difference in the values of D_e between the two works, it is very important in giving rise to more vibrational levels, which is discussed later. (b) The extra core - functions, that are present in cc - pCVQZ in Ref. [177], are not considered in our work. It appears that the omission of core functions overestimates

D_e by about 55.4 cm^{-1}. However, this difference lies within the reported error bars in our work. Only the experiments, when performed, can validate these different approximations.

From the non - relativistic and relativistic calculations shown in Table (4.2) and Table (4.3), respectively, we observe that the relativistic terms seem to have the effect of lowering the values of the spectroscopic constants that are reported. The value of R_e reduces by about 0.05%, D_e reduces by about 0.24%, ω_e decreases by 0.6%, and $\omega_e x_e$ decreases by 8%. Using CCSD(T)/QZ results of D_e and ω_e in Eq. (1.19), we have calculated the value of D_0 to be 6578.8 cm^{-1} at the non - relativistic level, while 6563.3 cm^{-1} at the relativistic level.

Our value of the dipole moment, given in Table (4.4), of $MgLi^+$ at the equilibrium point in its ground state is (2.135 ± 0.017) a.u., at the CCSD(T)/QZ level, and this compares well, to within 0.4% and 0.2%, with that of [197] and [177], respectively. However, these results, ours included, differ significantly, by about 44%, from that given in Ref. [4]. The results of QM and the static DPs for this ion are also reported in this work, most likely for the first time. The convergence trend in the correlation contributions may be seen in several molecular properties reported in Table (4.4). With reference to the SCF result, the contribution of the total electron correlations computed at the CCSD(T) level for Θ_{zz}, $\bar{\alpha}$ and γ is 5.1%, 7.7% and 10.7%, respectively. Further, we observe that the contribution of leading order triples to the CCSD values of Θ_{zz} and γ is $\sim 0.3\%$, while for $\bar{\alpha}$ it is $\sim 0.5\%$. The value of polarizability at the super molecular limit in our calculation is equal to 72.462 a.u., with an error bar of $\pm$ 1.115 a.u., and it compares well with the sum of the atomic polarizabilities, $\alpha_{Mg} + \alpha_{Li^+} = 71.37 + 0.191 = 71.561$ a.u. [192], at the similar level of approximation.

In this work, we have obtained the maximum number of vibrational states to be

59 (using CCSD(T)/QZ method), whereas, Fedorov *et al.* [177] have reported 54 vibrational states (at CCSDT/pCVQZ method). It has to be noted that the potential depths are different in both cases, the latter being $\sim 54\,\mathrm{cm}^{-1}$ smaller. However, the relative energy difference between the adjacent vibrational levels in our case are similar to those reported in Ref. [177] upto $v = 53$ and the last difference being larger than 2 cm^{-1} in both cases. This, however, is still far away from the continuum limit and hence, we have extrapolated our PEC up to $R = 52$ Å, and obtained additional five vibrational states, from $v = 53$ to $v = 58$.

The lifetime of the ro-vibronic ground state (*viz.* 2.81 s), reported in this work agrees well with the result, (*viz.*, 2.76 s) reported in Ref. [177]. The lifetimes of the higher vibrational levels close to dissociation limit are observed to be longer than that of the ro-vibronic ground state. To analyze this further, we have shown the variation of spontaneous- and BBR-transition rates separately for the vibrational states of $MgLi^+$ against the vibrational quantum number in Figure (4.6). The spontaneous-

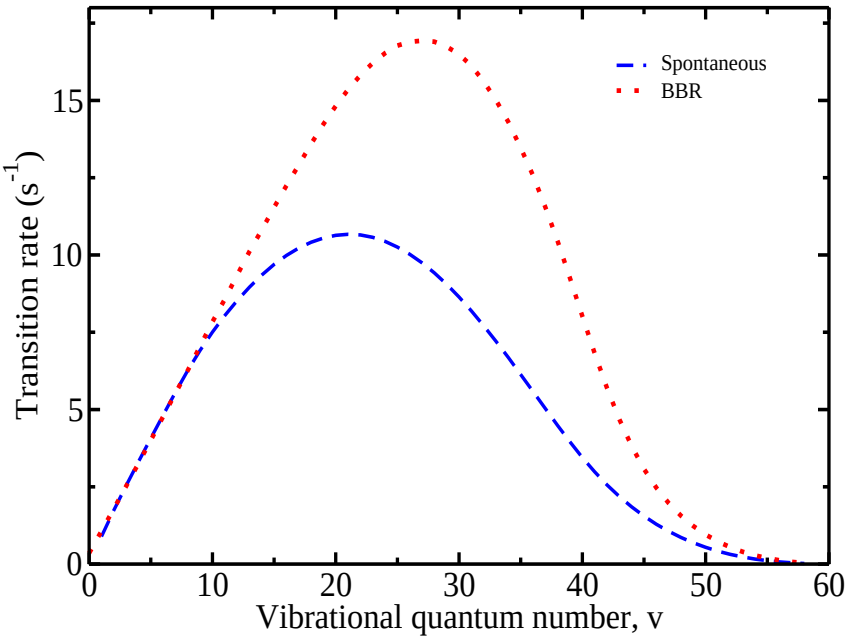

Figure 4.6: Spontaneous- and BBR-induced transition rates for the vibrational levels of electronic ground state of $MgLi^+$.

and the BBR - induced transition rates increase initially and they reach the peak at $v = 21$ and at $v = 27$, respectively. Thereafter, both the transition rates begin to decline. As the lifetime is the reciprocal of total transition rate, the lifetimes of the vibrational levels decrease upto $v = 25$, and then they begin to increase. For $v = 58$, the lifetime reaches the highest value of 19.3 s, which is about seven times larger than the lifetime of $v = 0$ state. For both spontaneous - and BBR - induced transition rates, we have observed that the transitions with $\Delta v = |1|$ are dominant for the lower vibrational levels. However, for intermediate and higher vibrational levels, the fundamental as well as the first few overtones contribute appreciably. The long lifetimes for highly excited vibrational states have also been predicted by Fedorov *et al.* [177] for alkali - alkaline - earth cations and by Zemke *et al.* [200] for neutral KRb molecule.

4.3.1.2 $CaLi^+$

The results of R_e, D_e and ω_e for the ground state of $CaLi^+$ molecular ion, computed at the equilibrium bond length using QCISD(T) method, reported by Russon *et al.* [89] differ from our CCSD(T) results, shown in Table (4.2), by about -1.7%, 0.8% and 2.5%, respectively. However, their QCISD(T, full) result of D_e differs from our result by 4.1%. On the other hand, our results for R_e, D_e and ω_e agree very well with those of Habli *et al.* [175] with a maximum disagreement being 1.26%. The value of $D_e = 8952.8$ cm^{-1} reported in [198] is quite small compared to all other published results, and it is about 11.3% smaller than our result. However, our value of the rotational constant, $B_e = (0.265 \pm 0.002)\,\text{cm}^{-1}$ agrees nicely with that of [198] where it is quoted as $0.263\,\text{cm}^{-1}$. The anharmonic frequencies are not available in the literature for comparison. From Table (4.3), we observe that the relativistic effects, at the CCSD(T)/QZ level, on R_e is a mere -0.08%, on D_e and on ω_e it is about -0.8%, and on $\omega_e x_e$ it is about -15%. The calculated results of D_0, using Eq. (1.19), at the non - relativistic (relativistic) level is $9970.4\,\text{cm}^{-1}$ ($9888.8\,\text{cm}^{-1}$) with values of D_e and ω_e calculated using the CCSD(T)/QZ method.

The only available result of the dipole moment for $CaLi^+$ in the literature is by Habli *et al.* [175] which reports its value to be ~ 2.713 a.u. at the equilibrium bond length. This is much larger than our CCSD(T) result (1.748 ± 0.066) a.u. There is no calculation available in the literature, known to our knowledge, which reports the results of QM and static DPs for this ion and hence, our results reported in this work are most likely the first. The sum of individual atomic polarizabilities, $\alpha_{Ca} + \alpha_{Li^+} = 155.9 + 0.191 = 156.091$ a.u. reported in Ref. [192] is very close to our result of molecular polarizability $(160.812 \pm 3.624$ a.u.) calculated at the super-molecular limit. The correlation contributions due to CCSD and CCSD(T) to SCF are positive for μ_0, while they are negative for the other calculated molecular properties, similar to the trends observed in the case of $MgLi^+$.

The computed lifetime of the ro-vibronic ground state of $CaLi^+$, at room temperature, is found to be 3.19 s. There is no other data available in the literature for

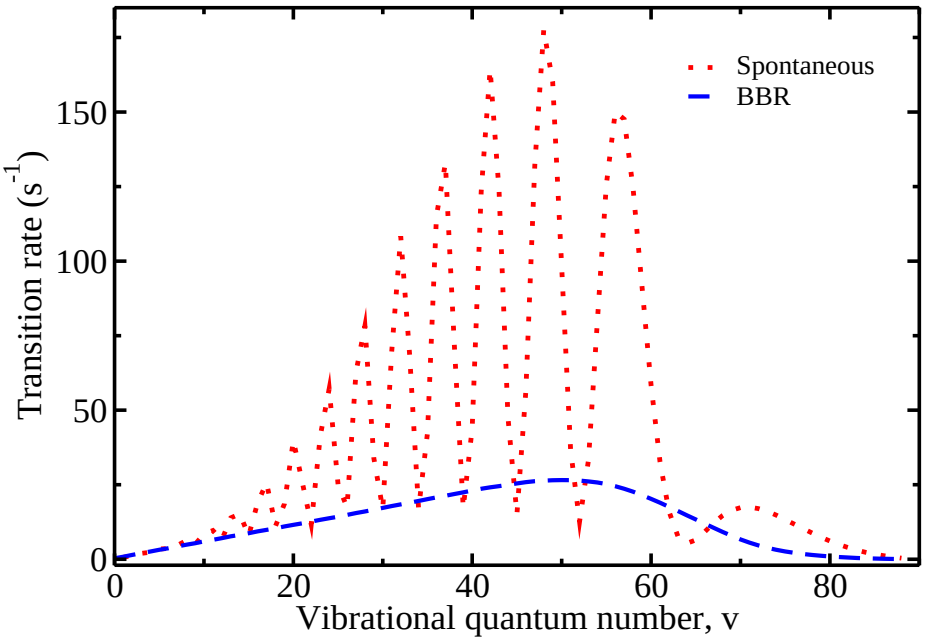

Figure 4.7: Spontaneous- and BBR-induced transition rates for the vibrational levels of electronic ground state of $CaLi^+$.

comparison. From Figure (4.5), we observe that the overall nature of the curve showing the lifetime of vibrational states of $CaLi^+$ against 'v' is similar to the case of $MgLi^+$. The lifetime for the highest vibrationally excited state is found to be 2.38 s, which is close to the value of the lifetime of the vibrational ground state. The behaviour of the BBR-induced transition rate with 'v' is analogous to that observed for $MgLi^+$, however, the spontaneous transition rate curve shows several minor oscillations between $v = 9$ and $v = 70$ (see Figure 4.7) and the same gets reflected in the lifetime curve as well.

4.3.2 Structure Constants & Properties of Excited states

4.3.2.1 $MgLi^+$

The PECs and PDM curves for the excited states of $MgLi^+$: $2\text{-}3\,^1\Sigma^+$, $1\,^3\Sigma^+$ and $1\,^3\Pi$, at EOM-CCSD/QZ level of the theory are shown in Figure (4.8) and Figure (4.9),

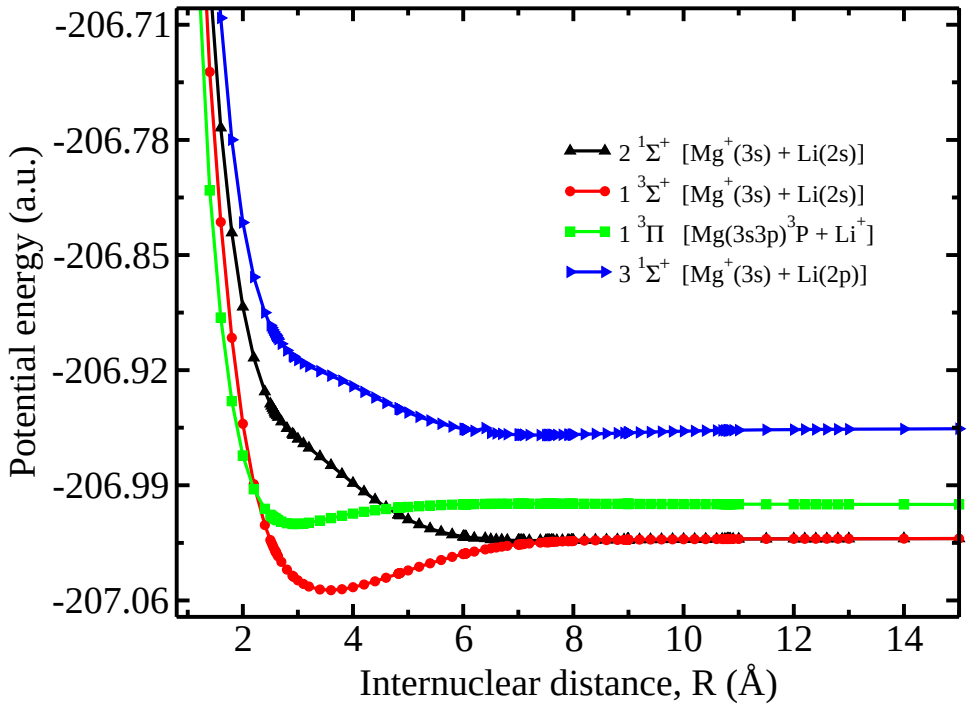

Figure 4.8: Potential energy curves for the electronic excited states of $MgLi^+$ using EOM-CCSD/QZ method.

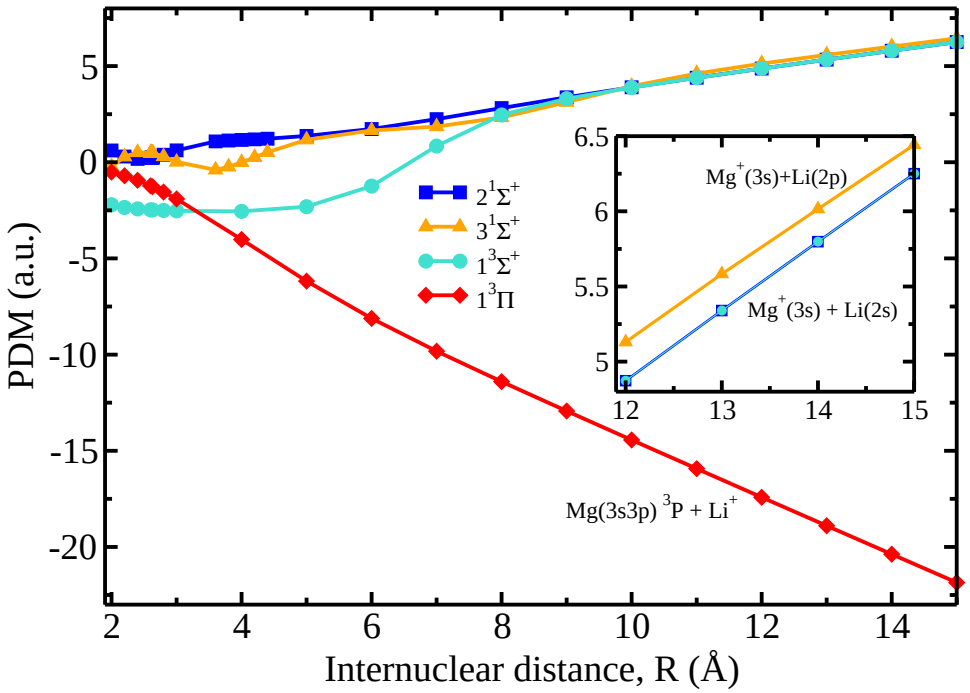

Figure 4.9: Permanent dipole moment curves for the electronic excited states of $MgLi^+$ using EOM - CCSD/QZ method.

respectively. The spectroscopic constants extracted from these PECs are tabulated in Table (4.7) and compared with the published results available in the literature. The spectroscopic constants: R_e, ω_e and B_e, for the triplet excited states reported in this work are in reasonable agreement with the other calculations performed at MRCI and FCI level of correlation [4, 197]. The value of $\omega_e x_e$, on the other hand, shows a noticeable difference in comparison to the published results. The spectroscopic constants for the $n\,^1\Sigma^+$ excited states show large disagreement with those of Ref. [4] mainly because our value of R_e is largely different from that considered in their work which renders the direct comparison of the two results meaningless. The dissociation energy D_e, and the electronic transition energy T_e for the triplet excited states reported in our work differ from those of published results for the following reasons: (i) the magnitude of these energies are sensitive to the size of the basis set, and also to the relativistic effects as seen from the results of Ref. [197] cited in Table (4.2) and Table (4.7) (ii) further, they have performed frozen core calculations

Table 4.7: The calculated spectroscopic constants for the low - lying excited states of $MgLi^+$ using EOM - CCSD/QZ method, compared with the available results in the literature.

State	$R_e\,(a_0)$	$D_e\,(\mathrm{cm}^{-1})$	$T_e\,(\mathrm{cm}^{-1})$	$\omega_e\,(\mathrm{cm}^{-1})$	$\omega_e x_e\,(\mathrm{cm}^{-1})$	$B_e\,(\mathrm{cm}^{-1})$	$\alpha_e\,(\mathrm{cm}^{-1})$	Ref.
$2^1\Sigma^+$	13.795	283.1	24618.03	39.955	1.97	0.0595	0.0031	This work
	10.73	1248	23647	79.59	1.12	0.096860	–	[4]
$1^3\Sigma^+$	6.752	6908.1	17992.74	179.490	0.45	0.2347	0.0007	This work
	6.712	7668.2	16339.1	188.8	0.90	0.2462	–	[197]^a
	6.701	7679.4	16441.5	187.8	0.84	0.2470	–	[197]^b
	6.705	7678.3	16292.2	189.4	0.92	0.2468	–	[197]^c
	6.703	7668.5	16355.6	189.3	0.92	0.2468	–	[197]^d
	6.64	7983	16912	189.96	1.43	0.252539	–	[4]
$1^3\Pi$	5.584	2578.6	26824.62	215.442	4.38	0.3567	0.0080	This work
	5.670	2782.6	24977.6	208.6	3.46	0.3452	–	[197]^a
	5.650	2822.9	25070.0	212.0	3.61	0.3475	–	[197]^b
	5.671	2742.3	24967.7	208.1	3.46	0.3449	–	[197]^c
	5.670	2726.2	25053.1	207.8	3.47	0.3451	–	[197]^d
	5.60	2561	26008	206.32	3.51	0.356099	–	[4]
$3^1\Sigma^+$	14.000	938.9	38691.4	61.7308	1.39	0.0573	0.0011	This work
	12.58	2548	37252	70.38	0.48	0.070509	–	[4]

^{a}MRCI/AV5Z + Q, ^{b}MRCI/AV5Z + Q + DK, ^{c}MRCI/AVQZ + Q, ^{d}MRCI/AVQZ + Q + DK.

in Refs. [4, 197] as against our all-electron correlation calculations (iii) The other reason could be the choice of the many-body method used in our work which is different from the other two.

We have observed that the two of the excited molecular states: $2\,^1\Sigma^+$ and $1\,^3\Sigma^+$ dissociate into $[Mg^+(3s) + Li(2s)]$ states, $1\,^3\Pi$ into $[Mg(3s\,3p) + Li^+(1s^2)]$ states, and $3\,^1\Sigma^+$ into $[Mg^+(3s) + Li(2p)]$ states. The Refs. [4, 197] also report the same observations on the dissociative nature of these molecular states. These asymptotic molecular states, and the corresponding electronic excitation energies with respect to the molecular ground state is given in Table (4.8) and compared with the sum of atomic/ionic energies taken from the NIST database [191]. The maximum difference

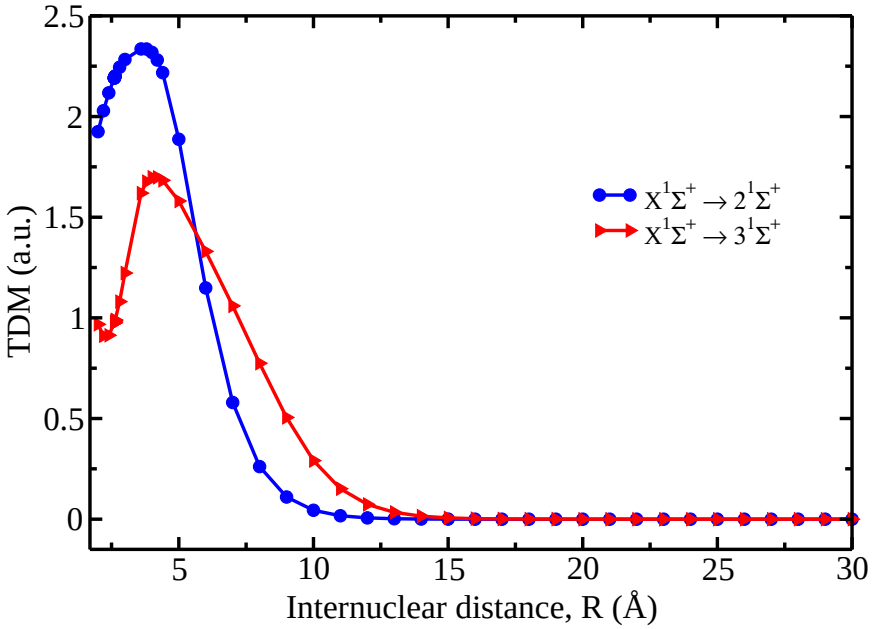

Figure 4.10: Transition dipole moment, as a function of R, from the ground state to the excited singlet electronic states of $MgLi^+$ using EOM-CCSD/QZ method.

between our results and those of [191] is 3.8%, which occurs for $1^3\Pi$. On correlating Figure (4.8) and Figure (4.9), we observe that the molecular states having positive values of dipole moment at large distances dissociate into $Mg^+(3s) + Li(2s\,\text{or}\,2p)$, whereas the states with negative value of dipole moment at large distances dissociate

Table 4.8: Energies of a few low-lying electronic states of $MgLi^+$ at the dissociative limit.

		E (cm^{-1})		
Molecular state	Asymptotic molecular state	This work	NIST [191]	% difference
$X^1\Sigma^+$	$Mg(3s^2) + Li^+$	0.0	0.0	–
$2^1\Sigma^+$	$Mg^+(3s) + Li(2s)$	18198.24	18183.94	0.08
$1^3\Sigma^+$	$Mg^+(3s) + Li(2s)$	18198.25	18183.94	0.08
$1^3\Pi$	$Mg(3s\,3p)\,^3P + Li^+$	22698.04	21877.23	3.75
$3^1\Sigma^+$	$Mg^+(3s) + Li(2p)$	32926.93	33087.77	0.49

into $Mg(3s^2 \text{ or } 3s\,3p) + Li^+$.

The TDM curves for the electronic transitions from the ground- to singlet excited states, are shown in Figure (4.10). The transitions, $X\,^1\Sigma^+ \rightarrow 2\,^1\Sigma^+$ and $X\,^1\Sigma^+ \rightarrow 3\,^1\Sigma^+$ have a maximum value of TDM at a distance of 3.6 Å and 4 Å, respectively. Further,

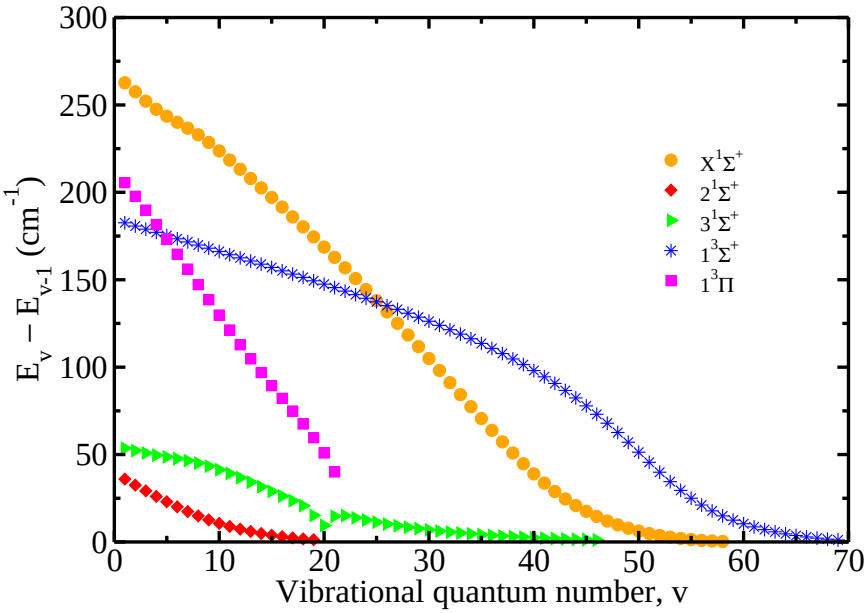

Figure 4.11: Energy spacing between the adjacent vibrational levels of the electronic ground state (using CCSD(T)/QZ method) and of the excited states (using EOM-CCSD/QZ method) of $MgLi^+$.

the number of vibrational states obtained within $2\,^1\Sigma^+$, $1\,^3\Sigma^+$, $1\,^3\Pi$ and $3\,^1\Sigma^+$ elec-

Table 4.9: Relative energies and rotational constants for vibrational levels of excited electronic states of $MgLi^+$. The results are quoted in cm^{-1}.

	$1^3\Sigma^+$		$2^1\Sigma^+$		$3^1\Sigma^+$		$1^3\Pi$	
v	ΔE_v	B_v	ΔE_v	B_v	ΔE_v	B_v	ΔE_v	B_v
0	–	0.2421	–	0.0571	–	0.0562	–	0.3519
1	182.57	0.2399	35.95	0.0547	53.59	0.0554	205.53	0.3442
2	180.74	0.2377	32.54	0.0522	52.25	0.0546	197.75	0.3362
3	178.93	0.2355	29.25	0.0495	50.88	0.0537	189.83	0.3280
4	177.12	0.2334	26.07	0.0467	49.65	0.0527	181.57	0.3194
5	175.28	0.2312	23.02	0.0438	48.64	0.0514	173.27	0.3105
6	173.46	0.2291	20.11	0.0408	47.68	0.0500	164.63	0.3012
7	171.66	0.2269	17.39	0.0379	46.54	0.0485	156.07	0.2917
8	169.86	0.2248	14.90	0.0350	45.10	0.0469	147.22	0.2819
9	168.03	0.2227	12.65	0.0321	43.37	0.0454	138.56	0.2717
10	166.17	0.2205	10.65	0.0293	41.37	0.0438	129.76	0.2614
11	164.33	0.2184	8.89	0.0266	39.16	0.0422	121.23	0.2509
12	162.51	0.2163	7.34	0.0239	36.76	0.0406	112.82	0.2403
13	160.73	0.2142	6.00	0.0213	34.23	0.0390	104.75	0.2297
14	158.91	0.2121	4.85	0.0189	31.60	0.0374	96.95	0.2191
15	157.02	0.2100	3.86	0.0165	28.93	0.0358	89.43	0.2084
16	155.11	0.2078	3.02	0.0143	26.26	0.0344	82.14	0.1976
17	153.23	0.2057	2.32	0.0121	23.61	0.0333	74.89	0.1864
18	151.34	0.2036	1.74	0.0102	20.74	0.0347	67.50	0.1745
19	149.40	0.2014	1.27	0.0083	15.22	0.0539	59.67	0.1613
20	147.46	0.1992	–	–	9.48	0.0451	50.89	0.1454
21	145.49	0.1970	–	–	14.75	0.0301	40.05	0.1229
22	143.49	0.1948	–	–	15.03	0.0268	–	–
23	141.48	0.1926	–	–	13.80	0.0250	–	–
24	139.42	0.1904	–	–	12.51	0.0234	–	–
25	137.34	0.1881	–	–	11.33	0.0221	–	–
26	135.22	0.1858	–	–	10.25	0.0208	–	–
27	133.06	0.1835	–	–	9.29	0.0196	–	–
28	130.84	0.1811	–	–	8.41	0.0185	–	–
29	128.58	0.1786	–	–	7.63	0.0174	–	–
30	126.26	0.1762	–	–	6.91	0.0164	–	–
31	123.88	0.1736	–	–	6.26	0.0154	–	–
32	121.43	0.1710	–	–	5.66	0.0145	–	–
33	118.90	0.1684	–	–	5.12	0.0136	–	–
34	116.28	0.1656	–	–	4.63	0.0127	–	–
35	113.56	0.1627	–	–	4.18	0.0119	–	–

Table 4.9: Continued...

	$1^3\Sigma^+$		$3^1\Sigma^+$	
v	ΔE_v	B_v	ΔE_v	B_v
36	110.74	0.1598	3.77	0.0112
37	107.79	0.1567	3.39	0.0104
38	104.71	0.1535	3.05	0.0097
39	101.47	0.1501	2.74	0.0090
40	98.06	0.1465	2.45	0.0084
41	94.47	0.1427	2.19	0.0078
42	90.67	0.1387	1.96	0.0072
43	86.64	0.1345	1.74	0.0066
44	82.37	0.1299	1.54	0.0061
45	77.83	0.1250	1.36	0.0056
46	73.02	0.1198	1.19	0.0051
47	67.94	0.1142	–	–
48	62.60	0.1083	–	–
49	57.04	0.1019	–	–
50	51.33	0.0953	–	–
51	45.57	0.0884	–	–
52	39.90	0.0814	–	–
53	34.50	0.0745	–	–
54	29.50	0.0678	–	–
55	25.03	0.0615	–	–
56	21.12	0.0556	–	–
57	17.77	0.0501	–	–
58	14.92	0.0451	–	–
59	12.48	0.0405	–	–
60	10.40	0.0362	–	–
61	8.62	0.0321	–	–
62	7.08	0.0284	–	–
63	5.77	0.0249	–	–
64	4.64	0.0216	–	–
65	3.68	0.0186	–	–
66	2.88	0.0158	–	–
67	2.18	0.0131	–	–
68	1.62	0.0108	–	–
69	1.16	0.0085	–	–

tronic states are 20, 70, 22 and 47, respectively. The relative energy separation between the last two vibrational states for $2\,^1\Sigma^+$, $3\,^1\Sigma^+$ and $1\,^3\Sigma^+$ is less than 1.2 cm^{-1}, whereas, it is about 40 cm^{-1} for $1\,^3\Pi$. We have plotted the energy spacing between adjacent vibrational states against 'v' for the ground- as well as for the excited electronic states in Figure (4.11). These results together with the vibrationally coupled rotational constants (B_v) for the excited electronic states are provided in the Table (4.9).

4.3.2.2 $CaLi^+$

The PECs and PDM curves for the low-lying electronic excited states of $CaLi^+$:

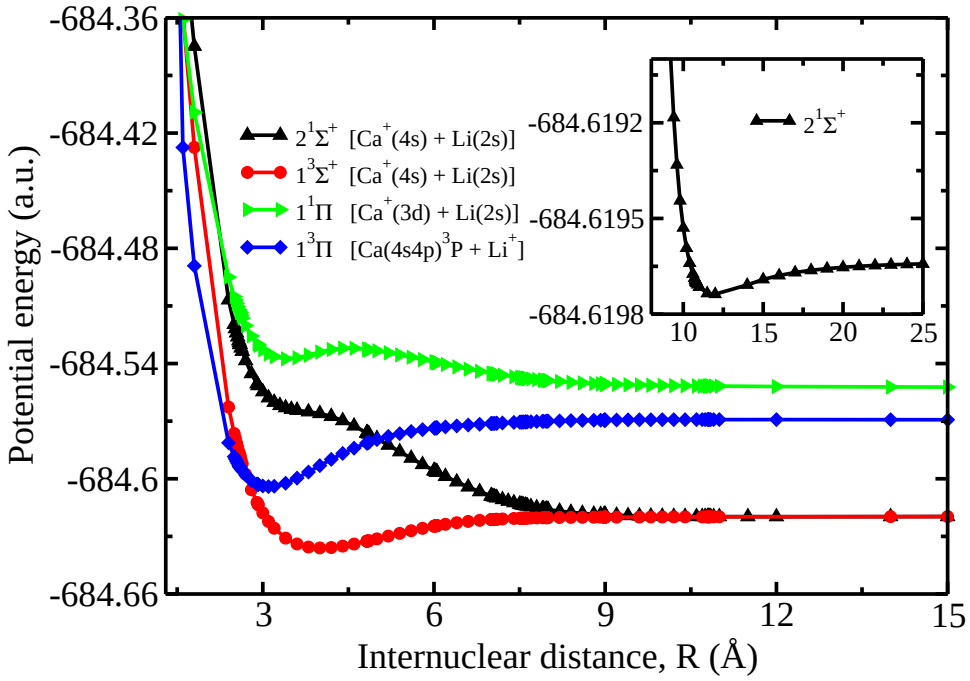

Figure 4.12: Potential energy curves for the electronic excited states of $CaLi^+$ using EOM-CCSD/QZ method.

$2\,^1\Sigma^+$, $1\,^3\Sigma^+$, $1\,^1\Pi$ and $1\,^3\Pi$ are plotted in Figure (4.12) and Figure (4.13), respectively. The extracted spectroscopic constants together with the available results in the literature are reported in Table (4.10). The values of equilibrium bond length and harmonic frequency reported in the present work for triplet states are in reasonable

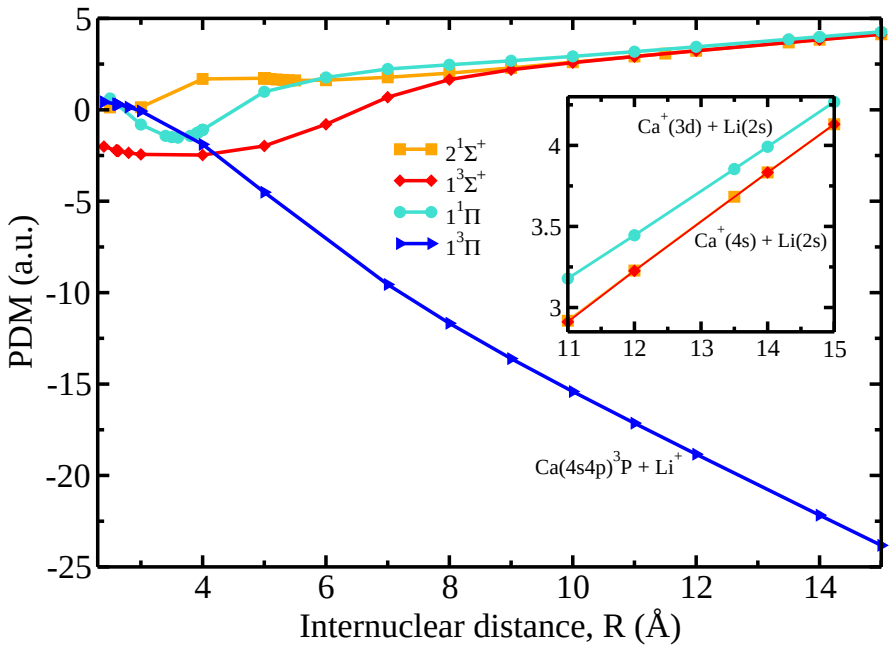

Figure 4.13: Permanent dipole moment curves for the electronic excited states of $CaLi^+$ using EOM - CCSD/QZ method.

agreement with the available results reported in Ref. [175]. However, their results for D_e are different from ours by 2195.52 cm^{-1} for $1\,^3\Sigma^+$, and 1361.06 cm^{-1} for $1\,^3\Pi$ state. The reasons for this large discrepancy are not different from those discussed earlier for the case of $MgLi^+$. Further, though the nature of our PEC for the $2\,^1\Sigma^+$ state is very similar to that of Ref. [175], it is weakly bound in our case and the potential minimum is situated at a distance almost twice of that of Ref. [175]. On the other hand, we have observed one bound minimum situated at a distance of 3.425 Å for the $1^1\Pi$ state and it becomes repulsive after a bond distance of 4.5 Å. In striking contrast, this PEC is reported to be attractive and the state is strongly bound with a potential depth of 6643.47 cm^{-1} in Ref. [175]. Therefore, our results of the diatomic constants which are extracted from the PECs of these singlet states should not be compared directly with that of Ref. [175]. Further theoretical or experimental works are necessary to verify these observations, and settle the discrepancies between these two works.

Table 4.10: The calculated spectroscopic constants for the low-lying excited states of $CaLi^+$ using EOM-CCSD/QZ method, compared with the available results in the literature.

State	$R_e\,(a_0)$	$D_e\,(\mathrm{cm}^{-1})$	$T_e\,(\mathrm{cm}^{-1})$	$\omega_e\,(\mathrm{cm}^{-1})$	$\omega_e x_e\,(\mathrm{cm}^{-1})$	$B_e\,(\mathrm{cm}^{-1})$	$\alpha_e\,(\mathrm{cm}^{-1})$	Ref.
$2^1\Sigma^+$	22.41	23.39	16500.54	6.474	0.63	0.0201	0.0020	This work
	13.68	412.37	–	41	–	–	–	[175]
$1^3\Sigma^+$	7.609	3596.4	12925.95	141.873	0.22	0.1663	0.0003	This work
	7.18	5791.92	–	136	–	–	–	[175]
$1^3\Pi$	5.879	7621.13	19933.56	255.875	1.57	0.2904	0.0021	This work
	5.71	8982.19	–	251	–	–	–	[175]
$1^1\Pi$	6.472	1371.90	34547.72	214.752	1.66	0.2397	0.0014	This work
	6.69	6643.47	–	193	–	–	–	[175]

Table 4.11: Energies of a few low-lying electronic states of $CaLi^+$ at the dissociative limit.

		E (cm^{-1})		
Molecular state	Asymptotic molecular state	This work	NIST [191]	% difference
$X^1\Sigma^+$	$Ca\,(4s^2) + Li^+$	0.0	0.0	–
$2^1\Sigma^+$	$Ca^+\,(4s) + Li(2s)$	6438.22	5818.82	10.6
$1^3\Sigma^+$	$Ca^+\,(4s) + Li(2s)$	6438.22	5818.82	10.6
$1^3\Pi$	$Ca\,(4s\,4p)\,^3P + Li^+$	17466.91	15227.97	15
$1^1\Pi$	$Ca^+\,(3d) + Li(2s)$	21170.74	19499.35	8.6

The atomic states to which these molecular states dissociate into, at the asymptotic distances, are calculated and the compilation is shown in Table (4.11). As it can be seen from this table that both the molecular states $2\,^1\Sigma^+$ and $1\,^3\Sigma^+$ dissociate into the same set of atomic states, *viz.*, $Ca^+\,(4s) + Li(2s)$. The excitation energy for these states with respect to the electronic ground state of neutral CaLi, at the asymptotic limit, is 49875.80 cm^{-1}, and that matches well with the first ionization energy of Ca, which is 49305.95 cm^{-1}. The other states $1\,^1\Pi$ and $1\,^3\Pi$ dissociate into $Ca^+(3d) + Li(2s)$ and $Ca\,(4s\,4p)\,^3P + Li^+\,(1s^2)$, respectively.

The dissociative nature of the molecular states reported in our work agrees with that reported in Ref. [175]. From Figure (4.13) and Table (4.11), it is clear that

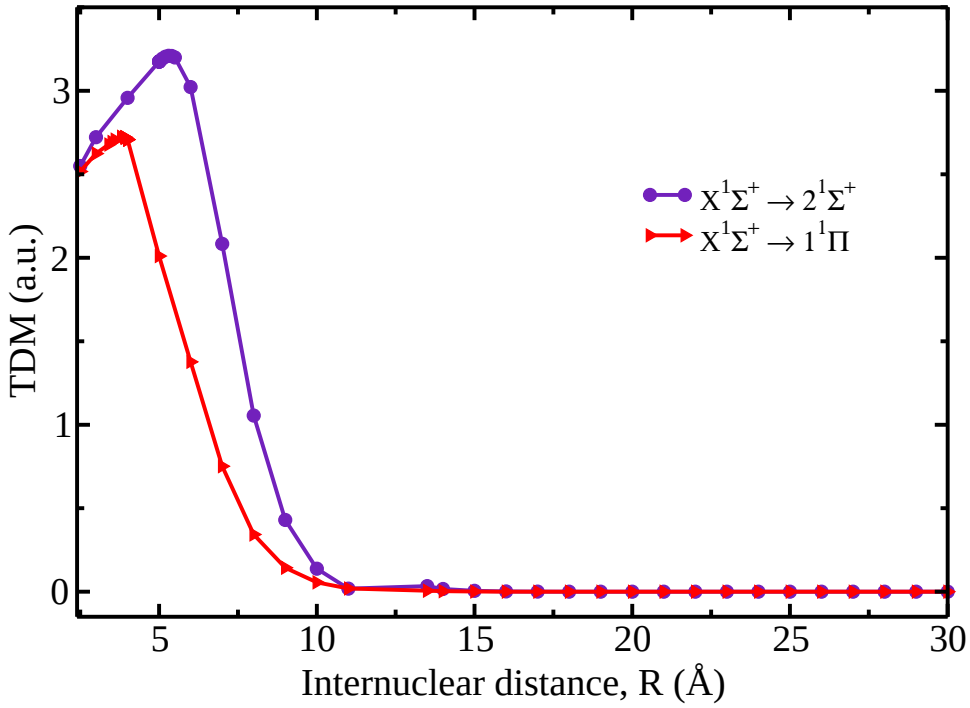

Figure 4.14: Transition dipole moment, as a function of R, from the ground state to the excited singlet electronic states of $CaLi^+$ using EOM - CCSD/QZ method.

those states which possess positive value of dipole moment at large distances dissociate into $Ca^+\,(4s \text{ or } 3d) + Li\,(2s)$, whereas, those states with negative value of dipole

moment dissociate into Ca ($4s^2$ or 4s 4p) + Li^+ ($1s^2$). This trend is exactly in line with that observed in the case of $MgLi^+$.

In order to estimate the effect of diffuse functions on the transition energies, we have used singly - augmented QZ basis sets. The contribution of these additional functions is observed to be less than 0.42% at the equilibrium point, and 0.063% at the asymptotic limit for both the molecular ions. The TDM curves for the transitions from the electronic ground state to the singlet excited states of $CaLi^+$ are shown in Figure (4.14). The maximum value of TDM for $X\,^1\Sigma^+ \rightarrow 2\,^1\Sigma^+$ and $X\,^1\Sigma^+ \rightarrow 1\,^1\Pi$, transition is found to be 3.210 a.u. at 5.3 Å and 2.725 a.u. at 3.8 Å, respectively. At

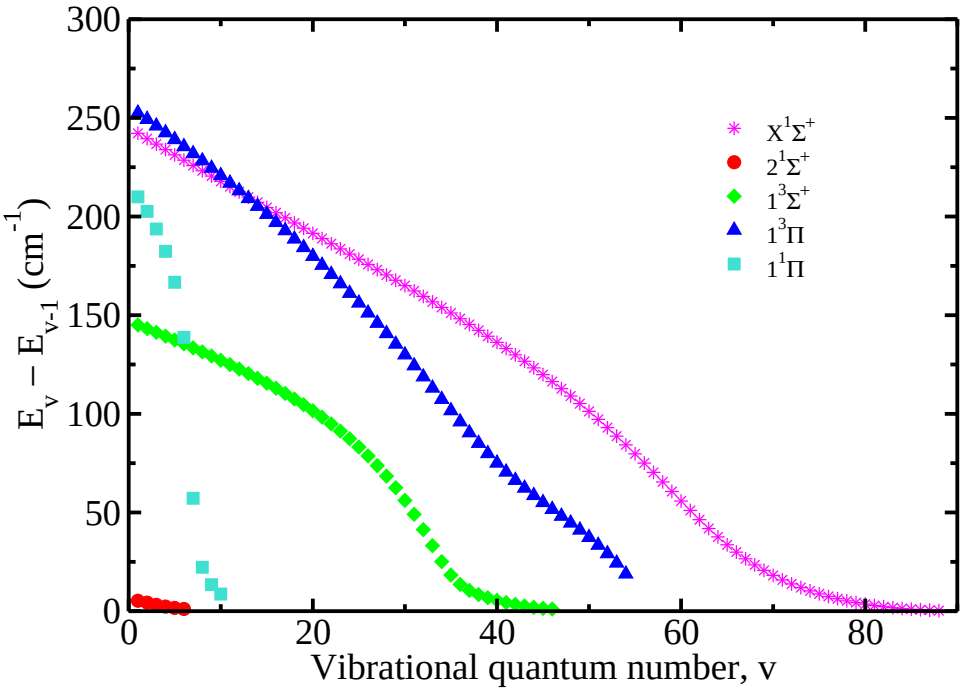

Figure 4.15: Energy spacing between the adjacent vibrational levels of the electronic ground state (using CCSD(T)/QZ level) and of the excited states (using EOM - CCSD/QZ method) of $CaLi^+$.

large distance the TDMs drop to zero.

We have obtained the maximum vibrational levels to be 7 for $2\,^1\Sigma^+$, 47 for $1\,^3\Sigma^+$, 55

for $1\,^3\Pi$ and 11 for $1\,^1\Pi$ state. The corresponding energy spacing between the last two vibrational levels in these states are 1.13, 1.05, 8.6 and 18.8 cm^{-1}, respectively. The relative vibrational energy spacing as a function of 'v' is plotted in Figure (4.15), and the trends are not uniform because of anharmonic effects. The details of the data related to the vibrational spacings and the rotational constants for the vibrational states are provided in the Table (4.12).

4.4 Summary

In conclusion, we have performed several *ab initio* calculations for the ground state and a few low - lying excited electronic states of $MgLi^+$ and $CaLi^+$. To obtain reliable results for the spectroscopic constants and molecular properties we have used higher - order correlation method such as CCSD(T) and also we have considered all - electron correlations even in large basis sets. Our results of diatomic constants and PDMs are compared with the published results, wherever available. The results of the QMs and various components of DPs of $MgLi^+$ and $CaLi^+$ are being reported for the first time. The errors arising both from the truncation of correlation effects and finite basis set size effects have also been estimated, and the recommended values are highlighted in bold fonts in the tables. Further, the adiabatic effects such as DBOC are estimated for both the ions at the CCSD level. The effect of augmenting the basis sets with diffuse functions on the molecular properties of the ground state and the transition energies for the excited states is also studied. Using PECs and PDM curves, the vibrational wavefunctions, constants of vibrational spectroscopy, TDMs between different vibrational states, spontaneous - and BBR - induced transition rates, and hence, the lifetimes of vibrational states are calculated. The lifetime of the $X\,^1\Sigma^+$ state in its ro - vibrational ground state is found to be 2.81 s for $MgLi^+$, and 3.19 s for $CaLi^+$, at room temperature. The lifetime of vibrational states as a function of the vibrational quantum number is studied, and it has been found that the higher vibrational states close to dissociation limit can have lifetimes larger than

Table 4.12: Relative energies and rotational constants for vibrational levels of excited electronic states of $CaLi^+$. The results are quoted in cm^{-1}.

	$2^1\Sigma^+$		$1^3\Sigma^+$		$1^3\Pi$		$1^1\Pi$	
v	ΔE_v	B_v	ΔE_v	B_v	ΔE_v	B_v	ΔE_v	B_v
0	–	0.0189	–	0.1733	–	0.2906	–	0.2392
1	5.27	0.0172	145.06	0.1715	252.47	0.2880	209.98	0.2358
2	4.34	0.0152	143.20	0.1697	249.26	0.2853	202.61	0.2320
3	3.20	0.0131	141.30	0.1679	245.89	0.2826	193.70	0.2273
4	2.33	0.0111	139.38	0.1661	242.49	0.2799	182.36	0.2213
5	1.65	0.0092	137.44	0.1643	239.02	0.2771	166.66	0.2124
6	1.13	0.0074	135.45	0.1625	235.46	0.2743	138.76	0.1917
7	–	–	133.44	0.1607	231.89	0.2714	57.23	0.1284
8	–	–	131.39	0.1588	228.24	0.2685	22.23	0.1031
9	–	–	129.30	0.1569	224.52	0.2655	13.44	0.0825
10	–	–	127.16	0.1550	220.76	0.2625	8.66	0.0647
11	–	–	124.96	0.1531	216.95	0.2594	–	–
12	–	–	122.71	0.1511	213.07	0.2563	–	–
13	–	–	120.39	0.1490	209.15	0.2531	–	–
14	–	–	118.00	0.1470	205.18	0.2499	–	–
15	–	–	115.53	0.1448	201.13	0.2466	–	–
16	–	–	112.97	0.1426	197.02	0.2432	–	–
17	–	–	110.31	0.1403	192.85	0.2397	–	–
18	–	–	107.53	0.1379	188.60	0.2362	–	–
19	–	–	104.61	0.1354	184.26	0.2326	–	–
20	–	–	101.55	0.1328	179.83	0.2290	–	–
21	–	–	98.32	0.1301	175.30	0.2253	–	–
22	–	–	94.90	0.1272	170.67	0.2215	–	–
23	–	–	91.25	0.1241	165.93	0.2177	–	–
24	–	–	87.37	0.1208	161.09	0.2137	–	–
25	–	–	83.19	0.1171	156.14	0.2097	–	–
26	–	–	78.67	0.1132	151.09	0.2055	–	–
27	–	–	73.78	0.1089	145.94	0.2013	–	–
28	–	–	68.44	0.1041	140.68	0.1968	–	–
29	–	–	62.58	0.0987	135.33	0.1923	–	–
30	–	–	56.14	0.0926	129.89	0.1875	–	–
31	–	–	49.06	0.0856	124.35	0.1826	–	–
32	–	–	41.33	0.0776	118.74	0.1775	–	–
33	–	–	33.15	0.0686	113.06	0.1722	–	–
34	–	–	25.11	0.0592	107.34	0.1667	–	–
35	–	–	18.31	0.0507	101.61	0.1611	–	–
36	–	–	13.56	0.0440	95.93	0.1555	–	–

Table 4.12: Continued...

	$1^3\Sigma^+$		$1^3\Pi$	
v	ΔE_v	B_v	ΔE_v	B_v
37	10.51	0.0386	90.40	0.1499
38	8.41	0.0340	85.08	0.1443
39	6.80	0.0299	79.87	0.1387
40	5.48	0.0261	75.03	0.1334
41	4.36	0.0226	70.50	0.1282
42	3.41	0.0192	66.27	0.1233
43	2.61	0.0161	62.33	0.1184
44	1.94	0.0133	58.61	0.1137
45	1.43	0.0109	55.04	0.1091
46	1.05	0.0087	51.58	0.1044
47	–	–	48.14	0.0996
48	–	–	44.66	0.0947
49	–	–	41.10	0.0895
50	–	–	37.37	0.0839
51	–	–	33.41	0.0778
52	–	–	29.12	0.0709
53	–	–	24.36	0.0628
54	–	–	18.83	0.0525

the lifetime of the ro - vibrational ground state. It is important to note that the long lifetimes of the highly excited vibrational states are desired for several ultracold experiments [177].

In addition, the behaviour of electronic TDM as a function of internuclear distance is also studied for the transitions from ground - to the singlet excited states for both $MgLi^+$ and $CaLi^+$. We believe that the all - electron *ab initio* results of various spectroscopic constants and properties that are presented here may serve as benchmarks for similar calculations in the future, and also they may be of interest to the experimental spectroscopists who would consider working on these molecular systems in the future.

CHAPTER 5

PROPERTIES OF ALKALINE-EARTH MONOFLUORIDES

"Mathematics began to seem too much like puzzle solving. Physics is puzzle solving, too, but of puzzles created by nature, not by the mind of man" – Maria Goeppert Mayer

5.1 Introduction

The alkaline-earth monofluorides (AEMFs) are currently in the forefront of several important theoretical as well as experimental research works not only in physics but also in chemistry. The AEMFs have attracted theorists because of their simple electronic structure: open-shell with their ground state being $^2\Sigma$, and the experimentalists because of the ease with which they could be laser-cooled. The latter is evident from the multitude of experiments that have been carried out to realize cooling and trapping of MgF [147], CaF [148, 149], SrF [150, 153, 201, 202] and

A part of the results presented in this chapter has been reported in a research publication [110].

BaF [152, 203] molecules. Some of the heavier members of AEMFs such as BaF [5] and RaF [6, 7] have been studied chiefly for fundamental symmetry violating effects which give rise to the nuclear anapole moment. Such effects bear vital implications for the physics beyond the standard model of particle physics. The chemical reaction between the SrF molecules at ultracold temperatures has been investigated by Meyer *et al.* [204] that can be used for the study of dipolar degenerate quantum gases.

The accurate theoretical predictions of various molecular properties are crucial in guiding the ongoing and forthcoming experiments with cold and ultracold diatomic molecules. To quote a few: the knowledge of PDMs of molecules is helpful for the study of long - range dipole - dipole interactions, EDM of an electron (eEDM), for qubits in quantum computations, and for several quantum phases in ultracold gases [43, 46, 47, 52, 71]. Similarly, the knowledge of electric DPs is one of the requisites for manipulating and for controlling the dynamics of molecules in laser fields [205–209]. Further, the knowledge of $\mathcal{P}$ & $\mathcal{T}$ - odd interaction constants such as W_d and W_s are crucial for resolving mysteries surrounding matter - antimatter asymmetry in the universe [210, 211].

A few theoretical studies of AEMF molecules that are being investigated in this work have already been reported in the literature. To mention: a detailed structural study of BaF molecule has been performed by Tohme and Korek [212]; the spectroscopy and evaluation of properties such as dipole moments of SrF molecules for the ground - and low - lying excited states has been performed by Jardali *et al.* [213]; the electronic structure calculations for the ground - and several excited states of AEMF (AE = Be, Mg, Ca) molecules have been performed by Kork *et al.* [214]. Further, the AEMF (AE = Be, Mg, Ca, Sr, Ba) molecules together with mercury halides and PbF have been studied by Abe *et al.* recently for the PDMs and for effective electric fields (ε_{eff}) using relativistic finite - field CCSD (FFCCSD) method [215]. The theoretical results for the isotropic and anisotropic components of molecular polariz-

ability ($\bar{\alpha}$ and γ) of BeF and MgF at the CASSCF level, and model - based predictions for AEMFs are available in Refs. [216, 217]. The polarizability components of SrF calculated using CCSD(T) method has been reported in Refs. [42,204], while only the z - component of polarizability for BaF has been calculated using MRCI method in Ref. [212]. Nevertheless, there are no experimental results available in the literature, known to our knowledge, for the DPs of these molecules.

The calculations of HFS constants of MgF and CaF have been performed by Sasmal *et al.* using Z - vector method in the relativistic CC approximation [218]. The experimental results for HFS constants of SrF and BaF with ^{87}Sr and ^{137}Ba, and also HFS constant of F atom in MgF and CaF molecule have been reported by Knight *et al.* [219]. The semi - empirical and *ab initio* calculations at SCF and RASSCF level for W_d, W_s and HFS constants of BaF have been estimated by Kozlov *et al.* in Ref. [220]. The RaF molecule with ^{223}Ra isotope has been studied by Kudashov *et al.* for their HFS and symmetry violating parameters [6].

In this chapter, we have studied the whole series of group - II monofluorides systematically and uniformly using the same quality of basis sets, and employing the same level of correlation method. In addition to the molecular properties: PDMs, components of molecular DPs, HFS and $\mathcal{P}$ & $\mathcal{T}$ - odd interaction constants of AEMFs, we have also calculated the atomic polarizabilities of alkaline - earth and fluorine atoms using GAS technique at the KRCISD level of theory. The theory and details of calculations along with the results are discussed below.

5.2 Theory

5.2.1 Permanent Dipole Moment and Dipole Polarizability

The valence electric properties: molecular PDMs and components of molecular polarizabilities for the ground state of open - shell AEMFs, and atomic polarizabilities of alkaline - earth and fluorine atoms are computed using the finite - field approach as discussed in Subsection (1.1.4). The relativistic energies of the systems (both atoms and molecules) considered in this work are calculated using weak perturbative electric field with varying strengths in the range; $(2 - 5) \times 10^{-4}\, E_h/ea_0$ along different coordinate axes. Further, by using the first - and the second - order polynomial fits to the data of $E(\varepsilon)$ against ε, we obtain PDMs and DPs, respectively.

5.2.2 Magnetic Dipole Hyperfine Interaction

The interaction of electric/magnetic moment of the nucleus with the electromagnetic field of the electron leads to the hyperfine structure splitting in atoms and molecules [120]. The magnetic vector potential $\vec{\mathcal{A}}(\vec{r})$ at a distance $\vec{r}$ from the center of nucleus of an atom is given by [115],

$$\vec{\mathcal{A}}(\vec{r}) \;=\; \frac{\mu_0}{4\pi}\,\frac{\vec{\mu}_N \times \vec{r}}{r^3}, \tag{5.1}$$

where $\vec{\mu}_N$ is the nuclear magnetic moment (NMM) and μ_0 is the vaccum permeability. The magnetic moment of a nucleus can be defined in terms of nuclear spin $\vec{\mathcal{I}}$ as [221],

$$\vec{\mu}_N \;=\; g_{\mathcal{I}}\,\vec{\mathcal{I}}\,\mu_N, \tag{5.2}$$

where $g_{\mathcal{I}}$ is the gyromagnetic ratio and $\mu_N \;=\; \dfrac{|e|\,\hbar}{2\,M_p}$ is the unit of NMM, known as nuclear magneton.

The HFS Hamiltonian of an atom due to the magnetic vector potential, $\vec{\mathcal{A}}(\vec{r})$, in

the Dirac theory is given by [218, 221, 222],

$$H_{HFS} \;=\; -e\,c\sum_{j=1}^{n}\vec{\alpha_j}\,.\,\vec{\mathcal{A}}_j(\vec{r}), \tag{5.3}$$

where α_j are the Dirac matrices for j^{th} electron; e is the electronic charge; and c is the speed of light.

By considering z-axis as the internuclear axis of a molecule, the z and x (or y) projections of the expectation values of the HFS Hamiltonian, we obtain the parallel ($A_\parallel$) and perpendicular ($A_\perp$) components of HFS constants as [6, 222],

$$\begin{aligned} A_\parallel \;&=\; \frac{1}{\mathcal{I}\Omega}\left\langle\Psi_\Omega\,|\,H_{HFS}\,|\,\Psi_\Omega\right\rangle, \\ &=\; \frac{\vec{\mu}_N}{\mathcal{I}\Omega}\;\cdot\;\left\langle\Psi_\Omega\right|\sum_{j=1}^{n}\left(\frac{\vec{\alpha_j}\times\vec{r_j}}{r_j^3}\right)_z\left|\Psi_\Omega\right\rangle, \\ &=\; \frac{\vec{\mu}_N}{\mathcal{I}\Omega}\;\cdot\;\left\langle\Psi_{^2\Sigma_{1/2}}\right|\sum_{j=1}^{n}\left(\frac{\vec{\alpha_j}\times\vec{r_j}}{r_j^3}\right)_z\left|\Psi_{^2\Sigma_{1/2}}\right\rangle, \end{aligned} \tag{5.4}$$

and

$$\begin{aligned} A_\perp \;&=\; \frac{1}{\mathcal{I}\,\Omega}\left\langle\Psi_\Omega\,|\,H_{HFS}\,|\,\Psi_{-\Omega}\right\rangle, \\ &=\; \frac{\vec{\mu}_N}{\mathcal{I}\Omega}\;\cdot\;\left\langle\Psi_\Omega\right|\sum_{j=1}^{n}\left(\frac{\vec{\alpha_j}\times\vec{r_j}}{r_j^3}\right)_{(x/y)}\left|\Psi_{-\Omega}\right\rangle, \\ &=\; \frac{\vec{\mu}_N}{\mathcal{I}\Omega}\;\cdot\;\left\langle\Psi_{^2\Sigma_{1/2}}\right|\sum_{j=1}^{n}\left(\frac{\vec{\alpha_j}\times\vec{r_j}}{r_j^3}\right)_{(x/y)}\left|\Psi_{^2\Sigma_{-1/2}}\right\rangle, \end{aligned} \tag{5.5}$$

respectively. Here n is the total number of electrons; Ω is the z-component of the total angular momentum of the diatomic molecule; and Ψ_Ω is the wavefunction for the ground state of AEMFs, *viz.*, $^2\Sigma$ state with $\Omega = 1/2$. The $^2\Sigma$ molecular electronic states with $\Omega = +1/2$ and $\Omega = -1/2$ are degenerate. However, their determinants differ by only spin of an electron. Further, the average and anisotropic parameters:

A and A_d, can be obtained, respectively, using [220]:

$$A = \frac{A_{\parallel} + 2\,A_{\perp}}{3}, \tag{5.6}$$

and

$$A_d = \frac{A_{\parallel} - A_{\perp}}{3}. \tag{5.7}$$

5.2.3 Intrinsic Electron Electric Dipole Moment

Classically, a free elementary particle cannot have an electric dipole moment. Nevertheless, in quantum field theory, each particle is surrounded by a virtual charge cloud of particles and anti - particles. A small deviation in the virtual charge cloud from the spherical symmetry can give a tiny eEDM [223]. Further, it has been predicted by several models of particle physics that the electron has a non - zero EDM, which arises due to the simultaneous violation of the $\mathcal{P}$ & $\mathcal{T}$ symmetries [224]. The expectation value of the operator describing the interaction of eEDM of a molecular system is given by [53, 225–228],

$$\begin{aligned}\left\langle \sum_{j=1}^{n} \hat{H}_{edm}(j) \right\rangle_{\Psi} &= -d_e \left\langle \sum_{j=1}^{n} \gamma_j^0\, \Sigma_j\, \varepsilon_j \right\rangle_{\Psi}, \\ &\approx \frac{2\,i\,c\,d_e}{e\,\hbar} \left\langle \sum_{j=1}^{n} \gamma_j^0\, \gamma_j^5\, p_j^2 \right\rangle_{\Psi},\end{aligned} \tag{5.8}$$

where d_e is the intrinsic electric dipole moment of an electron; γ^0 and γ^5 ($\equiv i\,\gamma^0\gamma^1\gamma^2\gamma^3$) are the 4 - component Dirac matrices; ε_j is the electric field at the position of j^{th} electron; p_j is the momentum operator; and Ψ is the molecular wavefunction determined from the many - body theory. Finally, the ε_{eff} experienced by the unpaired electron in a molecular system is defined as [6],

$$\varepsilon_{eff} = W_d\,\Omega, \tag{5.9}$$

where $W_d = (2\,i\,c/\Omega\,e\,\hbar)\langle\gamma^0\,\gamma^5\,p^2\rangle_\Psi$ is the $\mathcal{P}$ & $\mathcal{T}$ - odd interaction constant. A measurement of the shift in energy (ΔE) of a molecule in an electronic state (Ψ_Ω) due to eEDM (d_e), in conjunction with a theoretically estimated ε_{eff} (related by the equation $\Delta E = -d_e\,\varepsilon_{eff}$), provides a value of intrinsic eEDM [229].

5.2.4 Scalar - Pseudoscalar Interaction

The nucleon - electron interaction that arises due to the coupling between scalar - hadronic current and the pseudoscalar electronic current is known as scalar - pseudoscalar (S - PS) interaction. The S - PS interaction Hamiltonian for a molecular system is given by [6, 227],

$$H_{S-PS} = \frac{i}{e}\frac{G_F}{\sqrt{2}}\sum_{j=1}^{n}\sum_{A=1}^{N} k_{s,\,A}\,Z_A\,\gamma^0\,\gamma^5\,\rho_A(r_{Aj}), \tag{5.10}$$

where $G_F\,(=\,2.22249\times10^{-14}\,E_h a_0^3)$ is the Fermi coupling constant [6, 230]; ρ_A is the nuclear charge density; the summation running over j and A represent the number of electrons and nuclei, respectively. The $k_{s,\,A}$ is a dimensionless nucleus - electron S - PS coupling constant of an atom and it is defined as [230],

$$k_{s,\,A} = k_{s,p} + \frac{N_A}{Z_A}\,k_{s,n}, \tag{5.11}$$

where Z_A and N_A represent the number of protons and neutrons in a particular atom A, respectively. $k_{s,p}$ ($k_{s,n}$) is the S - PS constant of an electron and a proton (a neutron). Further, the $\mathcal{P}$ & $\mathcal{T}$ - odd interaction constant (W_s) that measures the shift in energy arising due to the nucleon - electron S - PS interaction, can be evaluated as,

$$W_s = \frac{1}{k_{s,\,A}\,\Omega}\,\langle\,H_{S-PS}\rangle_\Psi. \tag{5.12}$$

It is clear from Eq. (5.10) that the matrix element of H_{S-PS} varies roughly as $A\,Z^2 \approx Z^3$ [227] and hence, heavy polar molecules are preferred for the study of symmetry

violating effects. The contributions of the lighter atom in a diatomic molecule to the shift in energy due to S - PS interaction is negligibly small [230, 231].

5.3 Methodology

In order to compute the molecular properties discussed in Section (5.2), we have used the KRCI module of the DIRAC software suite [143]. After generating the reference state using the DF Hamiltonian, the KRCISD calculations are performed by employing the GAS technique. The Gaussian charge distribution for the nuclei is used in these calculations. All atomic and molecular properties are calculated using C_{2v} point group, while the C_2 subgroup is used to compute the perpendicular component of molecular polarizability. Further, we have used the uncontracted cc - pVQZ basis sets for Be, F, and Mg [128], and Dyall basis sets of similar quality (dyall.v4z) for Ca, Sr, Ba, and Ra [130]. These basis sets are quite large, when used in uncontracted form, as it can be seen from the explicit functions shown in Table (5.1). Such computationally expensive large basis sets are considered for obtaining reliable results.

We have adopted a frozen core (FC) approximation for atoms as well as for molecules

Table 5.1: Details of the basis sets for alkaline - earth and fluorine atoms in uncontracted form.

Atom	Basis
Be	cc - pVQZ: 12s, 6p, 3d, 2f, 1g
F	cc - pVQZ: 12s, 6p, 3d, 2f, 1g
Mg	cc - pVQZ: 16s, 12p, 3d, 2f, 1g
Ca	dyall.v4z: 30s, 20p, 6d, 5f, 3g
Sr	dyall.v4z: 33s, 25p, 15d, 4f, 3g
Ba	dyall.v4z: 35s, 30p, 19d, 4f, 3g
Ra	dyall.v4z: 37s, 34p, 23d, 15f, 3g

to make the correlation calculations manageable, particularly, for the heavy molecular systems. The atomic polarizability calculations are carried out with 10 outermost

electrons, *viz.*, ns, np and $(n+1)$s orbitals, where n being 2 for Mg, 3 for Ca, 4 for Sr, 5 for Ba, and 6 for Ra atom. However, for Be and F atoms, all electrons are kept active in the post - DF calculations. Further, a virtual cutoff energy of $10\,E_h$ is set uniformly for all atoms and molecules in order to truncate the orbitals having higher energies so that the computations can be made manageable.

The atomic orbitals are partitioned into four subspaces: frozen core, GAS1, GAS2 and GAS3, as shown in Table (5.2). The first subspace is the FC and it is excluded in

Table 5.2: Generalized active space model for the CI wavefunctions of atoms with $10E_h$ virtual cutoff energy.

Atom	Number of orbitals					Number of Slater determinants	Number of Slater determinants*
	Frozen core	GAS1	GAS2	GAS3	GAS3*		
Be	0	1	1	56	81	18929	39529
Mg	1	4	1	59	84	156056	316681
Ca	5	4	1	114	139	583681	868056
Sr	14	4	1	107	132	514136	782761
Ba	23	4	1	110	135	543401	818776
Ra	39	4	1	108	133	523801	794676
F	0	1	4	25	50	74630	299255

*Column with '$*$' for the augmented case replaces its preceding un - augmented column.

correlation calculations. For Be atom, filled 1s and 2s orbitals form GAS1 and GAS2 subspace, respectively. However, for other alkaline - earth atoms, GAS1 contain filled active [ns, np] and GAS2 contain filled active [$(n+1)$s] orbitals. On the other hand, for the open shell F atom, 1s orbital form GAS1, and [2s, 2p] orbitals form GAS2 subspace. All electrons available in GAS1 and GAS2 subspaces are allowed to excite to the virtual orbitals contained in GAS3 subspace. In case of augmented basis sets, GAS3* replaces GAS3. The number of resulting Slater determinants, for each atom, corresponding to QZ and aug - QZ basis sets are shown in the last two columns of

Table (5.2). For molecular property calculations, the DF orbitals having energy less than -2 E_h are considered as frozen core. The center of alkaline - earth atom is chosen as the coordinate origin of the corresponding diatomic molecule. In the GAS technique, active DF orbitals are divided into three subspaces: paired (GAS1), unpaired (GAS2), and virtual orbitals (GAS3). Similar to the atoms, the GAS3 is replaced by GAS3* for the augmentation calculations of AEMFs. The number of Slater determinants along with the number of orbitals in different subspaces for all molecules corresponding to QZ and aug - QZ basis sets are shown in Table (5.3).

The values of equilibrium bond lengths used in this work are: 1.359 Å for BeF [214], 1.778 Å for MgF [214], 2.015 Å for CaF [214], 2.124 Å for SrF [213], 2.162 Å for BaF [212] and 2.244 Å for RaF [7].

Table 5.3: Generalized active space model for the CI wavefunctions of alkaline - earth monofluorides with $10E_h$ virtual cutoff energy.

Molecule	Number of orbitals					Number of Slater determinants	Number of Slater determinants*
	Frozen core	GAS1	GAS2	GAS3	GAS3*		
BeF	2	4	1	80	128	410645	1050245
MgF	6	4	1	84	132	452681	1116857
CaF	7	7	1	139	188	3789982	6931568
SrF	15	8	1	132	180	4463853	8298909
BaF	24	8	1	134	183	4600095	8577768
RaF	40	8	1	133	183	4531718	8577768

*Column with '$*$' for the augmented case replaces its preceding un - augmented column.

5.4 Results and Discussion

5.4.1 Atomic Dipole Polarizabilities

Our results for atomic polarizabilities (α_A) for the alkaline - earth and fluorine atoms together with the available results in the literature are presented in Table (5.4). The correlation contributions to the α_A of alkaline - earth atoms at the level of KRCISD with reference to the DF results are negative. The magnitude of α_A increases as we go from Be to Ba. However, α_A decreases suddenly for Ra by about 8.2% when compared to Ba. It has been observed that the expectation value of $\langle r \rangle$ for 7s orbital of Ra is smaller than the 6s orbital of Ba and this is attributed as the reason for the decrease in α_A of Ra [232]. Our findings at the KRCISD/QZ level of correlation are in good agreement with the experimental data, well within their reported uncertainty limits [127, 233–235]. For Be and Ra, however, there are no experimental results available. Our results also compare quite well with the available theoretical calculations [232, 236–240].

In addition, we have investigated the effect of diffuse functions on the results by repeating the calculations with singly augmented QZ basis sets. The number of Slater determinants is considerably large with the augmented basis, as can be seen from Table (5.2), even while the number of active electrons and the virtual cutoff energy are the same as that of the un - augmented basis sets. The resulting computational costs get dearer especially while performing correlation calculations. These additional functions do not seem to alter the value of α_A much, particularly at the DF level. The maximum change is only about 0.6% for Mg. However, at the KRCISD level, the maximum change obtained in the result of α_A is about 4.1% for Be.

The relativistic CCSD calculations have been reported in Ref. [236], for alkaline - earth atoms along with He and Yb, and the contribution from the leading - order triples are quoted as error bars. Our KRCISD results compare quite well with those

Table 5.4: Results of dipole polarizabilities (in units of $e^2\,a_0^2\,E_h^{-1}$) for the ground state of alkaline-earth and fluorine atoms compared with the available results in the literature.

Method	Be	Mg	Ca	Sr	Ba	Ra	F
SCF/QZ	45.5	81.0	183.0	233.0	324.0	297.0	2.5
SCF/aug-QZ	45.5	80.5	182.5	232.0	323.5	297.0	3.5
KRCISD/QZ	37.0	73.0	157.0	194.0	269.5	247.5	3.0
KRCISD/aug-QZ	38.5	73.0	157.5	196.5	269.0	248.5	3.5
Expt.	–	70.89[a], 59 (16)[b]	169 (17)[c]	186 (15)[d]	268 (22)[c]	–	–
PRCC [232]	–	70.76	160.77	190.82	274.68	242.42	–
CCSD [236]	37.80 (47)	73.41 (2.32)	154.58 (5.42)	199.71 (7.28)	268.19 (8.74)	–	–
CI + MBPT2 [237]	37.76 (22)	71.3 (7)	157.1 (1.3)	197.2 (2)	273.5 (2.0)	–	–
DF [238]	–	–	182.79	232.66	323.82	299.59	–
CCSD(T) [238]	–	–	157.9	199	273.5	246.2	–
CCSD(T)	–	–	–	–	272.7[e]	242.8[e]	3.70[f]
CASPT2	37.2[g]	70.9[g]	163[g]	210[g]	312[g]	283[g]	3.76[h]
CASSCF [241]	–	–	–	–	–	–	3.68
MR-CCI† [241]	–	–	–	–	–	–	3.52

[a]Reference [127] [b]Reference [233]
[c]Reference [234] [d]Reference [235]
[e]Reference [240] [f]Reference [242]
[g]Reference [239] [h]Reference [243]
†Externally contracted multireference configuration interaction.

reported in Ref. [236]; the difference in the two being: 2.1% for Be, 0.6% for Mg, 1.6% for Ca, 2.9% for Sr and 0.5% for Ba. Our results at KRCISD level also agree well, to within 3.2%, with the results reported in Ref. [232], wherein they have used perturbed relativistic CC (PRCC) method.

The polarizability calculations with the inclusion of core - core and core - valence correlations using MBPT2 and valence - valence correlations using the CI method has been reported in Ref. [237]. Further, those authors have improved their results by obtaining the matrix elements using experimental lifetimes of the electronic states. In contrast, our *ab initio* results reported in this work are in good agreement with their recommended values, with the maximum deviation being 2.4%

The DF results of α_A for Ca through Ra, reported in our work, show excellent agreement with those given in Ref. [238] at the similar level. However, our fully relativistic KRCISD results vary from their recommended scalar relativistic results computed using the CCSD(T) method by 0.6% for Ca, 2.5% for Sr, 1.5% for Ba and 0.5% for Ra.

The calculated value of polarizability for F with and without augmentation comes out to be 3.5 a.u. and 3 a.u., respectively, at the KRCISD level. The former value is in good agreement with the other reported calculations [241–243].

5.4.2 Permanent Dipole Moments

The PDM values calculated using QZ basis sets in this work together with the available experimental, theoretical and semi - empirical model - based results are shown in Table (5.5), and our PDM results with aug - QZ basis sets are reported in Table (5.6).

Leaving aside BaF, our values of PDMs of all other AEMFs calculated at the KRCISD level show excellent agreement with the available results in the literature. To

Table 5.5: Results of permanent dipole moments (in Debye) for the ground state of alkaline - earth monofluorides at equilibrium bond length compared with the available results in the literature.

Molecule	Method	$\|\mu_0\|$	Ref.
BeF	SCF/QZ	1.246	This work
	KRCISD/QZ	1.116	This work
	FFCCSD	1.15	[215]
	SCF	1.30	[244]
	LCCSD[a]	1.10	[244]
	FD - HF	1.2727	[245]
	CISD	1.131	[246]
	CPF	1.086	[246]
	MP2	1.197	[247]
MgF	SCF/QZ	3.207	This work
	KRCISD/QZ	3.124	This work
	FFCCSD	3.13	[215]
	SCF	3.16	[244]
	LCCSD[a]	3.07	[244]
	FD - HF	3.1005	[245]
	CISD	3.048	[246]
	CPF	3.077	[246]
	MP2	3.186	[247]
	IM [b]	3.64	[248]
	EPM[c]	3.5	[249]
CaF	SCF/QZ	2.894	This work
	KRCISD/QZ	3.181	This work
	FFCCSD	3.19	[215]
	SCF	2.77	[244]
	LCCSD[a]	3.16	[244]
	FD - HF	2.6450	[245]
	CISD	2.590	[246]
	CPF	3.060	[246]
	MP2	3.190	[247]
	IM[b]	3.34	[248]
	LFA[d]	3.00	[250]
	EPM[c]	3.2	[249]
	MRD - CI[e]	3.01	[251]
	LFA[d]	3.36	[252]
	Exp.	3.07(7)	[253]

Table 5.5: Continued...

Molecule	Method	$\|\mu_0\|$	Ref.
SrF	SCF/QZ	2.930	This work
	KRCISD/QZ	3.395	This work
	CCSD(T)	3.4564	[42]
	FFCCSD	3.62	[215]
	SCF	3.01	[244]
	LCCSD[a]	3.60	[244]
	Z-vector	3.4504	[254]
	FD-HF	2.5759	[245]
	CISD	2.523	[246]
	CPF	3.199	[246]
	IM[b]	3.67	[248]
	EPM[c]	3.6	[249]
	LFA[d]	3.79	[252]
	Exp.	3.4676(10)	[255]
BaF	SCF/QZ	2.122	This work
	KRCISD/QZ	2.706	This work
	MRCISD	2.958	[212]
	FFCCSD	3.41	[215]
	SCF	2.65	[244]
	LCCSD[a]	3.40	[244]
	IM[b]	3.44	[248]
	EPM[c]	3.4	[249]
	LFA[d]	3.91	[252]
	Exp.	3.170(3)	[256]
RaF	SCF/QZ	3.045	This work
	KRCISD/QZ	3.621	This work

[a]Linearized coupled - cluster method with single - and double excitations
[b]Ionic model
[c]Electrostatic polarization model
[d]Ligand - field approach
[e]Multi - reference single - and double excitation configuration - interaction

the best of our knowledge, the PDM of RaF molecule is being reported, in this work, for the first time in the literature.

It has been observed that the correlation contributions to the PDMs of lighter

Table 5.6: Results of permanent dipole moments (in Debye) for the ground state of alkaline - earth monofluorides at equilibrium bond length calculated with aug - QZ basis sets.

Molecule	Method	$\|\mu_0\|$
BeF	SCF	1.246
	KRCISD	1.143
MgF	SCF	3.235
	KRCISD	3.177
CaF	SCF	2.893
	KRCISD	3.221
SrF	SCF	2.963
	KRCISD	3.465
BaF	SCF	2.122
RaF	SCF	3.050

molecules in this series are negative (-0.13 D for BeF and -0.083 D for MgF), while for the heavier molecules, these contributions are comparatively large and positive (0.287 D for CaF, 0.465 D for SrF, 0.584 D for BaF and 0.576 D for RaF). At the level of KRCISD, the magnitude of PDM increases gradually from BeF to RaF, with BaF as an exception. Further, the effect of adding diffuse functions to QZ basis sets on PDMs of these molecules is not more than 1.2% at the DF level. However, at the KRCISD level there is a maximum of 2.4% increase in the value of PDM among the four lower members of this series. Due to the lack of sufficient computational resources, we are unable to perform the calculations with the augmented basis sets for BaF and RaF. In the discussion that follows, we have compared our results with the experimental values and *ab initio* calculations that are available in the literature.

Our calculated PDM results differ from the corresponding experimental results by $\sim$ 3.6% for CaF [253], 2.1% for SrF [255] and 14.6% for BaF [256]. Further, it has to be noted that all available calculations, including ours, for BaF show a large deviation, ranging between 6.7% to 14.6%, from the experimental result reported in Ref. [256].

Recently, Prasannaa *et al.* [244] have performed CCSD calculations of PDMs by using only the linear terms in the CC wavefunction together with the cc - pVXZ (X = D, T, Q) basis sets for lighter elements (Be, Mg, Ca and F) and the combination of Dyall - and Sapporo basis sets for Sr and Ba atom. In Table (5.5), we have quoted their results only at the QZ basis level for a fair comparison with our results. Their results differ from ours by 0.016 D, 0.054 D, 0.021 D and -0.205 D for the first four members of the AEMF series. These differences lie within the error bars that they have reported (± 0.1 D for BeF, MgF and CaF, while ± 0.2 D for SrF). The PDM for BaF in our work deviates from their result by 0.694 D, which falls outside their estimated error bar of 0.2 D. However, they claim that their error estimate on this is completely uncertain due to numerical convergence issues and incompleteness of basis.

The FFCCSD results for PDMs by keeping all filled - and virtual orbitals as active have been reported in Ref. [215]. The basis sets used in this work are the same as that of Ref. [244] discussed in the preceding paragraph. The difference between the two results is only 0.034 D for BeF, 0.006 D for MgF, 0.009 D for CaF and 0.225 D for SrF. Furthermore, other recent calculations of PDM of SrF using the Z - vector method within CCSD approximation [254], and CCSD(T) method [42] differ from our KRCISD result by about 1.6% and 1.8%, respectively.

The absolute difference between our values of PDM at the DF level and those reported by Kobus *et al.* [245] at the finite difference HF (FD - HF) level increases from BeF to SrF. Similar is the situation between our relativistic findings at KRCISD/QZ level and the results reported by Langhoff *et al.* [246] using CISD and coupled pair functional (CPF) method together with the extended Slater type basis sets. The CPF results of Ref. [246] seem to be more closer to our KRCISD results as compared to their CISD results. It has to be noted that in both works, [245] and [246] the calculations have been performed in the non - relativistic framework. Therefore, the increase in difference between our results and those reported in the Refs. [245, 246]

could be due to the increase in relativistic effects as one go from BeF to SrF.

5.4.3 Molecular Dipole Polarizabilities

The results for polarizability components of AEMFs calculated in this work using QZ basis sets are tabulated along with those of other calculations in Table (5.7). The magnitudes of both polarizability components ($\alpha_{\parallel}$ and $\alpha_{\perp}$) increase as one goes from BeF to BaF. However, it has been observed that the magnitudes of $\alpha_{\parallel}$ and $\alpha_{\perp}$ for RaF are smaller than those of BaF. The contribution of fluorine to the DP of these molecules is small when compared to the contribution of alkaline - earth atom. The decrease in DP of RaF when compared to BaF can be explained in terms of the structure of radium atom itself, as discussed in the case of atomic polarizability.

All molecules of group - II monofluorides exhibit negative polarizability anisotropy (γ), which is supported by *ab initio* calculations in Ref. [216] and by several model-based predictions in Ref. [217]. All available calculations including ours for polarizability components are higher than those predicted by Davis in Ref. [217] using different electrostatic models.

The absolute value of correlation contribution to the average component of polarizability increases drastically as one traverses to higher members of AEMFs. Further, the correlation contributions for both $\bar{\alpha}$ and γ, as it can be seen from Table (5.7), are quite significant for the heavier molecules, *viz.*, CaF through RaF. The values of correlation contributions to the $\bar{\alpha}$ are: 13.63 a.u. for CaF, 31.16 a.u. for SrF, 68.67 a.u. for BaF, and 79.50 a.u. for RaF. These values of correlation contributions are one order of magnitude larger than that observed for the case of MgF (= - 1.33 a.u.) and by two orders of magnitude larger than that observed for the case of BeF (= - 0.67 a.u.). Similarly, for γ, these contributions are 22.1 a.u. for CaF, 34 a.u. for SrF, 110.5 a.u. for BaF and 70.5 a.u. for RaF, which are much larger than the value of 0.5 a.u.

Table 5.7: Results of dipole polarizabilities (in units of $e^2\,a_0^2\,E_h^{-1}$) for the ground state of alkaline - earth monofluorides at equilibrium bond length compared with the available results in the literature.

Molecule	Method	$\alpha_{\parallel}$	$\alpha_{\perp}$	$\bar{\alpha}$	γ	Ref.
BeF	SCF/QZ	18.0	29.0	25.33	-11.0	This work
	KRCISD/QZ	19.0	29.5	26.0	-10.5	This work
	CASSCF	–	–	27.30	-10.45	[216]
	T - Rittner	–	–	1.69	–	[217]
	TEK[a]	–	–	1.79	-0.19	[217]
	D - shell (-1)[b]	–	–	1.92	0.19	[217]
	D - shell (q)[c]	–	–	2.04	1.34	[217]
MgF	SCF/QZ	34.5	57.5	49.83	-23.0	This work
	KRCISD/QZ	37.5	58.0	51.16	-20.5	This work
	CASSCF	–	–	53.34	-22.79	[216]
	T - Rittner	–	–	3.69	–	[217]
	TEK[a]	–	–	4.10	-1.64	[217]
	D - shell (-1)[b]	–	–	4.27	-1.21	[217]
	D - shell (q)[c]	–	–	4.19	-0.02	[217]
CaF	SCF/QZ	91.4	172.0	145.13	-80.6	This work
	KRCISD/QZ	92.5	151.0	131.50	-58.5	This work
	T - Rittner	–	–	7.69	–	[217]
	TEK[a]	–	–	9.17	-5.77	[217]
	D - shell (-1)[b]	–	–	9.31	-5.20	[217]
	D - shell (q)[c]	–	–	9.03	-4.03	[217]
SrF	SCF/QZ	137.0	248.5	211.33	-111.5	This work
	KRCISD/QZ	128.5	206.0	180.17	-77.5	This work
	CCSD(T)	126	–	–	–	[204]
	CCSD(T)	125	–	170.05	-66.35*	[42]
	T - Rittner	–	–	9.69	–	[217]
	TEK[a]	–	–	11.69	-7.83	[217]
	D - shell (-1)[b]	–	–	11.82	-7.21	[217]
	D - shell (q)[c]	–	–	11.57	-6.35	[217]
BaF	SCF/QZ	214.5	413.5	339.33	-222.5	This work
	KRCISD/QZ	196.0	308.0	270.66	-112.0	This work
	MRCISD	182.590	–	–	–	[212]
	T - Rittner	–	–	12.69	–	[217]
	TEK[a]	–	–	15.71	-11.41	[217]
	D - shell (-1)[b]	–	–	15.81	-10.72	[217]
	D - shell (q)[c]	–	–	15.41	-9.50	[217]

Table 5.7: Continued...

Molecule	Method	$\alpha_{\parallel}$	$\alpha_{\perp}$	$\bar{\alpha}$	γ	Ref.
RaF	SCF/QZ	195.0	351.0	299.0	-156.0	This work
	KRCISD/QZ	162.5	248.0	219.5	-85.5	This work

[a]Törring - Ernst - Kindt
[b]Displaced shell model in which q_+ shell charges corresponding to valence shell electron, were set to -e.
[c]Displaced shell model where q_+ shell charges were treated as parameters.
*In Ref. [42], the authors have reported positive value of γ (or $\Delta\alpha$), however it comes out to be negative according to the definition given in Eq. (1.52).

(2.5 a.u.) for BeF (MgF) molecule.

The results of molecular polarizabilities using aug - QZ basis sets are tabulated in Table (5.8). We have observed that the augmentation of basis sets gives a positive contribution to the values of both $\alpha_{\parallel}$ and $\alpha_{\perp}$ components and is more effective for lower members of AEMFs rather than their heavier cousins at the DF level. Further, at the KRCI level, the augmented basis sets alter the value of $\alpha_{\parallel}$ by 7.9% (5.3%) and $\alpha_{\perp}$ by 5.1% (5.2%) for BeF (MgF) molecule. For other molecules, KRCISD calculations with the augmented basis sets are not performed due to the lack of sufficient computational resources. Nevertheless, we have estimated the effect of diffuse functions by adding the difference between the SCF energies calculated using the basis sets with and without augmentation, to the energies calculated at KRCISD level. With this energy correction, the estimated values of $\alpha_{\parallel}$ and $\alpha_{\perp}$ components increase, respectively, by 8.1% and 3.6% for CaF, 1.9% and 0.5% for SrF, 4% and 2.8% for BaF, and 4.3% and 3% for RaF.

Fowler and Sadlej [216] have employed the CASSCF method together with the contracted basis sets (10s 6p 4d) $\rightarrow$ [5s 3p 2d] for Be and F atom, and (13s 10p 4d) $\rightarrow$ [7s 5p 2d] for Mg, to compute the dipole polarizability components of BeF and MgF molecules. A total of 9 electrons are kept active in 4σ and 2π orbitals. We have also

Table 5.8: Results of dipole polarizabilities (in units of $e^2\,a_0^2\,E_h^{-1}$) for the ground state of alkaline - earth monofluorides at equilibrium bond length calculated with aug - QZ basis sets.

Molecule	Method	$\alpha_{\parallel}$	$\alpha_{\perp}$	$\bar{\alpha}$	γ
BeF	SCF	19.0	31.0	27.0	-12.0
	KRCISD	20.5	31.0	27.5	-10.5
MgF	SCF	37.5	60.5	52.83	-23.0
	KRCISD	39.5	61.0	53.83	-21.5
CaF	SCF	99.0	177.5	151.33	-78.5
	KRCISD†	100.0	156.5	137.67	-56.5
SrF	SCF	139.5	249.5	212.83	-110.0
	KRCISD†	130.9	207.0	181.63	-76.1
BaF	SCF	221.0	422.0	355.0	-201.0
	KRCISD†	203.9	316.5	278.97	-112.6
RaF	SCF	202.0	358.5	306.33	-156.5
	KRCISD†	169.5	255.5	226.83	-86.0

† These values are calculated by adding the difference between the SCF energies calculated using the basis sets with and without augmentation, to the energies calculated at KRCISD level.

included the same number of electrons (9) in our correlation calculation of BeF and MgF. However, our virtual space (80 and 84 molecular orbitals for BeF and MgF, respectively) is very large compared to that considered in Ref. [216]. For BeF, our values of $\bar{\alpha}$ and γ at KRCISD level differ from those reported in Ref. [216] by 4.8% and -0.5%, respectively, while for MgF, the difference between the results of two works is 4.1% for $\bar{\alpha}$ and 10% for γ.

Meyer and Bohn [204] have reported only the parallel component of polarizability for SrF using CCSD(T) method available in MOLPRO quantum chemistry package. They have used effective core potential (ECP28MDF) basis set for Sr and augmented correlation - consistent valence quadruple zeta basis set for F atom. Our value of $\alpha_{\parallel} = 128.5$ a.u. at KRCISD level agrees well with the value of 126 a.u. reported in Ref. [204] to within 2%. Quite recently, Kosicki *et al.* [42] have applied the CCSD(T) method in conjunction with the core - valence aug - cc - pCVQZ basis set for F and

ECP28MDF basis set for Sr atom to calculate the electric properties of SrF. The values of $\bar{\alpha}$ and γ reported in Ref. [42] differ from ours by 5.6% and 14.4%, respectively. It must be mentioned here that we have included 17 electrons to perform the correlation calculations in a virtual space of 132 orbitals. The similar information on number of correlated electrons and the size of virtual space is not clear from Ref. [42] for the comparison.

Tohme and Korek [212] have computed the z - component of polarizability for BaF molecule using MRCISD method. They have used ECP basis set (5s 5p 4d) for the Ba atom and valence double - zeta basis set (6s 3p) $\rightarrow$ [3s 2p] for F atom. Further, only five electrons are included in their correlation calculations. On the other hand, we have considered 17 electrons as active in a virtual space of 134 orbitals. The value of $\alpha_{\parallel}$ reported in Ref. [212] is smaller by 6.8% from our result at the similar level of approximation.

The computed values of $\alpha_{\parallel}$ and $\alpha_{\perp}$ for CaF (RaF) are 92.5 (162.5) a.u. and 151.0 (248.0) a.u., respectively, by considering 15 (17) electrons in the correlation calculation with 139 (133) virtual orbitals. There is no calculation available in the literature, known to our knowledge, to compare our results of polarizability components of CaF and RaF.

5.4.4 Magnetic Dipole Hyperfine Structure Constants

The reported results for the HFS constants are calculated using the locally modified DIRAC11 program package. The absolute values of the computed components of HFS constants at the DF and KRCISD level together with the existing results are given in Table (5.9). The values of nuclear spin and NMM for alkaline - earth and fluorine atoms and their different isotopes used to calculate the HFS constants are tabulated in Table (5.10) [258].

Table 5.9: Results of parallel ($A_{\parallel}$) and perpendicular ($A_{\perp}$) components of magnetic dipole HFS constants (in MHz) of alkaline - earth monofluorides using QZ basis sets, compared with the available results in the literature.

Molecule	Atom	Method	$A_{\parallel}$	$A_{\perp}$	Ref.
BeF	^{9}Be	SCF	237.28	227.62	This work
		KRCISD	236.37	227.16	This work
	^{19}F	SCF	190.20	137.75	This work
		KRCISD	253.50	128.95	This work
MgF	^{25}Mg	SCF	253.59	243.94	This work
		KRCISD	250.48	241.38	This work
		SCF	249.2	239.4	[222]
		RAS - CI	272.4	260.3	[222]
		ECC	282.6	270.4	[222]
		Z - vector	281.8	269.6	[218]
	^{19}F	SCF	162.63	92.45	This work
		KRCISD	271.09	136.47	This work
		SCF	168.0	99.8	[222]
		RAS - CI	255.4	139.4	[222]
		ECC	320.9	153.3	[222]
		Z - vector	322.6	148.7	[218]
		Exp.	331(3)	143(3)	[219]
CaF	^{43}Ca	SCF	316.69	305.68	This work
		KRCISD	342.27	326.83	This work
		Z - vector	426.4	408.9	[218]
	^{19}F	SCF	72.15	54.30	This work
		KRCISD	105.43	72.91	This work
		Z - vector	131.7	83.8	[218]
		Exp.	149	106	[219]
SrF	^{87}Sr	SCF	400.80	387.59	This work
		KRCISD	453.47	434.32	This work
		Exp.	591	570	[219]
	^{19}F	SCF	60.66	48.37	This work
		KRCISD	86.10	63.33	This work
		Exp.	126	95	[219]

In Ref. [219], the authors have reported the experimental results for the HFS constants of ^{19}F in the case of MgF, CaF, SrF and BaF molecules. They have observed

Table 5.9: Continued...

Molecule	Atom	Method	$A_{\parallel}$	$A_{\perp}$	Ref.
BaF	^{135}Ba	SCF	1430.49	1390.80	This work
		KRCISD	1611.87	1551.13	This work
	^{137}Ba	SCF	1600.22	1555.82	This work
		KRCISD	1803.12	1735.17	This work
		SCF*	1479	1446	[220]
		RASSCF*	1488	1455	[220]
		SCF - EO*†	2264	2186	[220]
		RASSCF - EO*†	2272	2200	[220]
		Exp.	2453(9)	2401(6)	[219]
		Exp.	2376	2301(9)	[257]
	^{19}F	SCF	38.77	35.68	This work
		KRCISD	47.82	41.27	This work
		Exp.	67	59	[219]
RaF	^{223}Ra	SCF	1573.11	1519.25	This work
		KRCISD	1737.15	1661.89	This work
		GHF - ZORA‡	1900	1860	[7]
		SODCI◇	1790	1720	[6]
		FS - RCCS⋆	1700	1630	[6]
		FS - RCCSD⋆	2100	2020	[6]
		CCSD	2090	–	[6]
		CCSD(T)	2110	–	[6]
		$\mathrm{CCSD}^{\oplus}_{enlarged}$	2080	–	[6]
		$\mathrm{CC}^{\odot}_{final}$	2110	2020	[6]
	^{225}Ra	SCF	4260.76	4114.88	This work
		KRCISD	4705.07	4501.22	This work
	^{227}Ra	SCF	2345.16	2264.86	This work
		KRCISD	2589.71	2477.51	This work
	^{19}F	SCF	55.40	48.11	This work
		KRCISD	74.09	60.02	This work

*These components are calculated from the results of A and A_d reported in Ref. [220] using Eqs. (5.6 - 5.7).
†SCF and RASSCF calculations with effective operator technique.
‡Generalized HF - zeroth - order regular approximation.
◇Spin - orbit direct CI.
⋆Relativistic 2 - component Fock - space CC approach.
$^{\oplus}$CCSD with larger basis sets.
$^{\odot}$CCSD results are corrected with triple excitations and basis set enlargement.

Table 5.10: Compilation of the values of nuclear spin quantum number ($\mathcal{I}$) and NMM (μ_N) of alkaline - earth and fluorine atoms used in this work.

Atom	$\mathcal{I}$	NMM
^{9}Be	3/2	-1.1779
^{19}F	1/2	2.628867
^{25}Mg	5/2	-0.85546
^{43}Ca	7/2	-1.31727
^{87}Sr	9/2	-1.09283
^{135}Ba	3/2	0.837943
^{137}Ba	3/2	0.37365
^{223}Ra	3/2	0.271
^{225}Ra	3/2	-0.734
^{227}Ra	3/2	-0.404

that the spin density on the F atom is much smaller than on the alkaline - earth atom, which thereby supports the ionic character of the AEMFs. Based on the orbital mixing theory, they have analyzed that the anisotropic values of the HFS constants (that can be calculated using Eq. (5.7)) of ^{19}F reveal the covalent character in the lighter molecules. It can be seen from Table (5.9) that as we go from MgF to BaF at the KRCISD level, the magnitude of HFS constants for F atom decreases similar to that reported in Ref. [219]. Therefore, one can conclude that the ionicity of the bond in BaF is greater than that for the case of MgF. The minimum and maximum difference between our computed values of F atom in molecular environment at the KRCISD level and experimental values reported in Ref. [219] for $A_{\|}$ is 19.18 MHz and 59.91 MHz, and for $A_{\perp}$, it is 6.53 MHz and 33.09 MHz, respectively.

Our findings for HFS constants at KRCISD level, are reasonably in good agreement with the available results in the literature. However, the recent calculations show that the CC together with the Z - vector method can construct accurate wavefunction near the nuclear region than that with the KRCISD method [218, 222]. For BeF, we have reported the results of HFS constants for the first time in our work, to the best of our knowledge. Except for Be and Mg, the correlation contribution to the

other alkaline - earth atoms is positive. Further, the absolute correlation contribution increases from Be to Ba and then decreases for Ra atom in monofluorides for both parallel and perpendicular components.

In order to understand the effect of the inclusion of core electrons and triple excitations, we have performed two additional calculations (i) by considering triple excitations at KRCI level in the FC approximation and (ii) by considering all electrons at the KRCISD level, for two lower members of the series, as shown in Table (5.11). From these additional calculations, we infer that the results for the HFS constant of

Table 5.11: Comparison of parallel ($A_{\parallel}$) and perpendicular ($A_{\perp}$) components of magnetic HFS constants (in MHz) of BeF and MgF at different level of approximations.

Molecule	Atom	Method	$A_{\parallel}$	$A_{\perp}$
BeF	^{9}Be	KRCISD + FC	236.37	227.16
		KRCISDT + FC	236.27	227.49
		KRCISD + All e^{-}	257.08	247.42
	^{19}F	KRCISD + FC	253.50	128.95
		KRCISDT + FC	267.92	112.19
		KRCISD + All e^{-}	253.25	133.25
MgF	^{25}Mg	KRCISD + FC	250.48	241.38
		KRCISDT + FC	250.29	241.61
		KRCISD + All e^{-}	276.70	264.74
	^{19}F	KRCISD + FC	271.09	136.47
		KRCISDT + FC	306.05	140.26
		KRCISD + All e^{-}	255.92	129.43

alkaline - earth atom is improved by keeping all electrons as active at the KRCISD level, while the results of F atom is improved with the inclusion of triple excitation within the FC approximation. Therefore, the simultaneous addition of triple excitation and all electrons are necessary to further improve the accuracy of HFS constants. Nevertheless, we have not reported these calculations in this work and we may consider it in our future work.

Further, for the quantitative comparison, we have considered the case of MgF system for which the HFS constants are available in the literature using both Z - vector method [222] and extended CC (ECC) theory [218]. We have observed that the inclusion of all electrons increases the results calculated with FC approximation at the KRCISD level for Mg atom by 10.5% for $A_{\parallel}$ and 9.7% for $A_{\perp}$ component. The computed values for HFS constants of Mg by considering all electrons as active at KRCISD level (KRCISD + All e^-) in the present work vary from the results reported in Refs. [218, 222] using ECC and Z - vector method by only 2.1% and 1.8%, respectively. The addition of triple excitations to KRCISD (KRCISDT + FC) increases the values of $A_{\parallel}$ and $A_{\perp}$ components of F atom by 13.3% and 2.8%, respectively. Our results at the KRCISDT + FC level of correlation differ from the experimental values of F atom by 7.2% for $A_{\parallel}$ and by 1.9% for the $A_{\perp}$ component [219], while our results for $A_{\parallel}$ and $A_{\perp}$ components deviate by 5.1% (4.6%) and 5.7% (8.5%), respectively, from *ab initio* calculations reported in Refs. [218, 222].

5.4.5 $\mathcal{P}$ & $\mathcal{T}$ - Odd Interaction Constants

The values of $\mathcal{P}$ & $\mathcal{T}$ - odd interaction constants (W_d) calculated using Eq. (5.9) at the KRCISD method in the present work together with the available results in the literature are collected in Table (5.12). Our results calculated at the KRCISD level using DIRAC17 program compare well with the existing semi - empirical and *ab initio* results reported in Refs. [5, 6, 155, 215, 220, 259]. The minimum and maximum difference between our results and those reported in Ref. [215] at FFCCSD level is 0.0003 ($\times 10^{25}$ Hz/e-cm) for BeF and 0.03814 ($\times 10^{25}$ Hz/e-cm) for BaF, respectively, at the similar level of basis set.

Nayak and Chaudhuri [5] have utilized the RASCI method together with the uncontracted Gaussian basis sets (27s 27p 12d 8f) for Ba and (15s 10p) for F to compute the W_d constant of BaF. Further, they have considered 17 electrons in 76 active or-

Table 5.12: Results of $\mathcal{P}$ & $\mathcal{T}$ - odd interaction constants, W_d (in Hz/e-cm) for the ground state of alkaline - earth monofluorides calculated using KRCISD/QZ method.

Molecule	$\lvert W_d\rvert$ ($\times 10^{25}$)	Ref.
BeF	0.00021	This work
	0.00024^{a*}	[215]
MgF	0.00269	This work
	0.00339^{a*}	[215]
CaF	0.01161	This work
	0.01354^{a*}	[215]
SrF	0.08979	This work
	0.10446^{a*}	[215]
BaF	0.27426	This work
	0.293^{b}, 0.352^{c}	[5]
	0.31240^{a*}	[215]
	0.26^{d}	[259]
	0.230^{e}, 0.224^{f}, 0.375^{g}, 0.364^{h}	[220]
	0.35^{i} 0.41^{i}	[155]
RaF	2.34303	This work
	2.40^{j}, 2.25^{k}, 2.65^{l}, 2.36^{m}, 2.33^{n}, 2.30^{o}, 2.56^{p}	[6]
	2.20^{d}	[259]

[a]FFCCSD, [b]DF, [c]RAS - CI, [d]Using numerically calculated value of W_S parameter, [e]SCF, [f]RASSCF, [g]SCF - EO, [h]RASSCF - EO, [i]semiempirical calculations, [j]SODCI, [k]FS - RCCS, [l]FS - RCCSD, [m]CCSD, [n]CCSD(T), [o]$\text{CCSD}_{enlarged}$, [p]CC_{final}
*These results are obtained using Eq. (5.9) with the values of ε_{eff} taken from Ref. [215].

bitals. We have, on the other hand, considered the same number of electrons in 143 active orbitals, which is very large in comparison to that included in Ref. [5]. Our computed result differs from the value given in Ref. [5] by 0.07774 ($\times 10^{25}$ Hz/e-cm) at the similar level of theory.

Isaev and Berger [259] have obtained the ε_{eff} for BaF and RaF numerically. Our value of W_d parameter is larger by 5.4% (6.5%) for BaF (RaF) from that computed using ε_{eff} reported in their work via Eq. (5.9).

Kudashov *et al.* [6] have performed spin - orbit direct CI (SODCI) calculations by

considering 19 electrons explicitly to report the W_d constant for RaF and our result varies by 2.4% from that estimated in their work. In the same Ref., the authors have also reported the W_d constant using relativistic 2 - component Fock - Space CCSD method. Further, the CCSD result is corrected by including the contributions due to triple excitations as well as basis set enlargement. Their final value ($= 2.56\,(\times 10^{25}\,\mathrm{Hz/e\text{-}cm})$) of W_d including these corrections is larger by 8.5% from our result ($= 2.34303\,(\times 10^{25}\,\mathrm{Hz/e\text{-}cm})$) at the KRCISD level.

The calculated S - PS $\mathcal{P}$ & $\mathcal{T}$ - odd interaction parameter (W_s) at the KRCISD level using QZ basis sets, along with the available results in the literature are given in Table (5.13). There is no calculation available in the literature to compare our results for the first four members of the series. For BaF, our value lies in between the results based on semi - empirical and *ab initio* calculations reported in Refs. [155, 220]. Our result of W_s at the KRCISD level for RaF shows excellent agreement with that reported in Ref. [6] at the SODCI level. The CC value that includes triple contributions as well as large basis set effects estimated in Ref. [6] is 6.1% larger than our result.

Table 5.13: Results of S - PS constants, W_s (in KHz) for the ground state of alkaline - earth monofluorides calculated using KRCISD/QZ method.

Molecule	Atom	W_s	Ref.
BeF	Be	0.0013	This work
MgF	Mg	0.0414	This work
CaF	Ca	0.1775	This work
SrF	Sr	1.7033	This work
BaF	Ba	7.286	This work
		11^{*}, 13^{*}	[155]
		$6.1^{\dagger}$, $5.9^{\ddagger}$	[220]
RaF	Ra	130.52	This work
		131^{a}, 122^{b}, 144^{c}, 128^{d}, 127^{e}, 125^{f}, 139^{g}	[6]

*Semi - empirical calculations, †SCF, ‡RASSCF.
^{a}SODCI, ^{b}FS - RCCS, ^{c}FS - RCCSD, ^{d}CCSD, ^{e}CCSD(T), $^{f}\mathrm{CCSD}_{enlarged}$, $^{g}\mathrm{CC}_{final}$

5.5 Summary

In summary, we have carried out the calculations for PDMs, molecular DPs, HFS and $\mathcal{P}$ & $\mathcal{T}$ - odd interaction constants of AEMFs and also, the polarizability calculations for atoms that form the diatomic molecules studied in this work using KRCISD method. These *ab initio* calculations are performed using GAS technique with the uncontracted quadruple - zeta quality basis sets. Some of the results, particularly, the PDM of RaF; components of molecular polarizability for CaF and RaF; W_s for BeF, MgF, CaF and SrF; and HFS constants of BeF, are computed and reported in this work for the first time, to the best of our knowledge. It has been found that the accurate calculations of the HFS constants require the inclusion of triple excitations as well as core electrons. Further, the effect of adding diffuse functions on the values of valence electric properties (PDMs and polarizabilities) are examined by considering the singly augmented QZ basis sets. Except F for which the effect of diffuse functions to the α_A is 16.7%, the change in the values of α_A for other atoms is not more than 4.1% at the KRCI level. The use of aug - QZ basis sets alters the results of molecular PDMs by a maximum of 2.4% among first four members of the series. In contrast, the contribution of diffuse functions are quite significant for the components of molecular polarizability ranging between 1.9% to 7.9% for $\alpha_{\parallel}$ and 0.5% to 5.2% for $\alpha_{\perp}$. We believe that our relativistic calculations performed with large optimized basis sets and with large active space would be considered more reliable and would serve as benchmarks for the future theoretical and experimental studies relevant to eEDM searches, laser spectroscopy and the collision physics.

CHAPTER 6

CONCLUSIONS AND FUTURE OUTLOOK

"I think nature's imagination is so much greater than man's, she's never going to let us relax" – Richard Phillips Feynman

6.1 Conclusions

This thesis work involves the structural study of diatomic molecules containing alkaline - earth atoms, particularly, singly charged alkaline - earth lithides ($AELi^+$) and neutral alkaline - earth monofluorides (AEMFs). After discussing the necessary basics of diatomic molecules and many - body theories briefly, we have chosen to investigate the simplest molecule amongst the $AELi^+$, i.e., $BeLi^+$, in Chapter 3 [108] because the feasibility of formation of this ion via photoassociation processes has been predicted recently [1]. We have calculated spectroscopic constants: equilibrium bond length (R_e), dissociation energy (D_e), harmonic frequency (ω_e), anharmonic frequency ($\omega_e\, x_e$) and rotational constants (B_e and α_e), and also the molecular

properties: permanent dipole moment (μ_0), quadrupole moment (Θ_{zz}), average and anisotropic components of dipole polarizability ($\bar{\alpha}$ and γ) and dipole polarizability at the asymptotic limit (α_{100}) for the ground state of $BeLi^+$ using SCF, MP2, CCSD, and CCSD(T) methods by including all the filled - as well as virtual orbitals explicitly in correlation calculations. These calculations are performed with successive hierarchy of basis sets, cc - pVXZ (X = D, T,Q) and the results are extrapolated to the CBS limit using exponential - Gaussian functions [188, 189]. Further, by taking the difference between CCSD(T) and CCSD results at the CBS level we have estimated the error bars, so as to report accurate and reliable results for $BeLi^+$.

We have examined the effects of adding diffuse functions on the ground state diatomic constants as well as on the molecular properties of $BeLi^+$ by considering the single augmentation of the basis sets. Except for $\omega_e x_e$, γ and α_{100}, the difference in our final results between the augmented and un - augmented basis sets for all parameters lie within the reported error bars. Further, the addition of DBOC at the CCSD level modifies energy by 332 cm^{-1} uniformly throughout the region of PEC. Therefore, the values of R_e and D_e will not get affected. Furthermore, the higher - order electron correlation effects beyond the CCSD(T) level of approximation are estimated by performing the PEC calculations using CCSDT/QZ method. It has been found that the values of R_e and B_e do not change with the inclusion of non - leading order triples to CCSD(T), at least for up to the accuracies reported in this work, whereas the value of D_e increases by 3 cm^{-1} and ω_e decreases by 0.06 cm^{-1}.

By using the PECs and PDM curves of ground electronic state at CCSD(T)/QZ level, we have obtained the vibrational properties: energies, wavefunctions, rotational constants, and TDMs between the vibrational levels. Further, lifetimes of the vibrational states have been computed using relative energy spacings and vibrational TDMs. The lifetime of ro - vibrational ground state has been found to be 4.67 s for $BeLi^+$, when BBR - induced transition rates are considered.

We have also studied a few low - lying excited states of $BeLi^+$ using EOM - CCSD/QZ method at the non - relativistic level. Further, the relativistic effects for the $1\,^3\Pi$ state have been evaluated using the DF Hamiltonian and the correlation calculation at the KRCISD level. We have observed that the $^3\Pi_1$ and $^3\Pi_2$ states lie $1.96\,cm^{-1}$ and $3.92\,cm^{-1}$, respectively, above the $^3\Pi_0$ state.

We have extended our work to higher members of $AELi^+$: $MgLi^+$ and $CaLi^+$, in Chapter 4 [109]. These ions have been considered for exploring the elastic - and inelastic processes occurring during the ion - atom collisions [3]. The feasibility of formation of these ions via photoassociation processes has also been studied recently [3,4]. Similar to $BeLi^+$, we have performed all - electron calculations for the structural parameters of ground states of these ions using TZ and QZ basis sets at various levels of correlations using relativistic and non - relativistic Hamiltonians. The derived diatomic constants and dipole moments have been compared with the available results in the literature. The results of quadrupole moments and dipole polarizabilities of $AELi^+$ have been reported in our work, for the first time. The maximum possible error bars arising due to the finite basis set and the exclusion of higher correlation effects beyond partial triples have been quoted for reliability. It has been found that the relativistic electronic energies for the ground states of these ions are lower than their non - relativistic counterparts. However, the difference between the results of spectroscopic constants calculated with the relativistic and the non - relativistic methods is small and lies within the estimated error bars.

Further, the adiabatic DBOC corrections and the correlation contributions due to the non - leading order triples which are absent in CCSD(T) have been calculated for these molecules. The addition of DBOC to the PEC does not change the value of R_e, while the D_e lowers by a negligibly small value for both ions. Performing the CCSD(T)/5Z and CCSDT/QZ calculations, we have concluded that our results are more saturated with respect to the correlation effects than the basis set size effects.

Thereafter, we have computed the vibrational properties and lifetimes of the vibrational states. The calculated value of the lifetime for ro - vibrational ground state of $MgLi^+$ is 2.81 s, while for $CaLi^+$ it is 3.19 s. The lifetime of ro - vibrational ground state for $MgLi^+$ agrees well with that reported in Ref. [177], while for $CaLi^+$, perhaps ours is the first result in the literature. It has further been observed that the lifetime of the highest vibrational state is several times larger than (comparable to) that of the vibrational ground state of $MgLi^+$ ($CaLi^+$). A knowledge of such states is desirable for several ultracold experiments.

In addition to the electronic ground state, the low - lying excited states of Σ and Π symmetries of these two ions have also been examined for their PECs, PDM curves and spectroscopic constants using EOM - CCSD/QZ method with non - relativistic Hamiltonian. The transition energies and the TDMs for the transitions arising from the ground state to the excited electronic states have been reported as well. Since a very few calculations, particularly for the excited states are available in the literature, our all - electron results computed with large active space should be helpful for future experimental and theoretical studies on these molecular ions.

The next chapter includes *ab initio* calculations for the molecular properties of ground electronic state of AEMFs. The heavier members of this series, especially BaF and RaF, have been identified as favourable candidates for the study of symmetry violating effects [5–7]. In this context, the molecular property calculations have been performed at the KRCISD level of theory by employing the GAS technique. Further, the frozen core approximation has been used together with the QZ quality basis sets. The valence properties: permanent dipole moments and molecular dipole polarizabilities of open - shell AEMFs, and atomic dipole polarizabilities of alkaline - earth and fluorine atoms have been reported using the finite - field method. In addition, the effect of augmentation of the basis sets on these properties has also been studied [110]. The augmentation of the basis sets alter the values for α_As of alkaline - earth atoms

by a maximum of 4.1%, while for F it is as high as 16.7% at the KRCISD level. On the other hand, the results for the components of molecular polarizability of AEMFs change significantly upto 7.9% for $\alpha_{\parallel}$ and upto 5.2% for $\alpha_{\perp}$. The maximum change in the values of molecular permanent dipole moments among first four members of the series is only 2.4% with the addition of diffuse functions to the basis sets. To the best of our knowledge, we are contributing to the literature for the first time the value of PDM of RaF, and the molecular polarizabilities for CaF and RaF.

Besides the valence properties, we have also studied the $\mathcal{P}$ & $\mathcal{T}$ - odd interaction constants: W_d and W_s, and HFS constants for the ground state of AEMFs using KRCISD/QZ method. The HFS constants of BeF, and W_s for BeF, MgF, CaF and SrF molecules have been computed and reported in this work for the first time. The calculated results of W_d and W_s have shown a good agreement with the existing results, wherever available. However, the results of HFS constants show noticeable deviation from the recent results calculated using ECC and Z - vector methods, and experiments. Therefore, to further improve the accuracy of our results, we have also performed the calculations of HFS constants for the lower members of the series for which computations were feasible. (i) by including triple excitations at KRCI level in the frozen core approximation and (ii) by including all core electrons for the correlation calculations at the KRCISD level. From these additional calculations, we have observed that the accurate calculations of the HFS constants require the inclusion of all - core electrons as well as the triple excitations at the KRCI level. We expect that our results of molecular properties will be useful for the future theoretical and experimental studies on the molecules, particularly, those which have been proposed for the search of eEDMs.

6.2 Future Outlook

We have reported several results related to structure and properties of the AELi$^+$ in this work. We have made all efforts to calculate these results as accurately as possible by employing large optimized basis sets, using large active space in correlation calculations and also, using higher - order correlation methods. Although, many of these results are more accurate than most of the available calculations, particularly, for the excited states, they can be improved further by using (a) full triple and quadruple excitations at the CC level of theory (b) basis sets larger than the QZ quality (c) several additional diffuse or core functions to the basis sets depending on the property to be calculated.

Further, only a few of the low - lying excited states of Σ and Π symmetries for AELi$^+$ have been studied in this thesis. This work may be extended to the study of higher excited states including Δ and Φ symmetry in the near future.

The molecular property calculations of AEMFs have been performed using frozen core approximation at the KRCISD level of correlation. However, those properties such as HFS that depend on the accuracy of the wavefunction near the nuclear region demand core - valence basis sets together with all - electron calculations and higher - order correlation methods to bring down the differences with the experimental results. It is, however, worth noting that all such improvements obviously demand high computational resources.

We have mostly used the non - relativistic theory for the calculations of excited state results. However, some of the systems that we have considered in this thesis have been proposed for the measurement of subtle effects involving the new physics beyond the standard model, which if measured successfully will demand sophisticated calculations including the full relativistic effects with Breit interactions and quantum

electrodynamic effects. Therefore, we wish to carry out the full relativistic calculations of not just the energies but also all the properties in the future.

The AEMFs that we have studied here for their properties such as permanent dipole moments, dipole polarizabilities, $\mathcal{P}$ & $\mathcal{T}$ - odd interaction constants and HFS constants are pursued in several ultracold experiments related to collision physics, eEDM studies, etc. New candidates are being proposed constantly for such sensitive experiments. Thus, theoretical investigations requiring accurate electronic structure and properties for such potential candidates are in great demand. Here, we mention a few such examples: (i) HfH^+ and PtH^+, have been proposed as favourable candidates for eEDM experiments [52]. For these molecular ions, the spectroscopic parameters are not yet reported. Even among the available calculations [260–263], there appears to be a contradiction in identifying the true electronic ground state and also in the energetic ordering of low - lying excited states of these systems. In this context, we have performed the spectroscopic study of $^1\Sigma^+$ states of these molecular ions, in a relativistic framework [264]. More accurate PEC calculations of $^3\Delta$ states are required in order to resolve the issue of the true ground state of these ionic systems and such calculations are being pursued by us currently. (ii) mercury $-$ alkali - metal molecules: HgLi, HgNa and HgK are also proposed as the potential candidates for the study of eEDM quite recently [231]. The results of PDMs, ε_{eff} and W_s constants for the ground electronic states of these molecules are reported in [231] where these properties are calculated as expectation values in a linearized CCSD approximation in conjunction with the TZ quality basis sets. Thus, there is a scope to improve these calculations further. (iii) polyatomic molecules having at least three atoms are being looked at in the recent times for probing new physics in PeV regime, for cold chemistry and photochemistry, for quantum informatics, etc. [265, 266]. We wish to take up the work on such interesting polyatomic molecules in the future.

Several molecular systems have been found in some astrophysical environments and

one can avail a wealth of information about their abundances, the ambient temperatures of the host astrophysical objects, etc. from the study of such systems. We wish to identify such molecular candidates which are of interest in astrophysics and carry out the calculations using many - body methods that we have employed in this work. We may consider exploring other methods based on effective core potentials [267] to carry out the molecular calculations, particularly that of polyatomic molecules, where all - electron calculations are challenging computationally.

APPENDIX A

MOLECULAR SYMMETRY AND SYMMETRY GROUPS

In this appendix, we have discussed the basic concepts of molecular symmetry that provides a formal and satisfying method for the illustration of the geometry of molecules by describing the various symmetry operations and symmetry elements.

Symmetry Operation

A symmetry operation is the transformation of atoms in a molecule such that the transformed state of a molecule is indistinguishable from its original state.

Symmetry Element

A symmetry element is a geometrical entity about which one or more symmetry operations can take place. The symmetry element can be a line, a plane, or a point. Corresponding to every symmetry element, there is a symmetry operation which is

given by the same symbol as the element. A molecule can have different symmetry elements that are given below [12, 13, 15, 22, 23]:

1. **Identity Element:** All molecules possess the identity element of symmetry, for which the symbol is E (or I). The symmetry operation E consists of doing nothing to the molecule, so that it may seem too trivial to be of importance but it is a necessary element required by the rules of group theory.

2. ***n*-Fold Axis of Symmetry:** If a molecule is brought into an equivalent configuration upon rotating it about an axis by $\frac{2\pi}{n}$ radians, the molecule has an n-fold axis of symmetry, where n (= 1, 2, 3, ..., ∞) represents the *order* of

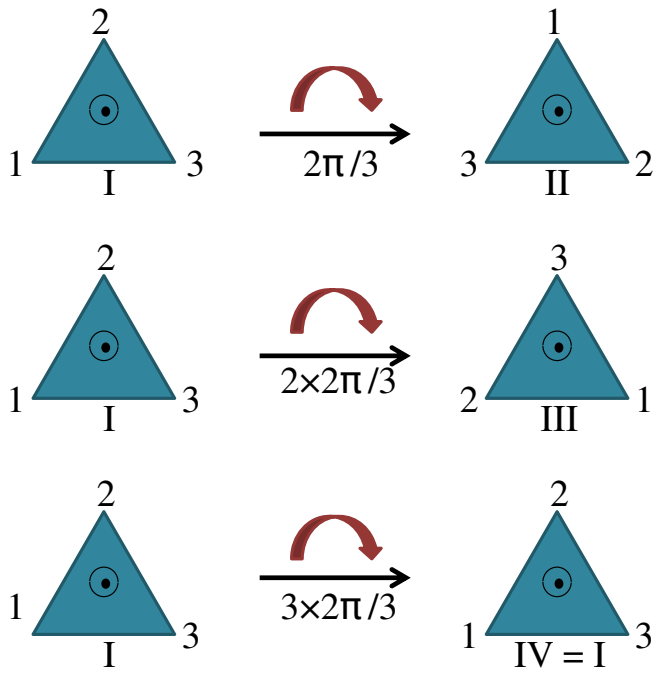

Figure A.1: An illustration of the three-fold symmetry axis operation.

the axis, i.e., the largest value of n that gives the equivalent configuration. This symmetry element is represented by Schönflies symbol C_n. Consider an example

of equilateral triangle as shown in Figure (A.1). A line drawn perpendicular to the plane of an equilateral triangle and intersecting it at its geometric center is called the axis of symmetry. It can be seen from Figure (A.1) that the II $\left(\text{obtained on rotating by } \frac{2\pi}{3}\right)$ and III $\left(\text{obtained on rotating by } 2 \times \frac{2\pi}{3}\right)$ configurations are equivalent to I. However, the configuration IV $\left(\text{obtained on rotating by } 3 \times \frac{2\pi}{3}\right)$ is exactly same as that of I. Therefore, the axis is known as three - fold symmetry axis and is given by symbol C_3. Similarly, for the case of a square, the symmetry axis is four - fold and is denoted by C_4.

3. **Plane of Symmetry:** If the reflection of all the nuclei through the plane to an equal distance on the opposite side produces a configuration equivalent to the

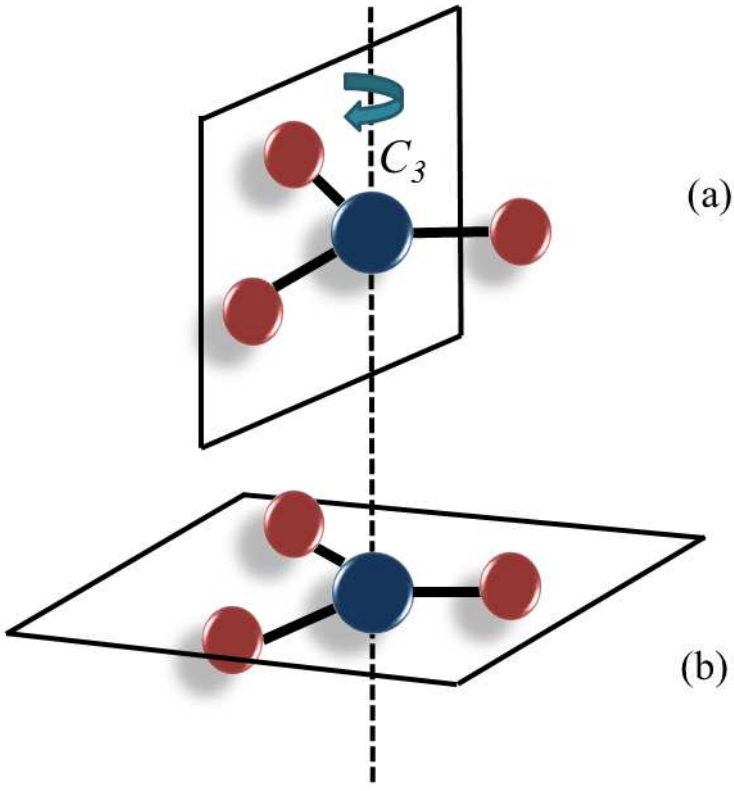

Figure A.2: An illustration of the reflection operation (a) about a vertical plane, σ_v (b) about a horizontal plane, σ_h.

initial one, the molecule is said to have a plane of symmetry. This symmetry element is given by the symbol σ. Any plane containing the principal rotation axis is known as vertical plane and it is represented by σ_v. On the other hand, the plane of a molecule that does not contain principal axis is known as horizontal plane and it is represented by σ_h. An example of a σ_v and a σ_h is shown in Figure (A.2a) and Figure (A.2b), respectively. In addition to σ_v and σ_h, there is one other plane called a dihedral plane that bisects the angles between dihedral axes. When we apply the same reflection operation twice, all atoms come back to their original positions, i.e., $\sigma^2 = E$ or

$$\begin{aligned} \sigma^n &= \sigma \ ; \text{when n is odd,} \\ &= E \ ; \text{when n is even.} \end{aligned}$$

If a molecules is linear, it has infinite number of symmetry planes, i.e., any plane containing the molecular axis is a symmetry plane. If a molecule has odd number of all atoms, it does not have any planar symmetry.

4. **Center of Inversion:** If a molecule can be brought into an equivalent configuration by changing the coordinates (x, y, z) of every atom into ($-x$, $-y$, $-z$) and the origin of coordinates lies at a point within a molecule, then the point at which the origin lies is said to be a center of symmetry or center of inversion. The molecules that contain an odd number of more than one species of atom do not show any inversion center. Similar to a symmetry plane, the inversion center also generates only one operation. This symmetry element is represented by a symbol i. The inversion operation is illustrated in Figure (A.3) with two pairs of points, A, A' and B, B', that each pair contain identical atoms in a molecule. Under the inversion operation, each atom in a molecule is moved through the inversion centre, i, to a position on the opposite side of the centre and at the same distance from the centre as the original point.

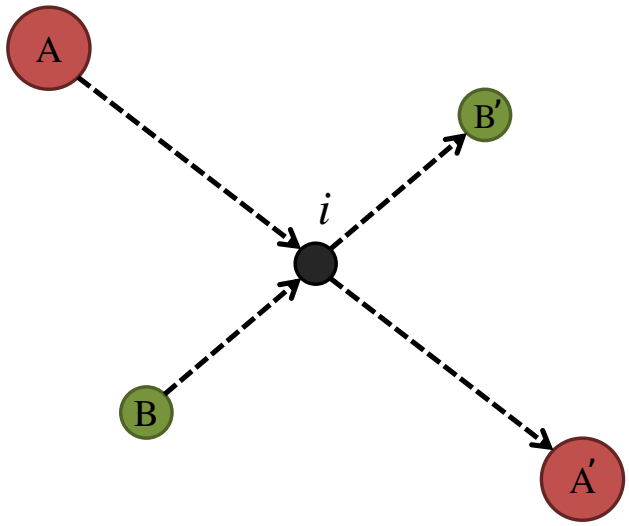

Figure A.3: An illustration of the inversion center operation.

5. ***n*-Fold Rotation-Reflection Axis of Symmetry:** This symmetry element is denoted by S_n. It maybe thought of as taking place in two steps: rotation by $\left(\frac{2\pi}{n}\right)$ radians about the axis (C_n), followed by reflection through a plane perpendicular to the rotation axis (σ_h):

$$\sigma_h \times C_n = S_n. \tag{A.1}$$

The axis about which this occurs is called n-fold rotation-reflection axis of symmetry or an axis of improper rotation or an improper axis. It follows from the definition given by Eq. (A.1) that $S_1 = \sigma$ and $S_2 = i$. In general, the existence of the S_n axis of even order always requires the existence of $C_{n/2}$ axis. On the other hand, the S_n axis with an odd-order requires that the C_n and a σ perpendicular to it must exist independently.

Point Group

A molecule can have a set of symmetry elements in which atleast one point is fixed in space that lies within all symmetry elements. Such set of symmetry elements are known as *point groups*. The total number of symmetry elements present in a particular point group represents the *order* of that group and is denoted by h. All point groups always contain an identity element. The commonly used point groups are given below [12, 22, 23]:

1. $\boldsymbol{C_n}$ **point groups:** A C_n point group contains C_n axis of symmetry. The symmetry elements of this point group are: C_n^2, C_n^3, ..., C_n^{n-1}.

2. $\boldsymbol{S_n}$ **point groups:** An S_n point group contains an S_n axis of symmetry. The group must contain S_n^2, S_n^3, ..., S_n^{n-1} elements.

3. $\boldsymbol{C_{nv}}$ **point groups:** A C_{nv} point group contains a C_n axis of symmetry and n σ_v planes of symmetry, all of which contain the C_n axis.

4. $\boldsymbol{D_n}$ **point groups:** A D_n point group contains a C_n axis and n C_2 axes. The C_2 axes are perpendicular to C_n and at equal angles to each other.

5. $\boldsymbol{C_{nh}}$ **point groups:** A C_{nh} point group contains a C_n axis and a σ_h plane, perpendicular to C_n. For even n, the point group contains a centre of inversion i.

6. $\boldsymbol{D_{nd}}$ **point groups:** A D_{nd} point group contains a C_n axis, an S_{2n} axis, n C_2 axes perpendicular to C_n and at equal angles to each other and n σ_d planes bisecting the angles between the C_2 axes. For odd n, the point group contains a centre of inversion i.

7. $\boldsymbol{D_{nh}}$ **point groups:** A D_{nh} point group contains a C_n axis, n C_2 axes perpendicular to C_n and at equal angles to each other, a σ_h plane and n other σ planes. For even n, the point group contains a centre of inversion i.

The groups: C_{nv}, D_n, C_{nh}, D_{nd}, and D_{nh}, also contain other elements which may be generated from the symmetry elements of a corresponding group. All point groups show the closure property, i.e., if we successively apply two operations, the combined operation must be the result of a single operation corresponding to a symmetry element of the same group. For instance, consider the point group (C_{2v}) associated with the H_2O molecule of AB_2 type that has four symmetry elements: E, C_2, $\sigma_v(xz)$ and $\sigma'_v(yz)$ as shown in Figure (A.4). The four symmetry elements can be combined and the results of all possible products are summarized in the group multiplication table (Table A.1). It can be seen from Table (A.1) that all the product elements are symmetry elements of the same group.

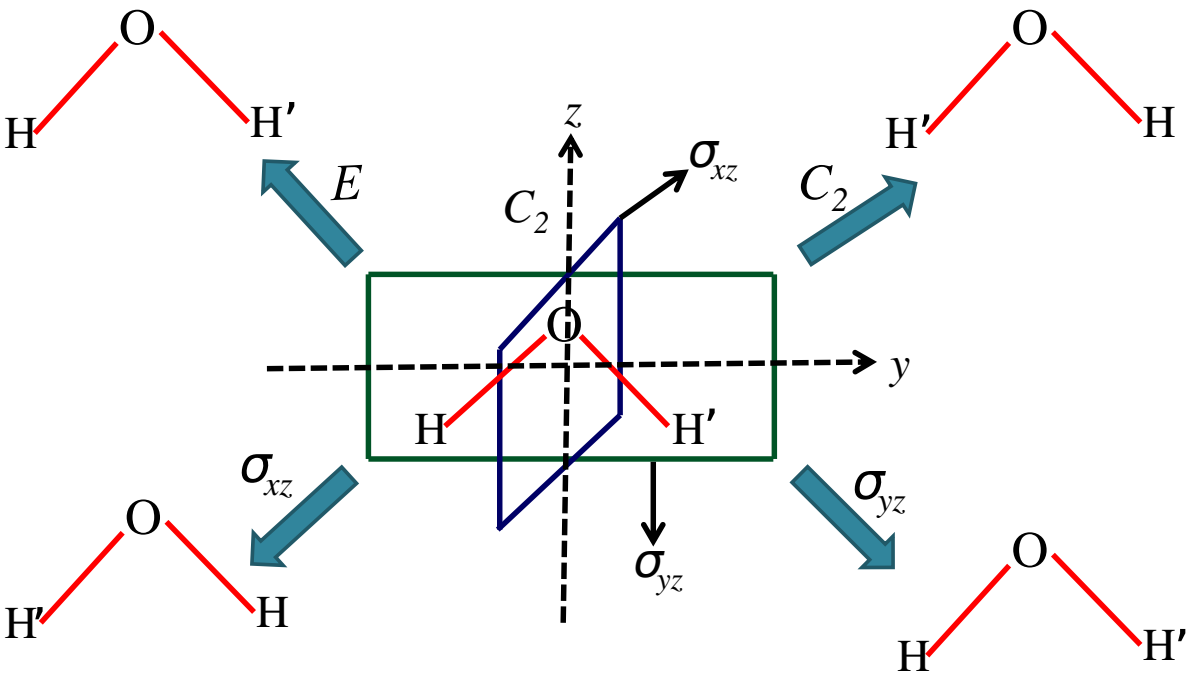

Figure A.4: An illustration of all symmetry operations in a H_2O molecule.

Table A.1: Group multiplication table for the symmetry operations associated with H_2O molecule.

C_{2v}	E	C_2	$\sigma_v(xz)$	$\sigma_v^{'}(yz)$
E	E	C_2	$\sigma_v(xz)$	$\sigma_v^{'}(yz)$
C_2	C_2	E	$\sigma_v^{'}(yz)$	$\sigma_v(xz)$
$\sigma_v(xz)$	$\sigma_v(xz)$	$\sigma_v^{'}(yz)$	E	C_2
$\sigma_v^{'}(yz)$	$\sigma_v^{'}(yz)$	$\sigma_v(xz)$	C_2	E

Character Table

It is a two - dimensional table whose rows correspond to the irreducible representations (IRs), χ_i, and columns correspond to the conjugate classes, Γ_i, of group elements.

Rules About the Irreducible Representations

The elements of a character table can be found using certain rules which are given below [15, 23]:

1. The sum of the squares of the dimensions of the IRs of a group is equal to h, i.e.,

$$\sum l_i^2 \;=\; l_1^2 \,+\, l_2^2 \,+\, l_3^2 \,+\, \ldots \,=\, h. \tag{A.2}$$

2. According to the *great orthogonality theorem (GOT)*,

$$\sum_R D_{ij}^{(l)}(R)^*\, D_{i'j'}^{(l')}(R) \;=\; \frac{h}{d_l}\,\delta_{ll'}\,\delta_{ii'}\,\delta_{jj'}, \tag{A.3}$$

   where $D^{(l)}(R)$ is the representative of the operation R in d_l - dimensional IR of symmetry species $\Gamma^{(l)}$ of the group.

3. According to the *little orthogonality theorem (LOT)*,

$$\sum_R \chi^{(l)}(R)^*\, \chi^{(l')}(R) \;=\; h\,\delta_{ll'}. \tag{A.4}$$

4. In a given representation, the characters of all matrices belonging to operations in the same class are identical.

5. The number of IRs of a group is equal to the number of classes in the group.

Consider, an abelian C_{2v} point group that has four symmetry elements as shown in Figure (A.4). As all symmetry elements of an abelian group form a separate class, there are four IRs (Rule [5]): Γ_1, Γ_2, Γ_3 and Γ_4, for this group. Therefore, the character table can be given as in Table (A.2).

The components of first IR are always 1 corresponding to E. The elements of first column in Table (A.2) represent the dimension of corresponding IR. Therefore, according to Rule [1],

$$1^2 + l_2^2 + l_3^2 + l_4^2 = 4. \tag{A.5}$$

Since dimensions can not be zero or negative, Eq. (A.5) implies,

$$l_1 = l_2 = l_3 = l_4 = 1. \tag{A.6}$$

Using Rules [2] - [4], there must be two '+1's and two '−1's in each class. Now,

Table A.2: Character table for C_{2v} point group with abstract elements.

C_{2v}	E	C_2	$\sigma_v(xz)$	$\sigma_v^{'}(yz)$
Γ_1	$l_1 = 1$	$p_1 = 1$	$q_1 = 1$	$r_1 = 1$
Γ_2	l_2	p_2	q_2	r_2
Γ_3	l_3	p_3	q_3	r_3
Γ_4	l_4	p_4	q_4	r_4

one has to find the Mulliken Symbol for each IR with respect to the dimension as shown in Table (A.3). Each Mulliken symbol given in Table (A.3) is featured with subscripts/superscripts to represent the different aspects of symmetry as given in Table (A.4).

Table A.3: Mulliken symbols for IRs.

Dimension of an IR	Mulliken symbol
1	A or B
2	E
3	T
4	G
5	H

As all IRs in C_{2v} point group are one - dimensional (A.6), the label (A or B) for

Table A.4: Subscripts/superscripts to Mulliken symbols representing different aspects of symmetry.

Subscript/ superscript	Symmetry with respect to symmetry operation
1	symmetric with respect to a vertical plane (σ_v)
2	anti - symmetric with respect to a vertical plane (σ_v)
g	symmetric with respect to inversion (i)
u	anti - symmetric with respect to inversion (i)
$'$	symmetric with respect to a horizontal plane (σ_h)
$''$	anti - symmetric with respect to a horizontal plane (σ_h)

each IR can be decided from the second column, i.e., symmetry with respect to C_2

Table A.5: Character table for C_{2v} point group with actual elements.

C_{2v}	E	C_2	$\sigma_v(xz)$	$\sigma_v^{'}(yz)$
A_1	1	1	1	1
A_2	1	1	-1	-1
B_1	1	-1	1	-1
B_2	1	-1	-1	1

rotation axis: label A is for '+1' and label B for '-1'. In C_{2v} case, there are two +1's and two -1's in second column, therefore, we will look for the third coloumn and add subscripts 1 or 2 to Mulliken labels according to symmetry and antisymmetry with respect to reflection $\sigma_v(xz)$. Consequently, the symmetry labels for IRs of C_{2v} are A_1, A_2, B_1, and B_2 as shown in Table (A.5).

Similar to C_{2v}, one can form the character table of any point group. Further details of point groups and their character tables can be found elsewhere [15, 22, 23].

APPENDIX B

SAMPLE INPUT FOR THE QUANTUM MANY-BODY SOFTWARES

B.1 ZMAT: Input File for the CFOUR Program

```
Beryllium lithium ion, CCSD(T)/cc-PVQZ PES
BE
LI 1 R
R=5
*CFOUR(CALC=CCSD(T),SCF_CONV=8,CC_CONV=8
BASIS=SPECIAL,CHARGE=1,MEM_UNIT=GB
MEMORY=10,ABCDTYPE=AOBASIS,PROPS=FIRST_ORDER)

BE:PVQZ
LI:PVQZ
```

B.2 Input Files for the DIRAC Program

B.2.1 BeLi+.mol

Following is the .mol file for $BeLi^+$ ion that uses cc - pVQZ basis sets for both Be and Li atom separated at a distance of 2 Å together with the C_{2v} point group.

```
DIRAC
BeLi+ molecule


C  2  2 Y  X  A
4.  1
Be  0.0  0.0  0.0
LARGE BASIS cc-pVQZ
3.  1
Li  0.0  0.0  2.0
LARGE BASIS cc-pVQZ
FINISH
```

B.2.2 CCenergy.inp

The sample input file that is required to be used combinedly with the .mol file given above to calculate the energies of $BeLi^+$ at the different levels of correlation. A threshold for convergence for energy is given as 10^{-8}.

```
**DIRAC
.TITLE
BeLi+
.WAVE F
.4INDEX

```

Continued . . .

```
**INTEGRALS
.NUCMOD
2
*READIN
.UNCONTRACT
**HAMILTONIAN
.LVCORR
**WAVE FUNCTIONS
.SCF
.RELCCSD
*SCF
.ERGCNV
1.0E-8
.CLOSED SHELL
6
.MAXITR
70
**MOLTRA
.ACTIVE
all
*END OF

&RELCCSD DOENER=T, TIMING=T &END
&CCENER DOMP2=T, DOCCSD=T DOCCSDT=T &END
```

B.2.3 KRCIenergy.inp

A sample input file for performing the field - dependent energy calculation for BeF using KRCISD method.

```
**DIRAC
.TITLE
BeF
.WAVE FUNCTION
**HAMILTONIAN
.LVCORR
.OPERATOR
ZDIPLEN
COMFACTOR
0.0002
**INTEGRALS
.NUCMOD
2
*READINP
.UNCONTRACT
**WAVE FUNCTION
.SCF
.KR CI
*SCF
.ERGCNV
1.0E-8
.MAXITR
250
*KRCICALC
.CI PROGRAM
LUCIAREL
```

Continued . . .

```
.INACTIVE
2
.GASSH
3
4
1
128
.GASSPC
6 8
7 9
9 9
.CIROOTS
3 1
.MAX CI
500
.MXCIVE
3
.THRECI
1.0d-08
*END OF
```

B.3 Input File for the VIBROT Program

This is a sample input file for the VIBROT program of MOLCAS, for the calculation of vibrational and rotational levels in an electronic state of $BeLi^+$ ion.

```
&VIBROT
RoVibrational spectrum
Title
Vib - Rot spectrum for BeLi+
Atoms
0 Be 0 Li
Potential
0.7558904511          -17.9807217737
0.9448630639          -19.7277485059
1.1338356767          -20.5450085857
1.3228082895          -20.9930522385
⋮                       ⋮
⋮                       ⋮
51.022605452           -21.9391488459
52.9123315798          -21.939148486
54.8020577077          -21.9391481761
56.6917838355          -21.9391479163
Range
0.7558904511          56.69178384
SCALe
Grid
2000
Vibrations
24
Rotations
0 3
```

Continued . . .

Orbital	
0	
OBSERVABLE	
Dipole Moment	
0.7558904511	0.1615558675
0.9448630639	-0.7565821882
1.1338356767	-0.8203353659
1.3228082895	-0.9243369832
⋮	⋮
⋮	⋮
51.022605452	-28.6743760369
52.9123315798	-29.7379077353
54.8020577077	-30.8013383912
56.6917838355	-31.8646812596

B.4 Input File for the LEVEL Program

Following is the sample input file for the calculation of vibrational parameters of $MgLi^+$ using LEVEL Program.

```
12  24  3  7  0  1                    % IAN1 IMN1 IAN2 IMN2 CHARGE NUMPOT
'Case 1.a: MgLi+ get all vib. levels and their TDMs'
0.001  1.51178  56.69178  1.d-5        % RH RMIN RMAX EPS
47  0  0  6712.39892                  % NTP LPPOT IOMEG VLIM
0   0   2   1   0                     % NUSE IR2 ILR NCN CNN
0.52917721    1.0D+0    0.d0          % RFACT EFACT VSHIFT
1.51178        291028.21196
1.70075        199501.83950
1.88973        144172.69789
2.07870        108985.42564
⋮                ⋮
⋮                ⋮
51.02261        6711.99508
52.91233        6712.15530
54.80206        6712.28698
56.69178        6712.39892
59 1 1 4 0 1 -1 0            % NLEV1 AUTO1 LCDC LXPCT NJM JDJR IWR LPRWF
0 0  1 0  2 0  3 0  4 0  5 0  6 0  7 0  8 0  9 0  10 0  11 0  12 0  13 0  14 0  15 0  16 0  17 0
18 0  19 0  20 0  21 0  22 0  23 0  24 0  25 0  26 0  27 0  28 0  29 0  30 0  31 0  32 0  33 0
34 0  35 0  36 0  37 0  38 0  39 0  40 0  41 0  42 0  43 0  44 0  45 0  46 0  47 0  48 0  49 0
50 0  51 0  52 0  53 0  54 0  55 0  56 0  57 0  58 0
1  10  0.D0                          % MORDR IRFN RREF

47        43.83909                   % NRFN RFLIM
0  2  1  0                          % NUSEF ILRF NCNF CNNF
0.52917721        2.54174691         % RFACT MFACT
```

Continued . . .

```
1.51178          0.15218
1.70075          0.31946
1.88973          0.48674
2.07870          0.64473
⋮                  ⋮
⋮                  ⋮
51.02261          39.44765
52.91233          40.91166
54.80206          42.37546
56.69178          43.83909
59  1  0  0  0                          % NLEV2 AUTO2 J2DL J2DU J2DD
0  1  2  3  4  5  6  7  8  9  10  11  12  13  14  15  16  17  18  19  20  21  22  23  24  24
25  26  27  28  29  30  31  32  33  34  35  36  37  38  39  40  41  42  43  44  45  46  47
48  49  50  51  52  53  54  55  56  57  58
```

BIBLIOGRAPHY

[1] A. Rakshit and B. Deb, *Formation of cold molecular ions by radiative processes in cold ion-atom collisions.* Phys. Rev. A, **83**, 022703, 2011.

[2] C. Ghanmi, M. Farjallah, and H. Berriche, *Theoretical study of the alkaline-earth $(LiBe)^+$ ion: structure, spectroscopy and dipole moments.* Journal of Physics B: Atomic, Molecular and Optical Physics, **50**, 055101, 2017.

[3] S. Haze, S. Hata, M. Fujinaga, and T. Mukaiyama, *Observation of elastic collisions between lithium atoms and calcium ions.* Phys. Rev. A, **87**, 052715, 2013.

[4] R. ElOualhazi and H. Berriche, *Electronic structure and spectra of the $MgLi^+$ ionic molecule.* The Journal of Physical Chemistry A, **120**, 452, 2016.

[5] M. K. Nayak and R. K. Chaudhuri, *Ab initio calculation of P, T-odd interaction constant in BaF: a restricted active space configuration interaction approach.* Journal of Physics B: Atomic, Molecular and Optical Physics, **39**, 1231, 2006.

[6] A. D. Kudashov, A. N. Petrov, L. V. Skripnikov, N. S. Mosyagin, T. A. Isaev, R. Berger, and A. V. Titov, *Ab initio study of radium monofluoride (RaF) as a candidate to search for parity- and time-and-parity−violation effects.* Phys. Rev. A, **90**, 052513, 2014.

[7] T. A. Isaev, S. Hoekstra, and R. Berger, *Laser-cooled RaF as a promising candidate to measure molecular parity violation.* Phys. Rev. A, **82**, 052521, 2010.

[8] https://www.nobelprize.org/prizes/physics/2005/summary/.

[9] https://www.nobelprize.org/prizes/physics/2012/summary/.

[10] C. N. Banwell, *Fundamentals of molecular spectroscopy.* Tata McGraw-Hill Publishing Company Limited, Third Edition.

[11] B. H. Bransden and C. J. Joachain, *Physics of atoms and molecules.* Prentice Hall Publication, 2003.

[12] J. M. Hollas, *Modern spectroscopy.* Wiley Publications, Fourth Edition.

[13] P. F. Bernath, *Spectra of atoms and molecules.* Oxford University Press, 1995.

[14] S. P. A. Sauer, *Molecular electromagnetism: A computational chemistry approach.* Oxford University Press, 2011.

[15] P. Atkins and R. Friedman, *Molecular quantum mechanics.* Oxford University Press, Fourth Edition, 2006.

[16] P. Atkins and J. de Paula, *Atkins' physical chemistry.* Eighth Edition, 2006.

[17] W. S. Struve, *Fundamentals of molecular spectroscopy.* John Wiley & Sons, 1989.

[18] W. Demtröder, *Molecular physics.* Wiley-VCH, Weinheim, 2005.

[19] G. H. F. Diercksen, B. O. Roos, and A. J. Sadlej, *Legitimate calculation of first-order molecular properties in the case of limited CI functions. Dipole moments.* Chemical Physics, **59**, 29, 1981.

[20] G. Maroulis, *Hyperpolarizability of H_2O revisited: Accurate estimate of the basis set limit and the size of electron correlation effects.* Chemical Physics Letters, **289**, 403, 1998.

[21] J. Noga and M. Urban, *On expectation value calculation of one-electron properties using the coupled cluster wave functions.* Theoretica Chimica Acta, **73**, 291, 1988.

[22] D. J. Willock, *Molecular symmetry.* A John Wiley and Sons, Ltd., Publication, 2009.

[23] F. A. Cotton, *Chemical applications of group theory.* Wiley India Pvt. Ltd., Third Edition.

[24] S. G. Karshenboim, *Lecture notes in physics 745: Precision physics of simple atoms and molecules.* Springer, Berlin Heidelberg, 2008.

[25] T. E. Chupp, P. Fierlinger, M. J. Ramsey-Musolf, and J. T. Singh, *Electric dipole moments of atoms, molecules, nuclei, and particles.* Reviews of Modern Physics, **91**, 015001, 2019.

[26] L. D. Carr, D. DeMille, R. V. Krems, and J. Ye, *Cold and ultracold molecules: Science, technology and applications*. New Journal of Physics, **11**, 055049, 2009.

[27] M. Saffman, T. G. Walker, and K. Mølmer, *Quantum information with Rydberg atoms*. Rev. Mod. Phys., **82**, 2313, 2010.

[28] R. Côté, *TUTORIAL: Quantum computing with Rydberg atoms*. Proc. SPIE, **6014**, 601415–1, 2005.

[29] M. Greiner, O. Mandel, T. Esslinger, T. W. Hänsch, and I. Bloch, *Quantum phase transition from a superfluid to a Mott insulator in a gas of ultracold atoms*. Nature, **415**, 39, 2002.

[30] S. Ramanan, T. Mishra, M. S. Luthra, R. V. Pai, and B. P. Das, *Signatures of the superfluid-to-Mott-insulator transition in cold bosonic atoms in a one-dimensional optical lattice*. Phys. Rev. A, **79**, 013625, 2009.

[31] I. Bloch, *Ultracold quantum gases in optical lattices*. Nature Physics, **1**, 23, 2005.

[32] D. Jiang, B. Arora, M. S. Safronova, and C. W. Clark, *Blackbody-radiation shift in a $^{88}Sr^+$ ion optical frequency standard*. Journal of Physics B: Atomic, Molecular and Optical Physics, **42**, 154020, 2009.

[33] B. Arora, M. S. Safronova, and C. W. Clark, *Blackbody-radiation shift in a $^{43}Ca^+$ ion optical frequency standard*. Phys. Rev. A, **76**, 064501, 2007.

[34] A. Roy, S. De, B. Arora, and B. K. Sahoo, *Accurate determination of blackbody radiation shift, magic and tune-out wavelengths for the $6S_{1/2} \rightarrow 5D_{3/2}$ clock transition in Yb^+*. Journal of Physics B: Atomic, Molecular and Optical Physics, **50**, 205201, 2017.

[35] M. Kállay, H. S. Nataraj, B. K. Sahoo, B. P. Das, and L. Visscher, *Relativistic general-order coupled-cluster method for high-precision calculations: Application to the Al^+ atomic clock*. Phys. Rev. A, **83**, 030503, 2011.

[36] S. M. Brewer, J.-S. Chen, A. M. Hankin, E. R. Clements, C. W. Chou, D. J. Wineland, D. B. Hume, and D. R. Leibrandt, *An $^{27}Al^+$ quantum-logic clock with systematic uncertainty below 10^{-18}*. arXiv:1902.07694v1.

[37] A. D. Ludlow, M. M. Boyd, J. Ye, E. Peik, and P. O. Schmidt, *Optical atomic clocks*. Reviews of Modern Physics, **87**, 637, 2015.

[38] A. Rastogi, N. Batra, A. Roy, J. Thangjam, V. P. S. Kalsi, S. Panja, and S. De, *Design of the ion trap and vacuum system for ^{171}Yb-ion optical frequency standard*. MAPAN, **30**, 169, 2015.

[39] E. D. Kaplan and C. J. Hegarty, *Understanding GPS: Principles and applications*. Artech House Publishers, Norwood, MA, 2006.

[40] R. V. Krems, W. C. Stwalley, and B. Friedrich, *Cold molecules: Theory, experiment, applications* (CRC press, Boca Raton, FL). Eds. 2009.

[41] S. Ospelkaus, K.-K. Ni, D. Wang, M. H. G. de Miranda, B. Neyenhuis, G. Quéméner, P. S. Julienne, J. L. Bohn, D. S. Jin, and J. Ye, *Quantum-state controlled chemical reactions of ultracold potassium-rubidium molecules*. Science, **327**, 853, 2010.

[42] M. B. Kosicki, D. Kedziera, and P. S. Żuchowski, *Ab initio study of chemical reactions of cold SrF and CaF molecules with alkali-metal and alkaline-earth-metal atoms: The implications for sympathetic cooling*. The Journal of Physical Chemistry A, **121**, 4152, 2017.

[43] D. DeMille, *Quantum computation with trapped polar molecules*. Phys. Rev. Lett., **88**, 067901, 2002.

[44] A. André, D. DeMille, J. M. Doyle, M. D. Lukin, S. E. Maxwell, P. Rabl, R. J. Schoelkopf, and P. Zoller, *A coherent all-electrical interface between polar molecules and mesoscopic superconducting resonators*. Nature Physics, **2**, 636, 2006.

[45] S. F. Yelin, K. Kirby, and R. Côté, *Schemes for robust quantum computation with polar molecules*. Phys. Rev. A, **74**, 050301, 2006.

[46] C. Menotti, M. Lewensteint, T. Lahaye, and T. Pfau, *Dipolar interaction in ultra-cold atomic gases*. AIP Conf. Proc., **970**, 332, 2008.

[47] C. Trefzger, C. Menotti, B. Capogrosso-Sansone, and M. Lewenstein, *Ultracold dipolar gases in optical lattices*. Journal of Physics B: Atomic, Molecular and Optical Physics, **44**, 193001, 2011.

[48] M. Kajita, G. Gopakumar, M. Abe, M. Hada, and M. Keller, *Test of m_p/m_e changes using vibrational transitions in N_2^+*. Phys. Rev. A, **89**, 032509, 2014.

[49] M. Kajita, G. Gopakumar, M. Abe, and M. Hada, *Sensitivity of vibrational spectroscopy of optically trapped SrLi and CaLi molecules to variations in m_p/m_e*. Journal of Physics B: Atomic, Molecular and Optical Physics, **46**, 025001, 2013.

[50] V. V. Flambaum and M. G. Kozlov, *Enhanced sensitivity to the time variation of the fine-structure constant and m_p/m_e in diatomic molecules*. Phys. Rev. Lett., **99**, 150801, 2007.

[51] M. Gacesa and R. Côté, *Photoassociation of ultracold molecules near a Feshbach resonance as a probe of the electron–proton mass ratio variation.* Journal of Molecular Spectroscopy, **300**, 124, 2014.

[52] E. R. Meyer, J. L. Bohn, and M. P. Deskevich, *Candidate molecular ions for an electron electric dipole moment experiment.* Phys. Rev. A, **73**, 062108, 2006.

[53] T. Fleig and M. K. Nayak, *Electron electric dipole moment and hyperfine interaction constants for ThO.* Journal of Molecular Spectroscopy, **300**, 1621, 2014.

[54] J. J. Hudson, B. E. Sauer, M. R. Tarbutt, and E. A. Hinds, *Measurement of the electron electric dipole moment using YbF molecules.* Phys. Rev. Lett., **89**, 023003, 2002.

[55] E. R. Meyer and J. L. Bohn, *Prospects for an electron electric-dipole moment search in metastable ThO and ThF^+.* Phys. Rev. A, **78**, 010502, 2008.

[56] M. G. Kozlov and D. DeMille, *Enhancement of the electric dipole moment of the electron in PbO.* Phys. Rev. Lett., **89**, 133001, 2002.

[57] S. Schiller and V. Korobov, *Tests of time independence of the electron and nuclear masses with ultracold molecules.* Phys. Rev. A, **71**, 032505, 2005.

[58] D. Bakalov and S. Schiller, *The electric quadrupole moment of molecular hydrogen ions and their potential for a molecular ion clock.* Applied Physics B, **114**, 213, 2014.

[59] J.-Ph. Karr, *H_2^+ and HD^+: Candidates for a molecular clock.* Journal of Molecular Spectroscopy, **300**, 37, 2014.

[60] U. Bissbort, D. Cocks, A. Negretti, Z. Idziaszek, T. Calarco, F. Schmidt-Kaler, W. Hofstetter, and R. Gerritsma, *Emulating solid-state physics with a hybrid system of ultracold ions and atoms.* Phys. Rev. Lett., **111**, 080501, 2013.

[61] S. S. Kondov, C.-H. Lee, K. H. Leung, C. Liedl, I. Majewska, R. Moszynski, and T. Zelevinsky, *Molecular lattice clock with long vibrational coherence.* arXiv:1904.04891v1.

[62] A. Roy and D. Angom, *Thermal suppression of phase separation in condensate mixtures.* Phys. Rev. A, **92**, 011601, 2015.

[63] A. Bhowmik, P. K. Mondal, S. Majumder, and B. Deb, *Density profiles of two-component Bose–Einstein condensates interacting with a Laguerre–Gaussian beam.* Journal of Physics B: Atomic, Molecular and Optical Physics, **51**, 135003, 2018.

[64] D. J. McCarron, H. W. Cho, D. L. Jenkin, M. P. Köppinger, and S. L. Cornish, *Dual-species Bose-Einstein condensate of ^{87}Rb and ^{133}Cs.* Phys. Rev. A, **84**, 011603, 2011.

[65] S. B. Papp, J. M. Pino, and C. E. Wieman, *Tunable miscibility in a dual-species Bose-Einstein condensate.* Phys. Rev. Lett., **101**, 040402, 2008.

[66] Thomas C. Killian, *Ultracold neutral plasmas.* Science, **316**, 705, 2007.

[67] J. P. Morrison, C. J. Rennick, J. S. Keller, and E. R. Grant, *Evolution from a molecular Rydberg gas to an ultracold plasma in a seeded supersonic expansion of NO.* Phys. Rev. Lett., **101**, 205005, 2008.

[68] J. J. Gilijamse, S. Hoekstra, S. Y. T. van de Meerakker, G. C. Groenenboom, and G. Meijer, *Near-threshold inelastic collisions using molecular beams with a tunable velocity.* Science, **313**, 1617, 2006.

[69] P. Staanum, S. D. Kraft, J. Lange, R. Wester, and M. Weidemüller, *Experimental investigation of ultracold atom-molecule collisions.* Phys. Rev. Lett., **96**, 023201, 2006.

[70] N. Zahzam, T. Vogt, M. Mudrich, D. Comparat, and P. Pillet, *Atom-molecule collisions in an optically trapped gas.* Phys. Rev. Lett., **96**, 023202, 2006.

[71] K. Góral, L. Santos, and M. Lewenstein, *Quantum phases of dipolar bosons in optical lattices.* Phys. Rev. Lett., **88**, 170406, 2002.

[72] J. D. Weinstein, R. deCarvalho, T. Guillet, B. Friedrich, and J. M. Doyle, *Magnetic trapping of calcium monohydride molecules at millikelvin temperatures.* Nature, **395**, 148, 1998.

[73] S. K. Tokunaga, J. M. Dyne, E. A. Hinds, and M. R. Tarbutt, *Stark deceleration of lithium hydride molecules.* New Journal of Physics, **11**, 055038, 2009.

[74] T. E. Wall, J. F. Kanem, J. M. Dyne, J. J. Hudson, B. E. Sauer, E. A. Hinds, and M. R. Tarbutt, *Stark deceleration of CaF molecules in strong- and weak-field seeking states.* Phys. Chem. Chem. Phys., **13**, 18991, 2011.

[75] J. M. Sage, S. Sainis, T. Bergeman, and D. DeMille, *Optical production of ultracold polar molecules.* Phys. Rev. Lett., **94**, 203001, 2005.

[76] G. Zinner, T. Binnewies, F. Riehle, and E. Tiemann, *Photoassociation of cold Ca atoms.* Phys. Rev. Lett., **85**, 2292, 2000.

[77] C. Gabbanini, A. Fioretti, A. Lucchesini, S. Gozzini, and M. Mazzoni, *Cold rubidium molecules formed in a magneto-optical trap.* Phys. Rev. Lett., **84**, 2814, 2000.

[78] T. Shimasaki, J. Kim, Y. Zhu, and D. DeMille, *Continuous production of rovibronic-ground-state RbCs molecules via short-range photoassociation to the* $b^3\Pi_1 - c^3\Sigma_1^+ - B^1\Pi_1$ *states.* Phys. Rev. A, **98**, 043423, 2018.

[79] K. M. Jones, E. Tiesinga, P. D. Lett, and P. S. Julienne, *Ultracold photoassociation spectroscopy: Long-range molecules and atomic scattering.* Rev. Mod. Phys., **78**, 483, 2006.

[80] M. Gacesa, J. A. Montgomery, Jr., H. H. Michels, and R. Côté, *Production of* $NaCa^+$ *molecular ions in the ground state from cold atom-ion mixtures by photoassociation via an intermediate state.* Phys. Rev. A, **94**, 013407, 2016.

[81] T. Köhler, K. Góral, and P. S. Julienne, *Production of cold molecules via magnetically tunable Feshbach resonances.* Rev. Mod. Phys., **78**, 1311, 2006.

[82] K.-K. Ni, S. Ospelkaus, M. H. G. de Miranda, A. Pe'er, B. Neyenhuis, J. J. Zirbel, S. Kotochigova, P. S. Julienne, D. S. Jin, and J. Ye, *A high phase-space-density gas of polar molecules.* Science, **322**, 231, 2008.

[83] H. da Silva Jr, M. Raoult, M. Aymar, and O. Dulieu, *Formation of molecular ions by radiative association of cold trapped atoms and ions.* New Journal of Physics, **17**, 045015, 2015.

[84] M. Drewsen, A. Mortensen, R. Martinussen, P. Staanum, and J. L. Sørensen, *Nondestructive identification of cold and extremely localized single molecular ions.* Phys. Rev. Lett., **93**, 243201, 2004.

[85] P. Blythe, B. Roth, U. Fröhlich, H. Wenz, and S. Schiller, *Production of ultracold trapped molecular hydrogen ions.* Phys. Rev. Lett., **95**, 183002, 2005.

[86] P. F. Staanum, K. Højbjerre, R. Wester, and M. Drewsen, *Probing isotope effects in chemical reactions using single ions.* Phys. Rev. Lett., **100**, 243003, 2008.

[87] T. E. Wall, *Preparation of cold molecules for high-precision measurements.* Journal of Physics B: Atomic, Molecular and Optical Physics, **49**, 243001, 2016.

[88] P. Staanum, A. Pashov, H. Knöckel, and E. Tiemann, $X\,^1\Sigma^+$ *and* $a\,^3\Sigma^+$ *states of LiCs studied by Fourier-transform spectroscopy.* Phys. Rev. A, **75**, 042513, 2007.

[89] L. M. Russon, G. K. Rothschopf, M. D. Morse, A. I. Boldyrev, and J. Simons, *Two - photon ionization spectroscopy and all-electron ab initio study of LiCa.* The Journal of Chemical Physics, **109**, 6655, 1998.

[90] S. Banerjee, J. A. Montgomery, J. N. Byrd, H. H. Michels, and R. Côté, *Ab initio potential curves for the $X\,^2\Sigma_u^+$, $A\,^2\Pi_u$ and $B\,^2\Sigma_g^+$ states of Ca_2^+*. Chemical Physics Letters, **542**, 138, 2012.

[91] B. Zhang, L.-E. Berg, and T. Hansson, *Wavepacket dynamics and predissociation of the $D^1\Pi_u$ state of Rb_2*. Chemical Physics Letters, **325**, 577, 2000.

[92] D. Edvardsson, S. Lunell, and C. M. Marian, *Calculation of potential energy curves for Rb_2 including relativistic effects*. Molecular Physics, **101**, 2381, 2003.

[93] R. Saito, S. Haze, M. Sasakawa, R. Nakai, M. Raoult, H. Da Silva, O. Dulieu, and T. Mukaiyama, *Characterization of charge-exchange collisions between ultracold ^6Li atoms and $^{40}Ca^+$ ions*. Phys. Rev. A, **95**, 032709, 2017.

[94] M. Abe, Y. Moriwaki, M. Hada, and M. Kajita, *Ab initio study on potential energy curves of electronic ground and excited states of $^{40}CaH^+$ molecule*. Chemical Physics Letters, **521**, 31, 2012.

[95] S. Azizi, M. Aymar, and O. Dulieu, *Prospects for the formation of ultracold ground state polar molecules from mixed alkali atom pairs*. The European Physical Journal D - Atomic, Molecular, Optical and Plasma Physics, **31**, 195, 2004.

[96] R. Côté, E. Juarros, and K. Kirby, *Formation of ultracold polar molecules in a single quantum state*. Phys. Rev. A, **81**, 060704, 2010.

[97] M. Aymar and O. Dulieu, *Calculation of accurate permanent dipole moments of the lowest $^{1,3}\Sigma^+$ states of heteronuclear alkali dimers using extended basis sets*. The Journal of Chemical Physics, **122**, 204302, 2005.

[98] D. Bhattacharya, N. Vaval, and S. Pal, *Electronic transition dipole moments and dipole oscillator strengths within Fock-space multi-reference coupled cluster framework: An efficient and novel approach*. The Journal of Chemical Physics, **138**, 094108, 2013.

[99] G. Gopakumar, M. Abe, M. Hada, and M. Kajita, *Dipole polarizability of alkali-metal (Na, K, Rb)−alkaline-earth-metal (Ca, Sr) polar molecules: Prospects for alignment*. The Journal of Chemical Physics, **140**, 224303, 2014.

[100] G. Gopakumar, M. Abe, M. Kajita, and M. Hada, *Ab initio study of permanent electric dipole moment and radiative lifetimes of alkaline-earth-metal−Li molecules*. Phys. Rev. A, **84**, 062514, 2011.

[101] S. Sasmal, H. Pathak, M. K. Nayak, N. Vaval, and S. Pal, *HgH: A potential candidate for the electron electric dipole moment experiment*. J. Chem. Phys., **144**, 124307, 2016.

[102] M. Abe, G. Gopakumar, M. Hada, B. P. Das, H. Tatewaki, and D. Mukherjee, *Application of relativistic coupled-cluster theory to the effective electric field in YbF.* Phys. Rev. A, **90**, 022501, 2014.

[103] J. Cheng, H. Zhang, and X. Cheng, *Spectral study of A* $^1\Pi$-X $^1\Sigma^+$ *transitions of CO relevant to interstellar clouds.* The Astrophysical Journal, **859**, 19, 2018.

[104] R. Sawant, O. Dulieu, and S. A. Rangwala, *Detection of ultracold molecules using an optical cavity.* Phys. Rev. A, **97**, 063405, 2018.

[105] J. C. J. Koelemeij, B. Roth, A. Wicht, I. Ernsting, and S. Schiller, *Vibrational spectroscopy of* HD^+ *with 2-ppb accuracy.* Phys. Rev. Lett., **98**, 173002, 2007.

[106] Y. You, C.-L. Yang, M.-S. Wang, X.-G. Ma, and W.-W. Liu, *Theoretical investigation of the laser cooling of a LiBe molecule.* Phys. Rev. A, **92**, 032502, 2015.

[107] Y. Hao, L. F. Pasteka, L. Visscher, the NL-eEDM collaboration: P. Aggarwal, H. L. Bethlem, A. Boeschoten, A. Borschevsky, M. Denis, K. Esajas, S. Hoekstra, K. Jungmann, V. R. Marshall, T. B. Meijknecht, M. C. Mooij, R. G. E. Timmermans, A. Touwen, W. Ubachs, L. Willmann, Y. Yin, and A. Zapara, *High accuracy theoretical investigations of CaF, SrF, and BaF and implications for laser-cooling.* arXiv:1904.02516v1.

[108] **R. Bala**, H. S. Nataraj, M. Abe, and M. Kajita, *Accurate ab initio calculations of spectroscopic constants and properties of* $BeLi^+$. Journal of Molecular Spectroscopy, **349**, 1, 2018.

[109] **R. Bala**, H. S. Nataraj, M. Abe, and M. Kajita, *Calculations of electronic properties and vibrational parameters of alkaline-earth lithides:* $MgLi^+$ *and* $CaLi^+$. Molecular Physics, **117**, 712, 2019.

[110] **R. Bala**, H. S. Nataraj, and M. K. Nayak, *Ab initio calculations of permanent dipole moments and dipole polarizabilities of alkaline-earth monofluorides.* Journal of Physics B: Atomic, Molecular and Optical Physics, **52**, 085101, 2019.

[111] A. Szabo and N. S. Ostlund, *Modern quantum chemistry: Introduction to advanced electronic structure theory.* Dover Publications, 1996.

[112] D. R. Hartree, *The wave mechanics of an atom with a non-Coulomb central field. Part II. Some results and discussion.* Mathematical Proceedings of the Cambridge Philosophical Society, **24**, 111, 1928.

[113] T. Saue, K. Faegri, T. Helgaker, and O. Gropen, *Principles of direct 4-component relativistic SCF: application to caesium auride.* Molecular Physics, **91**, 937, 1997.

[114] I. P. Grant, *Relativistic quantum theory of atoms and molecules*. Springer, 2006.

[115] K. G. Dyall, K. Fægri, and Jr., *Introduction to relativistic quantum chemistry*. Oxford University Press, 2007.

[116] F. Jensen, *Introduction to computational chemistry*. John Wiley & Sons Ltd., Second Edition, 2007.

[117] T. Helgaker, P. Jørgensen, and J. Olsen, *Molecular electronic-structure theory*. John Wiley & Sons Ltd., 2000.

[118] C. C. J. Roothaan, *New developments in molecular orbital theory*. Rev. Mod. Phys., **23**, 69, 1951.

[119] I. Shavitt and R. J. Bartlett, *Many-body methods in chemistry and physics, MBPT and coupled-cluster theory*. Cambridge University Press, 2009.

[120] I. Lindgren and J. Morrison, *Atomic many-body theory*. Springer-Verlag, Berlin, Second Edition, 1986.

[121] P. Schwerdtfeger, *Theoretical and computational chemistry: Relativistic electronic Structure Theory-Part 1. Fundamentals*. Elsevier, 2002.

[122] K. P. Geetha, *Relativistic many-body studies of parity non-conservation (PNC) in heavy atomic ions*. Ph.D. Thesis, URL: http://prints.iiap.res.in/, 2001.

[123] B. K. Sahoo, *Coupled-cluster theory of parity non - conservation in atoms*. Ph.D. Thesis, URL: http://prints.iiap.res.in/, 2005.

[124] R. F. Bishop, *Microscopic quantum many-body theories and their applications*, edited by Navarro, J. and Polls, A., Page 1. Springer-Verlag Berlin Heidelberg, 1998.

[125] R. F. Bishop and H. G. Kümmel, *The coupled Cluster Method*. Physics Today, **40**, 52, 1987.

[126] J. F. Stanton and R. J. Bartlett, *The equation of motion coupled-cluster method. A systematic biorthogonal approach to molecular excitation energies, transition probabilities, and excited state properties*. The Journal of Chemical Physics, **98**, 7029, 1993.

[127] P. Schwerdtfeger, *Table of experimental and calculated static dipole polarizabilities for the electronic ground states of the neutral elements (in atomic units), Centre for Theoretical Chemistry and Physics, Massey University*. 2015.

[128] T. H. Dunning, *Gaussian basis sets for use in correlated molecular calculations. I. The atoms boron through neon and hydrogen*. The Journal of Chemical Physics, **90**, 1007, 1989.

[129] J. Koput and K. A. Peterson, *Ab initio potential energy surface and vibrational-rotational energy levels of X $^2\Sigma^+$ CaOH.* The Journal of Physical Chemistry A, **106**, 9595, 2002.

[130] K. G. Dyall, *Relativistic double-zeta, triple-zeta, and quadruple-zeta basis sets for the 4s, 5s, 6s, and 7s elements.* The Journal of Physical Chemistry A, **113**, 12638, 2009.

[131] Peng Zhang, Enrico Bodo, and Alexander Dalgarno, *Near resonance charge exchange in ion−atom collisions of lithium isotopes.* The Journal of Physical Chemistry A, **113**, 15085, 2009.

[132] J. Koput, *The ab initio ground-state potential energy function of beryllium monohydride, BeH.* The Journal of Chemical Physics, **135**, 244308, 2011.

[133] N. S. Dattani, *Beryllium monohydride (BeH): Where we are now, after 86years of spectroscopy.* Journal of Molecular Spectroscopy, **311**, 76, 2015.

[134] N. S. Dattani, *Analytic potentials and vibrational energies for Li_2 states dissociating to Li (2S) + Li (3P). Part 1: The $^{2S+1}\Pi_u/g$ states.* e-print arXiv:1509.07041v1, 2015.

[135] W. Kutzelnigg, *The adiabatic approximation I. The physical background of the Born-Handy ansatz.* Molecular Physics, **90**, 909, 1997.

[136] E. F. Valeev and C. D. Sherrill, *The diagonal Born–Oppenheimer correction beyond the Hartree–Fock approximation.* The Journal of Chemical Physics, **118**, 3921, 2003.

[137] J. Gauss, A. Tajti, M. Kállay, J. F. Stanton, and P. G. Szalay, *Analytic calculation of the diagonal Born-Oppenheimer correction within configuration-interaction and coupled-cluster theory.* The Journal of Chemical Physics, **125**, 144111, 2006.

[138] N. C. Handy, Y. Yamaguchi, and H. F. Schaefer, *The diagonal correction to the Born–Oppenheimer approximation: Its effect on the singlet–triplet splitting of CH_2 and other molecular effects.* The Journal of Chemical Physics, **84**, 4481, 1986.

[139] J. F. Stanton, J. Gauss, M. E. Harding, P. G. Szalay with contributions from A. A. Auerand, R. J. Bartlett, U. Benedikt, C. Berger, D.E. Bernholdt, Y. J. Bomble, L. Cheng, O. Christiansen, M. Heckert, C. Huber O. Heun, T.-C. Jagau, D. Jonsson, J. Juslius, K. Klein, W.J. Lauderdale, D. A. Matthews, T. Metzroth, L. A. Mck, D. P. O'Neill, D. R. Price, E. Prochnow, C. Puzzarini, K. Ruud, F. Schiffmann, W. Schwalbach, C. Simmons, S. Stopkowicz, A. Tajti, J. Vzquez, F. Wang, J.D. Watts, the integral packages MOLECULE (J. Almlf,

ABACUS (T. Helgaker H. J. Aa. Jensen P. Jrgensen P. R. Taylor), PROPS (P. R. Taylor), J. Olsen), ECP routines by A. V. Mitin, and C. van Wllen., *CFOUR, a quantum chemical program package (http://www.cfour.de.).*

[140] M. J. Frisch, G. W. Trucks, H. B. Schlegel, G. E. Scuseria, M. A. Robb, J. R. Cheeseman, G. Scalmani, V. Barone, B. Mennucci, G. A. Petersson, H. Nakatsuji, M. Caricato, X. Li, H. P. Hratchian, A. F. Izmaylov, J. Bloino, G. Zheng, J. L. Sonnenberg, M. Hada, M. Ehara, K. Toyota, R. Fukuda, J. Hasegawa, M. Ishida, T. Nakajima, Y. Honda, O. Kitao, H. Nakai, T. Vreven, J. A. Montgomery, Jr., J. E. Peralta, F. Ogliaro, M. Bearpark, J. J. Heyd, E. Brothers, K. N. Kudin, V. N. Staroverov, R. Kobayashi, J. Normand, K. Raghavachari, A. Rendell, J. C. Burant, S. S. Iyengar, J. Tomasi, M. Cossi, N. Rega, J. M. Millam, M. Klene, J. E. Knox, J. B. Cross, V. Bakken, C. Adamo, J. Jaramillo, R. Gomperts, R. E. Stratmann, O. Yazyev, A. J. Austin, R. Cammi, C. Pomelli, J. W. Ochterski, R. L. Martin, K. Morokuma, V. G. Zakrzewski, G. A. Voth, P. Salvador, J. J. Dannenberg, S. Dapprich, A. D. Daniels, Ö. Farkas, J. B. Foresman, J. V. Ortiz, J. Cioslowski, and D. J. Fox, *Gaussian∼09 Revision E.01.* Gaussian Inc. Wallingford CT 2009.

[141] *GAMESS: The General Atomic and Molecular Electronic Structure System is a general ab initio quantum chemistry package*, http://www.msg.ameslab.gov/gamess/.

[142] H.-J. Werner, P. J. Knowles, G. Knizia, F. R. Manby, M. Schütz, P. Celani, W. Györffy, D. Kats, T. Korona, R. Lindh, A. Mitrushenkov, G. Rauhut, K. R. Shamasundar, T. B. Adler, R. D. Amos, A. Bernhardsson, A. Berning, D. L. Cooper, M. J. O. Deegan, A. J. Dobbyn, F. Eckert, E. Goll, C. Hampel, A. Hesselmann, G. Hetzer, T. Hrenar, G. Jansen, C. Köppl, Y. Liu, A. W. Lloyd, R. A. Mata, A. J. May, S. J. McNicholas, W. Meyer, M. E. Mura, A. Nicklass, D. P. O'Neill, P. Palmieri, D. Peng, K. Pflüger, R. Pitzer, M. Reiher, T. Shiozaki, H. Stoll, A. J. Stone, R. Tarroni, T. Thorsteinsson, and M. Wang, *MOLPRO, version 2015.1, a package of ab initio programs.* 2015. (http://www.molpro.net).

[143] R. Bast, T. Saue, L. Visscher, H. J. Aa. Jensen with contributions from V. Bakken, K. G. Dyall, S. Dubillard, U. Ekstroem, E. Eliav, T. Enevoldsen, E. Fasshauer, T. Fleig, O. Fossgaard, A. S. P. Gomes, T. Helgaker, J. Henriksson, M. Ilias, Ch. R. Jacob, S. Knecht, S. Komorovsky, O. Kullie, J. K. Laerdahl, C. V. Larsen, Y. S. Lee, H. S. Nataraj, M. K. Nayak, P. Norman, G. Olejniczak, J. Olsen, Y. C. Park, J. K. Pedersen, M. Pernpointner, R. Di Remigio, K. Ruud, P. Salek, B. Schimmelpfennig, J. Sikkema, A. J. Thorvaldsen, J. Thyssen, J. van Stralen, S. Villaume, O. Visserand T. Wintherand, and S. Yamamoto, *DIRAC, a relativistic ab initio electronic structure program, Release DIRAC15.* 2015 (http://www.diracprogram.org).

[144] G. Karlström, R. Lindh, P.-Å. Malmqvist, B. O. Roos, U. Ryde, V. Veryazov, P.-O. Widmark, M. Cossi, B. Schimmelpfennig, P. Neogrady, and L. Seijo, *MOLCAS: a program package for computational chemistry*. Computational Materials Science, **28**, 222, 2003. Proceedings of the Symposium on Software Development for Process and Materials Design.

[145] R. J. Le Roy, *LEVEL: A computer program for solving the radial Schrödinger equation for bound and quasibound levels*. Journal of Quantitative Spectroscopy and Radiative Transfer, **186**, 167, 2017. Satellite Remote Sensing and Spectroscopy: Joint ACE-Odin Meeting, October 2015.

[146] M. Kállay, Z. Rolik, J. Csontos, P. Nagy, G. Samu, D. Mester, J. Csóka, B. Szabó, I. Ladjánszki, L. Szegedy, B. Ladóczki, K. Petrov, M. Farkas, P. D. Mezei, and B. Hégely, *MRCC, a quantum chemical program suite*. See also Z. Rolik, L. Szegedy, I. Ladjánszki, B. Ladóczki, and M. Kállay, J. Chem. Phys., **139**, 094105, 2013 (www.mrcc.hu.).

[147] Y. Yin, Y. Xia, X. Li, X. Yang, S. Xu, and J. Yin, *Narrow-linewidth and stable-frequency light source for laser cooling of magnesium fluoride molecules*. Applied Physics Express, **8**, 092701, 2015.

[148] M. R. Tarbutt and T. C. Steimle, *Modeling magneto-optical trapping of CaF molecules*. Phys. Rev. A, **92**, 053401, 2015.

[149] V. Zhelyazkova, A. Cournol, T. E. Wall, A. Matsushima, J. J. Hudson, E. A. Hinds, M. R. Tarbutt, and B. E. Sauer, *Laser cooling and slowing of CaF molecules*. Phys. Rev. A, **89**, 053416, 2014.

[150] J. F. Barry, D. J. McCarron, E. B. Norrgard, M. H. Steinecker, and D. DeMille, *Magneto-optical trapping of a diatomic molecule*. Nature, **512**, 286, 2014.

[151] D. J. McCarron, E. B. Norrgard, M. H. Steinecker, and D. DeMille, *Improved magneto–optical trapping of a diatomic molecule*. New Journal of Physics, **17**, 035014, 2015.

[152] W. Bu, T. Chen, G. Lv, and B. Yan, *Cold collision and high-resolution spectroscopy of buffer-gas-cooled BaF molecules*. Phys. Rev. A, **95**, 032701, 2017.

[153] E. S. Shuman, J. F. Barry, and D. DeMille, *Laser cooling of a diatomic molecule*. Nature, **467**, 820, 2010.

[154] S. Hou, B. Wei, L. Deng, and J. Yin, *A novel molecular synchrotron for cold collision and EDM experiments*. Scientific Reports, **6**, 32663, 2016.

[155] M. G. Kozlov and L. N. Labzowsky, *Parity violation effects in diatomics*. Journal of Physics B: Atomic, Molecular and Optical Physics, **28**, 1933, 1995.

[156] K. Sinha and B. M. Tripathi, *On ionized molecules in the solar atmosphere.* Bull. Astr. Soc. India, **18**, 33, 1990.

[157] P. S. Ramachandran, N. Rajamanickam, and S. P. Bagare, *Evaluation of astrophysically useful parameters for strontium monohydride and deuteride.* Serb. Astron. J. N., **172**, 13, 2006.

[158] J. D. Kirkpatrick, *New Spectral Types L and T.* Annual Review of Astronomy and Astrophysics, **43**, 195, 2005.

[159] L. Wallace, K. Hinkle, G. Li, and P. Bernath, *The MgH B' $^2\Sigma^+$-X $^2\Sigma^+$ transition: A new tool for studying magnesium isotope abundances.* The Astrophysical Journal, **524**, 454, 1999.

[160] P. Sotirovski, *Table of solar diatomic molecular lines spectral lines spectral range 4900-6441Å.* Astron. Astrophys. Suppl., **6**, 85, 1972.

[161] M. Abe, M. Kajita, M. Hada, and Y. Moriwaki, *Ab initio study on vibrational dipole moments of XH^+ molecular ions: X = ^{24}Mg, ^{40}Ca, ^{64}Zn, ^{88}Sr, ^{114}Cd, ^{138}Ba, ^{174}Yb and ^{202}Hg.* Journal of Physics B: Atomic, Molecular and Optical Physics, **43**, 245102, 2010.

[162] J. B. Roos, M. Larsson, Å. Larson, and A. E. Orel, *Dissociative recombination of BeH^+.* Phys. Rev. A, **80**, 012501, 2009.

[163] H. Habli, R. Dardouri, B. Oujia, and F. X. Gadéa, *Ab initio adiabatic and diabatic energies and dipole moments of the CaH^+ molecular ion.* The Journal of Physical Chemistry A, **115**, 14045, 2011.

[164] F. B. C. Machado and F. R. Ornellas, *A theoretical investigation of the low-lying electronic states of the molecule BeH^+.* The Journal of Chemical Physics, **94**, 7237, 1991.

[165] M. Aymar, R. Guérout, M. Sahlaoui, and O. Dulieu, *Electronic structure of the magnesium hydride molecular ion.* Journal of Physics B: Atomic, Molecular and Optical Physics, **42**, 154025, 2009.

[166] Y. Gao and T. Gao, *Laser cooling of the alkaline-earth-metal monohydrides: Insights from an ab initio theory study.* Phys. Rev. A, **90**, 052506, 2014.

[167] L. Mejrissi, H. Habli, H. Ghalla, B. Oujia, and F. X. Gadéa, *Adiabatic ab initio study of the BaH^+ ion including high energy excited states.* The Journal of Physical Chemistry A, **117**, 5503, 2013.

[168] X. Liu, G. Liang, X. Zhang, H. Xu, and B. Yan, *Configuration interaction study on the ground and excited electronic states of the SrH molecule.* Journal of Quantitative Spectroscopy and Radiative Transfer, **170**, 169, 2016.

[169] D.-L. Wu, B. Tan, X.-F. Zeng, H.-J. Wan, A.-D. Xie, B. Yan, and D.-J. Ding, *Theoretical study on the spectroscopic parameters and transition properties of MgH radical including spin-orbit coupling.* Chinese Physics Letters, **33**, 063102, 2016.

[170] K. Mølhave and M. Drewsen, *Formation of translationally cold MgH^+ and MgD^+ molecules in an ion trap.* Phys. Rev. A, **62**, 011401, 2000.

[171] A. Shayesteh, K. A. Walker, I. Gordon, D. R. T. Appadoo, and P. F. Bernath, *New Fourier transform infrared emission spectra of CaH and SrH: combined isotopomer analyses with CaD and SrD.* Journal of Molecular Structure, **695 - 696**, 23, 2004. Winnewisser Special Issue.

[172] V. Laporta, K. Chakrabarti, R. Celiberto, R. K. Janev, J. Zs Mezei, S. Niyonzima, J. Tennyson, and I. F. Schneider, *Theoretical resonant electron-impact vibrational excitation, dissociative recombination and dissociative excitation cross sections of ro-vibrationally excited BeH^+ ion.* Plasma Physics and Controlled Fusion, **59**, 045008, 2017.

[173] R. Celiberto, R. K. Janev, and D. Reiter, *State-to-state electron impact cross sections for BeH^+ molecular ions in ITER-like fusion edge plasmas with Be walls.* Plasma Physics and Controlled Fusion, **54**, 035012, 2012.

[174] M. Kajita, M. Abe, M. Hada, and Y. Moriwaki, *Estimated accuracies of pure XH^+ (X: even isotopes of group II atoms) vibrational transition frequencies: towards the test of the variance in m_p/m_e.* Journal of Physics B: Atomic, Molecular and Optical Physics, **44**, 025402, 2011.

[175] H. Habli, L. Mejrissi, H. Ghalla, S. J. Yaghmour, B. Oujia, and F. Xavier Gadéa, *Ab initio investigation of the electronic and vibrational properties for the $CaLi^+$ ionic molecule.* Molecular Physics, **114**, 1568, 2016.

[176] S. Jellali, H. Habli, L. Mejrissi, M. Mohery, B. Oujia, and F. X. Gadéa, *Theoretical study of the $SrLi^+$ molecular ion: structural, electronic and dipolar properties.* Molecular Physics, **114**, 2910, 2016.

[177] D. A. Fedorov, D. K. Barnes, and S. A. Varganov, *Ab initio calculations of spectroscopic constants and vibrational state lifetimes of diatomic alkali-alkaline-earth cations.* The Journal of Chemical Physics, **147**, 124304, 2017.

[178] A. A. Safonov, V. F. Khrustov, and N. F. Stepanov, *Calculation of the potential curves of the low-lying electronic states of LiBe and $LiBe^+$ in a mixed orbital basis by the SCF method.* Journal of Structural Chemistry, **24**, 321, 1983.

[179] C. A. Nicolaides, M. Chrysos, and P. Valtazanos, *Stability and physicochemical reactions of light dications.* Journal of Physics B: Atomic, Molecular and Optical Physics, **23**, 791, 1990.

[180] A. I. Boldyrev, J. Simons, and P. von R. Schleyer, *Ab initio study of the electronic structures of lithium containing diatomic molecules and ions.* The Journal of Chemical Physics, **99**, 8793, 1993.

[181] M. Farjallah, C. Ghanmi, and H. Berriche, *Theoretical study of the low-lying sigma electronic states Of the alkaline earth $BeLi^+$ ion.* AIP Conference Proceedings, **1370**, 215, 2011.

[182] S. Baoguang, C. Hengjie, L. Fengkui, and Y. Yaohui, *Ground and low-lying excited states of $LiBe^+$.* Acta Chim. Sin., **69**, 761, 2011.

[183] Y. You, C. Yang, M. Wang, X. Ma, and W. Liu, *An ab initio study of the ground and low-lying excited states of $LiBe^+$.* J. At. Mol. Sci., **6**, 63, 2015.

[184] https://bse.pnl.gov/bse/portal.

[185] S. Kotochigova and E. Tiesinga, *Ab initio relativistic calculation of the RbCs molecule.* The Journal of Chemical Physics, **123**, 174304, 2005.

[186] L. Visscher, *Approximate molecular relativistic Dirac-Coulomb calculations using a simple Coulombic correction.* Theoretical Chemistry Accounts, **98**, 68, 1997.

[187] L. Visscher, T. J. Lee, and K. G. Dyall, *Formulation and implementation of a relativistic unrestricted coupled-cluster method including noniterative connected triples.* J. Chem. Phys., **105**, 8769, 1996.

[188] K. A. Peterson, D. E. Woon, and T. H. Dunning, *Benchmark calculations with correlated molecular wave functions. IV. The classical barrier height of the $H + H_2 \rightarrow H_2 + H$ reaction.* The Journal of Chemical Physics, **100**, 7410, 1994.

[189] D. Feller and J. A. Sordo, *A CCSDT study of the effects of higher order correlation on spectroscopic constants. I. First row diatomic hydrides.* The Journal of Chemical Physics, **112**, 5604, 2000.

[190] W. Pewestorf, V. Bonačić-Koutecký, and J. Koutecký, *Ab initio configuration interaction study of mixed $BeLi_k$ clusters (k=1–9).* The Journal of Chemical Physics, **89**, 5794, 1988.

[191] https://www.nist.gov/pml/atomic-spectra database.

[192] I. Miadoková, V. Kellö, and A. J. Sadlej, *Standardized basis sets for high-level-correlated relativistic calculations of atomic and molecular electric properties in the spin - averaged Douglas-Kroll approximationII. Groups Ia and IIa.* Theoretical Chemistry Accounts, **96**, 166, 1997.

[193] D. A. Fedorov, A. Derevianko, and S. A. Varganov, *Erratum: "Accurate potential energy, dipole moment curves, and lifetimes of vibrational states of heteronuclear alkali dimers [J. Chem. Phys. 140, 184315 (2014)]"*. The Journal of Chemical Physics, **147**, 209901, 2017.

[194] C. A. Nicolaides, D. R. Beck, and O. Sinanoglu, *Theoretical oscillator strengths for the beryllium $1s^2$ $2s^2$ ^1S-$1s^2$ $2s2p$ $^1P^0$, $1s^2$ $2s2p$ $^1P^0$-$1s^2$ $2p^2$ ^1D and $1s^2$ $2s2p$ $^1P^0$-$1s^2$ $2p^2$ ^1S isoelectronic sequences.* Journal of Physics B: Atomic and Molecular Physics, **6**, 62, 1973.

[195] R. E. Irving, M. Henderson, L. J. Curtis, Martinson I, and P. Bengtsson, *Accurate transition probabilities for the $2s^2$ ^1S - $2s2p$ ^1P transition in Be I and B II.* Canadian Journal of Physics, **77**, 137, 1999.

[196] P. PyykkÖ, *Ab initio study of bonding trends among the 14-electron diatomic systems: from B_2^{4-} to F_2^{4+}.* Molecular Physics, **67**, 871, 1989.

[197] Y. Gao and T. Gao, *Ab initio study of ground and low-lying excited states of MgLi and $MgLi^+$ molecules with valence full configuration interaction and MRCI method.* Molecular Physics, **112**, 3015, 2014.

[198] M. Kimura, H. Sato, and R. E. Olson, *Molecular treatment of charge transfer in Li^+ + Ca collisions.* Phys. Rev. A, **28**, 2085, 1983.

[199] P. Fantucci, V. Bonačić-Koutecký, W. Pewestorf, and J. Koutecký, *Ab initio configuration interaction study of the electronic and geometric structure of small, mixed neutral and cationic $MgNa_k$ and $MgLi_k$ (k=2–8) clusters.* The Journal of Chemical Physics, **91**, 4229, 1989.

[200] W. T. Zemke and W. C. Stwalley, *Radiative transition probabilities, lifetimes and dipole moments for the vibrational levels of the X $^1\Sigma^+$ ground state of $^{39}K^{85}Rb$.* The Journal of Chemical Physics, **120**, 88, 2004.

[201] J. F. Barry, E. S. Shuman, E. B. Norrgard, and D. DeMille, *Laser radiation pressure slowing of a molecular beam.* Phys. Rev. Lett., **108**, 103002, 2012.

[202] S. Truppe, H. J. Williams, M. Hambach, L. Caldwell, N. J. Fitch, E. A. Hinds, B. E. Sauer, and M. R. Tarbutt, *Molecules cooled below the Doppler limit.* Nature Physics, **13**, 1173, 2017.

[203] E. Altuntaş, J. Ammon, S. B. Cahn, and D. DeMille, *Measuring nuclear-spin-dependent parity violation with molecules: Experimental methods and analysis of systematic errors.* Phys. Rev. A, **97**, 042101, 2018.

[204] E. R. Meyer and J. L. Bohn, *Chemical pathways in ultracold reactions of SrF molecules.* Phys. Rev. A, **83**, 032714, 2011.

[205] B. Friedrich and D. Herschbach, *Alignment and trapping of molecules in intense laser fields.* Phys. Rev. Lett., **74**, 4623, 1995.

[206] B. Friedrich and D. Herschbach, *Polarization of molecules induced by intense nonresonant laser fields.* J. Phys. Chem., **99**, 15686, 1995.

[207] B. Friedrich and D. Herschbach, *Enhanced orientation of polar molecules by combined electrostatic and nonresonant induced dipole forces.* The Journal of Chemical Physics, **111**, 6157, 1999.

[208] B. Friedrich and D. Herschbach, *Manipulating molecules via combined static and laser fields.* The Journal of Physical Chemistry A, **103**, 10280, 1999.

[209] J. Deiglmayr, M. Aymar, R. Wester, M. Weidemüller, and O. Dulieu, *Calculations of static dipole polarizabilities of alkali dimers: Prospects for alignment of ultracold molecules.* The Journal of Chemical Physics, **129**, 064309, 2008.

[210] D. DeMille, J. M. Doyle, and A. O. Sushkov, *Probing the frontiers of particle physics with tabletop-scale experiments.* Science, **357**, 990, 2017.

[211] K. Fuyuto, J. Hisano, and E. Senaha, *Toward verification of electroweak baryogenesis by electric dipole moments.* Physics Letters B, **755**, 491, 2016.

[212] S. N. Tohme and M. Korek, *Theoretical study of the electronic structure with dipole moment calculations of barium monofluoride.* Journal of Quantitative Spectroscopy and Radiative Transfer, **167**, 82, 2015.

[213] F. Jardali, M. Korek, and G. Younes, *Theoretical calculation of the low-lying doublet electronic states of the SrF molecule.* Canadian Journal of Physics, **92**, 1223, 2014.

[214] N. El-Kork, N. Abu el kher, F. Korjieh, J. A. Chtay, and M. Korek, *Electronic structure of the polar molecules XF (X: Be, Mg, Ca) with rovibrational and dipole moment calculations.* Spectrochimica Acta Part A: Molecular and Biomolecular Spectroscopy, **177**, 170, 2017.

[215] M. Abe, V. S. Prasannaa, and B. P. Das, *Application of the finite-field coupled-cluster method to calculate molecular properties relevant to electron electric-dipole-moment searches.* Phys. Rev. A, **97**, 032515, 2018.

[216] P. W. Fowler and A. J. Sadlej, *Correlated studies of electric properties of ionic molecules: alkali and alkaline-earth hydrides, halides and chalcogenides.* Molecular Physics, **73**, 43, 1991.

[217] S. L. Davis, *Model polarizabilities and multipoles for ionic compounds. Alkaline-earth monohalides.* The Journal of Chemical Physics, **89**, 3, 1988.

[218] S. Sasmal, K. Talukdar, M. K. Nayak, N. Vaval, and S. Pal, *Calculation of hyperfine structure constants of small molecules using Z-vector method in the relativistic coupled-cluster framework*. Journal of Chemical Sciences, **128**, 1671, 2016.

[219] L. B. Knight, W. C. Easley, W. Weltner, and M. Wilson, *Hyperfine interaction and chemical bonding in MgF, CaF, SrF, and BaF molecules*. The Journal of Chemical Physics, **54**, 322, 1971.

[220] M. G. Kozlov, A. V. Titov, N. S. Mosyagin, and P. V. Souchko, *Enhancement of the electric dipole moment of the electron in the BaF molecule*. Phys. Rev. A, **56**, R3326, 1997.

[221] W. R. Johnson, *Atomic structure theory: Lectures on atomic physics*. Springer-Verlag Berlin Heidelberg, 2007.

[222] S. Sasmal, H. Pathak, M. K. Nayak, N. Vaval, and S. Pal, *Relativistic extended-coupled-cluster method for the magnetic hyperfine structure constant*. Phys. Rev. A, **91**, 022512, 2015.

[223] H. S. Nataraj, *Electric dipole moment of the electron and its implications on matter-antimatter asymmetry in the universe*. Ph.D. Thesis, 2009.

[224] W. Bernreuther and M. Suzuki, *The electric dipole moment of the electron*. Rev. Mod. Phys., **63**, 313, 1991.

[225] B. P. Das. *Relativistic many-body theory of electric dipole moment of atoms due to parity and time reversal violation*. In D. Mukherjee, editor, *Aspects of Many-Body Effects in Molecules and Extended Systems*, page 411, Berlin, Heidelberg, 1989. Springer Berlin Heidelberg.

[226] T. Fleig and M. K. Nayak, *Electron electric-dipole-moment interaction constant for HfF^+ from relativistic correlated all-electron theory*. Phys. Rev. A, **88**, 032514, 2013.

[227] E. D. Commins. *Electric dipole moments of leptons*. volume 40 of *Advances In Atomic, Molecular, and Optical Physics*, page 1. Academic Press, 1999.

[228] V. S. Prasannaa, A. C. Vutha, M. Abe, and B. P. Das, *Mercury monohalides: Suitability for electron electric dipole moment searches*. Phys. Rev. Lett., **114**, 183001, 2015.

[229] The ACME Collaboration, J. Baron, W. C. Campbell, D. DeMille, J. M. Doyle, G. Gabrielse, Y. V. Gurevich, P. W. Hess, N. R. Hutzler, E. Kirilov, I. Kozyryev, B. R. O'Leary, C. D. Panda, M. F. Parsons, E. S. Petrik, B. Spaun, A. C. Vutha, and A. D. West, *Order of magnitude smaller limit on the electric dipole moment of the electron*. Science, **343**, 269, 2014.

[230] A. Sunaga, M. Abe, M. Hada, and B. P. Das, *Relativistic coupled-cluster calculation of the electron-nucleus scalar-pseudoscalar interaction constant W_s in YbF.* Phys. Rev. A, **93**, 042507, 2016.

[231] A. Sunaga, V. S. Prasannaa, M. Abe, M. Hada, and B. P. Das, *Ultracold mercury−alkali-metal molecules for electron-electric-dipole-moment searches.* Phys. Rev. A, **99**, 040501, 2019.

[232] S. Chattopadhyay, B. K. Mani, and D. Angom, *Electric dipole polarizability of alkaline-earth-metal atoms from perturbed relativistic coupled-cluster theory with triples.* Phys. Rev. A, **89**, 022506, 2014.

[233] L. Ma, J. Indergaard, B. Zhang, I. Larkin, R. Moro, and W. A. de Heer, *Measured atomic ground-state polarizabilities of 35 metallic elements.* Phys. Rev. A, **91**, 010501, 2015.

[234] T. M. Miller and B. Bederson, *Measurement of the polarizability of calcium.* Phys. Rev. A, **14**, 1572, 1976.

[235] T. M. Miller, *Handbook of chemistry and physics.* Ed. D. R. Lide, 2002.

[236] B. K. Sahoo and B. P. Das, *Relativistic coupled-cluster studies of dipole polarizabilities in closed-shell atoms.* Phys. Rev. A, **77**, 062516, 2008.

[237] S. G. Porsev and A. Derevianko, *High - accuracy calculations of dipole, quadrupole, and octupole electric dynamic polarizabilities and van der Waals coefficients C_6, C_8, and C_{10} for alkaline-earth dimers.* Journal of Experimental and Theoretical Physics, **102**, 195, 2006.

[238] I. S. Lim and P. Schwerdtfeger, *Four-component and scalar relativistic Douglas-Kroll calculations for static dipole polarizabilities of the alkaline-earth-metal elements and their ions from Ca^n to Ra^n ($n = 0,+1,+2$).* Phys. Rev. A, **70**, 062501, 2004.

[239] B. O. Roos, V. Veryazov, and P.-O. Widmark, *Relativistic atomic natural orbital type basis sets for the alkaline and alkaline-earth atoms applied to the ground-state potentials for the corresponding dimers.* Theoretical Chemistry Accounts, **111**, 345, 2004.

[240] A. Borschevsky, V. Pershina, E. Eliav, and U. Kaldor, *Ab initio predictions of atomic properties of element 120 and its lighter group-2 homologues.* Phys. Rev. A, **87**, 022502, 2013.

[241] C. Nelin, B. O. Roos, A. J. Sadlej, and P. E. M. Siegbahn, *Complete active space (CAS) SCF and externally contracted multireference CI studies of atomic and molecular properties. Static dipole polarizabilities of F, F^-, and Ne.* The Journal of Chemical Physics, **77**, 3607, 1982.

[242] A. K. Das and A. J. Thakkar, *Static response properties of second-period atoms: coupled cluster calculations.* Journal of Physics B: Atomic, Molecular and Optical Physics, **31**, 2215, 1998.

[243] M. Medveď, P. W. Fowler, and J. M. Hutson, *Anisotropie dipole polarizabilities and quadrupole moments of open-shell atoms and ions: O, F, S, Cl, Se, Br and isoelectronic systems.* Molecular Physics, **98**, 453, 2000.

[244] V. S. Prasannaa, S. Sreerekha, M. Abe, V. M. Bannur, and B. P. Das, *Permanent electric dipole moments of alkaline-earth-metal monofluorides: Interplay of relativistic and correlation effects.* Phys. Rev. A, **93**, 042504, 2016.

[245] J. Kobus, D. Moncrieff, and S. Wilson, *Comparison of the electric moments obtained from finite basis set and finite-difference Hartree-Fock calculations for diatomic molecules.* Phys. Rev. A, **62**, 062503, 2000.

[246] S. R. Langhoff, C. W. Bauschlicher, H. Partridge, and R. Ahlrichs, *Theoretical study of the dipole moments of selected alkaline-earth halides.* The Journal of Chemical Physics, **84**, 5025, 1986.

[247] A. D. Buckingham and R. M. Olegário, *Hyperfine coupling in alkaline earth monofluorides. Limitations of the ionic model.* Chemical Physics Letters, **212**, 253, 1993.

[248] T. Törring, W. E. Ernst, and S. Kindt, *Dipole moments and potential energies of the alkaline earth monohalides from an ionic model.* The Journal of Chemical Physics, **81**, 4614, 1984.

[249] J. M. Mestdagh and J. P. Visticot, *Semiempirical electrostatic polarization model of the ionic bonding in alkali and alkaline earth hydroxides and halides.* Chemical Physics, **155**, 79, 1991.

[250] S. F. Rice, H. Martin, and R. W. Field, *The electronic structure of the calcium monohalides. A ligand field approach.* The Journal of Chemical Physics, **82**, 5023, 1985.

[251] P. Bündgen, B. Engels, and S.D. Peyerimhoff, *An MRD - CI study of low-lying electronic states in CaF.* Chemical Physics Letters, **176**, 407, 1991.

[252] A. R. Allouche, G. Wannous, and M. Aubert-Frécon, *A ligand-field approach for the low-lying states of Ca, Sr and Ba monohalides.* Chemical Physics, **170**, 11, 1993.

[253] W. J. Childs, L. S. Goodman, U. Nielsen, and V. Pfeufer, *Electric-dipole moment of CaF ($X\ ^2\Sigma^+$) by molecular beam, laser-rf, double-resonance study of Stark splittings.* The Journal of Chemical Physics, **80**, 2283, 1984.

[254] S. Sasmal, H. Pathak, M. K. Nayak, N. Vaval, and S. Pal, *Implementation of the Z - vector method in the relativistic - coupled - cluster framework to calculate first - order energy derivatives: Application to the SrF molecule.* Phys. Rev. A, **91**, 030503, 2015.

[255] W. E. Ernst, J. Kändler, S. Kindt, and T. Törring, *Electric dipole moment of SrF $X\ ^2\Sigma^+$ from high-precision Stark effect measurements.* Chemical Physics Letters, **113**, 351, 1985.

[256] W. E. Ernst, J. Kändler, and T. Törring, *Hyperfine structure and electric dipole moment of BaF $X\ ^2\Sigma^+$.* The Journal of Chemical Physics, **84**, 4769, 1986.

[257] Ch. Ryzlewicz, H.-U. Schütze-Pahlmann, J. Hoeft, and T. Törring, *Rotational spectrum and hyperfine structure of the $^2\Sigma$ radicals BaF and BaCl.* Chemical Physics, **71**, 389, 1982.

[258] http://www.webelements.com/isotopes.html.

[259] T. A. Isaev and R. Berger, *Lasercooled radium monofluoride: A molecular all-in-one probe for new physics.* arXiv:1302.5682.

[260] L. V. Skripnikov, A. N. Petrov, A. V. Titov, and N. S. Mosyagin, *Electron electric dipole moment: Relativistic correlation calculations of the P,T-violation effect in the $^3\Delta_3$ state of PtH^+.* Phys. Rev. A, **80**, 060501, 2009.

[261] K. Shen, B. Suo, and W. zou, *Theoretical study of low-lying Ω electronic states of PtH and PtH^+.* The Journal of Physical Chemistry A, **121**, 3699, 2017.

[262] K. G. Dyall, *Relativistic effects on the bonding and properties of the hydrides of platinum.* The Journal of Chemical Physics, **98**, 9678, 1993.

[263] G. Ohanessian, M. J. Brusich, and W. A. Goddard, *Theoretical study of transition-metal hydrides. 5. HfH^+ through HgH^+, BaH^+, and LaH^+.* J. Am. Chem. Soc., **112**, 7179, 1990.

[264] **R. Bala**, H. S. Nataraj, and M. Abe, *Spectroscopic studies of $^1\Sigma^+$ states of HfH^+ and PtH^+ molecular ions* (Accepted for publication in Springer Proceedings of ISAMP TC-7).

[265] I. Kozyryev and N. R. Hutzler, *Precision measurement of time-reversal symmetry violation with laser-cooled polyatomic molecules.* Phys. Rev. Lett., **119**, 133002, 2017.

[266] T. A. Isaev, A. V. Zaitsevskii, and E. Eliav, *Laser-coolable polyatomic molecules with heavy nuclei.* Journal of Physics B: Atomic, Molecular and Optical Physics, **50**, 225101, 2017.

[267] M. Dolg, *Effective core potentials*. Modern Methods and Algorithms of Quantum Chemistry, Proceedings, Second Edition, J. Grotendorst (Ed.), John von Neumann Institute for Computing, Jülich, NIC Series, **3**, 507, 2000.